

Award Number: W81XWH-12-2-0123

TITLE: Rapid Field-Usable Cyanide Sensor Development for Blood and Saliva

PRINCIPAL INVESTIGATOR: Brian A. Logue

CONTRACTING ORGANIZATION: South Dakota State University
Brookings, SD 57007

REPORT DATE: December 2014

TYPE OF REPORT: Final

PREPARED FOR: U.S. Army Medical Research and Materiel Command
Fort Detrick, Maryland 21702-5012

DISTRIBUTION STATEMENT:

Approved for public release; distribution unlimited

The views, opinions and/or findings contained in this report are those of the author(s) and should not be construed as an official Department of the Army position, policy or decision unless so designated by other documentation.

REPORT DOCUMENTATION PAGE

Form Approved
OMB No. 0704-0188

Public reporting burden for this collection of information is estimated to average 1 hour per response, including the time for reviewing instructions, searching data sources, gathering and maintaining the data needed, and completing and reviewing the collection of information. Send comments regarding this burden estimate or any other aspect of this collection of information, including suggestions for reducing this burden to Washington Headquarters Service, Directorate for Information Operations and Reports, 1215 Jefferson Davis Highway, Suite 1204, Arlington, VA 22202-4302, and to the Office of Management and Budget, Paperwork Reduction Project (0704-0188) Washington, DC 20503.

PLEASE DO NOT RETURN YOUR FORM TO THE ABOVE ADDRESS.

1. REPORT DATE December 2014	2. REPORT TYPE FINAL	3. DATES COVERED (From - To) 29 Sep 2012 to 25 Sep 2014
--	--------------------------------	---

4. TITLE AND SUBTITLE Rapid Field-Usable Cyanide Sensor Development for Blood and Saliva	5a. CONTRACT NUMBER
	5b. GRANT NUMBER W81XWH-12-2-0123
	5c. PROGRAM ELEMENT NUMBER

6. AUTHOR(S) Brian A. Logue; Michael W. Stutelberg, Erica Manandhar, Joseph K. Dzisam, Brendan L. Mitchell, Randy E. Jackson, Wenhui Zhou, Robert P. Oda, and Raj K. Bhandari email: brian.logue@sdstate.edu	5d. PROJECT NUMBER
	5e. TASK NUMBER
	5f. WORK UNIT NUMBER

7. PERFORMING ORGANIZATION NAME(S) AND ADDRESS(ES) South Dakota State University Brookings, SD 57007-0001	8. PERFORMING ORGANIZATION REPORT NUMBER
--	---

9. SPONSORING / MONITORING AGENCY NAME(S) AND ADDRESS(ES) U.S. Army Medical Research and Materiel Command Fort Detrick, Maryland 21702-5012	10. SPONSOR/MONITOR'S ACRONYM(S)
	11. SPONSORING/MONITORING AGENCY REPORT NUMBER

12. DISTRIBUTION AVAILABILITY STATEMENT
Approved for Public Release; Distribution Unlimited

13. SUPPLEMENTARY NOTES

14. ABSTRACT Cyanide is a deadly poison which may be ingested or inhaled and can cause severe incapacitation or death. The diagnosis of cyanide exposure is critical to speed treatment and reduce harm. The development of a diagnostic sensor device and the identification and analysis of novel biomarkers of cyanide exposure and the development of methods of analysis for novel cyanide therapeutics are the major objectives of this research. Since the onset of toxic outcome from cyanide exposure is very fast, a rapid and portable sensor for the detection of cyanide exposure was developed and tested. The sensor utilized a cyanide-selective fluorescent reaction as the core chemical reaction with micro-diffusion sample preparation and can determine exposure <60s. Multiple novel markers of cyanide exposure were also identified as having potential advantages to cyanide and thiocyanate, and methods of analysis for these markers were developed or are in the process of being developed. Specifically, 2-amino-2-thiozoline-4-carboxylic acid (ATCA), alpha-ketoglutarate, and a cyanide-glutathione adduct were investigated and obtained. Methods of analysis for DMTS, Cbi, and sulfanegen were developed and utilized.

15. SUBJECT TERMS
Sensor, cyanide, thiocyanate, 2-amino-2-thiazolino-4-carboxylic acid (ATCA), toxicokinetics, biomarker, diagnostics, therapeutics, sulfanegen, cobinamide, DMTS.

16. SECURITY CLASSIFICATION OF:			17. LIMITATION OF ABSTRACT UU	18. NUMBER OF PAGES 222	19a. NAME OF RESPONSIBLE PERSON USAMRMC
a. REPORT U	b. ABSTRACT U	c. THIS PAGE U			19b. TELEPHONE NUMBER (Include area code)

TABLE OF CONTENTS

LIST OF FIGURES (vi)

LIST OF TABLES (xiii)

INTRODUCTION (1)

SECTION I. DEVELOP A DIAGNOSTIC SENSOR THAT COMBINES RAPID AND ACCURATE DETERMINATION OF CYANIDE EXPOSURE WITH SIMPLISTIC USE AND PORTABILITY. (6)

CHAPTER 1. DEVELOPMENT OF A FLUORESCENCE-BASED SENSOR FOR RAPID DIAGNOSIS OF CYANIDE EXPOSURE (6)

CHAPTER 2. DESIGN OF PROTOTYPE 2 CARTRIDGE FOR CYANIDE SENSOR (7)

CHAPTER 3. DESIGN OF TWO-CHAMBER PROTOTYPE SENSORS (10)

SECTION II. EVALUATE NOVEL MARKERS OF CYANIDE EXPOSURE TO HELP DETERMINE THE MOST APPROPRIATE CYANIDE EXPOSURE MARKER(28)

CHAPTER 4. ANALYSIS OF CYANIDE AND THIOCYANATE BY GC-MS (28)

CHAPTER 5. TOXICOKINETICS OF CN, SCN, AND ATCA BY GC-MS (29)

CHAPTER 6. SIMULTANEOUS DETERMINATION OF CN AND SCN BY LC-MS-MS (30)

CHAPTER 7. DETERMINATION OF THE CYANIDE ADDUCT OF GLUTATHIONE BY HPLC (31)

CHAPTER 8. DETERMINATION OF α -KETOGLUTARATE CYANOHYDRIN (46)

CHAPTER 9. TOXICOKINETIC PROFILE OF α -KETOGLUTARATE CYANOHYDRIN (47)

SECTION III. DEVELOPMENT OF METHODS FOR NEXT GENERATION CYANIDE THERAPEUTICS (48)

CHAPTER 10. DETERMINATION OF DMTS BY GC-MS (48)

CHAPTER 11. DETERMINATION OF DMTS BY LC-MS-MS (62)

CHAPTER 12. DETERMINATION OF 3-MERCAPTOPYRUVATE BY LC-MS-MS (88)

CHAPTER 13. SIMULTANEOUS ANALYSIS OF 3-MERCAPTOPYRUVATE AND COBINAMIDE BY LC-MS-MS (89)

CHAPTER 14. DETERMINATION OF MULTIPLE SPECIES OF COBINAMIDE BY LC-MS-MS (104)

KEY RESEARCH ACCOMPLISHMENTS (146)

REPORTABLE OUTCOMES (147)

CONCLUSION (149)

REFERENCES (150)

APPENDICES (160)

LIST OF FIGURES

Figure I.2.1. Configuration of the bubble pack microdiffusion cartridge.

Figure I.2.2. Bubble portion of the bubble cartridge. A) The bubble mounting pegs and B) the bubbles (modified latex balloons) attached to the bubble mounting pegs.

Figure I.3.1. The cyanide sensor prototype: A) the front, left-hand view of the sensor; B) the response for no exposure; and C) the flashing response for exposure.

Figure I.3.2. Optical configuration of the miniature sensor cartridge chamber.

Figure I.3.3. Time delay for sample excitation and A/D sampling and conversion.

Figure I.3.4. Short-term reaction rate for the production of the NDA-Taurine-CN complex.

Figure I.3.5. Air volume optimization for the transfer of HCN gas-containing headspace from the sample chamber to the capture chamber.

Figure I.3.6. The cyanide sensor prototypes: A) the front, top view of the both the original sensor and the miniature sensor; B) the response for no exposure; and C) the flashing response for exposure.

Figure I.3.7. Experimental configuration for determination of the location of HCN gas within the side-by-side cyanide capture apparatus.

Figure I.3.8. Schematic for the experimental configurations used in the attempt to increase cyanide recovery.

Figure I.3.9. Schematic for the experimental configurations used in the rearrangement of the air inlet.

Figure II.7.1. Reaction scheme for the condensation of cyanamide with reduced glutathione (GSH), and possible rearrangement of the initial product.

Figure II.7.2. Reaction scheme for the addition of cyanide to oxidized glutathione (GSSG), and possible products.

Figure II.7.3. Overlaid HPLC chromatograms of a reagent blank, the reaction mixture from GSH and cyanamide, and Fraction 8 eluted by 20% methanol in chloroform solvent from the silica column. HPLC conditions: Column: Zorbax C-18, 4.6 X 150 mm; Mobile phase: 1mM ammonium formate in water/ methanol; Flow: 1.0 mL/ min; Detection: 270 nm.

Figure II.7.4. Overlaid HPLC chromatograms of a reagent blank, the reaction mixture from GSH and cyanamide, and Fractions 11 and 22 eluted by 50% methanol in water from the silica column. HPLC conditions: Column: Zorbax C-18, 4.6 X 150 mm; Mobile phase: ammonium formate (1 mM) in water/methanol; Flow: 1.0 mL/ min; Detection: 270 nm.

Figure II.7.5. Overlaid mass spectra of the cyanide-spiked plasma reaction mixtures. 100 mM CN (red) , 10 mM CN (green) and a plasma blank (blue). AB Sciex Q-trap 5500 Mass Spectrometer in positive ion mode with an ESI source.

Figure II.7.6a. Possible structure for the observed $m/z = 279$ fragment.

Figure II.7.6b. Possible structures for the $m/z = 213$ fragment.

Figure III.10.1. Overlaid chromatograms of 10 μM DMTS (blue) and a methanol blank (red).

Figure III.10.2. Overlaid chromatograms of 1 mM DMTS (purple), DMTS-spiked blood (green) and a blood blank (red).

Figure III.10.3 Overlaid chromatograms of 100 μM DMTS (red) and a water blank (blue).

Figure III.10.4. Average peak area of 100 μM DMTS by using different initial CIS temperature.

Figure III.10.5. Average peak area of 100 μM DMTS by using different headspace incubation time.

Figure III.10.6. Average peak area of 100 μM DMTS by using different transfer heater temperature of DHS.

Figure III.10.7. Average peak area of 100 μM DMTS by using different agitator temperature.

Figure III.10.8. Overlaid chromatograms of 0.8 μM DMTS (blue) and a water blank (red).

Figure III.11.1. Overlaid chromatograms of 10 μM DMTS (blue) and a methanol blank (red).

Figure III.11.2. Overlaid chromatograms of 1 mM DMTS (purple), DMTS-spiked blood (green) and a blood blank (red).

Figure III.11.3. Overlaid chromatograms of $[C_4H_{17}S_6Br]$ transition $m/z = 336.5 \rightarrow 220$. LC conditions are as described in the text.

Figure III.11.4. Mass spectra of increasing concentrations of DMTS in 0.1% Propionic acid. Mass/charge of the ions of interest are labeled.

Figure III.11.5. Chromatograms showing the oxidized reaction product (eluting at 6.5 min) and unreacted starting material DMTS (eluting at 15.5 min) when increasing the acetic acid concentration. The LC conditions are described in the text.

Figure III.11.6. Chromatograms of 0.5 mM product from oxidation of increasing DMTS (10 mM-100 mM) at 1.3 M peroxide and 8 M acetic acid concentrations. The LC parameters are described in the text in detail.

Figure III.11.7. Chromatogram showing loss of DMTS after drying for 15 minutes under N_2 air. A (before drying) shows the DMTS peak, which disappears in B (after drying).

Figure III.11.8. Chromatograms showing the oxidized product before (A), and after drying (B). The oxidized product is completely lost after drying for 15 minutes under N_2 air.

Figure III.11.9. Overlaid HPLC chromatograms of the reaction product after undergoing different quenching steps.

Figure III.11.10. Overlaid chromatograms showing analysis of the aqueous layer before and after extraction using organic solvents. The reaction product peak elutes at 6.5 min, and DMTS peak elutes at 15 min.

Figure III.11.11. Chromatograms showing the oxidized reaction product (eluting at 6.5 min) and unreacted starting material DMTS (eluting at 15.5 min) using different acids. The LC conditions are described in the text.

Figure III.11.12. Chromatograms of the collected oxidation product in positive ionization mode by infusion analysis with ESI mass spectroscopy.

Figure III.11.13. Chromatograms of the collected oxidation product in negative ionization mode by Infusion analysis with ESI-mass spectroscopy.

Figure III.13.1. Overlaid chromatograms of $CbiSO_3$ eluting at 2.74 min, 3-MPB eluting at 2.69 min, $Cbi(CN)_2$ eluting at 2.94 min, and $Cbi(CN)$ eluting at 2.94 min, spiked in rabbit plasma. The chromatograms represent the signal response of the MRM transitions of $CbiSO_3$ $1092.8 \rightarrow 989.9$, 3-MPB $311.0 \rightarrow 223.1$, $Cbi(CN)_2$ $1064.9 \rightarrow 1010.8$, and $Cbi(CN)$ $1015.0 \rightarrow 930.5$ m/z .

Figure III.13.2. Calibration curve for CbiSO₃ spiked in rabbit plasma.

Figure III.13.3. Calibration curve for Cbi(CN)₂ spiked in rabbit plasma.

Figure III.13.4. Calibration curve for Cbi(CN) spiked in rabbit plasma.

Figure III.13.5. Chromatograms of Cbi(NO₂)₂ eluting at 0.75 min, and Cbi eluting at 0.8 min spiked in swine plasma. The chromatograms represent the signal response of the MRM transitions of Cbi(NO₂)⁺ 1035.9 → 989.9 and Cbi 989.0 → 916.9 *m/z* and total ion chromatograph of the blank.

Figure III.13.6. Chromatograms of Cbi(CN)₂ eluting at 2.9 min and 3-MPB eluting at 2.67 min, in swine plasma. The chromatograms represent the signal response of the MRM transitions of Cbi(CN)₂ 1015.9-930.9 and 3-MP 311.0 → 223.1 *m/z*.

Figure III.13.7. Chromatograms of Cbi(CN)₂ eluting at 2.95 min spiked in swine plasma.

Figure III.13.8. The chromatograms represent the signal response of 3-MP, eluting at 2.67 min, in plasma with varying Cbi species and excess cyanide. The MRM transitions observed are 311-223 *m/z*.

Figure III.13.9. Chromatograms of varying species of Cbi with 3-MP and excess cyanide after conversion to Cbi(CN)₂ eluting at 2.9 min. The chromatograms represent the signal response of the MRM transitions of Cbi(CN)₂ 1015.9-930.9 *m/z*.

Figure III.14.1. Schematic of the cyanide apparatus used to create sodium- and potassium-free Cbi-cyanide species. The lower chamber contained KCN solution to which acid was added to generate HCN(g). Air was bubbled through the lower chamber via the air injection syringe to deliver HCN(g) to cobinamide solution in the upper chamber.

Figure III.14.2. Mass spectrum of cobinamide-sulfite. The sodium adduct, [CbiSO₃Na]⁺, is clearly observed at 1092.5 *m/z*.

Figure III.14.3. Mass spectra of aquo- and hydroxo- Cbi species with tentative assignment of the peaks at 1022.5-1026.5.

Figure III.14.4. Plots of intensities of 1022.5, 1023.5, 1024.5, 1025.5 and 1026.5 divided by the intensity of 1024.5. **A, B and C** were conducted in Days 1, 3 and 5, respectively. The trend reveals a direct correlation between 1024.5 (green), 1025.5 (purple) and 1026.5 (light blue). Similarly, 1022.5 (deep blue) and 1023.5 (red) are also correlated. The correlation shows isotopic relations. Day 1 and 5 solutions were not thermodynamically stable, but Day 3 solutions were

very stable, as they showed the trends of the Cbi species at the expected pH values.

Figure III.14.5. Chromatograms showing the elution of diaquocobinamide (100 μM) from the LC column in water (blue) and in plasma (red). LC conditions: mobile phase A ; 90 % 5 mM ammonium formate and 10 % methanol, mobile phase B has 90% methanol and 10% ammonium formate (5 mM). MS transition: 1024.4 \rightarrow 930.5.

Figure III.14.6. Chromatogram of Cbi species prepared at pH 11 after 3 days. LC conditions were as described earlier. MS transition: 1022.7 \rightarrow 946.8.

Figure III.14.7. Chromatogram of $[\text{Cbi}(\text{S})_2]^0$ transition 1053 \rightarrow 916. LC Conditions were as described above.

Figure III.14.8. Overlaid chromatograms of Cbi species prepared at pH 11 after 3 days. LC conditions were as described earlier. MS transition: $m/z = 1022.7 \rightarrow 946.8$.

Figure III.14.9. Overlaid chromatograms of $[\text{Cbi}(\text{S})_2]^0$ at transition $m/z = 1053 \rightarrow 916$. LC conditions were as described above.

Figure III.14.10. Overlaid chromatograms of $[\text{CbiS}_2]$. The solution prepared in aqueous medium (100 μM) became thermodynamically stable within 24 hours (blue chromatogram is blank). The intensity for the solution prepared within 4 hours (red) was not as much as that for the 24 hour period (green).

Figure III.14.11. Overlaid chromatograms from $[\text{CbiS}_2]^0$ swine plasma. The transitions shown here is $m/z = 1092 \rightarrow 989$. The $m/z = 1053 \rightarrow 989$ transitions (not shown) were unresolved.

Figure III.14.12. Mass spectrum (MS1) showing the dinitrocobinamide with the sodium adduct, $[\text{Cbi}(\text{NO}_2)_2\text{Na}]^+$ with $m/z=1104.5$, mononitrocobinamide with sodium adduct, $[\text{Cbi}(\text{NO}_2)\text{Na}]^{2+}$, $m/z=1058.5$, mononitrocobinamide with no sodium adduct, $[\text{Cbi}(\text{NO}_2)]^+$, $m/z=1035$, and the cobinamide (Cbi) with no ligands at $m/z=989.5$.

Figure III.14.13. SPE of $[\text{Cbi}({}^{13}\text{C}{}^{15}\text{N})_2]^0$. Spectral intensities of 'free' cyanide in acidified solution (red) and non-acidified solution containing the internal standard (blue). The standard cyanide spectra intensity is shown in green, and the blank is shown in yellow. The concentration of cyanide verified (standard and free) with NDA/ Taurine reagent was 100 μM .

Figure III.14.14. Chromatograms showing the elution of isotopically-labelled dicyanocobinamide, the internal standard, spiked into swine plasma. MS transition: $m/z = 1068.5 \rightarrow 1010.7$. There is no evidence of peak in the blank (red) and the acidified solution (green).

Figure III.14.15. Overlaid chromatograms of $[\text{Cbi}(\text{NO}_2)_2]^0$ at transition $m/z = 1104.5 \rightarrow 1058.8$ and $1104.5 \rightarrow 1013.8$, respectively, in water and plasma. LC conditions were as described above.

Figure III.14.16. Overlaid chromatograms of $[\text{Cbi}(\text{NO}_2)_2]^0$ in swine plasma at different concentrations. The peak intensity for the blank (deep blue) is significant and more conspicuous than the $0.5 \mu\text{M}$ (red). Transitions monitored were $1104 \rightarrow 1058$.

Figure III.14.17. Overlaid chromatograms of $1104 \rightarrow 1058$ transitions for the positive controls (shown in red and grey,) spiked mononitromonocyano (yellow) and dicyano (blue) derivatives of cobinamide. The blank is shown in green with a significant peak for the $1104 \rightarrow 1058$ transitions. The presence of $1104 \rightarrow 1058$ transitions in all the samples prepared could be due to an interferent in the plasma, and may not be due to a residual or contaminant of the aquo or hydroxo forms or other derivatives of the cobinamides.

Figure III.14.18. Overlaid chromatograms $1064.5 \rightarrow 1010.8$ transitions. The positive control is spiked dicyano cobinamide (blue). The red is mononitromonocyanocobinamide spiked in plasma; the large intensity seen could be due to the presence of dicyanocobinamide formed after cyanide was added to the dinitrocobinamide. Cyanide spiked into blank plasma is shown in yellow; any free cobinamide in the blank plasma should have converted to dicyanocobinamide so that the $1064.5 \rightarrow 1010.8$ transitions could be seen. The absence of a peak for the transition $1064.5 \rightarrow 1010.8$ in the spiked -CN blank plasma suggests that there is no form of cobinamide in the unspiked plasma (similar to results in Figure II.4.3 -2. above).

Figure III.14.19. Overlaid chromatograms $1084.5 \rightarrow 1038$ transitions. The positive control is spiked mononitromonocyanocobinamide (blue and red). The grey peak is spiked dinitrocobinamide spiked in plasma. The yellow represents spiked dicyanocobinamide, and the deep blue (tiny) is the peak for spiked CN into the blank plasma. By the same analogy described earlier any free cobinamide in the unspiked plasma should have been converted to cyanide derivatives when the CN was spiked into it. The absence of any conspicuous peaks for the spiked-CN plasma could be an indication of lack of any cobinamide in the blank plasma. The large peak seen for this transition in the blank (green) could possibly be an interferent or a contamination that is not in the plasma but probably from other sources such as the injector of the LC.

Figure III.14.20. Stacked chromatogram for 'neutral' spiked and unspiked plasma (blank) prepared at 0 hour and 1 hour, respectively, prior to analysis. The intensity for the blank plasma (light blue) analyzed after 1 hour is very much higher than that for 0 hour (deep blue). 'DN' is spiked dinitrocobinamide into the plasma at 1 hour (red) or 0 hour (green). The intensities for the spiked DN samples were almost the same.

Figure III.14.21. Stacked chromatogram for 'acidified' spiked and unspiked plasma (blank) prepared at 0 hour and 1 hour, respectively, prior to analysis. The intensity for the acidified blank plasma (light blue) analyzed after 1 hour is very much higher than that for 0 hour (deep blue). 'DN' is spiked dinitrocobinamide into the plasma at 1 hour (red) or 0 hour (green). The intensity for the spiked DN analyzed after 1 hour diminished almost to undetectable limits, as compared to all other peaks.

Figure III.14.22. Overlaid chromatogram for 'alkalinized' spiked and unspiked plasma (blank) prepared at 0 hour and 1 hour, respectively, prior to analysis. The intensity for the alkalinized blank plasma (light blue) analyzed after 1 hour is very much lower than that for 0 hour (deep blue). 'DN' is spiked dinitrocobinamide into the plasma at 1 hour (red) or 0 hour (green). The intensity for the spiked DN analyzed after 1 hour was significantly enhanced.

LIST OF TABLES

Table III.11.1 Composition of reaction mixture for oxidation of DMTS using different acids.

Table III.11.2. MRM ions and associated parameters corresponding to some form of DMTS-Br adduct in negative ionization mode.

Table III.11.3. MRM ions and associated parameters corresponding to potential DMTS-propionic acid adducts.

Table III.14.1. MRM ions and associated parameters corresponding to some Cbi forms of interest.

Table III.14.2. MRM ions and associated parameters corresponding to some Cbi forms of interest.

Table III.14.3. The occurrence of various transitions of cobinamide analogues in plasma and aqueous medium (water).

INTRODUCTION

One of the long-term goals of the *Strategic Plan and Research Agenda for Medical Countermeasures Against Chemical Threats* (August, 2007)¹ is the development of “rapid diagnostic tests and assays to identify biological markers consistent with cyanide exposure and the level of exposure”. Dr. Logue has been working to identify and study biological marker behavior and to develop rapid, portable cyanide diagnostics over the last several years.^{2,3} Multiple sensor technologies have been developed by the PI to move towards the ultimate sensor technology that combines rapid and accurate determination of cyanide exposure with simplistic use. The combination of these technologies should prove to be the most rapid path towards the long-term research goal of cyanide diagnostic development. Therefore, one objective of the proposed work is to develop a diagnostic sensor that combines rapid and accurate determination of cyanide exposure with simplistic use. A diagnostic sensor will be developed from a combination of the most promising current sensor technologies for rapid cyanide diagnosis. The sensor technology will utilize the change in fluorescence from the reaction of naphthalene dialdehyde (NDA), taurine, and cyanide as the core chemical process. This chemical process has shown excellent sensitivity and selectivity for cyanide analysis in past work.

The choice of biomarker and biological matrix for diagnosing cyanide poisoning is dependent on multiple factors. While definitive determination of cyanide exposure is essential, the ability to quickly and non-invasively gather the biological matrix of interest is also desirable, especially in a mass casualty

situation. Currently, cyanide exposure is typically determined by analysis of blood for elevated cyanide concentrations, although it may not be the best matrix/biomarker combination. Therefore, multiple biomarkers will be evaluated as potential alternatives to direct analysis of cyanide by developing analytical methods for their analysis.

Pharmacokinetic, stability, and other studies, which are necessary for FDA approval, require an analytical method. 3-Mercaptopyruvate (3-MP), dimethyltrisulfide (DMTS), and cobinamide (Cbi) are promising cyanide therapeutic lead candidates, including combinations of the three, that are currently being studied for potential FDA approval. Some of these therapeutics currently have associated analytical methods, but some do not. Furthermore, no methods are available for the simultaneous detection of two or more of these therapeutics during combination therapies. Therefore, we will develop multiple methods for the analysis of cyanide therapeutics from blood or its components.

Technical Objectives

1. Develop a diagnostic sensor that combines rapid and accurate determination of cyanide exposure with simplistic use and portability.
2. Identify alternative biomarkers of cyanide exposure by developing analytical methods for their analysis and determining the toxicokinetics of these biomarkers.

3. Develop assays to detect next generation cyanide antidotes from biological fluids that are accurate and robust.

Specific Tasks

1a) Develop an easy-to-use two-chamber type diagnostic sensor technology that has the ability to determine cyanide exposure rapidly and accurately.

Previously, the development of a simple, field-portable fluorometric sensor platform was undertaken. Although extremely promising, the analysis time for cyanide by the initial sensor was slow (5-minute analysis) compared to the onset of the symptoms of cyanide exposure. Thus, the development of the next-generation portable fluorometric cyanide diagnostic sensor will be pursued.

1b) Test the sensor developed in Task 1 using an appropriate animal model to confirm the ability of the sensor to diagnose cyanide exposure.

2) Evaluate novel markers of cyanide exposure to help determine the most appropriate cyanide exposure marker.

A rat model was used in the initial toxicokinetic experiment and may not be appropriate for this study. Therefore, a rabbit model (reported last year) and a swine model will be used to verify the toxicokinetic data. To increase the

chances of finding a suitable cyanide diagnostic bio-marker, we shall also investigate the cyanide adduct of α -ketoglutarate, α -ketoglutarate cyanohydrin, and the cyanide adduct(s) of glutathione.

2a) Verify the toxicokinetics of ATCA, cyanide, and thiocyanate in an appropriate animal model post-cyanide exposure

2b) Optimize and validate an analytical method to analyze ATCA, cyanide, and thiocyanate simultaneously.

To lessen the burden of analyzing three compounds with three different methods, an analytical method to determine all three metabolites simultaneously will be developed at SDSU. This method will be utilized to determine ATCA, cyanide, and thiocyanate concentrations from the biological samples produced in Task 1, if validated prior to the toxicokinetic study.

2c) Determination of the cyanide metabolite α -ketoglutarate cyanohydrin by liquid chromatography tandem mass-spectrometry

2d) Determination of the cyanide adduct of glutathione by high performance liquid chromatography

3) Development of an assay for 3-mercaptopyruvate (sulfanegen), dimethyl trisulfide, and multiple forms of cobinamide from blood (i.e., plasma, RBCs or whole blood) and test methods to analyze combinations of each.

REFERENCES

1. *Strategic Plan and Research Agenda for Medical Countermeasures Against Chemical Threats* (August, 2007), http://www.ninds.nih.gov/research/counterterrorism/counterACT_home.htm. Accessed 8/29/2012.2.
2. Youso, S. L.; Rockwood, G. A.; Lee, J. P.; Logue, B. A. 2010. *Anal Chim Acta* 677 24-28.
3. Logue, B. A.; Hinkens, D. M.; Baskin, S. I.; Rockwood, G. A. 2010. *Crit Rev Anal Chem* 44 122-147.

SECTION I

DEVELOP A DIAGNOSTIC SENSOR THAT COMBINES RAPID AND ACCURATE DETERMINATION OF CYANIDE EXPOSURE WITH SIMPLISTIC USE AND PORTABILITY

CHAPTER 1

DEVELOPMENT OF A FLUORESCENCE-BASED SENSOR FOR RAPID DIAGNOSIS OF CYANIDE EXPOSURE

Randy E. Jackson and Brian A. Logue

I.1. The effort for this portion of the report was published as a peer-reviewed manuscript which is attached as Appendix I.

CHAPTER 2

DESIGN OF PROTOTYPE 2 CARTRIDGE FOR CYANIDE SENSOR

Randy E. Jackson and Brian A. Logue

1.2.1. Microdiffusion Cartridge Design Evolution.

The current microdiffusion cartridge utilizes a “bubble pack” for reagent introduction (Figure 1.2.1) with external dimensions of 45 x 30 x 40 mm (l x w x h). The bubble pack microdiffusion cartridge utilizes side-by-side positioning of the sample and capture chambers, contains channels to deliver the reagents to their designated chambers, and uses a bubble pack to house the reagents. Several materials, including bubble wrap, nitrile, and latex, were evaluated to create a leak proof bubble. Modified latex balloons (35 cm long with a 0.8 mm diameter) were determined to be the best material to create short-term leak proof seal (see Figure 1.2.2). The balloons were able to create a leak-free seal and could be modified to hold the correct amount of solution for the designated reagents. The latex material created the leak-free seal due to the attached o-ring and the flexibility of the material. Also, it is important to note that over time the latex became brittle and less flexible which lead to tearing. This issue may be eliminated in the manufacturing process with the use of a plastic material (i.e., the use of polyethylene) to create the bubbles. The current cartridge design allows the expulsion of capture solution through the air outlet in the capture chamber and the junction between the bubble portion and the chamber portion of the cartridge leaks at times. Currently, a new cartridge design that increases the

size of the capture chamber and uses the incorporation of preformed plastic material (i.e., needle and syringe Luer locks, metal tubing) into the fused deposition modeling (FDM) printed material is being developed. The design changes will ensure the preservation of capture solution as well as ensure liquid and air tight seals for junctions and channels within the microdiffusion cartridge.

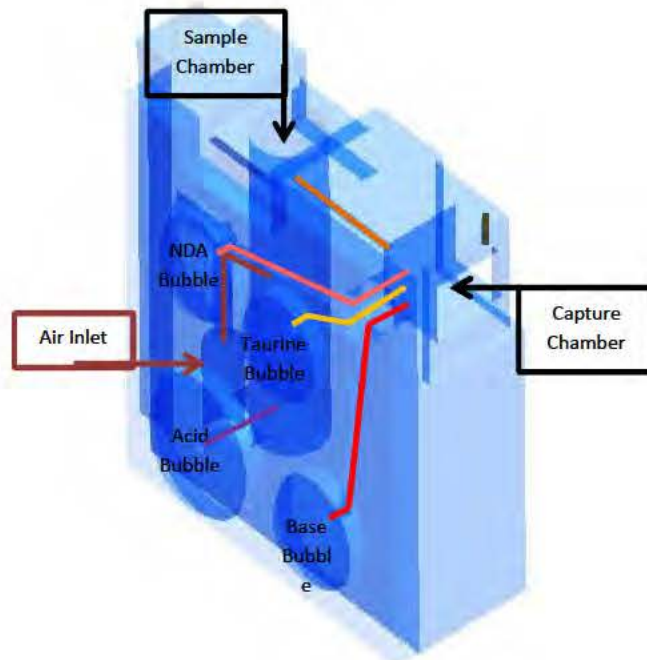


Figure I.2.1. Configuration of the bubble pack microdiffusion cartridge.

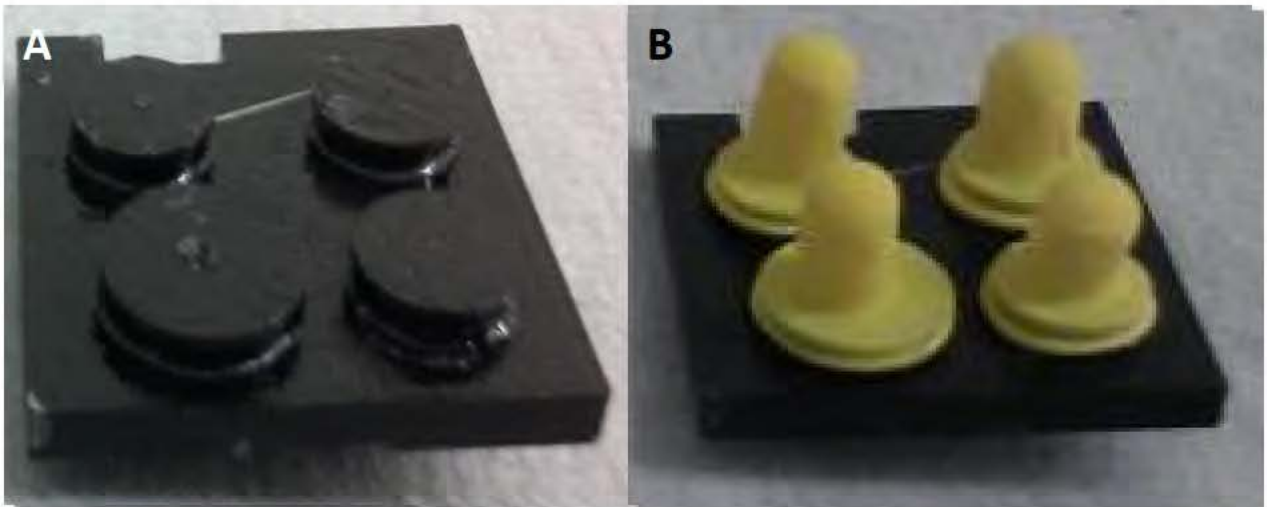


Figure I.2.2. Bubble portion of the bubble cartridge. A) The bubble mounting pegs and B) the bubbles (modified latex balloons) attached to the bubble mounting pegs.

CHAPTER 3

DESIGN OF TWO-CHAMBER PROTOTYPE SENSORS

Randy E. Jackson and Brian A. Logue

1.3.1. Sensor Circuit Design for Prototype

The sensor casing was designed in our laboratory and manufactured by Falcon Plastics using their fused deposition modeling (FDM) Printing Technology (i.e., rapid prototyping or 3D printing). The current sensor has a base for mounting all components, a cartridge and detector holder (mounted to the base and holds the microdiffusion cartridge and USB2000+ Spectrometer), and a cover, which houses the display and is secured in place to the base. The circuitry consists of a Microchip Explorer 16 PIC development board joined to an Electronic Assembly display development board, and a Firgelli linear actuator control board. The sensor (Figure II.3.1A) was programmed and can differentiate between below threshold (display reads “No Exposure” seen in Figure II.3.1B) and above threshold (display flashes “Exposure Detected” seen in Figure II.3.1C) concentrations of cyanide. The threshold for exposure was set at 15 μM cyanide in whole blood. The circuit design, implementation, and programming were performed at Midwest Micro-Tek and in our laboratory. For laboratory testing, further programming is needed to create an administrator screen such that numerical data can be obtained from the sensor and analyzed. The current sensor is portable, but still bulky measuring 28.5 x 19.5 x 15 cm (l x w x h). The use of bulky components such as the 50 mm linear actuator, the large

development circuit board, and the USB2000+ Spectrometer makes the sensor much larger than necessary. We identified smaller components and have designed a photodiode-based spectrophotometer to replace the larger components in order to miniaturize the sensor and increase instrument portability. These changes were incorporated into a new circuit design, which was built in lab. The new circuit design is centered around the same Microchip Explorer 16 PIC development board joined to an Electronic Assembly display development board in order to manipulate the coding that currently exists. The code for the display screens (altered and new) and the microcontroller code to navigate through the screens were written. The coding and communication programming for all the additional peripheral components (i.e., linear actuator, pressure pump, etc.) and the microcontroller unit were developed. The circuitry for the new miniature sensor is complete and the manufacture of a custom circuit board is underway with the electrical engineers at Midwest Micro-Tek. Lastly, the coding for the miniature sensor is ~90% complete; some coding for displaying detector signals as numerical values, and the optimization of LED illumination, light capture, and analog-to-digital conversion is underway. These items will be developed concurrently with circuit board manufacture.

I.3.2. RESULTS AND DISCUSSION

I.3.2.1. Sensor Optics Optimization

To obtain the highest fluorescence signal within the desired analysis time (>1 min), the initiation time for the LED irradiation and the time interval for

photodiode sampling and analog to digital (A/D) conversion were optimized. This evaluation was performed using a 410nm LED with no focusing lens, a 1 cm path length cuvette (placed in the cartridge chamber of the sensor), and a photodiode with a focusing lens (1.5 cm focal length) positioned perpendicular to the LED, see Figure II.3.2. Samples consisted of 100 μL of the specified CN standard (0, 1, and 10 μM NaCN in 10 mM NaOH) and 200 μL of each capture solution reagent (0.5 mM NDA, 0.05 M taurine, and 0.1 M NaOH). The time delays used to analyze fluorescence ranged from 15.625 – 125 ms. The sample analysis sequence was as follows, the LED was turned on and the timer began counting, analog sampling was performed when the counter reached the designated time and the LED was turned off immediately after analog sampling. The increased fluorescent signal for 62.5 ms time delay shown in Figure II.3.3 indicates that it was the optimum time delay between sample excitation and analog sampling for A/D conversion.

1.3.2.2. Evaluation of Analysis Time

The analysis time was evaluated to determine the time (after NDA and taurine addition) needed to distinguish a blank sample from a CN spiked sample. This evaluation was performed using same optical configuration as previously described. For the initial analysis using the cuvette, samples for the cuvette consisted of the CN standard (100 μL of 0 and 10 μM NaCN in 10 mM NaOH) and 200 μL of each 0.5 mM NDA, and 0.1 M NaOH), and 200 μL of 0.05 M taurine was added at time of analysis. Upon the introduction of taurine the

“capture” button was pressed and fluorescence was measured. For the cartridge samples, the CN Std (100 μ L of 0 and 10 μ M NaCN in 0.010 M NaOH) were placed in the capture chamber and reagent bubbles were prepared containing 200 μ L of NDA, 250 μ L of taurine, and 250 μ L of NaOH. The cartridge was placed in the cartridge holder, automatically injects NaOH, and both the NDA and taurine bubbles were depressed and the capture button was pressed. Once the capture button was pressed, the sample solutions were allowed to passively mix for time periods ranging from 1 – 90 s before fluorescence was measured. Figure II.3.4 shows the comparison of the cuvette and cartridge and the rate of observed fluorescence signal differentiation for the NDA-aurine-CN complex. The use of the cartridge is favorable due to the fact that it decreases the background signal and reduced the standard deviation observed between samples. The 20 s time period for both reaction vessels was the first time period that allows for reproducible and significant distinction between CN containing samples and blanks and this time period was considered best compromise between quick analysis and accurate differentiation between exposed and non-exposed samples.

1.3.2.3. Transfer Pump Flow Rate

The flow rate of the transfer pump was evaluated to determine the optimum volume of air for the transfer of HCN containing headspace from the sample chamber to the capture chamber. The pump flow rate was analyzed by attaching the pump to the air inlet luer (located beneath the cartridge chamber)

using an 11 cm long piece of Nalgene tubing with a 3 mm I.D., the outlet side of the air inlet luer was attached to a 50.5 cm long Nalgene tubing that steps up from 3 mm I.D. to 12.5 mm I.D. The end of the tubing measuring 12.5 mm I.D. was placed in a beaker of water and the pump was turned on for 10 s. The bubbles which evolved were counted and the pump flow rate was estimated by multiplying the number of bubbles by the calculated volume of a 12.5 mm bubble. The flow rate was estimated to be 3.5 mL/s or 0.211 L/min. This calculated flow rate was lower than the manufacturer's rating but the pump was powered with a 5 V power supply rather than the 6 V supply recommended by the manufacturer.

1.3.2.4. Air Volume Optimization

Once the pump flow rate was determined, the air volume necessary to transfer the HCN containing headspace from the sample chamber to the capture chamber was evaluated. Samples consisted of a CN standard (100 μ L of 0 or 10 μ M NaCN in 10 mM NaOH) placed in the sample chamber of the analysis cartridge while 300 μ L of H₂SO₄ (1 M) 200 μ L of NDA (0.5 mM), 250 μ L of taurine (0.05 M), and 250 μ L of NaOH (0.1 M) were placed in their specified reagent bubbles. The cartridge was placed in the cartridge holder which automatically injects H₂SO₄ and NaOH and the start button was pressed. The air pump delivered air volumes ranging from 30-70 mL. Once the pump stopped, NDA and taurine bubbles were depressed using the linear actuator injector arm and the reaction was allowed to proceed for 20 s before fluorescence was measured. Preliminary results (Figure II.1-5) indicate that 60-70 mL of air may be the

optimum for transferring HCN gas to the capture chamber, although additional air volumes, as well as blank samples and replicate analysis, must be performed to obtain definitive information about the transfer of HCN gas. If these preliminary results hold true, the overall analysis time is expected to be ~40 s, which is well below the goal of <1 min.

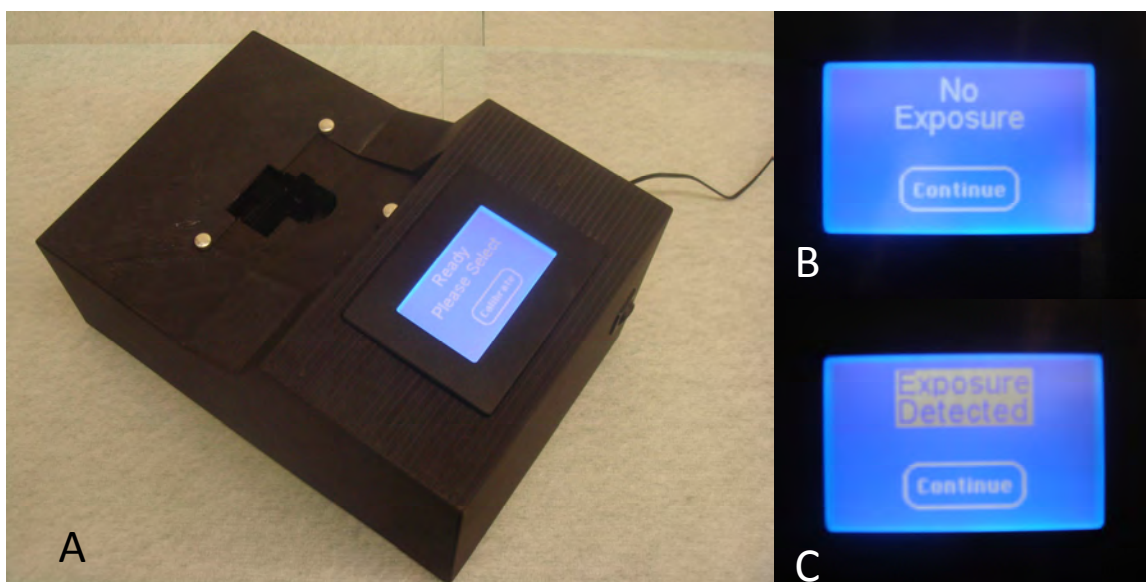


Figure I.3.1. The cyanide sensor prototype: A) the front, left-hand view of the sensor; B) the response for no exposure; and C) the flashing response for exposure.

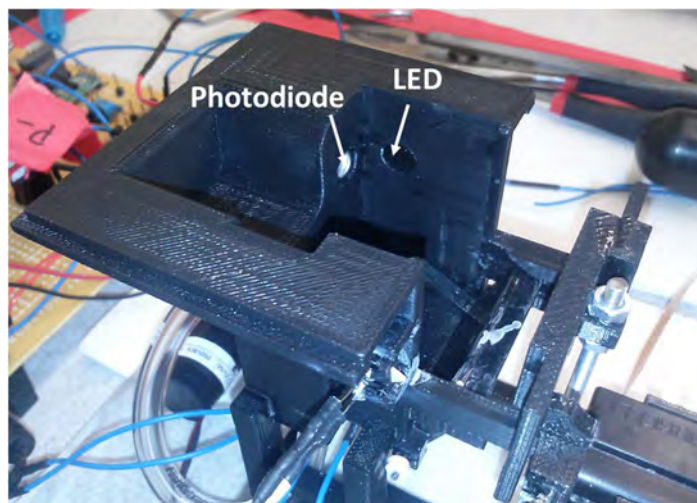


Figure II.3.2. Optical configuration of the miniature sensor cartridge chamber.

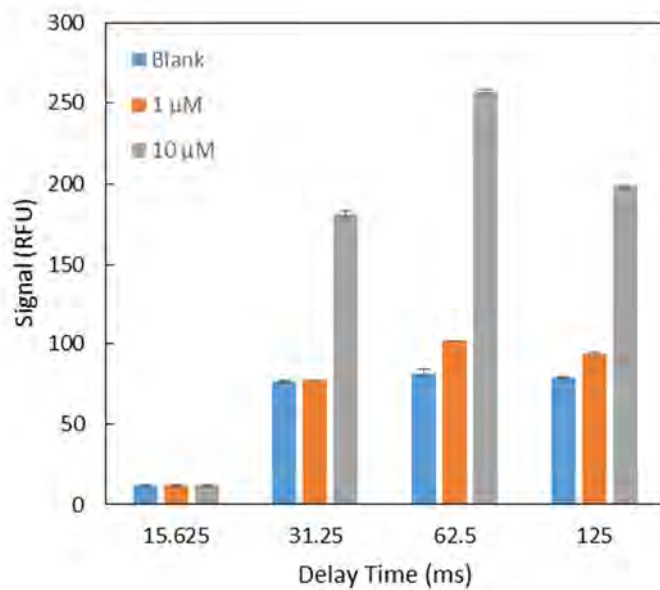


Figure II.3.3. Time delay for sample excitation and A/D sampling and conversion.

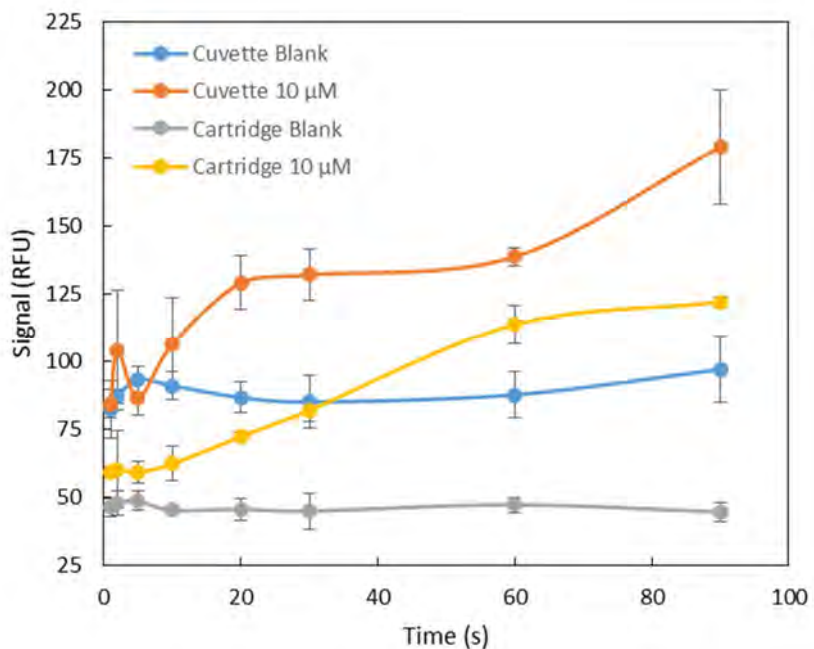


Figure II.3.4. Short-term reaction rate for the production of the NDA-Taurine-CN complex.

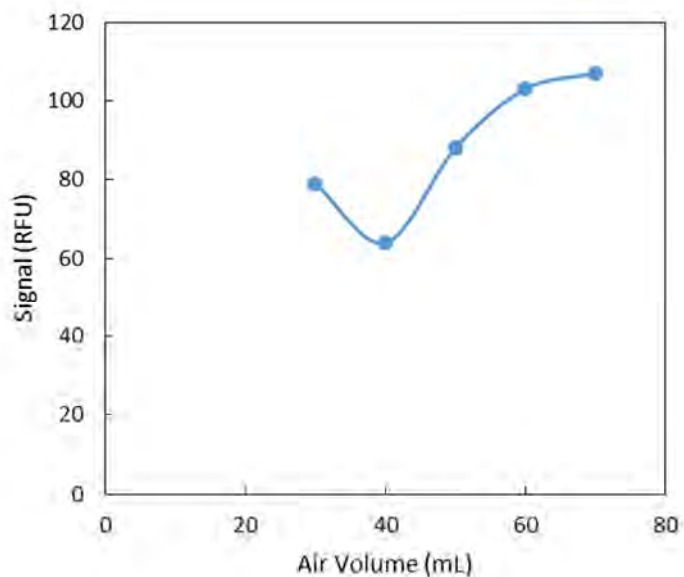


Figure II.3.5. Air volume optimization for the transfer of HCN gas-containing headspace from the sample chamber to the capture chamber.

II.3.2.5. Sensor Circuit Design for Prototype

The sensor casing was designed in our laboratory and manufactured by Falcon Plastics using their fused deposition modeling (FDM) Printing Technology (i.e., rapid prototyping or 3D printing). The current sensor has a base for mounting all components, a cartridge and detector holder (mounted to the base and holds the microdiffusion cartridge and USB2000+ Spectrometer), and a cover which houses the display and is secured in place to the base. The circuitry consists of a Microchip Explorer 16 PIC development board joined to an Electronic Assembly display development board, and a Firgelli linear actuator control board. The sensor (Figure II.3.6A) was programmed and can differentiate between below threshold (display reads “No Exposure” seen in Figure II.3.6B) and above threshold (display flashes “Exposure Detected” seen in Figure II.3.6C) concentrations of cyanide. The threshold for exposure was set at 15 μM cyanide in whole blood. The circuit design, implementation, and programming were performed at Midwest Micro-Tek and in our laboratory. For laboratory testing, further programming is needed to create an administrator screen such that numerical data can be obtained from the sensor and analyzed. The current sensor is portable, but still bulky measuring 28.5 x 19.5 x 15 cm (l x w x h) taking up $\sim 8300 \text{ cm}^3$. The use of bulky components such as the 50 mm linear actuator, the large development circuit board, and the USB2000+ Spectrometer makes the sensor much larger than necessary. We identified smaller components and have designed a photodiode-based spectrophotometer to replace the larger components in order to miniaturize the sensor and increase instrument

portability. These changes were incorporated into a new circuit design, which was built in lab. The new circuit design is centered around the same Microchip Explorer 16 PIC development board joined to an Electronic Assembly display development board in order to manipulate the coding that currently exists. The code for the display screens (altered and new) and the microcontroller code to navigate through the screens were written. The coding and communication programming for all the additional peripheral components (i.e., linear actuator, pressure pump, etc.) and the microcontroller unit were developed. A custom circuit board was designed and a sensor casing were designed in our laboratory and manufactured by the electrical engineers at Midwest Micro-Tek and the printing technicians at Falcon Plastics, respectively. The miniature sensor has increased portability and measures 19.6 x 13.2 x 9.5 cm (l x w x h) taking up $\sim 2500 \text{ cm}^3$, which is $\sim 1/3$ the size of the original cyanide sensor (for comparison see Figure II.3.6A). Lastly, the coding for the miniature sensor is $\sim 95\%$ complete; some coding for displaying detector signals as numerical values is underway.

II.3.2.6. Investigation of Loss of Cyanide Recovery

Initial cyanide recovery data that led to the side-by-side cyanide capture apparatus, indicated $\geq 80\%$ recovery. While using the cartridge, only 5% recovery was being observed. The initial thought was that the cyanide was being lost to the atmosphere due to the high flow rate of 0.211 L/min. To test this hypothesis, the cartridge was mimicked using 1 cm cuvettes cut to designated

dimensions. The experimental setup consisted of three consecutive chambers, the sample chamber (1 cm cuvette cut 33 mm tall) was joined to the capture chamber (1 cm cuvette cut 13 mm tall) which was joined to the air outlet chamber, see Figure II.3.7 for the schematic. The chambers were joined using 0.010 I.D. Tygon tubing pushed over varying lengths of 18 ga stainless steel tubing that was puncturing polypropylene push cap. The caps on the sample and air outlet chambers had one additional hole for either an inlet for air introduction or outlet for air after cyanide capture. The 100 μL (50 μM NaCN) sample was placed in the sample chamber, acidified (300 μL of 1 M H_2SO_4), then 60 mL of air was forced through the capture chamber and bubbled through the solution in the air outlet chamber, which both contained 200 μL of 0.1 M NaOH. For fluorometric analysis of the sample chamber, 200 μL of 8M base was added to neutralize the acid and trap any cyanide that was still present, then 100 μL of the resulting solution was reacted with 200 μL of each capture solution reagent, 0.1 M NaOH, 0.5 mM NDA, and 12.5 mM taurine. For fluorometric analysis of the capture and air outlet chambers, 200 μL of each, 0.5 mM NDA, and 12.5 mM taurine, were added to each chamber. Fluorometric analysis was performed using the miniature sensor. The sample, capture, and air outlet chambers were found to contain 8.4, 4.4, and 1.2% of the cyanide available in the original 100 μL sample, respectively. This experiment indicates that 86% of the available cyanide is not being transferred from the sample chamber to the capture chamber. The cyanide may be interacting with or adhering to the materials that the cyanide capture apparatus is made of or could possibly be contained in the

headspace of the sample chamber due to the small volume (60 mL) of air being used to transfer the HCN gas. This data also indicates that there is minuscule loss of HCN to the atmosphere so the use of bubbling through the capture solution could aid in the increase of cyanide recovery.

II.3.2.7. Attempts to Increase Cyanide Recovery

In an attempt to increase the cyanide recovery for the side-by-side cyanide capture apparatus, various parameters were tested (i.e., chamber size, air volume, chamber size, etc.). The experimental setup consisted of the sample chamber (1 cm cuvette cut 16.5 or 33 mm tall) was joined to the capture chamber (1 cm cuvette cut 13 mm tall), see Figure II.3.8 for the schematic. The chambers were joined using 0.010 I.D. Tygon tubing pushed over varying lengths of 18 ga stainless steel tubing that was puncturing polypropylene push cap. The caps on the sample and capture chambers had one additional hole for either an inlet for air introduction or outlet for air after cyanide capture. In the capture chamber the piece of 18 ga stainless steel inlet (from the sample chamber) was submerged (to allow bubbling) into the 200 μL of 0.1 M NaOH present. The 100 μL (50 μM NaCN) sample was placed in the sample chamber, acidified (300 μL of 1 M H_2SO_4), then 60/120 mL of air was bubbled through the 200 μL of 0.1 M NaOH in the capture chamber. The sample chamber was tested with and without bubbling, and one set of samples were tested using a smaller sample chamber size (with bubbling only). For fluorometric analysis of the capture chamber, 200 μL of each, 0.5 mM NDA, and 12.5 mM taurine, were added and fluorometric

analysis was performed using the miniature sensor. When no bubbling was used in the sample chamber the cyanide recovery for 60 and 120 mL of air were 5 and 18%. When bubbling was employed and 120 mL of air was introduced in to the sample chamber, the 32 mm sample chamber produced a cyanide recovery of 44% while the use of the 16.5 mm sample chamber produced a cyanide recovery of 79%. This data indicates that the HCN gas is likely accumulating at the surface of the solution in the sample chamber and only a small amount is being swept into the air and being transferred to the capture chamber. The use of a smaller volume sample chamber, larger volume of air and bubbling the sample solution aid in the increased recovery of cyanide. This may be an issue since all these experiments were carried out using aqueous samples rather than blood as the sample matrix.

II.3.2.8. Blood as a Sample Matrix

Compared to aqueous solutions, blood is a very complex matrix and may not interact in the same manner. Experiments to determine if blood diluted with H_2SO_4 will exhibit similar bubbling pattern as aqueous solutions were performed. Water (400 μL), rabbit whole blood (20, 50, and 100 μL) and 0.01 M NaOH (100 μL , cyanide is typically made up in this) were placed in a 20 mm tall 1 cm cuvette, 300 μL of H_2SO_4 was added to blood or 0.01 M NaOH samples, and capped. The cap was joined to an empty capture chamber to assess solution transfer. The air inlet needle was submerged into the sample solution and 60 mL of air was introduced as fast as possible to mimic the sensors pressure pump.

The water sample had medium bubbles (~6 mm in diameter) that popped at the top of the chamber, and ~10 μL of solution was transferred within the introduction of the full 60 mL of air. For all sample volumes of blood, there were medium bubbles (also ~6 mm in diameter) that did not pop at the top of the chamber and ~20 μL solution was transferred within the introduction of only 15 mL of air. The 0.01 M NaOH sample had large bubbles (8-10 mm in diameter) that popped half way up the chamber and no solution was transferred within the introduction of the full 60 mL of air. The data indicates that when using blood as the sample matrix, bubbling is not plausible for the side-by-side cyanide capture apparatus because it causes sample solution to transfer from the sample chamber to the capture chamber.

II.3.2.9. Air Inlet Rearrangement

The use of blood as a sample matrix makes the use of bubbling through the sample solution impractical. Since the HCN gas is believed to be concentrated near the surface of the sample solution, it may be possible to increase cyanide recovery by adjusting the placement of the air inlet tube. A 20 mm tall sample chamber with an air inlet positioned 6 mm high (1 mm higher than the sample solution level) (see Figure II.3.9) was made for these experiments. Since there was no bubbling with this setup it was elected that aqueous samples would be used for the assessment of cyanide recovery. The 100 μL (10 μM NaCN) sample was placed in the sample chamber, acidified (300 μL of 1 M H_2SO_4), then 120 mL of air was bubbled through 200 μL of 0.1 M

NaOH in the capture chamber. The sample chamber was tested with and without bubbling, and one set of samples were tested using a smaller sample chamber size (with bubbling only). For fluorometric analysis of the capture chamber, 200 μ L of each, 0.5 mM NDA, and 12.5 mM taurine, were added and fluorometric analysis was performed using the miniature sensor. The new placement of the air inlet produced 31% cyanide recovery with 15.9% RSD. This indicates that increased recovery without bubbling through the sample solution is possible and confirms that HCN gas is located near the surface of the sample solution within the sample chamber. These design changes may yield higher cyanide recovery and precision once they are incorporated in the bubble cartridge.

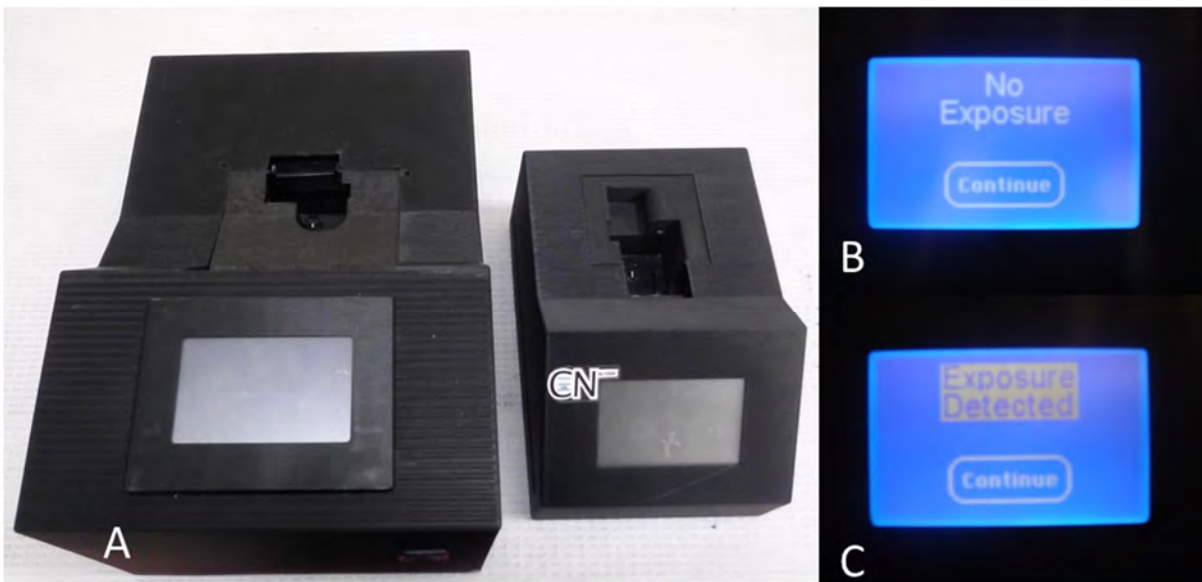


Figure II.3.6. The cyanide sensor prototypes: A) the front, top view of the both the original sensor and the miniature sensor; B) the response for no exposure; and C) the flashing response for exposure.

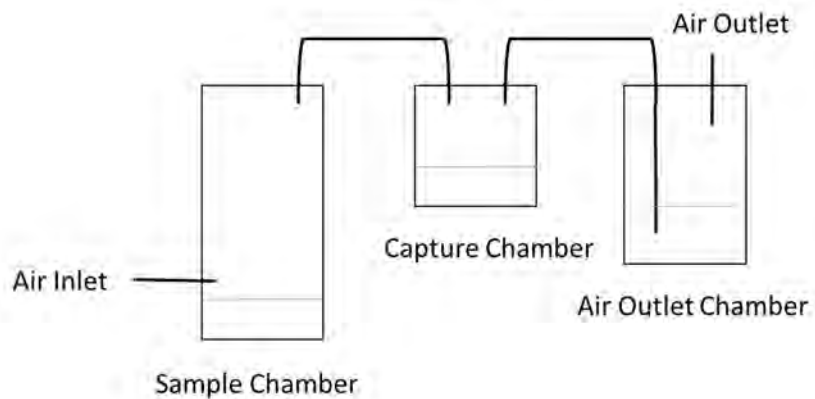


Figure II.3.7. Experimental configuration for determination of the location of HCN gas within the side-by-side cyanide capture apparatus.

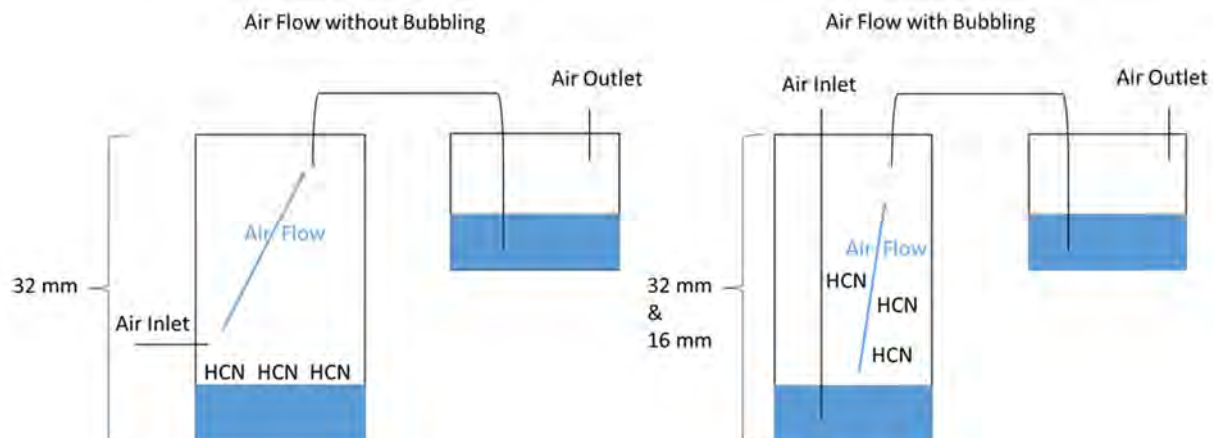


Figure II.3.8. Schematic for the experimental configurations used in the attempt to increase cyanide recovery.

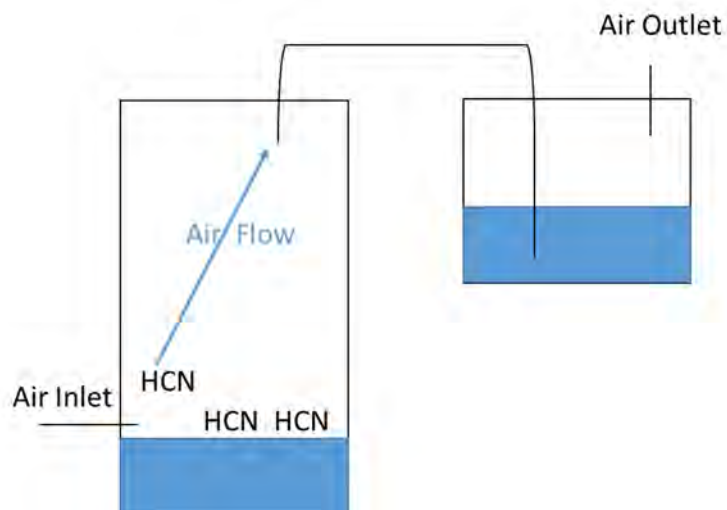


Figure II.3.9. Schematic for the experimental configurations used in the rearrangement of the air inlet.

II.3.3. CONCLUSION

A smaller, more portable miniaturized sensor was manufactured by teamwork between our laboratory, the electrical engineers at Midwest Micro-Tek and the print technicians at Falcon Plastics. Initially it was thought that loss of HCN gas to the atmosphere was the cause of poor cyanide recovery, but data indicates that HCN gas was not being transferred from the sample chamber to the capture chamber. The use of a smaller volume sample chamber, larger volume of air and bubbling the sample solution aid in the increased recovery of cyanide up to 79%. Experiments using blood as the sample matrix indicate that bubbling is not plausible for the side-by-side cyanide capture apparatus because it causes sample solution to transfer to the capture chamber; however, the rearrangement of the air inlet indicates that increased recovery without bubbling through the sample solution is possible and confirms that HCN gas is located near the surface of the sample solution within the sample chamber. This new information is currently being applied to design modifications for the bubble cartridge.

SECTION II
EVALUATE NOVEL MARKERS OF CYANIDE EXPOSURE TO DETERMINE
THE MOST APPROPRIATE CYANIDE EXPOSURE MARKER

CHAPTER 4
ANALYSIS OF CYANIDE AND THIOCYANATE BY GC-MS

Raj K. Bhandari and Brian A. Logue

II.4. The effort for this portion of the report was published as a peer-reviewed manuscript, which is attached as Appendix II.

CHAPTER 5

TOXICOKINETICS OF CYANIDE, THIOCYANATE AND ATCA BY GC-MS

Raj K. Bhandari and Brian A. Logue

II.5. The effort for this portion of the report was published as a peer-reviewed manuscript, which is attached as Appendix III.

CHAPTER 6
SIMULTANEOUS DETERMINATION OF CYANIDE AND THIOCYANATE BY
LC-MS-MS

Raj K. Bhandari and Brian A. Logue

II.6. The effort for this portion of the report was published as a peer-reviewed manuscript, which is attached as Appendix IV.

CHAPTER 7

DETERMINATION OF THE CYANIDE ADDUCT OF GLUTATHIONE BY HIGH PERFORMANCE LIQUID CHROMATOGRAPHY

Wenhui Zhou, Robert P. Oda and Brian A. Logue

II.7.1. INTRODUCTION

Glutathione (GSH) is the primary intra-cellular reducing agent, and is active in many metabolic processes, including the detoxification of xenobiotics and removal of peroxides¹. In maintaining the oxidative state of the cell, glutathione reduces disulfides to thiols, while becoming oxidized to the glutathione homo-disulfide (or glutathiol, GSSG). Although intra-cellular levels of glutathione may range from 1-10 mM, the extra-cellular levels are low^{1,2}. Within blood, most of the glutathione is contained within the erythrocytes, where it may reach mM concentrations²⁻⁴. However, circulating extra-cellular GSSG concentrations may be as high as 200 μ M in plasma, while glutathione levels are in the 2-5 μ M range²⁻⁴. The detoxification of cyanide with GSH or GSSG may be a first-line defense against cyanide intoxication, as studies have demonstrated a reduced toxicity of cyanide in glutathione and glutathione-disulfide-pretreated mice⁵. Although the mechanism of toxic reduction is unknown, it is possible that the reaction of cyanide with circulating GSH or GSSG might reduce the availability of cyanide to produce cellular toxicity.

Protein-bound thiocyanate ion was released from serum proteins following reaction with cyanide^{6,7}, which demonstrated that the disulfide bond would react

with cyanide under alkaline conditions. GSSG might react with cyanide, since it contains a reactive disulfide bond. Therefore, we investigated the possibility of a non-enzymatic cyanide reaction with GSH and/or GSSG, producing adduct(s) which might serve as a bio-marker(s) for cyanide exposure.

Cyanamide was used to create a possible GS-CN adduct analogous to the reaction by Nagasawa⁸ to create ATCA from cysteine for use as a standard compound. Possible adducts from the reaction of GSH with cyanamide are depicted in Figure II.7.1. Possible products from the reaction of GSSG with CN are depicted in Figure II.7.2. It should be noted that the initial products from the reaction depicted in Figure II.7.2 could undergo the rearrangements pictured in Figure II.6-1.

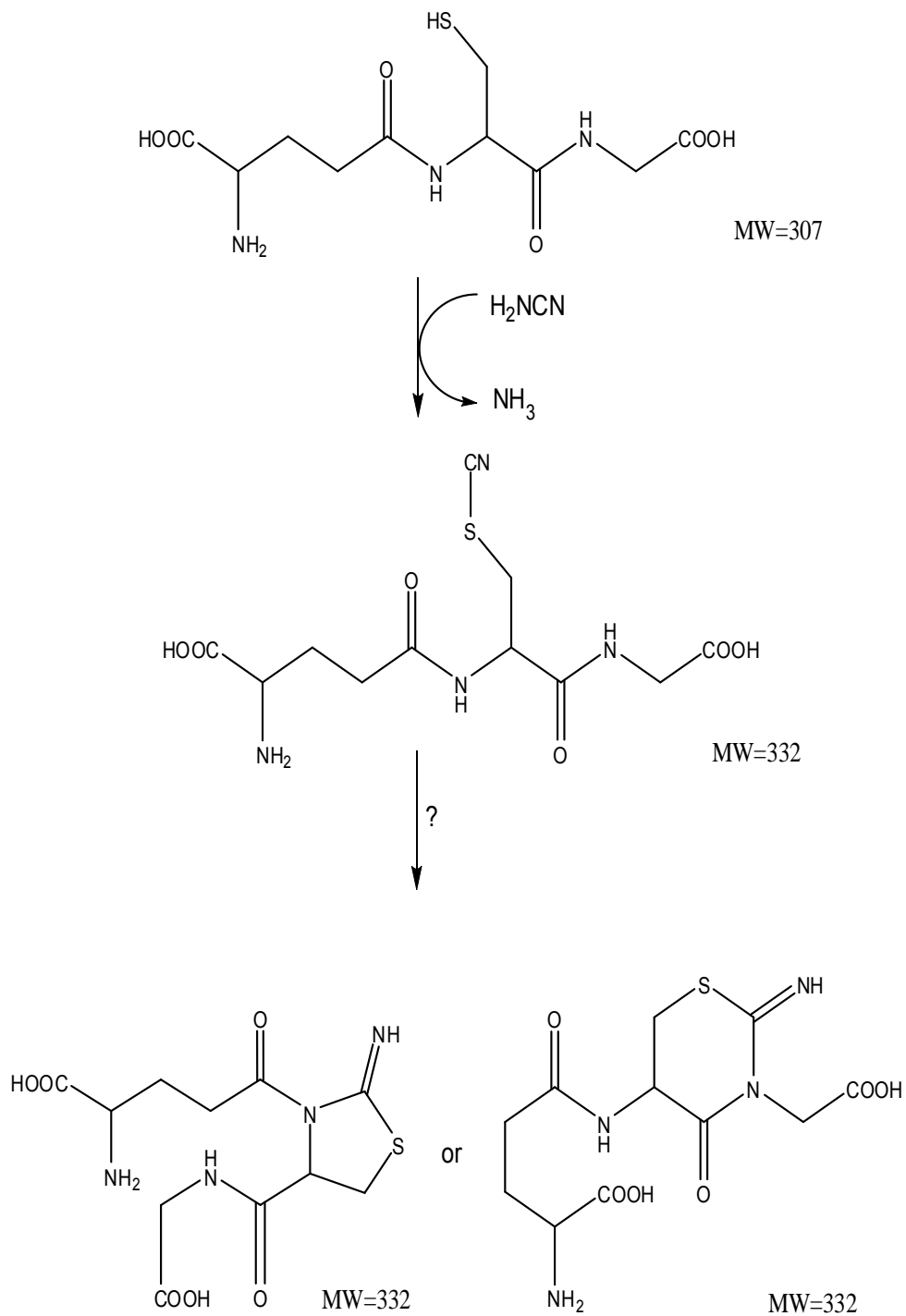


Figure II.7.1. Reaction scheme for the condensation of cyanamide with reduced glutathione (GSH), and possible rearrangement of the initial product.

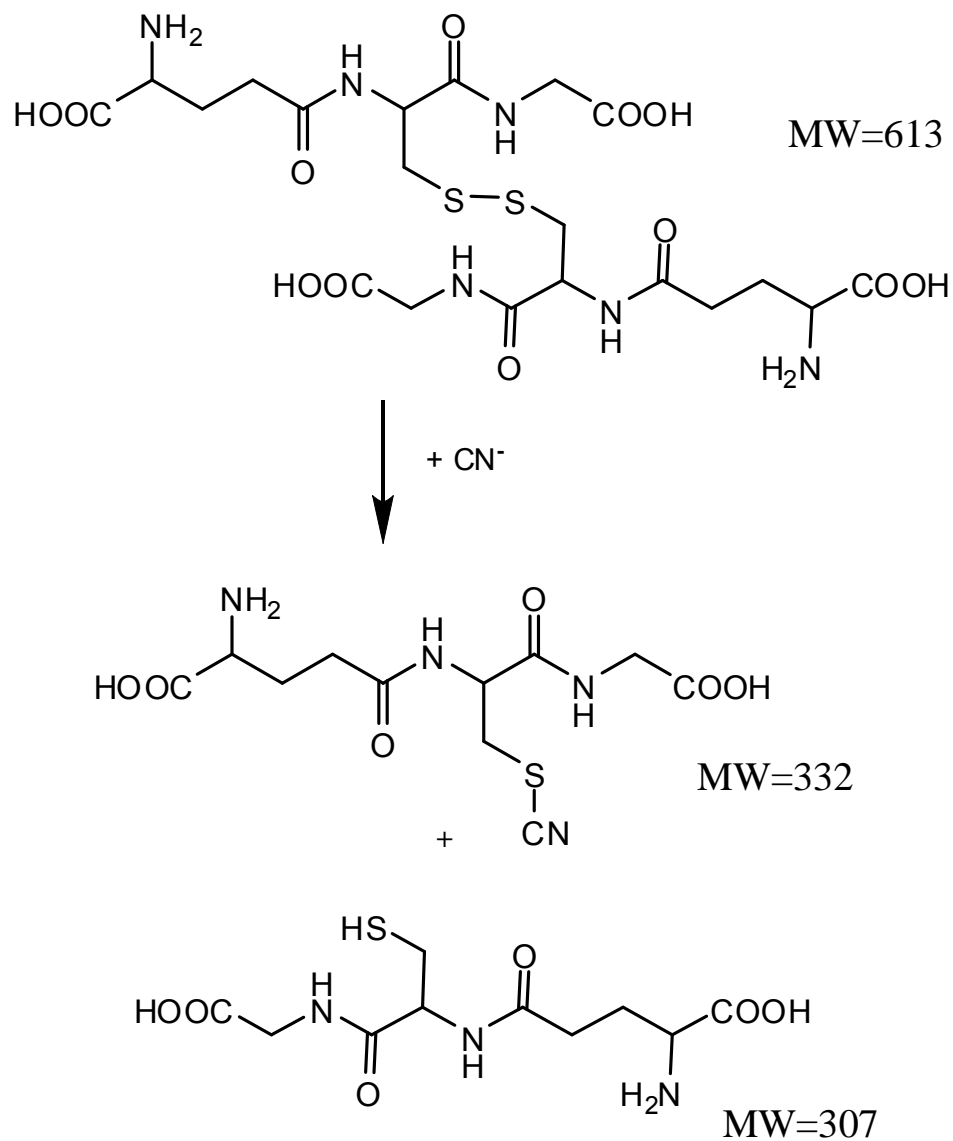


Figure II.7.2. Reaction scheme for the addition of cyanide to oxidized glutathione (GSSG), and possible products.

II.7.2 EXPERIMENTAL

II.7.2.1. Reagents and Materials

All reagents were at least reagent grade. Sodium cyanide (NaCN), sodium phosphate salts, and methanol (HPLC grade) were purchased from Fisher Scientific (Fair Lawn, NJ, USA). Glutathione (reduced, GSH), ammonium formate, Ellman's reagent, ninhydrin, monobromobimane, and sodium carbonate were products of Sigma-Aldrich (St. Louis, MO, USA). LC/MS grade formic acid and Ellman's Reagent [5, 5'-dithio-bis(2-nitrobenzoic acid)] were purchased from Thermo Scientific (Rockford, IL, USA). Reverse-osmosis water was passed through a polishing unit and had a conductivity of 18.2 M-Ω.

Oxidized glutathione (glutathiol, GSSG) was produced by taking 50 mL of a 1 mM solution of glutathione (GSH) in 0.1 M phosphate buffer, pH 7.27, and adding 5 mL 3% hydrogen peroxide drop-wise over several minutes with constant stirring. The lack of reaction with Ellman's reagent was used as an indicator for completion of the reaction. In later experiments, GSH (61.4 mg; 200 μmoles) was dissolved in 10 ml water to which 15 drops of 3% hydrogen peroxide was added over several minutes with constant stirring.

II.7.2.2. Preparation of Cyanide Adducts

Aliquots (1 mL of 1 mM solution) of glutathione or glutathione-disulfide in phosphate buffer (pH 7.27), borate buffer (pH 8.3 and 9.25), or sodium carbonate (pH 10.6) were mixed with a cyanide solution in a 1:10 or 1:20 molar ratio to present a ten-fold molar excess ratio of cyanide to sulfur and allowed to react for up to 2 hours at room temperature. The reaction mixtures were assayed for the presence of CN-adducts by HPLC. The high salt content of the reaction mixture

required the samples to be diluted or dialyzed to reduce the salt load onto the HPLC column. This was best accomplished by “float dialysis”, in which an aliquot (200 μ L) of reaction mixture was placed on a 0.2 μ 47 mm nylon filtration membrane (Millipore, Billerica, MA, USA) floated on about 20 mL deionized water. After 10 minutes of dialysis, the residual sample was filtered through a 0.2 μ filter into a 150 μ L insert in a 2 mL vial, capped, and analyzed by HPLC.

II.7.2.3. Assay of Free Thiols with Ellman’s Reagent^{9,10}

An aliquot of sample (0.1 mL) was mixed with an equal volume of 0.1 M sodium phosphate buffer, pH 7.27, to which was added 0.1 mL Ellman’s reagent (5, 5’-dithio-bis(2-nitrobenzoic acid), 1.7 mM) in phosphate buffer, pH 7.27, containing 0.1 mM EDTA. The yellow product was analyzed at 412 nm.

II.7.2.4. Mass Spectrum Analysis

A Thermoquest Finnigan LCQ Deca Mass Spectrometer (Thermo Scientific, Waltham, MA, USA) with a turbo electrospray ion source was used to screen the GSH –cyanamide and GSSG-cyanide reactions for products. A 5500 Q-Trap (Applied Biosystems, Foster City, CA, USA) was used for MS-MS analysis of presumed cyano-adducts. Samples from the original reaction mixtures and various extraction solutions and collected fractions were analyzed as appropriate.

II.7.2.4. Reverse Phase-High Performance Liquid Chromatography

HPLC analysis was performed on an Agilent 1200 HPLC system consisting of a quaternary pump, auto-sampler, vacuum degasser, multi-wavelength detector, and a fluorescence detector (Agilent Technologies, Wilmington, DE, USA). A Discovery Bio wide pore C-18 column (150 mm x 2.1 mm i.d.; 5- μ m particle size; Supelco, Bellefonte, PA, USA) and a mobile phase containing 0.1% formic acid (Pierce Chemical, Rockford, IL, USA) was used to separate the analytes at a flow rate of 0.350 mL/min. 0.1% Formic acid in methanol was used in a gradient elution from 10% (held for 1 min), linearly increased to 100% over 21 min and held for 2 min. The mobile phase was then linearly converted to the initial composition over 2 min and subsequently held for 2 min prior to the next analysis. A multi-wavelength detector monitored absorbance at 270 nm.

In later experiments a Zorbax C-18 column (150 mm x 4.6 mm i.d.; 5- μ m particle size; Agilent Technologies, Wilmington, DE, USA) with a flow rate of 1.00 mL/min were used. The mobile phase consisted of 1 mM ammonium formate, pH 4.0 in water. Methanol containing 1 mM ammonium formate, pH 4.0 was used in a gradient elution from 0% (held for 3 min), linearly increased to 20% over 2 min, to 40% over 10 min, to 100% over 2 min and held at 100% for 3 min. The mobile phase was then linearly decreased to the initial composition over 2 min and subsequently held for 3 min prior to the next analysis. A multi-wavelength detector monitored absorbance at 230 and/or 270 nm. Fluorescent monobromo-bimane reaction products were excited at 390 nm and the emission was monitored at 490 nm.

II.7.3. RESULTS AND DISCUSSION

A glutathione adduct was prepared by a procedure adapted from Nagasawa⁸. GSH (3 g) was mixed with 0.822 g sodium bicarbonate, and placed under a nitrogen atmosphere. Cyanamide (0.4287 g) and water (15 mL) were added to dissolve the mixture, and the mixture refluxed for five hours. The reaction mixture was separated by using a normal-phase silica gravity column. Different chloroform/methanol solvent mixtures from 0% to 100% were used to elute compounds from the column. A mobile phase of 50% methanol in water was then used to elute highly polar compounds. Fractions were collected and analyzed by HPLC. The peak at 3.87 minutes in the chromatogram of the reaction mixture in Figure 2.6-3 was presumed to be main product from the GSH-cyanamide reaction. Fraction 8, from 20% methanol in chloroform, has a single peak which eluted at 1.72 minutes (Figure II.7.3), was presumed to be unreacted GSH by comparison of the retention time of an aqueous solution of GSH. Fractions 11 and 12 were eluted by 50% methanol in water. Fraction 11 displayed two early eluting peaks (Figure II.7.4) which appear to be GSSG and GSH by comparison of retention times with standard aqueous solutions. Fraction 12 has two peaks. The first peak (1.5 min) elutes with the retention time of GSSG. The second peak which eluted at 3.37 minutes may be the desired product (Figure II.7.4), but did elute prior to the peak identified in the reaction mixture. More work must be done to identify this peak.

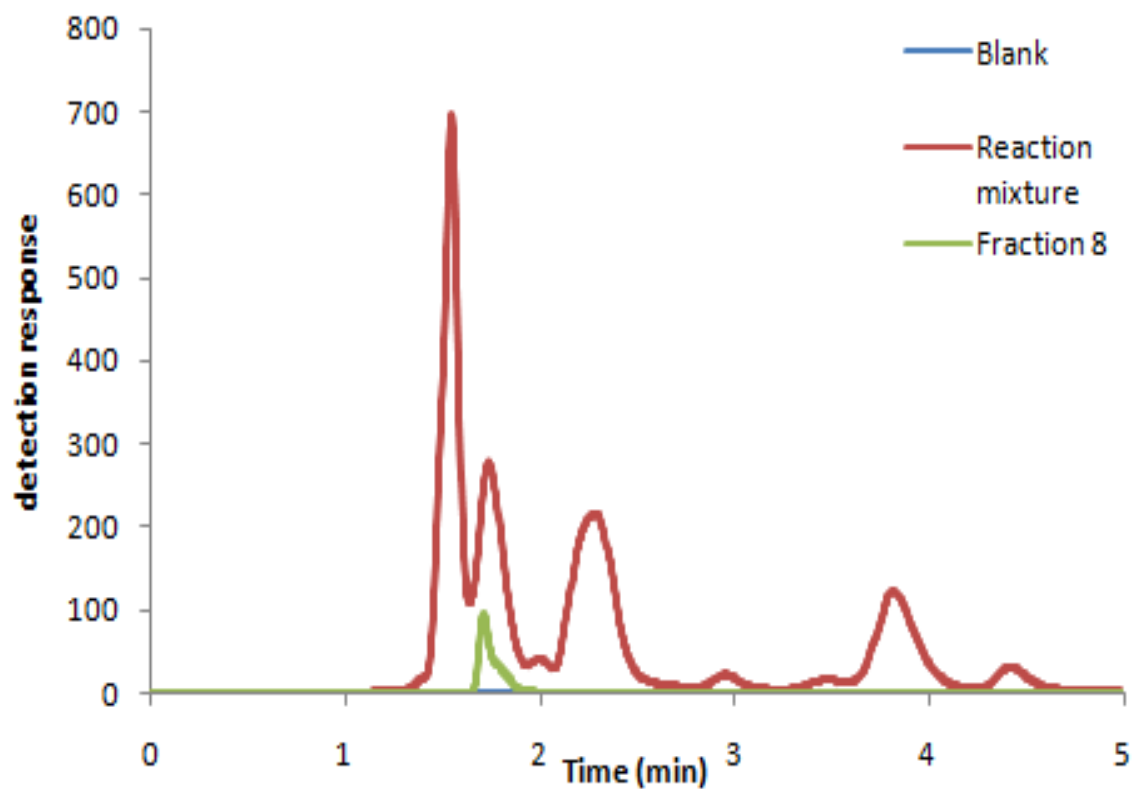


Figure II.7.3. Overlaid HPLC chromatograms of a reagent blank, the reaction mixture from GSH and cyanamide, and Fraction 8 eluted by 20% methanol in chloroform solvent from the silica column. HPLC conditions: Column: Zorbax C-18, 4.6 X 150 mm; Mobile phase: 1mM ammonium formate in water/ methanol; Flow: 1.0 mL/ min; Detection: 270 nm.

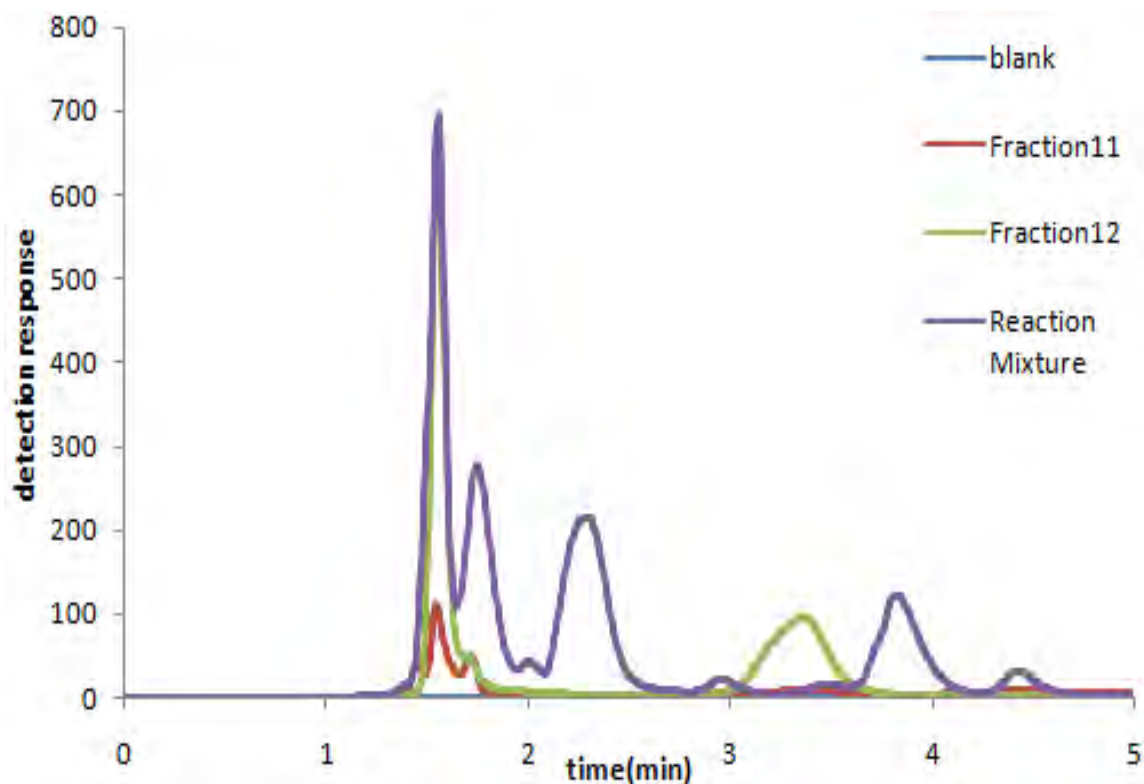


Figure II.7.4. Overlaid HPLC chromatograms of a reagent blank, the reaction mixture from GSH and cyanamide, and Fractions 11 and 22 eluted by 50% methanol in water from the silica column. HPLC conditions: Column: Zorbax C-18, 4.6 X 150 mm; Mobile phase: ammonium formate (1 mM) in water/methanol; Flow: 1.0 mL/ min; Detection: 270 nm.

Swine plasma (1 mL) was spiked with 6.5 mg KCN and 65.2 mg KCN separately to form 10 mM and 100 mM cyanide-spiked plasma. After a couple of hours' reaction, acetone (3 mL) was added to the sample to precipitate proteins, and the sample kept at 4°C for 15 minutes. The samples were then centrifuged for 10 minutes at 10,000 RPM ($9.6 \times 10^3 \times g$), the supernatants were removed and dried with N₂ gas, and reconstituted with 2 mL buffer (1% NH₄OOC in water). Samples were then filtered (0.22 μm PVDF filter) and analyzed by LC-MS.

High-performance liquid chromatography-tandem mass spectrometry (UHPLC-MS) conducted on a Shimadzu HPLC (LC-20AD, Shimadzu Corp., Kyoto, JPN) coupled to an AB Sciex Q-Trap 5500 MS (Applied Biosystems, Foster City, CA, USA). Samples were separated by reversed-phase (RP) chromatography using a Phenomenex Synergi 4 μ RP Max column (2.0 x 50mm) (Phenomenex, Torrance, CA, USA) as a stationary phase. A mobile phase containing 1 mM ammonium formate (Sigma-Aldrich, St. Louis, MO, USA) was used at a flow rate of 0.25 mL/min. Methanol was used in a gradient elution from 0% (held for 3 min), linearly increased to 20% over 2 min, to 40% over 10 min, to 100% over 2 min and held at 100% for 3 min. The mobile phase was then linearly decreased to the initial composition over 2 min and subsequently held for 3 min prior to the next analysis.

Mass spectrometry was used to assess if there was a putative product in the reaction mixture. The spectra of the reaction mixtures of cyanide-spiked plasma (10 μ M and 100 μ M) are pictured in Figure II.7.5. The peaks at m/z = 213 and 279 from the 100 mM reaction mixture were higher than those in the 10 mM solution and are presumed to be the putative product(s) of the reaction. Further analysis is required to confirm the identity of these peaks. Possible structures for the presumed products are depicted in Figure II.7.6a and b.

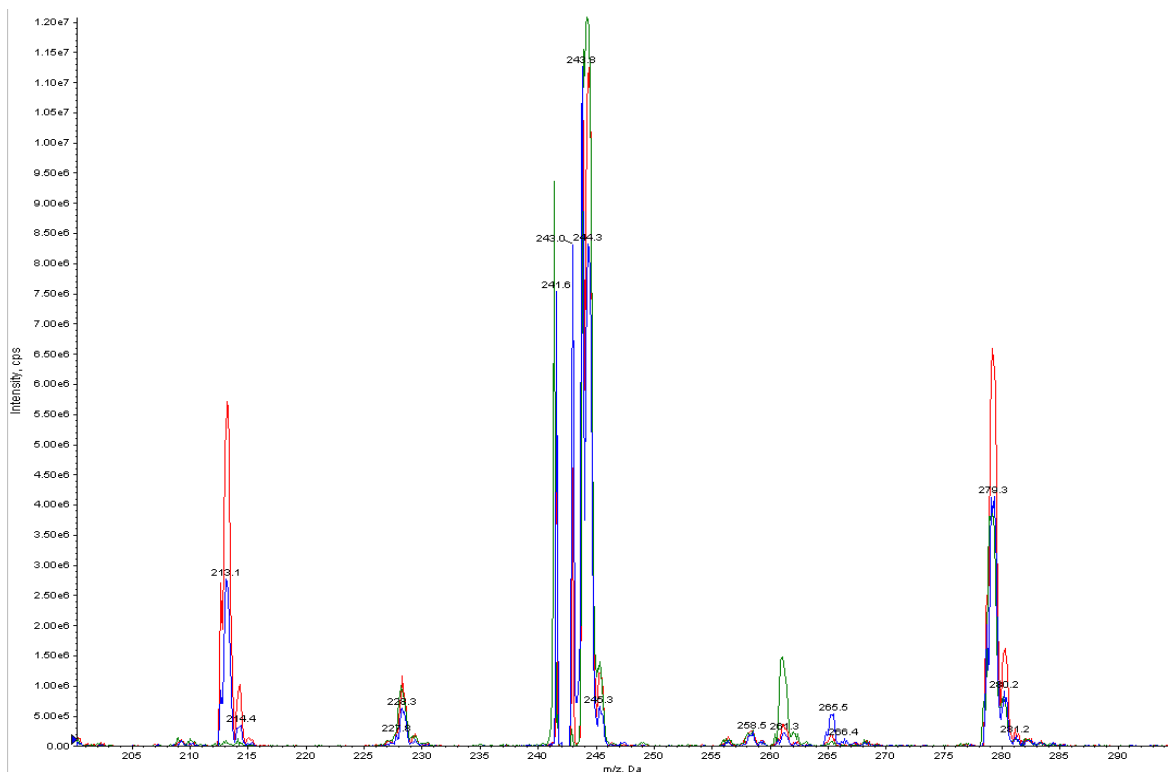


Figure II.7.5. Overlaid mass spectra of the cyanide-spiked plasma reaction mixtures. 100 mM CN (red) , 10 mM CN (green) and a plasma blank (blue). AB Sciex Q-trap 5500 Mass Spectrometer in positive ion mode with an ESI source.

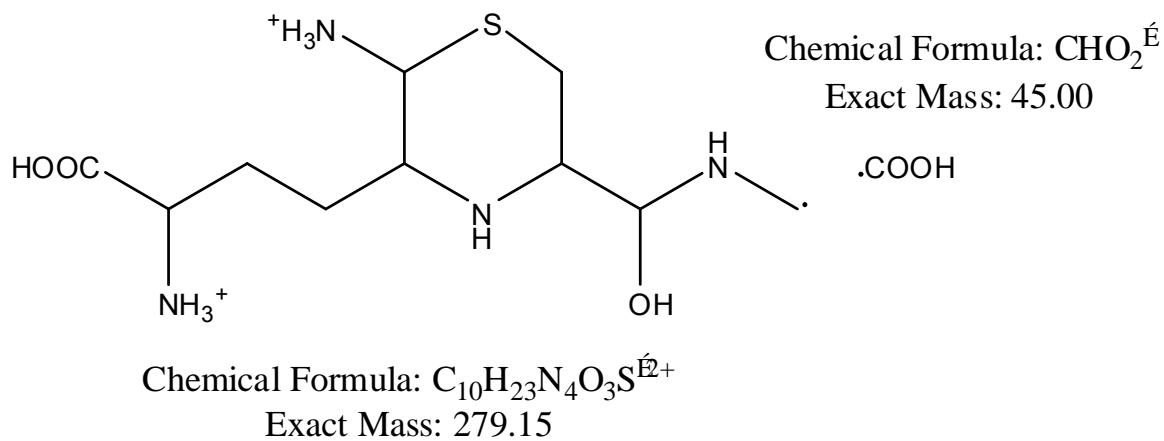


Figure II.7.6a. Possible structure for the observed $m/z = 279$ fragment.

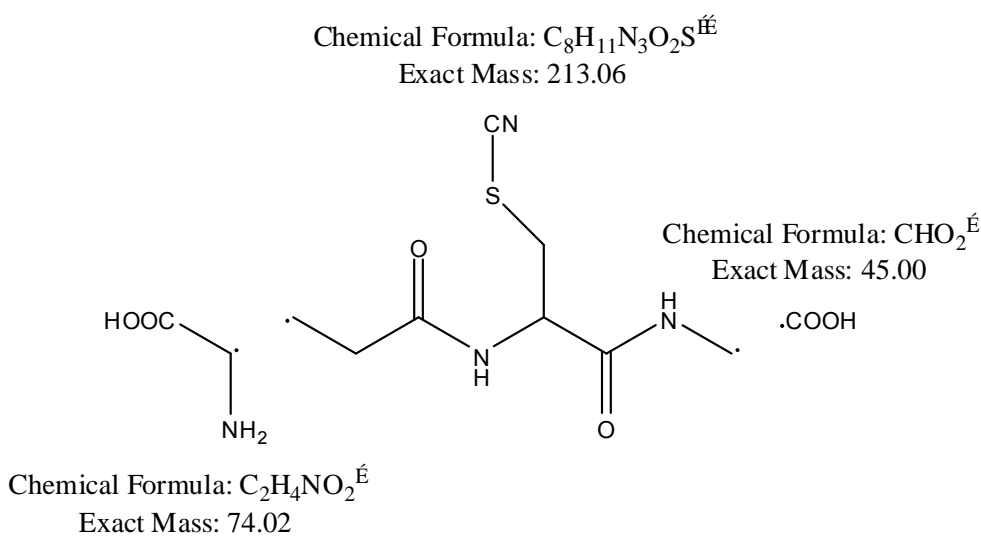
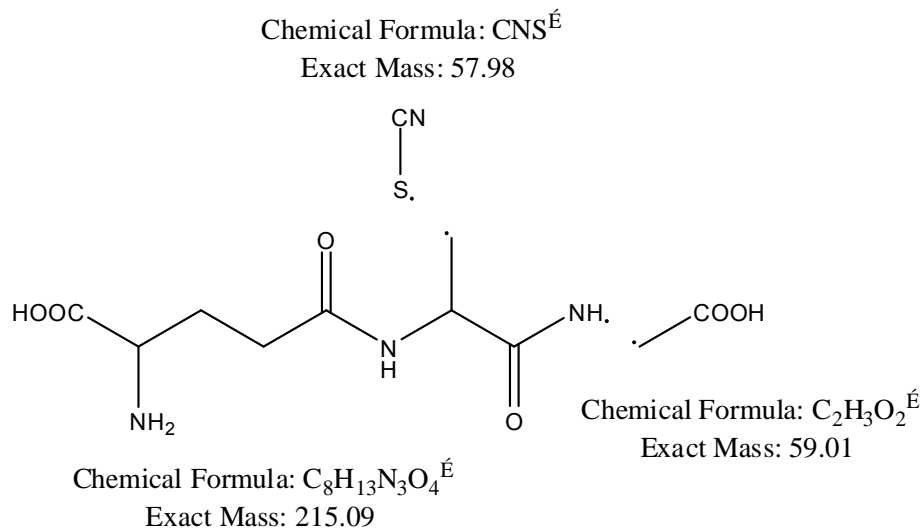


Figure II.7.6b. Possible structures for the $m/z = 213$ fragment.

For the determination of the glutathione-cyanide adducts, there are numerous by-products from the reaction which make the interpretation of structural and chromatographic information difficult. The use of the LC-MS should enable the putative adducts to be resolved and characterized.

The person most responsible for this project has left the laboratory. Therefore, minimal progress was made on this project.

II.7.4. REFERENCES

1. Meister, A. and Anderson, M. E., 1983. Glutathione. *Ann Rev Biochem* 52, 711-760.
2. Jose, C. J., Jacob, R. H., Gardner, G. E., Pethick, D. W., and Liu, S. M., 2010. Selenium supplementation and increased muscle glutathione concentration do not improve the color stability of lamb meat. *J Agric Food Sci* 58 (12), 7389-7393.
3. Serru, V., Baudin, B., Ziegler, F., David, J-P., Cals, M-J., Vaubourdolle, M., and Mario, N., 2001. Quantification of reduced and oxidized glutathione in whole blood samples by capillary electrophoresis. *Clin Chem* 47 (7), 1321-1324.
4. Michelet, F., Gueguen, R., Leroy, P., Wellman, M., Nicolas, A., and Siest, G., 1995. Blood and plasma glutathione measured in healthy subjects by HPLC: Relation to sex, aging, biological variables, and life habits. *Clin Chem* 41 (10), 1509-1517.
5. Hatch, R. C., Laflamme, D. P., and Jain, A. V., 1990. Effects of various known and potential cyanide antagonists and a glutathione depletor on acute toxicity of cyanide in mice. *Vet Human Toxicol* 32 (1), 9-16.
6. Catsimpoolas, N., and Wood, J. L., 1964. The reaction of cyanide with bovine serum albumin. *J Biol Chem* 239 (12), 4132-4137.
7. Youso, S. L., Rockwood, G. A., Lee, J. P., Logue, B. A., 2010. Determination of cyanide exposure by gas chromatography-mass spectrometry analysis of cyanide-exposed plasma proteins. *Anal Chim Acta* 677 (1), 24-28.

8. Nagasawa, H. T., Cummings, S. E., and Baskin, S. I., 2004. The structure of "ITCA", a urinary metabolite of cyanide. *Organic Prep and Proc Int'l* 36 (2), 178-182.

9. Ellman, G. L., 1959. Tissue sulfhydryl groups. *Arch Biochem Biophys* 82, 70-77.

10. Habeeb, A. F. S. A., 1972. Reaction of protein sulfhydryl groups with Ellman's reagent. *Methods Enzymol.* 25 (part B), 457-464.

CHAPTER 8

DETERMINATION OF THE CYANIDE METABOLITE A-KETOGLUTARATE CYANOHYDRIN BY LIQUID CHROMATOGRAPHY TANDEM MASS- SPECTROMETRY

Brendan L. Mitchell and Brian A. Logue

II.8. The effort for this portion of the report was published as a peer-reviewed manuscript, which is attached as Appendix V.

CHAPTER 9

TOXICOKINETIC PROFILE OF α -KETOGLUTARATE CYANOHYDRIN

Brendan L. Mitchell and Brian A. Logue

II.9. The effort for this portion of the report was published as a peer-reviewed manuscript, which is attached as Appendix VI.

SECTION III
DEVELOP ASSAYS FOR CYANIDE THERAPEUTICS
CHAPTER 10
DETERMINATION OF DMTS BY GC-MS
Wenhui Zhou and Brian A. Logue

III.10.1. INTRODUCTION

Cyanide has figured as a prominent human toxicant over the years as a result of both accidental and intentional exposure. Within the purview of cyanide detoxification, DMTS was shown to effectively function as sulfur donor for rhodanese *in vitro*¹. In addition, it was demonstrated that DMTS by itself is a very efficient converter of cyanide to thiocyanate²⁻⁴. Compared with current cyanide therapeutics which have some disadvantages, DMTS is safer and more efficient with good lipophilicity. So far, there is no published method to determine DMTS in biofluids. Thus, an assay for detecting DMTS in blood would be necessary should it become useful as a therapeutic agent.

III.10.2. EXPERIMENTAL

All reagents were at least reagent grade. Methanol (LC-MS grade) was purchased from Fisher Scientific (Fair Lawn, NJ, USA). Reverse-osmosis water was passed through a polishing unit (Lab Pro, Labconco, Kansas City, KS, USA) and had a conductivity of 18.2 MΩ-cm. Dimethyl trisulfide (DMTS) was a product of Sigma-Aldrich (St. Louis, MO, USA). Dimethyl disulfide (DMDS) was a product of Alfa Aesar (Ward Hill, MA, USA).

Analysis was performed by headspace on an Agilent GC-MS system (Agilent Technologies, Wilmington, DE, USA) consisting of a 6890N series gas chromatograph, a 5975 series mass detector, and a Gerstel MPS sampler (Gerstel Inc., Linthicum, MD, USA). A DB5-MS bonded-phase column (30 m x 0.25 mm I.D., 0.25 μ m film thickness; J&W Scientific, Folsom, CA, USA) was used with nitrogen as the carrier gas at a flow rate of 1.0 mL/min and a column head pressure of 10.0 psi. An aliquot (100 μ L) of solution containing DMTS was placed in a 20 mL headspace vial with a Teflon-lined septum. The vial was incubated at 115 $^{\circ}$ C for up to 5 min, before a 100 μ L sample was withdrawn. The auto-sampler injected a 100 μ L headspace sample into the splitless injection port which was held at 120 $^{\circ}$ C. A deactivated, straight-through glass inlet liner packed with about 1 cm of glass wool was used. The GC oven temperature was initially held at 30 $^{\circ}$ C for 2 min, then elevated at a rate of 15 $^{\circ}$ C/min up to 120 $^{\circ}$ C. The gradient was increased to 120 $^{\circ}$ C/min up to 300 $^{\circ}$ C where it was held constant for 1.5 min, before returning to the initial temperature. The injection syringe temperature was 115 $^{\circ}$ C. The GC was interfaced with a mass selective detector with electron ionization. Selective-ion-monitoring (SIM) mode was used, detecting ions with m/z of 79, 94, 111, and 126. DMTS was identified at m/z = 126/111 and DMDS by m/z = 94/79.

In an initial experiment, DMTS was spiked into rabbit plasma. An aliquot of plasma (900 μ L) was spiked with 100 μ L DMTS (in methanol) to make a final concentration of 1 mM. An aliquot (100 μ L) was taken for assay by GC/MS headspace.

III.10.2.1. DMTS Analysis by TDU

An aliquot (100 μ L) of solution containing DMTS was placed in a 20 mL headspace vial with a Teflon-lined septum. The vial was incubated at 115 $^{\circ}$ C for up to 1 min, the septum was punctured using dual needles and nitrogen was delivered through the headspace of the vial. The use of the dual needle configuration enables DMTS to be trapped by a TDU tube filled with adsorptive material (Tenax[®]). A dry purge technique was used to remove water from the TDU tube. The tube was inserted into the TDU injection source and heated from 60 $^{\circ}$ C to 250 $^{\circ}$ C at 720 $^{\circ}$ C/min. The DMTS was desorbed from the adsorptive material and transferred to the GC column using a cooled injection system (CIS) PTV-type inlet, whose initial temperature was set at 30 $^{\circ}$ C. Cooling of the CIS with liquid nitrogen was attempted but found to be unnecessary for DMTS.

For GC, a DB5-ms bonded-phase column (30 m x 0.25 mm I.D., 0.25 μ m film thickness; J&W Scientific, Folsom, CA, USA) was used with nitrogen as the carrier gas at a flow rate of 1.0 mL/min and a column head pressure of 10.0 psi. The GC oven temperature was initially held at 30 $^{\circ}$ C for 1 min, then elevated at a rate of 30 $^{\circ}$ C/min up to 120 $^{\circ}$ C. The gradient was increased at 120 $^{\circ}$ C/min up to 250 $^{\circ}$ C where it was held constant for 1 min, before returning to the initial temperature. The injection syringe temperature was 115 $^{\circ}$ C. The GC was interfaced with a mass selective detector with electron ionization. Selective-ion-monitoring (SIM) mode was used, detecting ions with m/z of 79, 94, 111, and 126. DMTS was identified at m/z = 126/111 and DMDS by m/z = 94/79.

III.10.2.2. Finalized Experimental for DMTS by GC-MS

Analysis was performed by dynamic headspace on an Agilent GC-MS system (Agilent Technologies, Wilmington, DE, USA) consisting of a 6890N series gas chromatograph, a 5975 series mass detector, and a Gerstel MPS sampler (Gerstel Inc., Linthicum, MD, USA). An aliquot (100 μ L) of solution containing DMTS was placed in a 20 mL headspace vial with a Teflon-lined septum. The vial was incubated at 115 $^{\circ}$ C for up to 1 min, the septum was punctured using dual needles and nitrogen is delivered through the headspace of the vial. The use of dual needle system enables to trap the DMTS to a TDU tube filled with adsorptive materials (Tenax[®] TA). A dry purge technique was also applied (5 min) to the TDU tube for water removal. The TDU tube was inserted into the TDU injector and was heated from 60 $^{\circ}$ C to 250 $^{\circ}$ C at 720 $^{\circ}$ C/min. The analytes were desorbed from the Tenax[®] and transferred to the GC/MS system using a cooled injection system (CIS) PTV-type inlet, whose initial temperature was set at -30 $^{\circ}$ C. The sample was injected into the system by heating the cooled injector to 200 $^{\circ}$ C at 12 $^{\circ}$ C/min.

A DB5-MS bonded-phase column (30 m x 0.25 mm I.D., 0.25 μ m film thickness; J&W Scientific, Folsom, CA, USA) was used with nitrogen as the carrier gas at a flow rate of 1.0 mL/min and a column head pressure of 5.6 psi. The GC oven temperature was initially held at 30 $^{\circ}$ C for 2 min, then elevated at a rate of 20 $^{\circ}$ C/min up to 250 $^{\circ}$ C, where it was held constant for 1.0 min, before returning to the initial temperature. The injection syringe temperature was 115 $^{\circ}$ C. The GC was interfaced with a mass selective detector with electron ionization. Selective-ion-monitoring (SIM) mode was used, detecting ions with

m/z of 79, 94, 111, and 126. DMTS was identified at m/z = 126/111 and DMDS by m/z = 94/79.

III.10.3. RESULTS AND DISCUSSION

Water was found to produce the lowest detection limit at 10 μ M (Figure III.10.1). The chromatogram of the DMTS-spiked blood is shown in Figure III.10.2; DMDS and DMTS eluted at 3.94 and 6.98 minutes, respectively, which demonstrates that DMTS can be detected in blood. The ramp rate of the GC oven temperature program was reset at 30 $^{\circ}$ C to reduce the retention time of DMTS. Compared with the same concentration of DMTS in methanol, DMTS was degraded to DMDS in blood as shown in Figure III.10.2. Overall, a simple GC/MS headspace method for the analysis of DMTS from biological fluids was developed; however, further optimization is necessary to obtain a lower detection limit of DMTS.

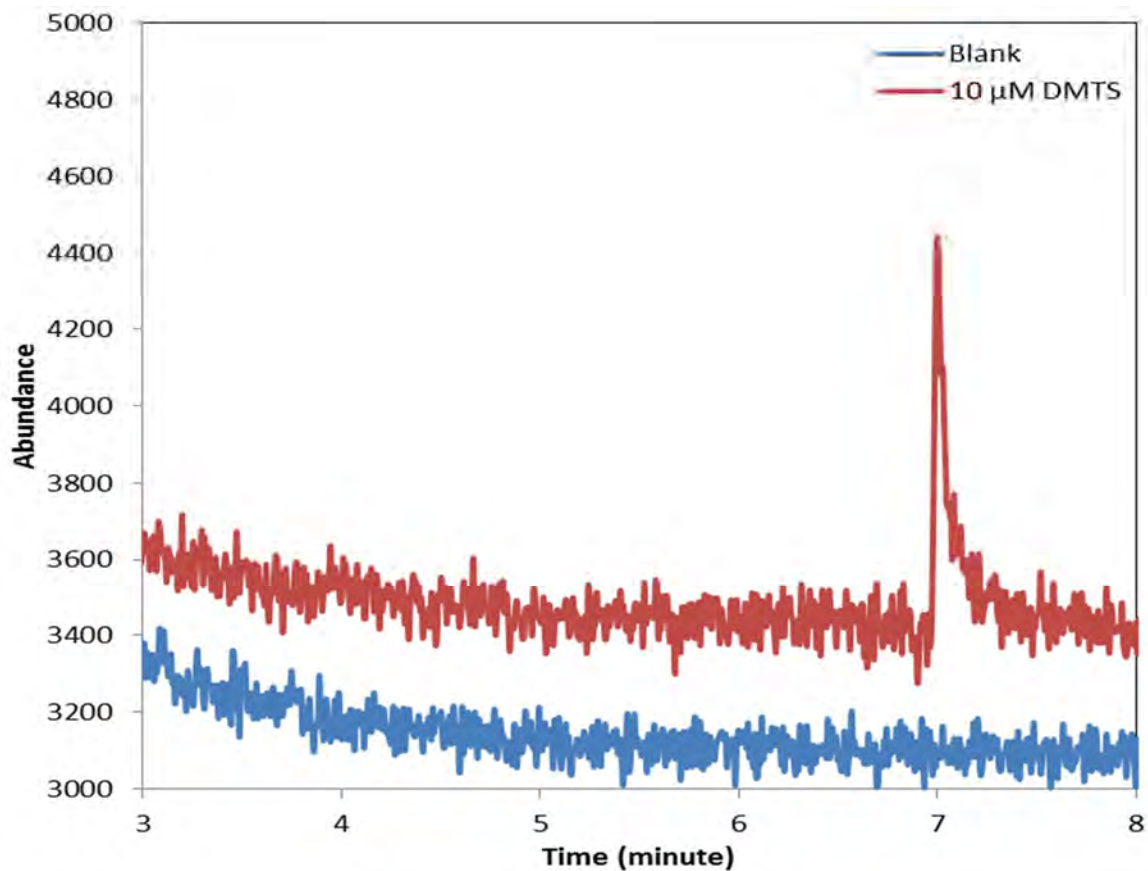


Figure III.10.1. Overlaid chromatograms of 10 μM DMTS (blue) and a methanol blank (red).

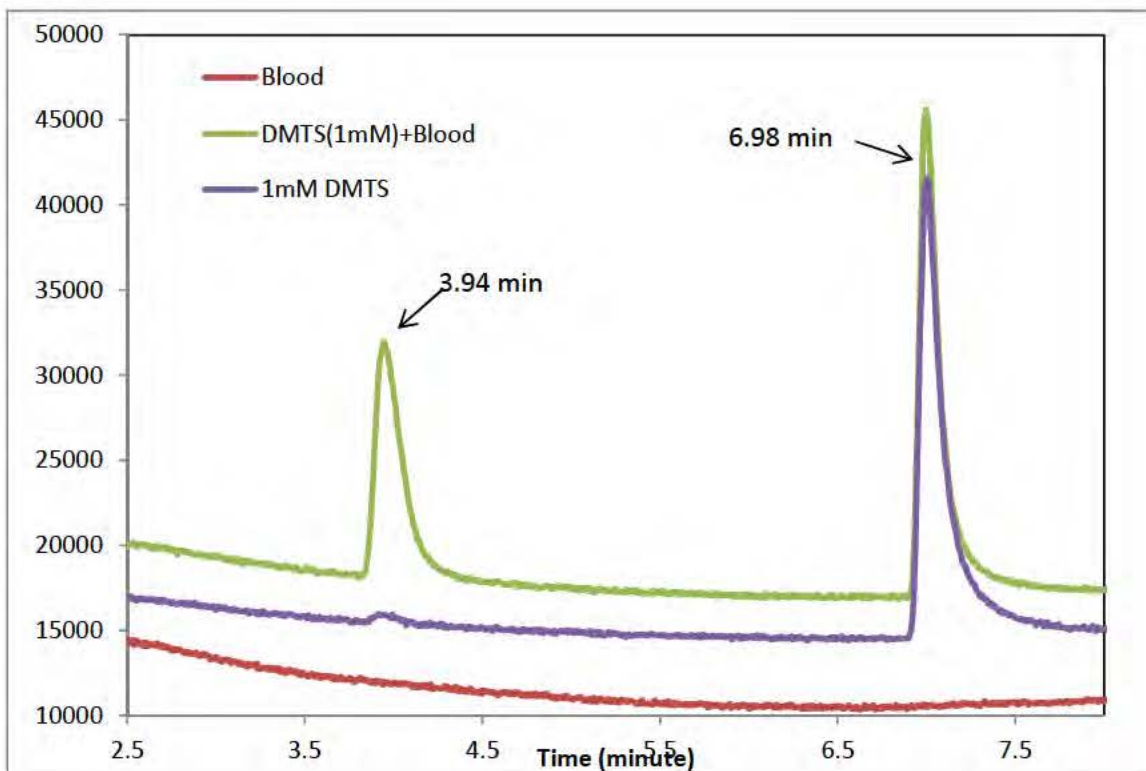


Figure III.10.2. Overlaid chromatograms of 1 mM DMTS (purple), DMTS-spiked blood (green) and a blood blank (red).

III.10.3.1. Optimization of TDU Capture Temperature

The current method shows that DMTS can be detected from aqueous solution with DHS-GC/MS. DMTS eluted at 5.57 minutes was shown in Figure III.10.3. The ramp rate of the GC oven temperature program was reset at 30 °C to reduce the retention time of DMTS. By using the same concentration of DMTS in water (100 µM), an initial CIS temperature at 0° C was found to be the ideal temperature for analyte capture (Figure III.10.4). Overall, a simple DHS/GC/MS

headspace method for the analysis of DMTS was developed; however, further optimization is necessary to obtain a lower detection limit for DMTS.

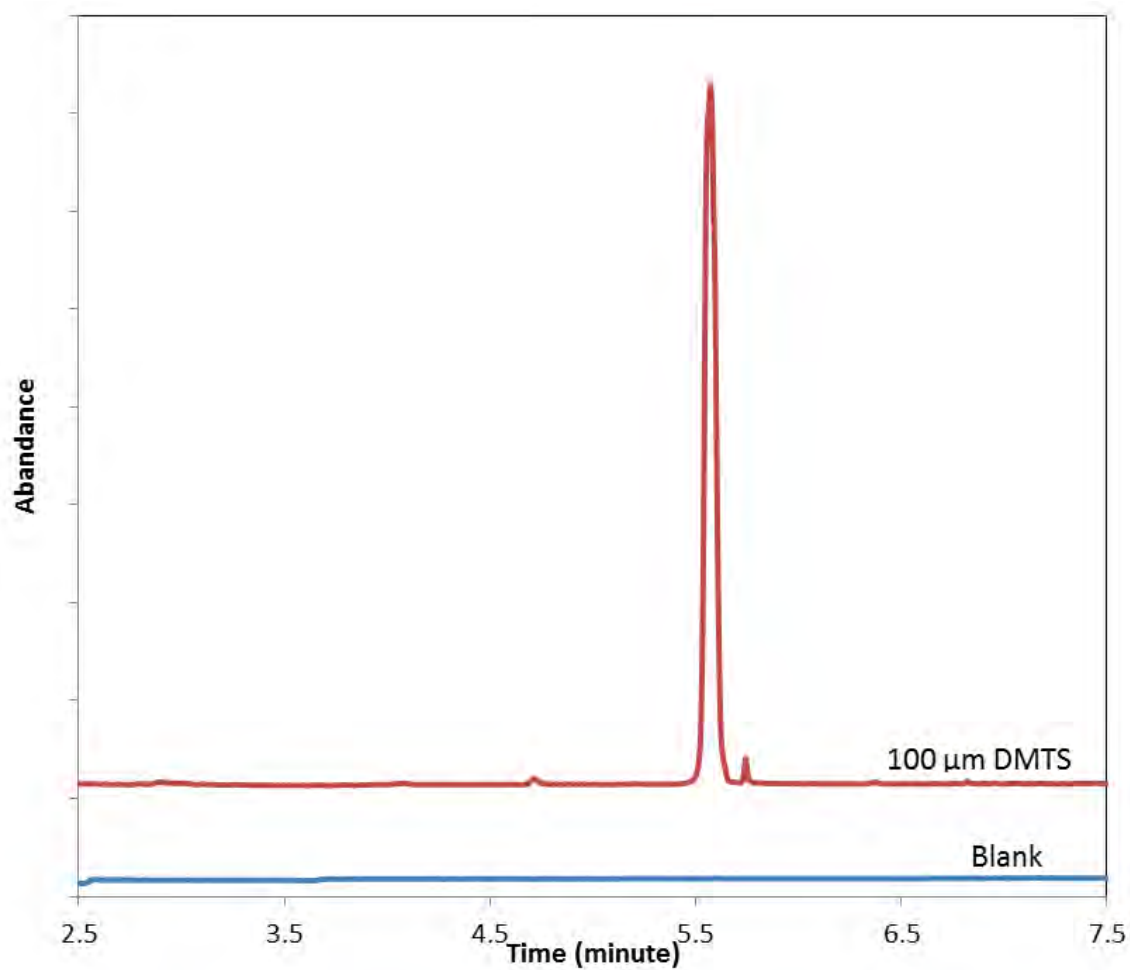


Figure III.10.3. Overlaid chromatograms of 100 μM DMTS (red) and a water blank (blue).

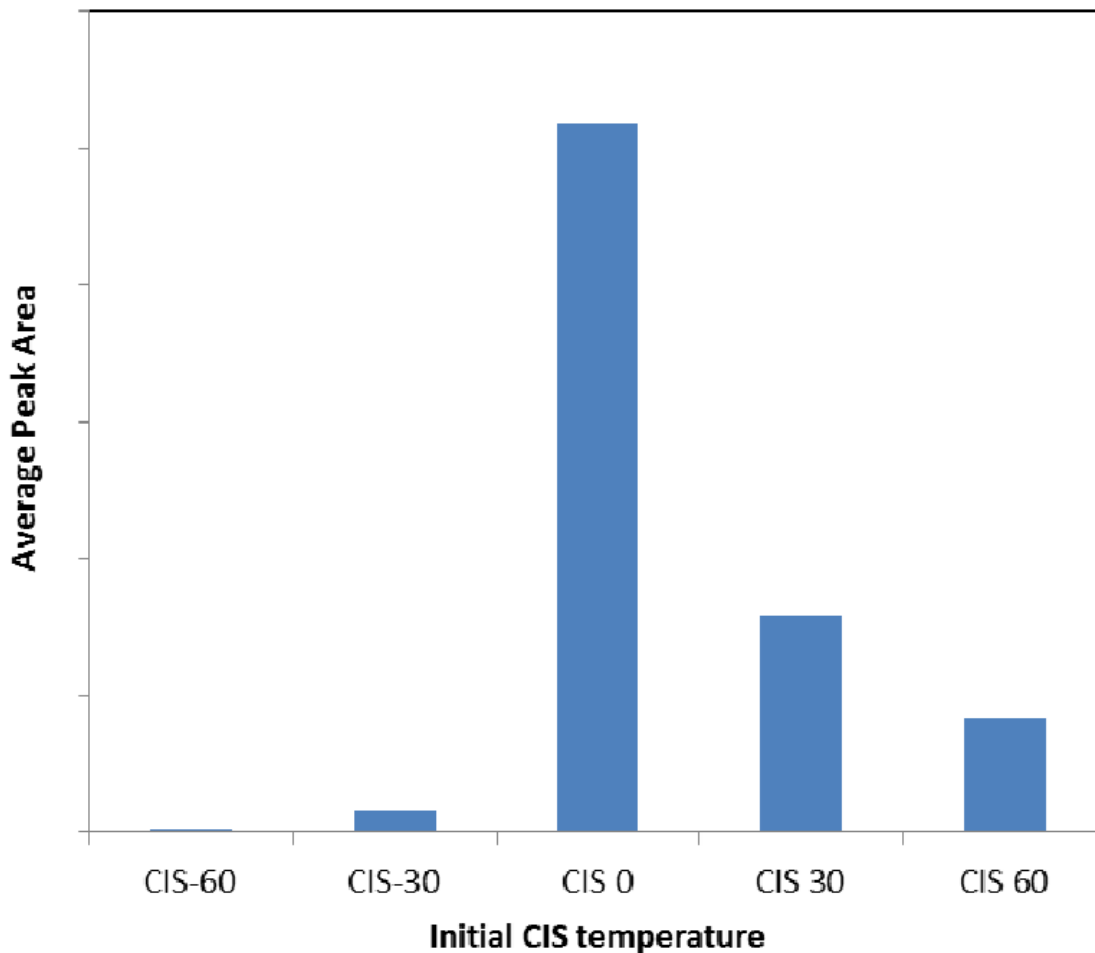


Figure III.10.4. Average peak area of 100 µM DMTS by using different initial CIS temperature.

III.10.3.2. Optimization of parameters for LOD

By evaluating an aqueous DMTS standard multiple times, the ideal parameters for analyte capture (Figures III.10.5 to 7) were an incubation time of 1 minute, a transfer heater temperature at 50 °C, and an agitator temperature of 110 °C. The optimized DHS/GC/MS method produced a detection limit of 0.8 µM in water. The chromatogram of DMTS at its detection limit (0.8 µM) is shown in Figure II.4.2-4; DMTS eluted at 4.66 minutes. The ramp rate of the GC oven temperature program was reset at 30 °C to reduce the retention time of DMTS.

Overall, a simple DHS/GC/MS headspace method for the analysis of DMTS in water was developed.

It was found that either 1 minute or 2 minutes was ideal incubation time for DMTS analysis since they produced bigger average peak area (Figure II.4.2-1). One minute was selected finally to minimize analysis time.

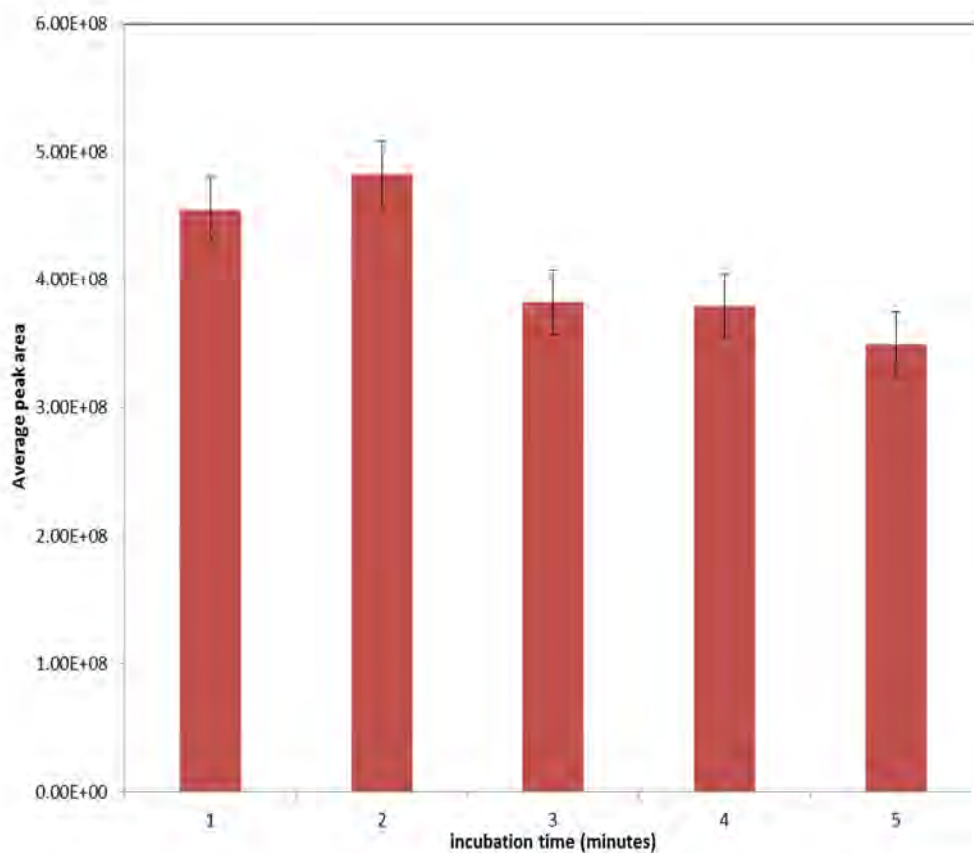


Figure III.10.5. Average peak area of 100 µM DMTS by using different headspace incubation time.

It was found that 50 °C was the ideal transfer heater temperature according to the average peak area (Figure III.10.6).

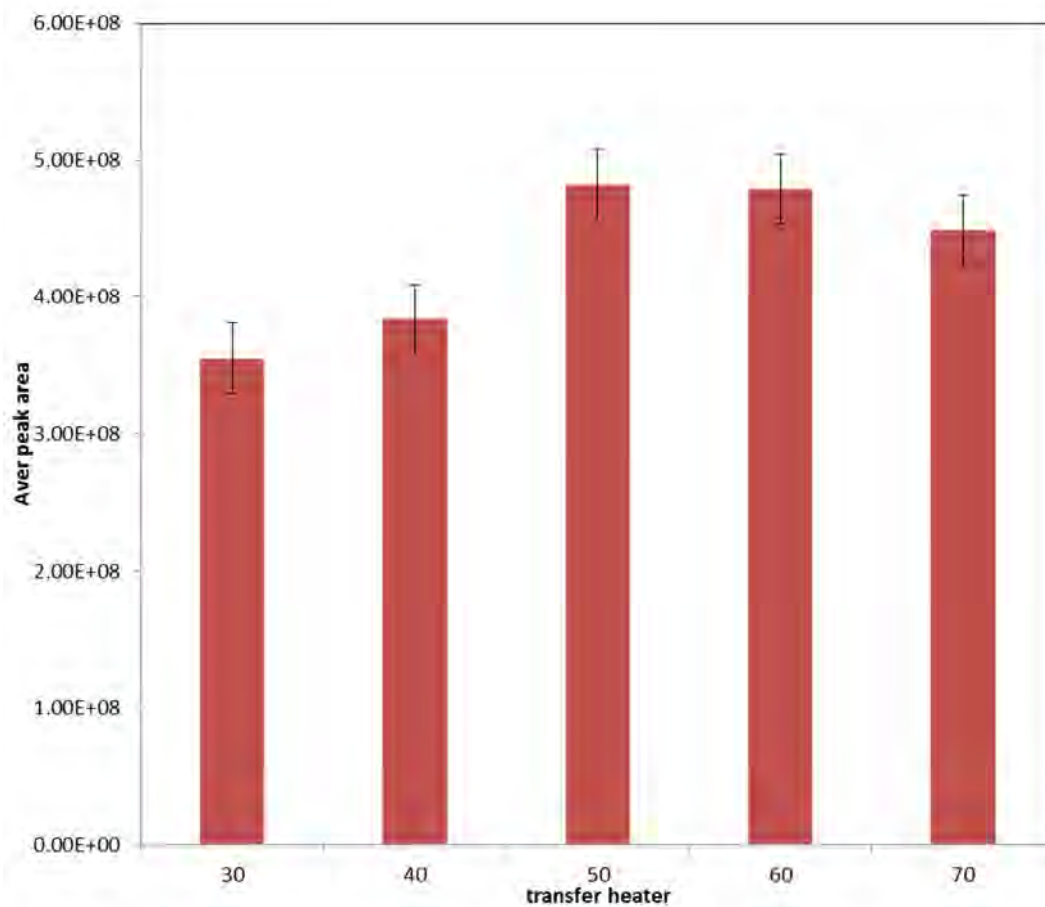


Figure III.10.6. Average peak area of 100 μM DMTS by using different transfer heater temperature of DHS.

It was found that 110 $^{\circ}\text{C}$ was the ideal agitator temperature according to the average peak area (Figure III.10.7).

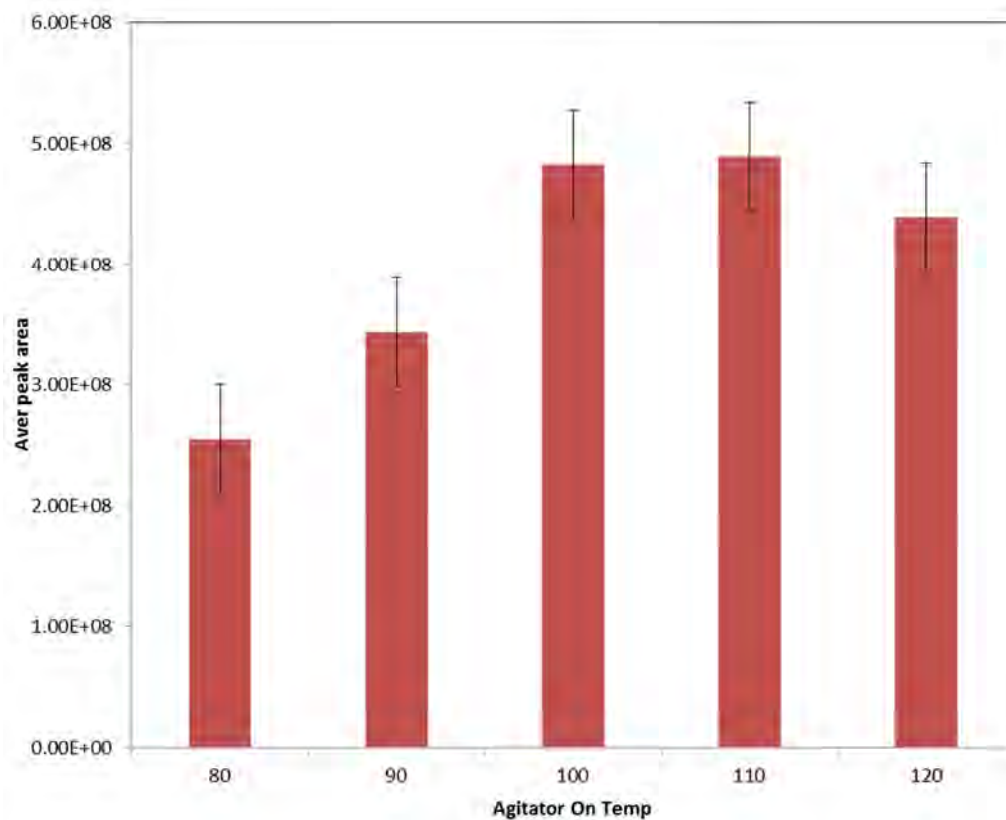


Figure III.10.7. Average peak area of 100 µM DMTS by using different agitator temperature.

It was found that 0.8 µM was the detection of limit of DMTS in water (Figure III.10.8).

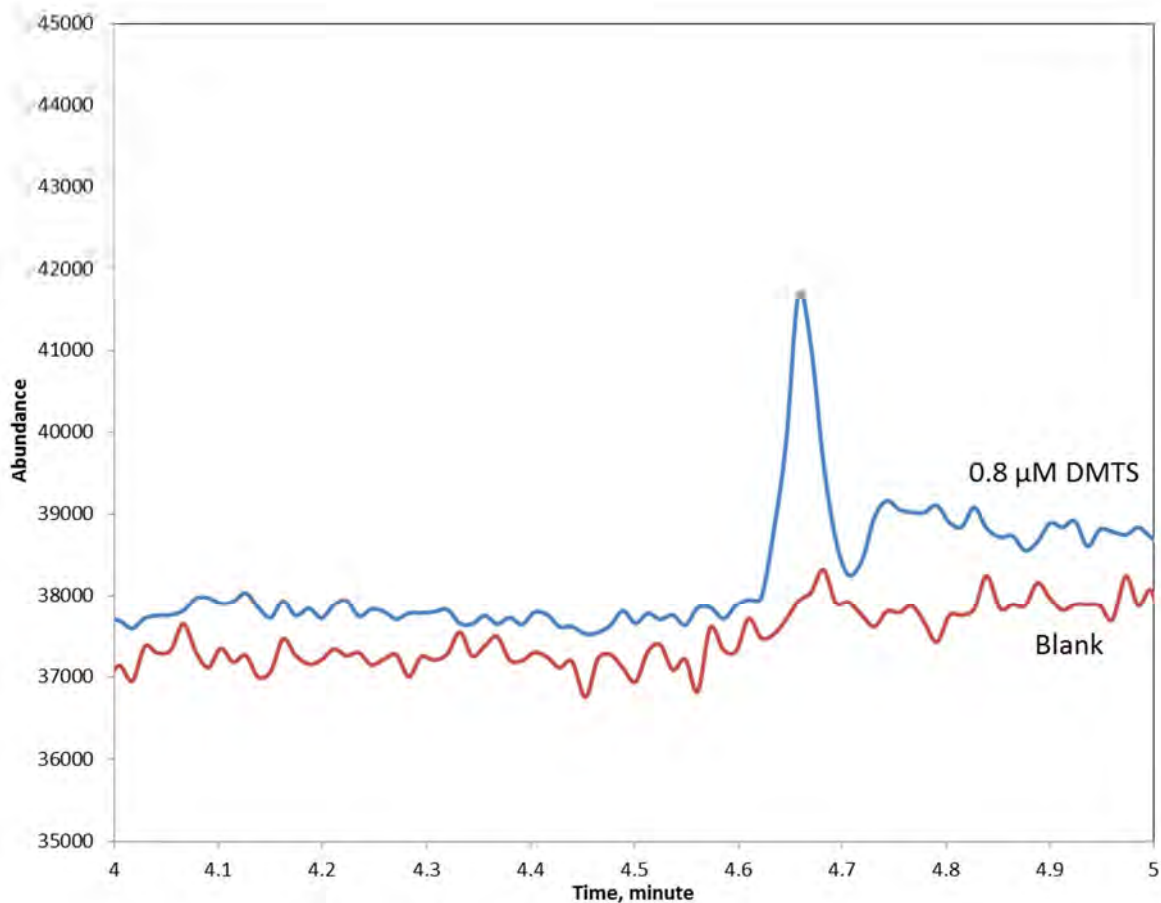


Figure III.10.8. Overlaid chromatograms of 0.8 μM DMTS (blue) and a water blank (red).

III.10.3.3. Determination of DMTS from whole blood

The current method shows that DMTS can be detected by DHS/GC/MS with good sensitivity. The limit of detection from aqueous samples was found to be 0.5 μM (Figure III.10.8). Chromatograms of DMTS-spiked blood are shown in Figure III.10.2; DMTS eluted at 4.45 minutes, and demonstrates that DMTS can be detected from whole blood. By altering the incubation temperature for the headspace analysis, 130 $^{\circ}\text{C}$ was found to be optimal, resulting in the largest peak area for DMTS. The detection limit from whole blood was decreased to 10 μM .

Utilizing the optimized conditions for analysis from whole blood, a concentration curve was found to be non-linear. Therefore, we utilized an isotope-labelled internal standard, DMTS-d₆, to correct for analytical variance. Plotting the peak area ratios of the DMTS divided by the internal standard peak area resulted in a linear concentration range of over two orders of magnitude.

III.10.4 CONCLUSIONS

Overall, a simple DHS/GC/MS headspace method for the analysis of DMTS was developed. Sensitivity of the detection of DMTS is increased by optimizing the DHS/GC-MS method. Detection of limit of DMTS in water is 0.8 µM. The limit of detection from aqueous medium was 0.5 µM. However, the limit of detection from whole blood was much higher at 10 µM. Further optimization may result in a lower detection limit for DMTS from whole blood.

III.10.5. REFERENCES

1. Petrikovics I, Kuzmitcheva G, Budai M, Haines D, Nagy A, Rockwood GA, Way JL (2010) Encapsulated rhodanese with two new sulfur donors in cyanide antagonism. In *XII International Congress of Toxicology*. Barcelona, Spain.
2. Frankenberg L (1980) Enzyme therapy in cyanide poisoning: effect of rhodanese and sulfur compounds. *Arch Toxicol* **45**: 315-323.
3. Iciek M, Wlodek L (2001) Biosynthesis and biological properties of compounds containing highly reactive, reduced sulfane sulfur. *Pol J Pharmacol* **53**: 215-225.
4. Petrikovics I, Pei L, McGuinn W, Cannon E, Way J (1994) Encapsulation of rhodanese and organic thiosulfonates by mouse erythrocytes. *Fund and Appl Toxicol* **23**: 70-75.

CHAPTER 11

DETERMINATION OF DMTS BY LC-MS-MS

Erica Manandhar, Wenhui Zhou, and Brian A. Logue

III.11.1. INTRODUCTION

Cyanide has figured as a prominent human toxicant over the years as a result of both accidental and intentional exposure. Within the purview of cyanide detoxification, DMTS was shown to effectively function as sulfur donor for rhodanese *in vitro*¹. In addition, it was demonstrated that DMTS by itself is a very efficient converter of cyanide to thiocyanate²⁻⁴. Thus, an assay for detecting DMTS would be necessary should it become useful as a therapeutic agent.

The motivation for this project is to develop a high performance liquid chromatography-tandem mass spectrometry (HPLC-MS-MS) method to analyze dimethyl trisulfide (DMTS), a potential novel antidote for cyanide poisoning. Dimethyl trisulfide functions as a sulfur donor converting cyanide to a less toxic thiocyanate. Classical sulfur donor antidotes (i.e., thiosulfate) require the help of a sulfur transferase enzyme, namely rhodanese, to transfer its sulfur to cyanide. However, due to its limited lipophilicity, thiosulfate is not very efficient at reaching the endogenous rhodanese enzyme^{1,2}, which is primarily located in the mitochondria. Unlike the conventional sulfur donors that require sulfur transferase enzymes to catalyze detoxification of cyanide, DMTS is capable of functioning on its own without the need of rhodanese¹⁻³. Currently, there is limited published literature on the analysis of DMTS. Therefore, an analytical

method to detect and analyze DMTS is vital for it to become available as a therapeutic agent for cyanide poisoning.

Initially, DMTS was analyzed as adducts with sodium bromide, and propionic acid. However, due to instability of the adducts formed, these approaches did not lead to reproducible or productive results. Therefore, it was decided that DMTS could be analyzed as a more stable oxidized product formed from the oxidation reaction between hydrogen peroxide and DMTS in presence of acetic acid⁵.

Next, DMTS was oxidized using peroxide in the presence of 8M acetic acid. However, due to practical limitations of the column, the reaction mixture containing concentrated acetic acid and peroxide could not be directly injected into the HPLC system. Upon investigating methods to isolate the product from the reaction mixture, it was found that drying or quenching processes would compromise recovery of the product. Extraction experiments using different organic solvents showed that ethyl acetate was capable of extracting the product from an aqueous mixture. However, miscibility of acetic acid and ethyl acetate posed a problem in using ethyl acetate as an extracting solvent in presence of acetic acid. Therefore, in order to use the extraction step, the oxidation reaction was tested with different mineral acids.

III.11.2. EXPERIMENTAL

All reagents were at least reagent grade. Methanol (LC-MS grade) was purchased from Fisher Scientific (Fair Lawn, NJ, USA). Reverse-osmosis water

was passed through a polishing unit (Lab Pro, Labconco, Kansas City, KS, USA) and had a conductivity of 18.2 M Ω -cm. Dimethyl trisulfide (DMTS) was a product of Sigma-Aldrich (St. Louis, MO, USA). 30% Hydrogen peroxide, chloroform (HPLC grade), sulfuric acid, nitric acid, and hydrochloric acid were purchased from Fisher Scientific. Glacial acetic acid and ethyl acetate are products of Acros Organics (Morris Plains, NJ, USA). Dichloromethane was purchased from Sigma Aldrich (St. Louis, MO, USA).

DMTS was oxidized using 1:4 molar ratio of DMTS: 30% Hydrogen peroxide in the presence of glacial acetic acid. The reaction mixture consisted of 83 μ L of pure DMTS solution, 396 μ L of 30% hydrogen peroxide solution, and 1521 μ L of glacial acetic acid, such that the concentration of DMTS, peroxide and acetic acid in the reaction were 0.4 M, 1.3 M and 13.2 M respectively. The reaction was carried out for 60 minutes at 30 $^{\circ}$ C. The oxidized product was monitored using thin layer chromatography (TLC), and then a 10 μ L aliquot was analyzed using high performance liquid chromatography (HPLC). The products obtained from the reactions were diluted to 0.5 mM in methanol prior to analyzing by HPLC.

An Agilent 1200 Series HPLC system, and an Agilent Eclipse XDB-C18 column (5 μ m packing material, and 2.1 x 150 mm dimensions) were used for the HPLC analysis of the oxidized product. Mobile phases A (100% water) and B (100% methanol) were prepared using HPLC grade methanol and water, and were filtered using vacuum filtration through a 0.45 μ m nylon membrane filter. Gradient elution was performed with 30% B and linearly increasing mobile phase

B to 100% over 15 minutes. The mobile phase composition was held constant for 3 minutes, and was then linearly decreased to 0% B over 5 minutes at a flow rate of 0.35 mL/minute. UV detection was performed at 280 nm.

Reaction conditions such as temperature, time, and concentration (peroxide and acetic acid) were optimized. Acetic acid concentrations of 1, 2, 5, 8, and 13.2 M were tested for acid optimization. Reaction time and temperature were kept constant at 30°C and 60 minutes. Longer reaction time (> 1hr) and higher reaction temperatures (>40 °C) were avoided for the purpose of preventing long sample preparation time, and uncontrolled oxidation or decomposition of DMTS, respectively.

For some oxidation reactions, sodium hydroxide (NaOH) was used to quench acetic acid in the reaction mixture. A 4 M NaOH solution was added to the 2 mL reaction mixture drop wise until the pH of the solution was neutral. Peroxide quenching for some reactions was performed using sodium chloride (NaCl) and sodium sulfite (Na₂SO₃). A 400 µL aliquot of 1.3 M NaCl or Na₂SO₃ was used for quenching the residual peroxide in the 2 mL reaction product mixture. The product was analyzed by HPLC before and after the quenching.

In an attempt to determine if drying was an option for analysis of the oxidized DMTS, DMTS and oxidation product in methanol, 100 µL each were taken in individual vials and were dried under N₂ for 15 minutes, reconstituted with 100 µL of methanol, and then analyzed by HPLC.

Chloroform, dichloromethane, hexane, and ethyl acetate were used to determine extraction efficiency of each solvent for DMTS and oxidized product.

Initially, the reaction was performed at 0.4 M DMTS, 1.3 M hydrogen peroxide, and 13.2 M acetic acid for 60 mins at 30 °C. Assuming that all of the DMTS was converted to product, the product was first diluted to 10 mM in methanol, and then to 1 mM in water. A 300 µL aliquot of the reaction product was transferred to a 4 mL vial, to which 200 µL of organic solvent was added. The mixture was vortexed for 1 min and allowed to settle for 3 mins. The organic layer was removed, and a 2nd extraction was performed for each sample by further adding 200 µL of the same solvent, and removing the organic layer again. The aqueous layer before and after extraction for each organic solvent was analyzed using HPLC. The difference between the initial and final concentration of the analytes in the aqueous layer was used to estimate the amount that was extracted into the organic solvent. All of the extractions were performed at room temperature.

III.11.2.1. Experimental with Mineral Acids

DMTS was oxidized using 30% hydrogen peroxide with acetic acid and different mineral acids. The composition of the reaction mixture for different acids is recorded in Table II.4.3-1. The reaction was carried out for 60 minutes at 30 °C. The oxidation product was analyzed using high performance liquid chromatography (HPLC).

Table III.11.1. Composition of reaction mixture for oxidation of DMTS using different acids.

Acid type	DMTS	Peroxide	Acid volume	Water
Acetic	200 μ L of 0.1 M DMTS	400 μ L of 30% peroxide	920 μ L of 17.4 M	480 μ L
HCl			50 μ L of 1M	1350 μ L
H ₂ SO ₄			50 μ L of 0.5 M	1350 μ L
HNO ₃			50 μ L of 1 M	1350 μ L

An Agilent 1200 Series HPLC system, with an Agilent Eclipse XDB-C18 column (5 μ m silica particles and 2.1 x 150 mm dimensions) was used for the HPLC analysis of the oxidized product. Mobile phases A (100% water) and B (100% methanol) were prepared using HPLC grade water and methanol, and were filtered by vacuum filtration through a 0.45 μ m nylon membrane filter. Gradient elution was performed with 30% B from 0 to 4 mins, which linearly increased to 100% B at 6 minutes. The mobile phase composition was held constant at 100% B for 2 minutes, and was then linearly decreased to 30% B over 4 minutes at a flow rate of 0.35 mL/minute. UV detection was performed at 280 nm.

An aliquot (40 μ L) of oxidation product was injected into the HPLC, and the product peak was collected. The oxidation product collected from HPLC was analyzed in mass spectrometry via Infusion analysis.

The oxidation product was also analyzed using a DB5 column by GCMS for information about mass and structure by direct injection of product, and after collection from the HPLC. For direct analysis, the product after reaction was extracted in ethyl acetate, and diluted to 500, and 1000 μ M in ethyl acetate, and

injected into GCMS directly. For analysis after purifying the product by HPLC, the extracted oxidation product analyzed by HPLC was collected, dried using anhydrous sodium sulfate, and analyzed with GCMS. GCMS analysis was done in positive and negative ionization modes using both the strong ionization EI mode and softer ionization CI mode.

III.11.3. RESULTS AND DISCUSSION

Water was found to produce the lowest detection limit at 10 μM (Figure III.11.1). The chromatogram of the DMTS-spiked blood is shown in Figure III.11.2; DMDS and DMTS eluted at 3.94 and 6.98 minutes, respectively, which demonstrates that DMTS can be detected in blood. The ramp rate of the GC oven temperature program was reset at 30 $^{\circ}\text{C}$ to reduce the retention time of DMTS. Compared with the same concentration of DMTS in methanol, DMTS was degraded to DMDS in blood as shown in Figure III.11.2. Overall, a simple GC/MS headspace method for the analysis of DMTS from biological fluids was developed; however, further optimization is necessary to obtain a lower detection limit of DMTS.

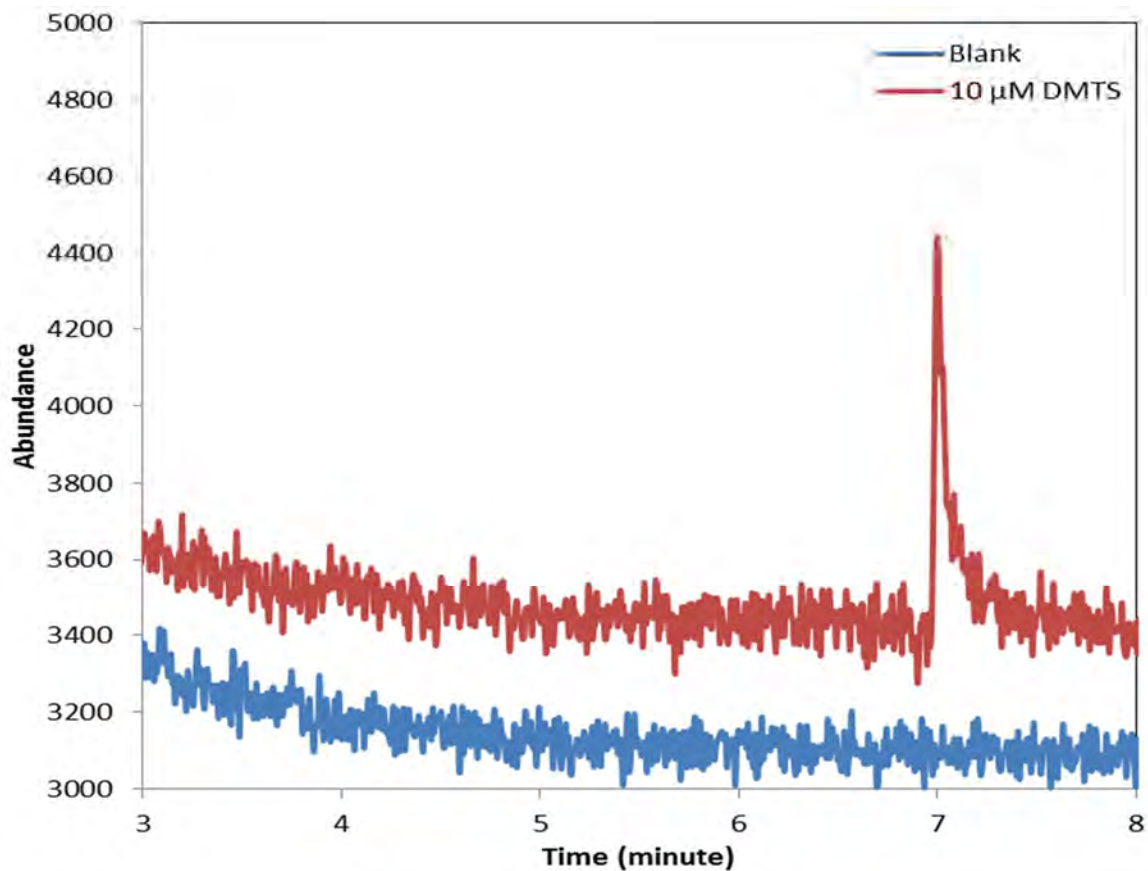


Figure III.11.1. Overlaid chromatograms of 10 μM DMTS (blue) and a methanol blank (red).

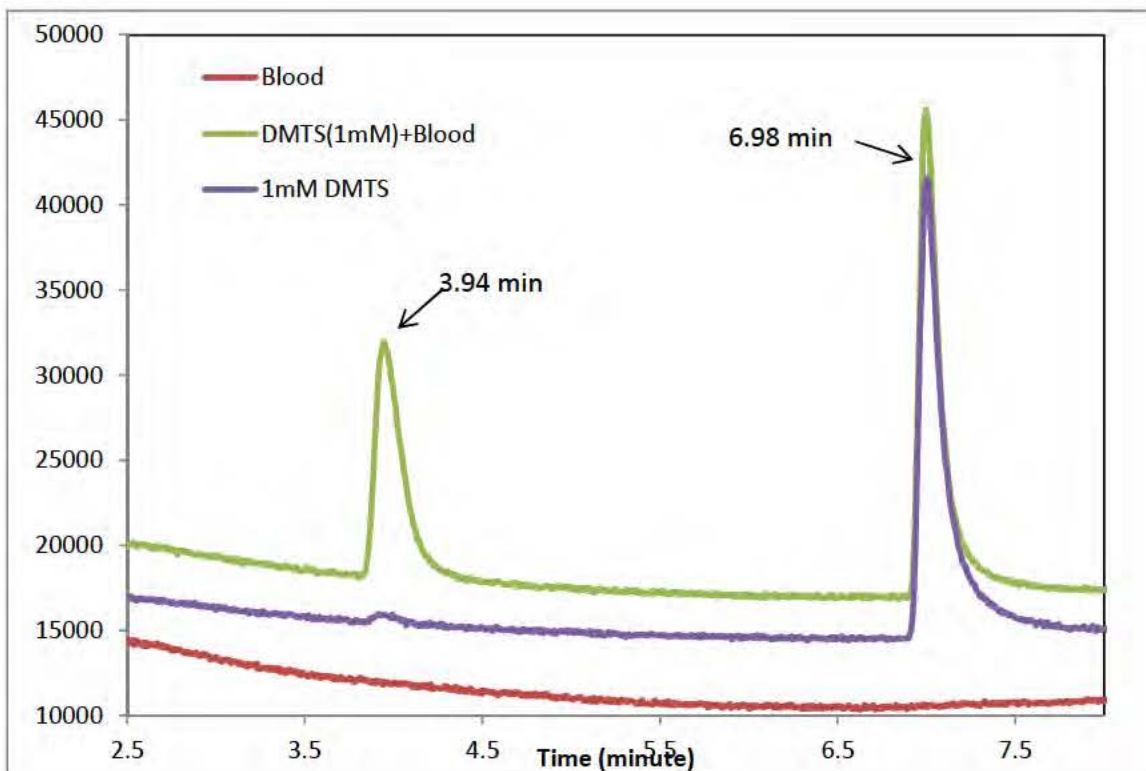


Figure III.11.2. Overlaid chromatograms of 1 mM DMTS (purple), DMTS-spiked blood (green) and a blood blank (red).

III.11.3.1. DMTS-NaBr Analysis

A 1 mM stock solution of NaBr and a 100 mM stock solution of DMTS were made in LC-MS-grade water and methanol, respectively. DMTS standards (0 μM , 500 μM , 1000 μM) with constant concentration of NaBr at i) 100 μM , and ii) 50 μM were made for infusion analysis. All standards were filtered through a 0.22 μm filter prior to infusing into mass spectrometer.

Mobile phases A (90% water, 10% methanol), and B (90% methanol and 10% water) were prepared using LC-MS-grade methanol and water, and were filtered using vacuum filtration. Different concentration ratios of DMTS:NaBr (5:1,

6:1, 4:1, 1:2) were prepared and analyzed for a comparative study. All standards were filtered through a 0.22 µm filter prior to injecting into the HPLC-MS-MS.

An AB Sciex Q-Trap 5500 MS (Applied Biosystems, Foster City, CA, USA) with electrospray ionization in negative and positive mode was used to perform the mass spectrometric analysis. A direct infusion (10 µL/min) of DMTS-NaBr standard was done to acquire mass spectra monitoring scans from 20-400 Da. Product ion scans were completed using both MS1 and MS3.

High-performance liquid chromatography-tandem mass spectrometry (HPLC-MS-MS) was conducted on a Shimadzu HPLC (LC-20AD, Shimadzu Corp., Kyoto, Japan) coupled to the AB Sciex Q-Trap 5500 MS. Gradient elution was used with initial mobile phase of 0% B, which linearly increased to 100% B over 7 minutes, held constant for 1 minute, and linearly decreased to 0% B over 2 minutes at a flow rate of 0.25 mL/min.

III.11.3.2. DMTS-Propionic Acid Analysis:

Propionic acid solutions (0.1% and 1%) were prepared in HPLC grade methanol: water (90:10) solution. DMTS standards (0 µM, 5 µM, 10 µM, 50 µM, and 100 µM) were made in both 0.1% and 1% propionic acid solutions for a comparative analysis. All standards were filtered through a 0.22 µm filter prior to HPLC-MS-MS analysis.

An AB Sciex Q-Trap 5500 MS (Applied Biosystems, Foster City, CA, USA) with electrospray ionization in negative mode was used to perform the mass spectrometric analysis. A direct infusion (10 µL/min) of DMTS-propionic acid

standard was done to acquire mass spectra monitoring scans from 20-400 Da. Product ion scans were completed using both MS1 and MS3.

III.11.4. RESULTS AND DISCUSSION

DMTS analysis using NaBr was performed in both negative and positive ionization mode. Optimized MRM parameters for tentative DMTS adduct in negative ionization mode are presented in Table III.11.2.

Table III.11.2. MRM ions and associated parameters corresponding to some form of DMTS-Br adduct in negative ionization mode.

Compound	MS1 (m/z Da)	MS3 (m/z Da)	CE (Volts)	DP (Volts)
$C_4H_{17}S_6Br$	336.5	206.2	19.75	168.89
	336.5	220.2	26.22	29.85

Different concentration ratios of DMTS and NaBr were tested for comparative study, in order to get to the optimal NaBr concentration for adduct formation. However, after multiple approaches, it was found that DMTS-NaBr adduct formation was not uniform, and did not increase with increasing concentration. Both low concentration standards (1, 5, 10, and 50 μ M) and high concentration standards (100, 500, and 1000 μ M) were tested. The mass spectrum obtained from infusion analysis indicated that ion $m/z = 336.5$ could be the fragment of interest. An m/z of 336.5 is predicted to be a dimerized DMTS with a bromine atom, but its presence in positive ionization mode was deemed unlikely. Furthermore, after continued replicate analysis, it was seen that an

increase in concentration of DMTS did not increase the abundance of $m/z = 336.5$ (Figure III.11.3) which led to the conclusion that it is likely not an adduct of interest.

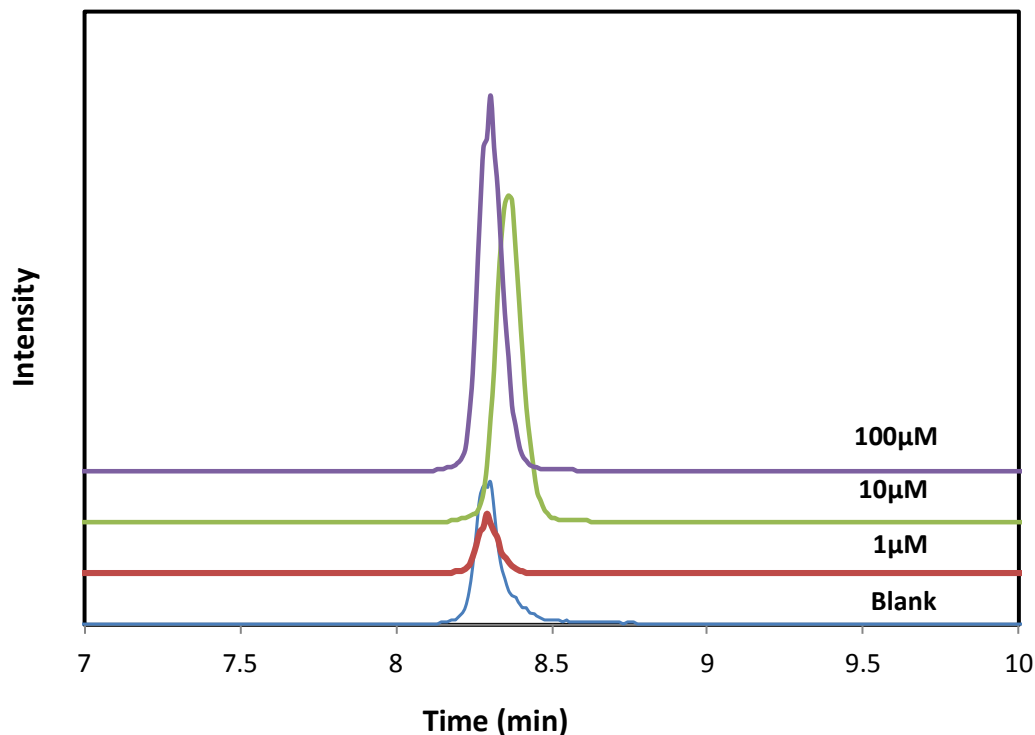
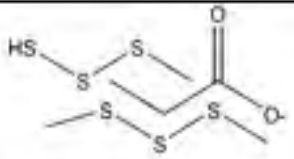
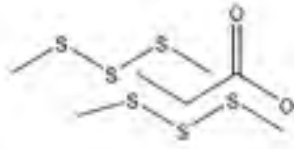


Figure III.11.3. Overlaid chromatograms of $[C_4H_{17}S_6Br]$ transition $m/z = 336.5 \rightarrow 220$. LC conditions are as described in the text.

Tentative MS1 adduct structure, masses of MS3 fragments, collision energy, and declustering potential of the species of interest are listed in Table III.11.4. The tentative structures show that the hydrophobic part of a propionic acid could be interacting with two dimethyl trisulfides. The m/z of $325 \rightarrow 311.1$ corresponds to the loss of a methyl group. Ions of $m/z = 283.1$ and 255.2 did not produce any Q3 fragments and were not studied further. Ion 169.2 gave a 73.1 Q3 fragment, which correlates to the mass of a propionic acid. Mass spectra of

DMTS-propionic acid with possible adducts of interest are shown in Figure III.11.4.

Table III.11.4. MRM ions and associated parameters corresponding to potential DMTS-propionic acid adduct.

Compound	MS1 (m/z Da)	MS3 (m/z Da)	Collision Energy (volts)	Declustering Potential (volts)
	311.1	80.0	-169.46	-105.62
		119.1	-189.44	-68.73
		182.9	-164.51	-105.62
C₆H₁₅O₂S₆⁻ 	325	80	-177.28	-113.43
		118.9	-176.16	-72.10
		182.9	-190.44	-47.93
C₇H₁₇O₂S₆⁻				

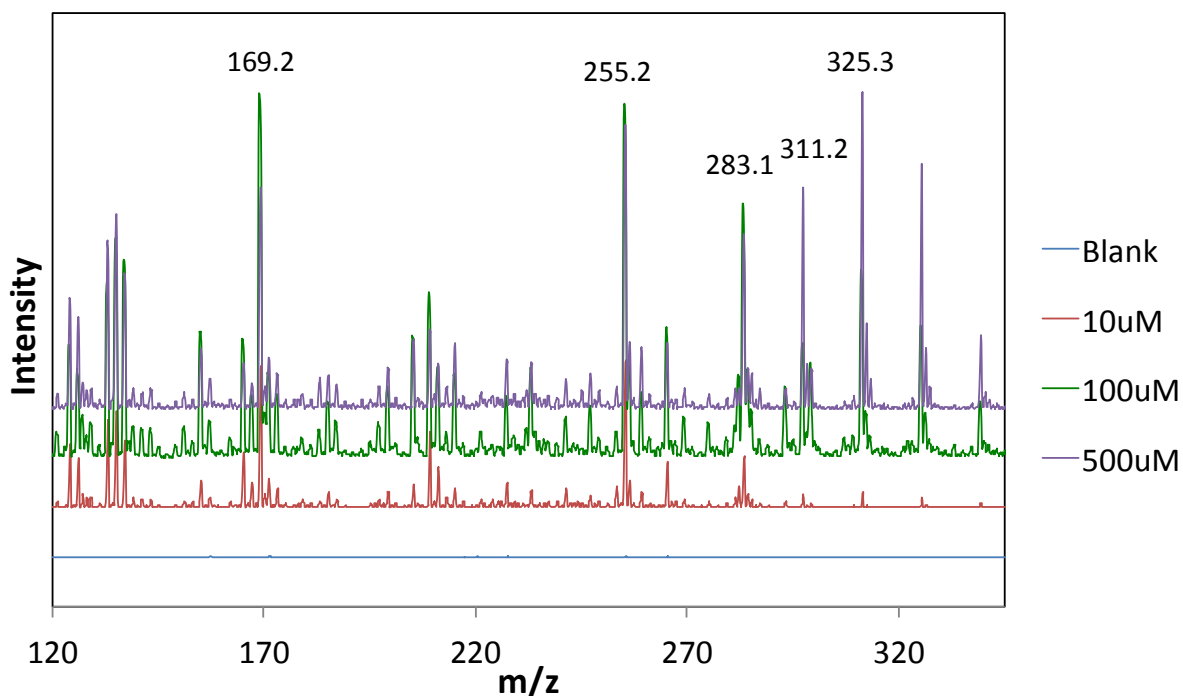


Figure III.11.4. Mass spectra of increasing concentrations of DMTS in 0.1% Propionic acid. Mass/charge of the ions of interest are labeled.

III.11.4.1. Optimization of Reaction Parameters:

The oxidation of 0.4 M DMTS with 1.3 M hydrogen peroxide and increasing concentration of acetic acid is presented in Figure III.11.5. From HPLC analysis, the reaction at 8 M acid results in the highest yield of oxidized product.

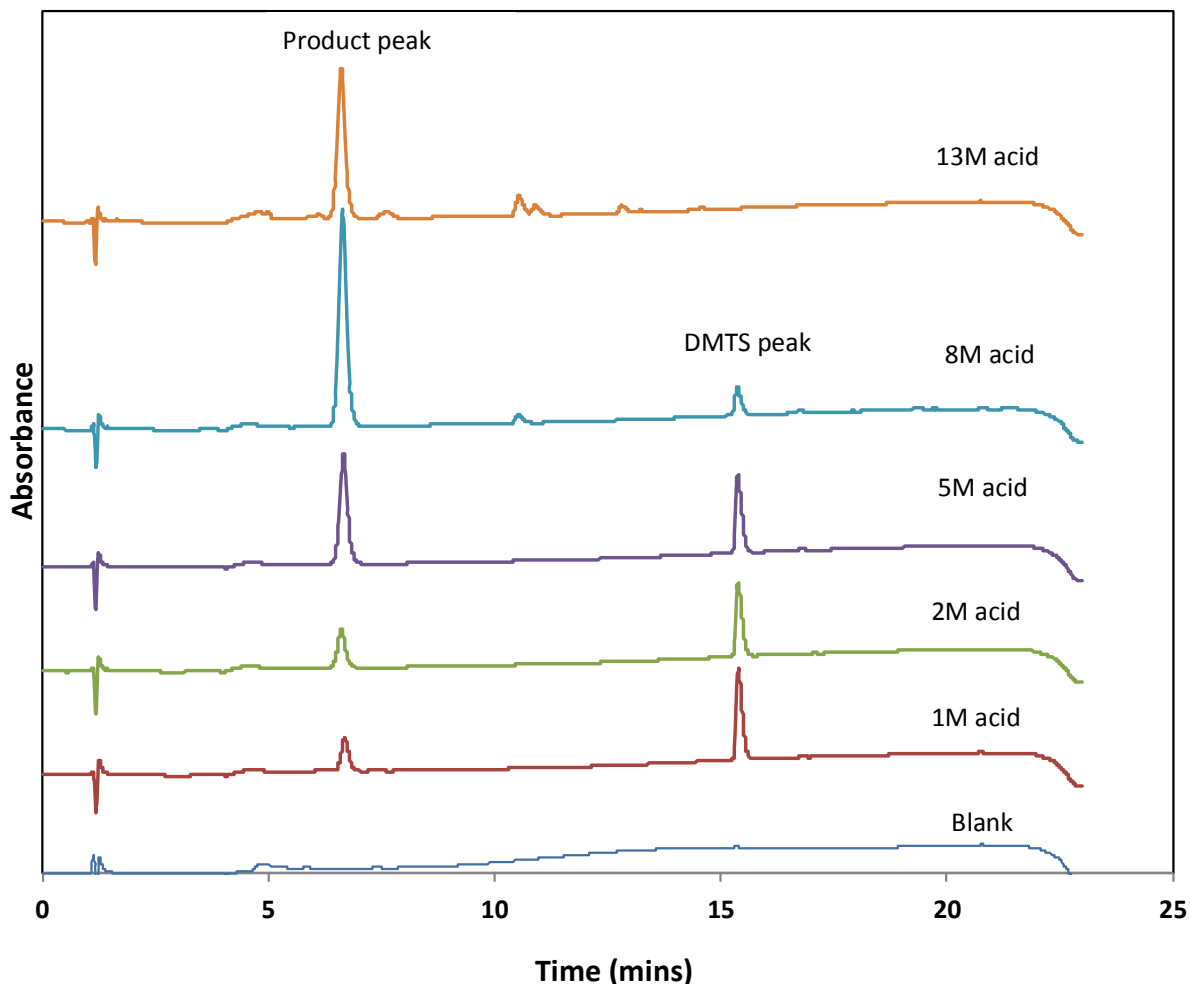


Figure III.11.5. Chromatograms showing the oxidized reaction product (eluting at 6.5 min) and unreacted starting material DMTS (eluting at 15.5 min) when increasing the acetic acid concentration. The LC conditions are described in the text.

HPLC chromatograms for reactions performed at 8 M acid, 1.3 M hydrogen peroxide, and increasing DMTS concentration (10 mM, 50 mM and 100 mM) are shown in Figure III.11.6. Before analysis, the reaction product was diluted to 0.5 mM in methanol. For each DMTS concentration, only the oxidized product peak was observed and the DMTS peak was negligible (Figure III.11.6).

Therefore, the reaction conditions are optimized for DMTS oxidation, for at least the concentration range studied. The reaction may still need to be optimized for DMTS concentrations below 10 mM.

Because of practical limitations of the HPLC instrumentation, large concentrations of acid and peroxide cannot be used. Therefore, in order to successfully optimize the parameters for lower DMTS concentration, the acid and peroxide either need to be quenched or the product needs to be extracted using an LC-compatible organic solvent.

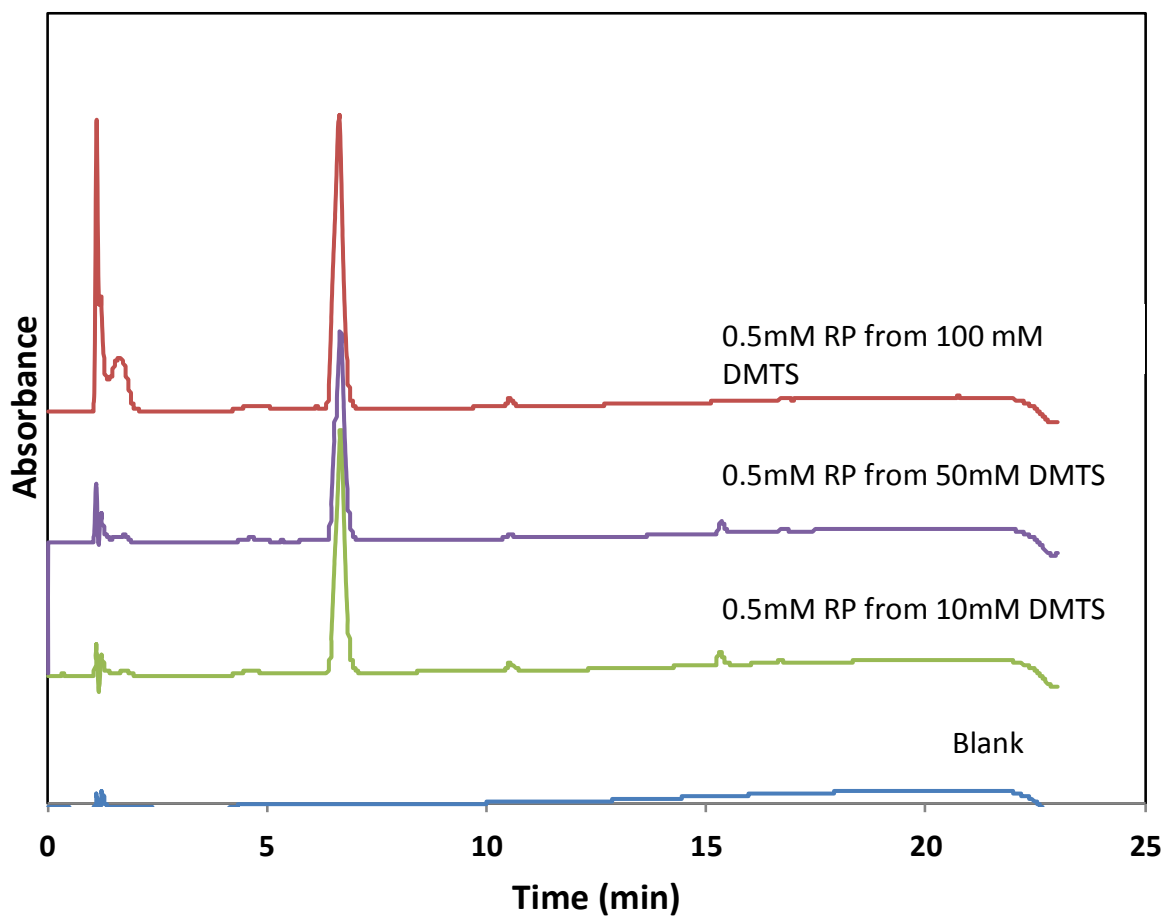


Figure III.11.6. Chromatograms of 0.5 mM product from oxidation of increasing DMTS (10 mM-100 mM) at 1.3 M peroxide and 8 M acetic acid concentrations. The LC parameters are described in the text in detail.

III.11.4.2. Drying and Quenching

Quenching and solvent drying analysis was also done on the product mixture prior to analyzing the product via HPLC or MS in order to prevent corrosion of injector, column, and infusion syringe from high concentrations of acid or peroxide.

Drying experiments showed that DMTS as well as the oxidized product are both easily lost when dried under N₂. The chromatograms of before and after drying for DMTS (Figure III.11.7), and reaction product (Figure III.11.8) shows that DMTS and the product are volatile, and are lost in the drying process. These results indicate that any drying process should be avoided in the sample preparation and extraction process.

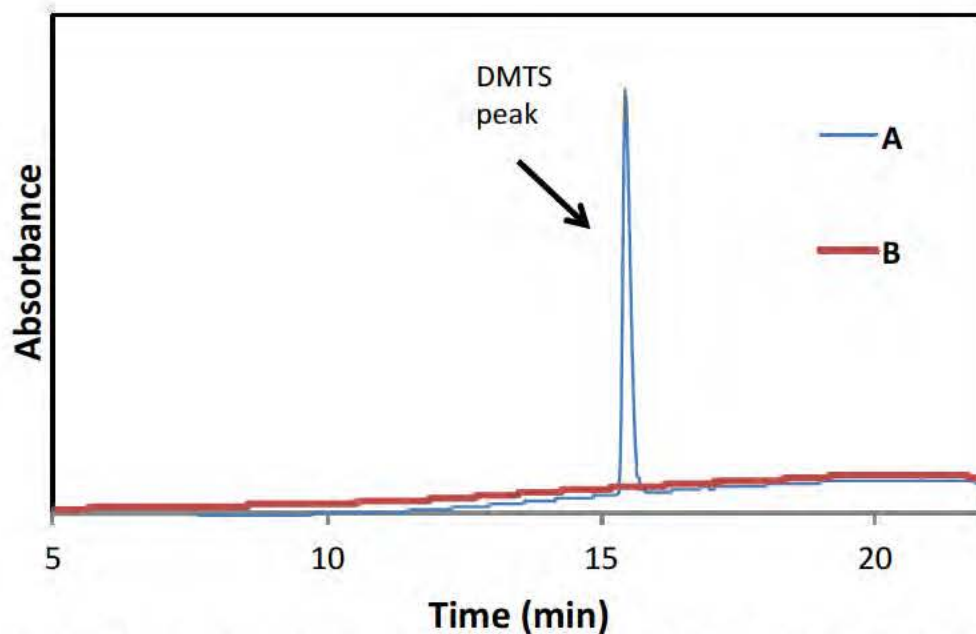


Figure III.11.7. Chromatogram showing loss of DMTS after drying for 15 minutes under N_2 air. A (before drying) shows the DMTS peak, which disappears in B (after drying).

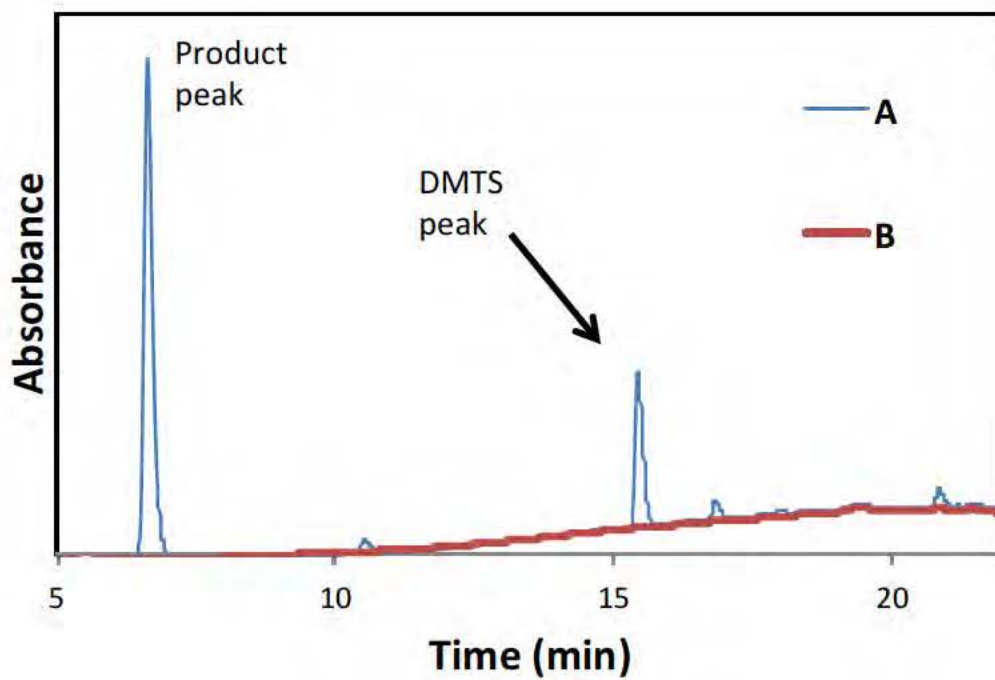


Figure III.11.8. Chromatograms showing the oxidized product before (A), and after drying (B). The oxidized product is completely lost after drying for 15 minutes under N₂ air.

Quenching analysis presented in Figure III.11.9 shows that acid quenching using sodium hydroxide degrades the product completely. Similarly, peroxide quenching using sodium sulfite and sodium chloride converts some of the oxidized product back to DMTS. This analysis indicates that quenching using hydroxide, and sulfite should be avoided. Quenching with chloride is observed to preserve most of the product, but still converts some of it to DMTS. Failure of the quenching and drying experiments necessitated an extraction step to extract the product using an organic solvent prior to HPLC or MS analysis.

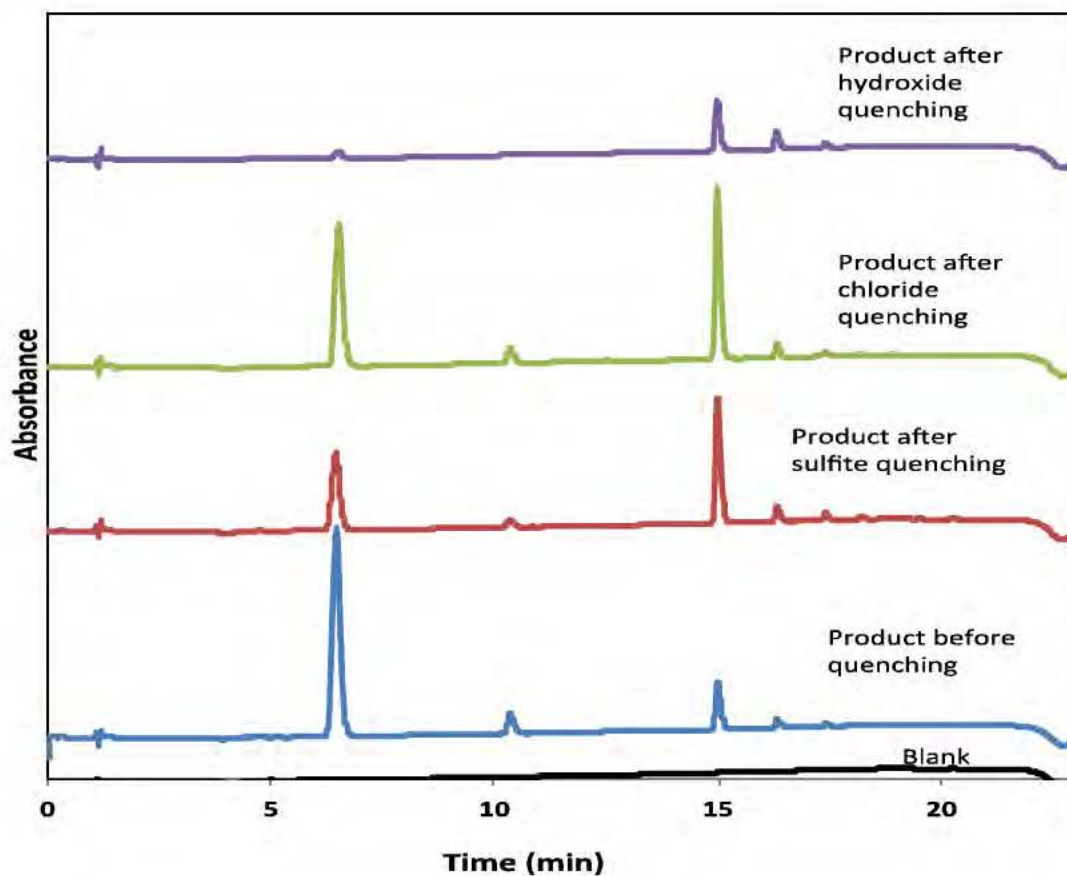


Figure III.11.9. Overlaid HPLC chromatograms of the reaction product after undergoing different quenching steps.

III.11.4.3. Extraction of DMTS and Reaction Product

Among the different organic solvents tested for extraction, hexane worked best for extraction of DMTS and ethyl acetate is capable of extracting both DMTS as well as the oxidized product. Results of extraction using hexane, ethyl acetate, and 50:50 hexane: ethyl acetate are presented in Figure III.11.10.

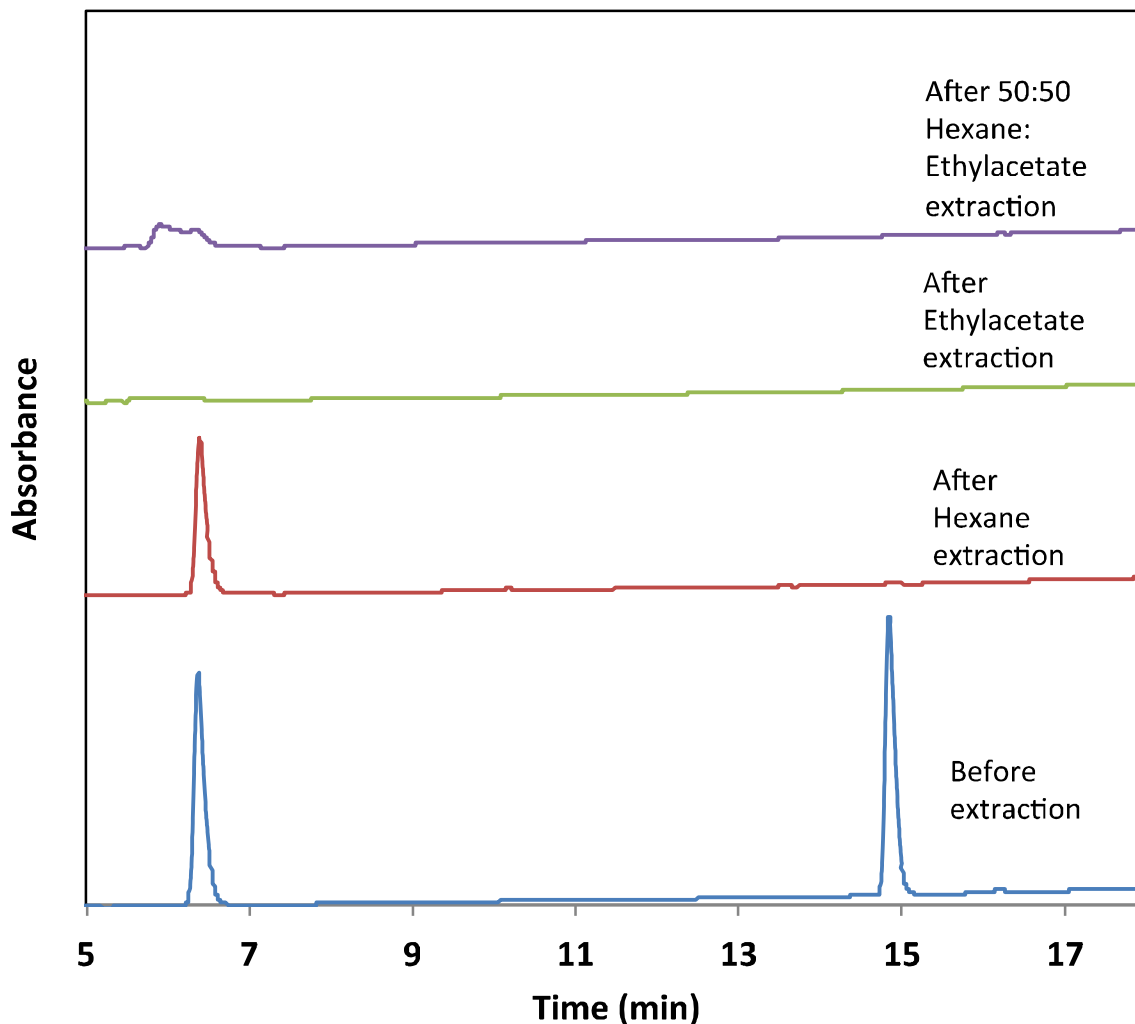


Figure III.11.10. Overlaid chromatograms showing analysis of the aqueous layer before and after extraction using organic solvents. The reaction product peak elutes at 6.5 min, and DMTS peak elutes at 15 min.

III.11.4.4. Oxidation reaction using mineral acids

The chromatogram of the oxidation product formed in the presence of different acids is shown in Figure III.11.11. From HPLC analysis, it was found that reaction using different mineral acids resulted in similar yield when compared to the yield using acetic acid.

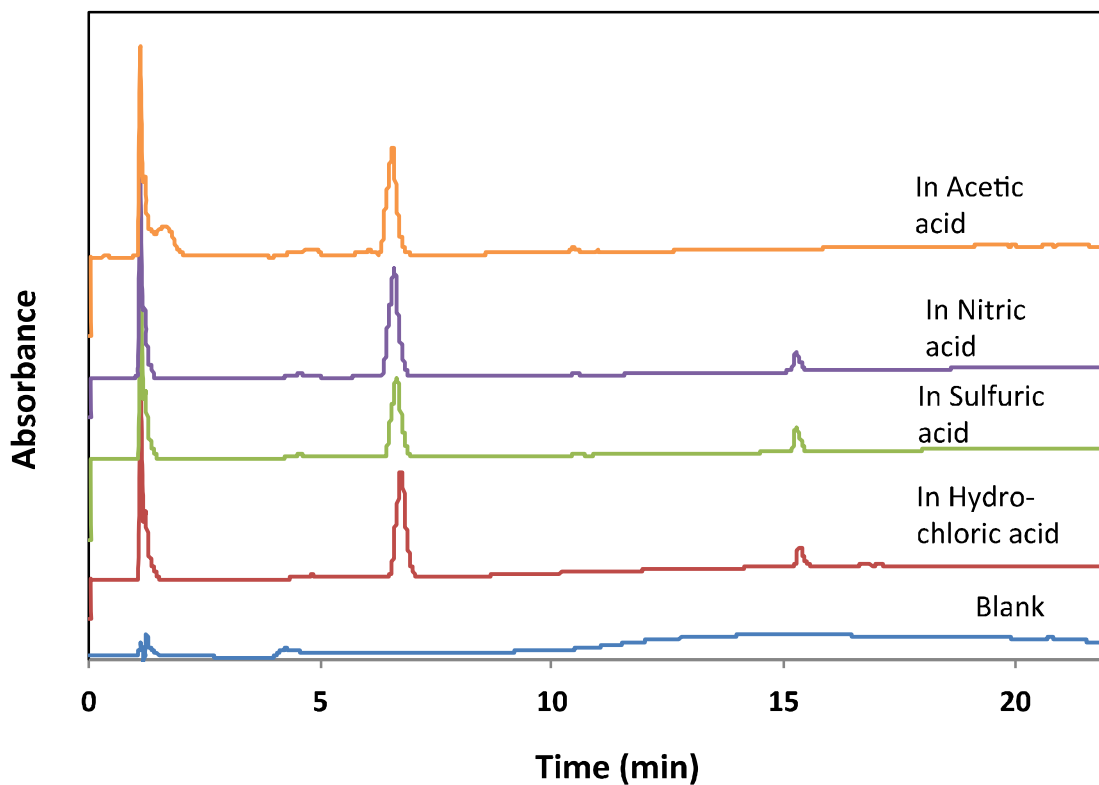


Figure III.11.11. Chromatograms showing the oxidized reaction product (eluting at 6.5 min) and unreacted starting material DMTS (eluting at 15.5 min) using different acids. The LC conditions are described in the text.

The infusion analysis of the purified oxidation product by mass spectroscopy in positive and negative ionization mode is reported in Figures III.11.12 and 11.13, respectively.

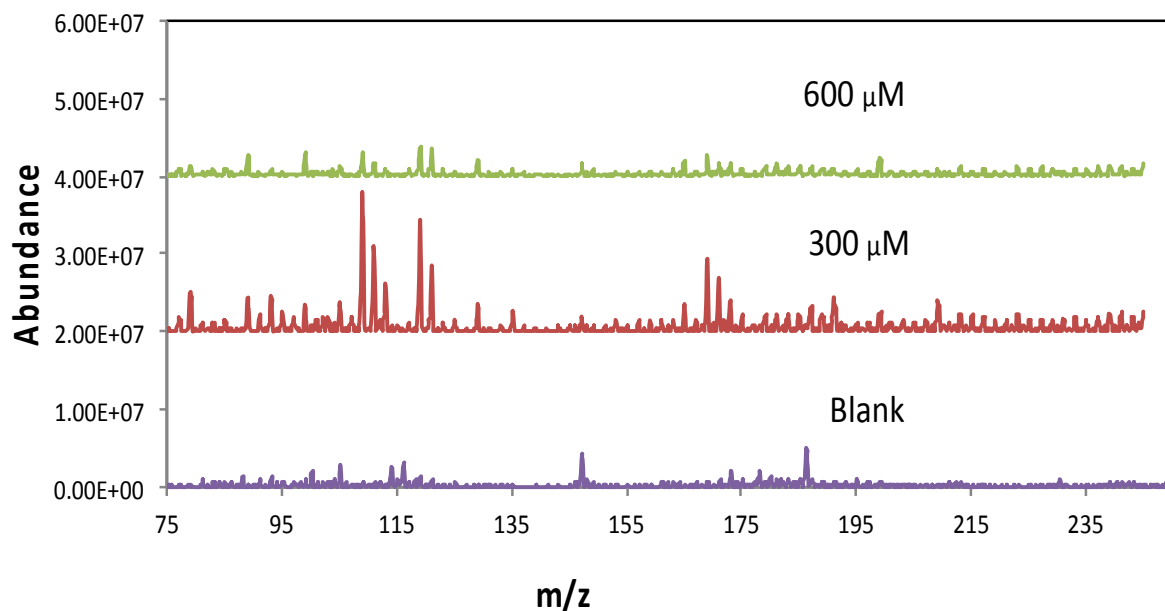


Figure III.11.12. Chromatograms of the collected oxidation product in positive ionization mode by infusion analysis with ESI mass spectroscopy.

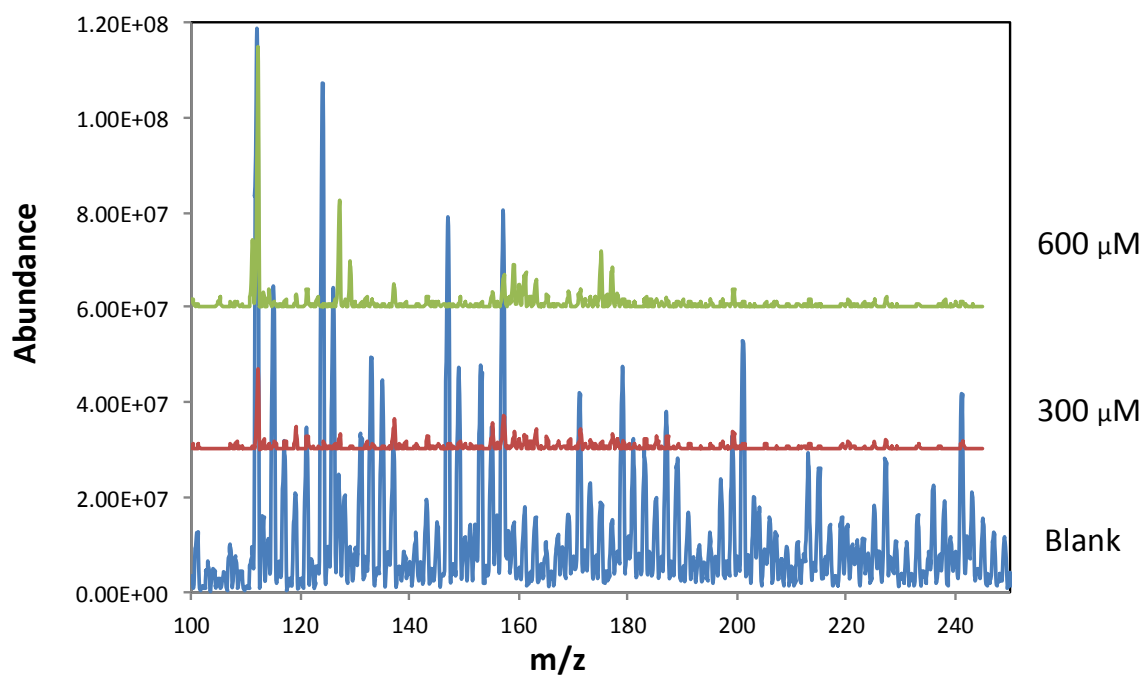


Figure III.11.13. Chromatograms of the collected oxidation product in negative ionization mode by Infusion analysis with ESI-mass spectroscopy.

The oxidation product was not detected in either of the ionization modes in the mass spec. The oxidation product was not detected by GCMS in either approaches of with and without purifying the product by HPLC.

III.11.5. CONCLUSIONS

The DMTS-propionic acid method is a promising approach. Further analysis will be done by setting up an HPLC-MS-MS method using the information obtained from infusion studies. A reverse phase C-12 column will be used because of the hydrophobic nature of DMTS. A 0.1% propionic acid in methanol and water will be used for Mobile phases A and B, respectively. So far, it has been noticed that DMTS does not form stable adducts easily. It is also possible that the adducts formed are too fragile, and are degrading rapidly into smaller ions. Hence, if this approach fails, then oxidation of the sulfur bond will be the next approach to analyze DMTS using HPLC-MS-MS.

Analyzing DMTS as an oxidized product appears to be a promising approach if the product can be isolated from acid and peroxide prior to analysis in HPLC-MSMS. Unlike DMTS, the oxidized product is ionizable and does not require other compounds to form ionizable adducts for detection in the mass spectrometer. The higher mass of the product will also provide advantages in MS detection. From multiple experiments, it has been found that ethyl acetate is a potential extracting solvent for the oxidized product. However, miscibility of

acetic acid and ethyl acetate pose a limitation in using ethyl acetate as an extracting solvent. Therefore, future work will include performing this reaction in strong mineral acids such as hydrochloric, sulfuric and nitric. Strong mineral acids will dissociate completely during the reaction process, and will not mix with ethyl acetate in the extraction step. Once the product is extracted in ethyl acetate, it will be diluted in methanol such that it can be analyzed in the LC. After the reaction and extraction conditions are optimized, the product will be analyzed using HPLC-MSMS to achieve desirable low detection limits (<5 μ M).

DMTS was oxidized using mineral acid, such that the oxidized product could be extracted using ethyl acetate. The product was not detected by infusion analysis with mass spectroscopy, which could be due to high background noise in the instrument, ion suppression, or a neutral molecule not ionizing. Different concentrations of product, higher than 700 μ M and lower than 300 μ M can be tested to verify the problem of detection. The product might also be undergoing fragmentation into smaller masses due to the strong ESI ionization, or forming uncharged species, leading to difficulty in detection. The product was not detected in either of the ionization modes using both EI, and CI sources in GCMS. Failure in detection with both strong and weak ionization sources points to the possibility of the product degrading at the high temperatures used in the GC. Future work include headspace- GCMS analysis of the product using GCMS, and further analysis by mass spec via infusion.

III.11.6. REFERENCES

1. Petrikovics I, Kuzmitcheva G, Budai M, Haines D, Nagy A, Rockwood GA, Way JL (2010) Encapsulated rhodanese with two new sulfur donors in cyanide antagonism. In *XII International Congress of Toxicology*. Barcelona, Spain.
2. Frankenberg L (1980) Enzyme therapy in cyanide poisoning: effect of rhodanese and sulfur compounds. *Arch Toxicol* **45**: 315-323.
3. Iciek M, Wlodek L (2001) Biosynthesis and biological properties of compounds containing highly reactive, reduced sulfane sulfur. *Pol J Pharmacol* **53**: 215-225.
4. Petrikovics I, Pei L, McGuinn W, Cannon E, Way J (1994) Encapsulation of rhodanese and organic thiosulfonates by mouse erythrocytes. *Fund and Appl Toxicol* **23**: 70-75.
4. Golchoubian, H.; Hosseinpoor, F., Effective oxidation of sulfides to sulfoxides with hydrogen peroxide under transition-metal-free conditions. *Molecules* **2007**, *12* (3), 304-311.

CHAPTER 12

DETERMINATION OF 3-MERCAPTOPYRUVATE BY LC-MS-MS

Michael W. Stutelberg and Brian A. Logue

III.12. The effort for this portion of the report was published as a peer-reviewed manuscript, which is attached as Appendix VII.

CHAPTER 13

SIMULTANEOUS DETERMINATION OF COBINAMIDE AND 3-MERCAPTOPYRUVATE IN SWINE PLASMA BY LIQUID CHROMATOGRAPHY-TANDEM MASS SPECTROMETRY

Michael W. Stutelberg and Brian A. Logue

III.13.1. Introduction

With the development of novel cyanide antidotes, there is a need to simultaneously determine 3-mercaptopyruvate (3-MP) and cobinamide (Cbi). 3-MP acts as a sulfur donor to produce thiocyanate^{1,2} when cyanide is present, though when administered 3-MP rapidly metabolizes in the blood. Therefore, dimer prodrugs (sulfanegen³) were developed to deliver 3-MP upon administration into the blood, which proved to be more efficacious than current antidotes.

Another antidote being investigated, Cbi, the penultimate derivative of hydroxocobalamin, is also being utilized as a cyanide antidote. The enhancement from hydroxocobalamin, currently used as a cyanide antidote, is that Cbi has greater water solubility, higher affinity for cyanide, and can bind two cyanides.⁴ The dinitrocobinamide salt has been shown to have greater efficacy when compared to other cyanide antidotes and cobinamides.^{5,6}

For further development of these next generation cyanide antidotes, a method to simultaneously determine both antidotes together is needed. The focus of this project is to develop an analytical method to simultaneously

determine total cobinamide (Cbi) and 3-mercaptopyruvate (3-MP) using high performance liquid chromatography tandem mass spectrometry (HPLC-MS-MS).

III.13.2. Experimental

III.13.2.1. Preparation of $Cbi(SO_3)$, $Cbi(CN)(H_2O)$, and $Cbi(CN)_2Na$ with 3-MP

Spiked plasma (100 μ L) of $CbiSO_3$ and 3-MP was added to a 2 mL centrifuge tube along with an internal standard (100 μ L of 15 μ M 3-MP- $^{13}C_3$). For the cyanide analogs, spiked plasma (100 μ L) with $Cbi(CN)(H_2O)$ and $Cbi(CN)_2Na$, was also added to a separate 2 mL centrifuge tube. In place of the 3-MP internal standard, an equal volume of water (100 μ L) was added to the $Cbi(CN)_2$ and $Cbi(CN)$.

III.13.2.2. Preparation of Dinitrocobinamide ($Cbi(NO_2)_2$)

Spiked plasma (100 μ L) of $Cbi(NO_2)_2$ and 3-MP was added to a 2 mL centrifuge tube along with an internal standard (100 μ L of 15 μ M 3-MP- $^{13}C_3$). The $Cbi(NO_2)_2$ was prepared by adding excess sodium nitrite (4:1 $NO_2:[Cbi(H_2O)_2]^{2+}$) to forcibly bind nitrite to cobinamide. Protein from the plasma was precipitated by addition of acetone (300 μ L) and the samples were cold-centrifuged (Thermo Scientific Legend Micro 21R centrifuge, Waltham, MA, USA) at 8 $^{\circ}C$ for 20 min at 13,100 RPM (16,500 x g). An aliquot (450 μ L) of the supernatant was then transferred into a 4 mL glass vial and dried under N_2 . (Note: Glass vials were used in our laboratory mainly because of practical limitations of the N_2 drier.)

III.13.2.3. Preparation for Analysis of Total Cobinamide

The $\text{Cbi}(\text{NO}_2)_2$ was prepared by adding excess sodium nitrite (4:1 $\text{NO}_2:\text{[Cbi}(\text{H}_2\text{O})_2]^{2+}$) to forcibly bind nitrite to cobinamide. The $\text{Cbi}(\text{CN})_2$ was prepared by adding 3x the concentration of cyanide to $\text{Cbi}(\text{H}_2\text{O})_2^{2+}$ in water spiked into plasma and diaquocobinamide ($\text{Cbi}(\text{H}_2\text{O})_2^{2+}$) was spiked directly into plasma. To determine total cobinamide conversion, $\text{Cbi}(\text{CN})_2$, $\text{Cbi}(\text{NO}_2)_2$, $\text{Cbi}(\text{H}_2\text{O})_2^{2+}$, or mix (1:1:1, $\text{Cbi}(\text{CN})_2:\text{Cbi}(\text{NO}_2)_2:\text{Cbi}(\text{H}_2\text{O})_2^{2+}$) (100 μL , 100 μM) were spiked into swine plasma. Then cyanide (10x concentration of Cbi's) was added to convert all the species to $\text{Cbi}(\text{CN})_2$. Protein from the plasma was precipitated by addition of acetone (300 μL) and the samples were cold-centrifuged (Thermo Scientific Legend Micro 21R centrifuge, Waltham, MA, USA) at 8 °C for 20 min at 13,100 RPM (16,500 x g). An aliquot (450 μL) of the supernatant was then transferred into a 4 mL glass vial and dried under N_2 . (Note: Glass vials were used in our laboratory mainly because of practical limitations of the N_2 drier). The samples were reconstituted with 5 mM ammonium formate in 9:1 water:methanol (100 μL) and monobromobimane (MBB, 100 μL , 500 μM). The samples were heated on a block heater (VWR International, Radnor, PA, USA) at 70 °C for 15 min (3-MP derivatization step). The samples were then filtered with a 0.22 μm tetrafluoropolyethylene membrane syringe filter into autosampler vials fitted with 150 μL deactivated glass inserts for LC-MS-MS analysis.

Mobile phase solutions for LC-MS-MS consisted of 5 mM aqueous ammonium formate with 10% methanol (Mobile Phase A) and 5 mM ammonium formate in 90% methanol (Mobile Phase B). A gradient of 0 to 100% B was applied over 3 min, held constant for 0.5 min, then reduced to 0% B over 1.5 min for the determination of Cbi(CN)₂. The total run-time was 5.1 min with a flow rate of 0.25 mL/min. For validation of the analytical method, we generally followed the FDA bioanalytical method validation guidelines.⁷

III.13.2.4. Preparation for Simultaneous Analysis of 3-MP and Total Cbi

For initial method development, samples were prepared by combining Cbi(CN)₂ plasma (50 µL) with plasma containing 3-MP (50 µL) in a 2 mL centrifuge tube along with an internal standard (100 µL of 15 µM 3-MP-¹³C₃). Excess cyanide (100 µL) was pipetted into samples or standards in an attempt to convert all cobinamide species into Cbi(CN)₂. The rest of the procedure for total cobinamide followed total Cbi procedure, as outlined above.

To verify Cbi could be converted to Cbi(CN)₂ in the presence of 3-MP, spiked plasma (50 µL) of 3-MP was added to a 2 mL centrifuge tube along with an internal standard (100 µL of 15 µM 3-MP-¹³C₃). Then Cbi species Cbi(CN)₂, Cbi(NO₂)₂, Cbi(H₂O)₂²⁺ (50 µL, 200 µM) spiked in plasma were added. Then excess cyanide (10x Cbi concentration) was added to convert species to Cbi(CN)₂ and the rest of the procedure followed as outlined above. The Cbi(NO₂)₂ was prepared by adding excess sodium nitrite (4:1 NO₂: [Cbi(H₂O)₂]²⁺) to forcibly bind nitrite to cobinamide.

III.13.3. Results

III.13.3.1. *Analysis of Cbi(SO₃), Cbi(CN)(H₂O), and Cbi(CN)₂Na with 3-MP in plasma*

For validation of the analytical method, we generally followed the FDA bioanalytical method validation guidelines.⁷ The lower limit of quantification (LLOQ) and upper limit of quantification (ULOQ) were defined using the following inclusion criteria: 1) calibrator precision of <15% RSD, and 2) accuracy of $\pm 15\%$ of the nominal calibrator concentration back-calculated from the calibration curve. The linear range for 3-MP was previously determined.⁸ The linear dynamic ranges for CbiSO₃, Cbi(CN)₂, and Cbi(CN)(H₂O) were separately determined in plasma using standards from 5-1000 μM (5, 10, 20, 50, 100, 200, 500, 1000 μM). The range was decreased to 10-1000 for CbiSO₃ (Figure III.13.1). For Cbi(CN)₂ (Figure III.13.2) and Cbi(CN)(H₂O) (Figure III.13.3), the linear range was decreased to 5-200 μM with each calibration weighted by $1/x^2$. Note: The parent ion for Cbi(CN)(H₂O) is 1015.5, which is assumed to be Cbi(CN)⁺ due to the loss of water during the electrospray ionization.

The limit of detection (LOD) of 3-MP previously determined⁸ was determined by analyzing multiple concentrations of 3-MP below the LLOQ and determining the lowest 3-MP concentration that reproducibly produced a signal-to-noise ratio of 3, with noise measured as the peak-to-peak noise directly adjacent to the 3-MP peak. For determining the LOD for the Cbi species, calibration curves below the LLOQ, near the estimated LOD from 1-5 μM (1, 2, 3,

4, and 5 μM), were created. Following the RMSE method⁹, the LOD was calculated from each calibration curve with a LOD of CbiSO_3 (Figure III 13.2) at 5.7 μM , $\text{Cbi}(\text{CN})_2$ (Figure III.13.3) at 3.5 μM , and $\text{Cbi}(\text{CN})(\text{H}_2\text{O})$ (Figure III.13.4) at 4 μM .

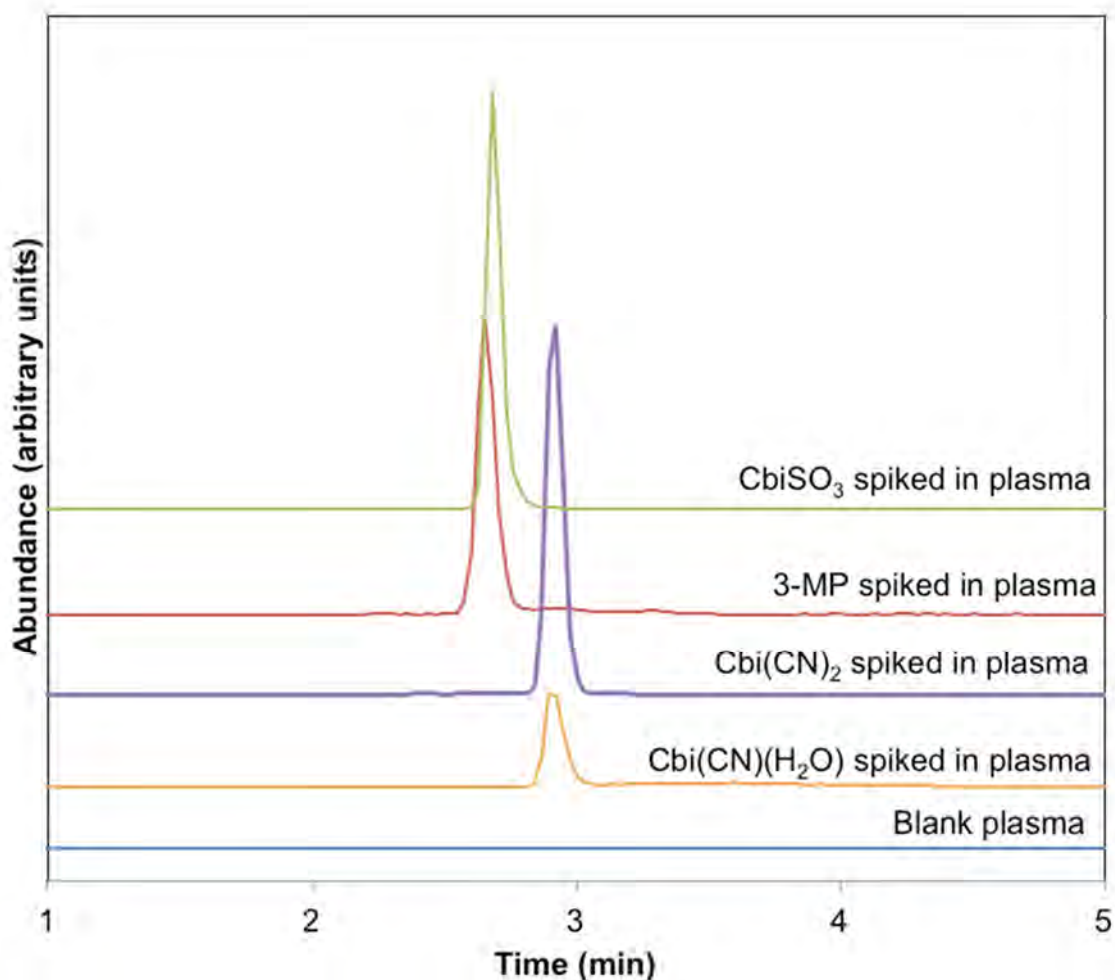


Figure III.13.1. Overlaid chromatograms of CbiSO_3 eluting at 2.74 min, 3-MPB eluting at 2.69 min, $\text{Cbi}(\text{CN})_2$ eluting at 2.94 min, and $\text{Cbi}(\text{CN})$ eluting at 2.94 min, spiked in rabbit plasma. The chromatograms represent the signal response of the MRM transitions of CbiSO_3 1092.8 \rightarrow 989.9, 3-MPB 311.0 \rightarrow 223.1, $\text{Cbi}(\text{CN})_2$ 1064.9 \rightarrow 1010.8, and $\text{Cbi}(\text{CN})$ 1015.0 \rightarrow 930.5 m/z .

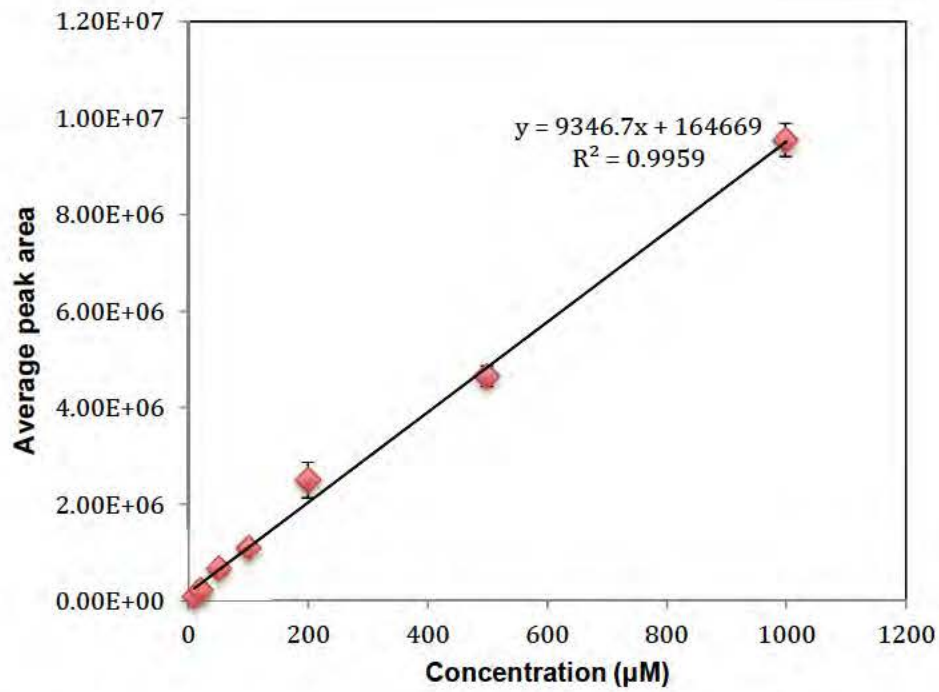


Figure III.13.2. Calibration curve for CbiSO₃ spiked in rabbit plasma.

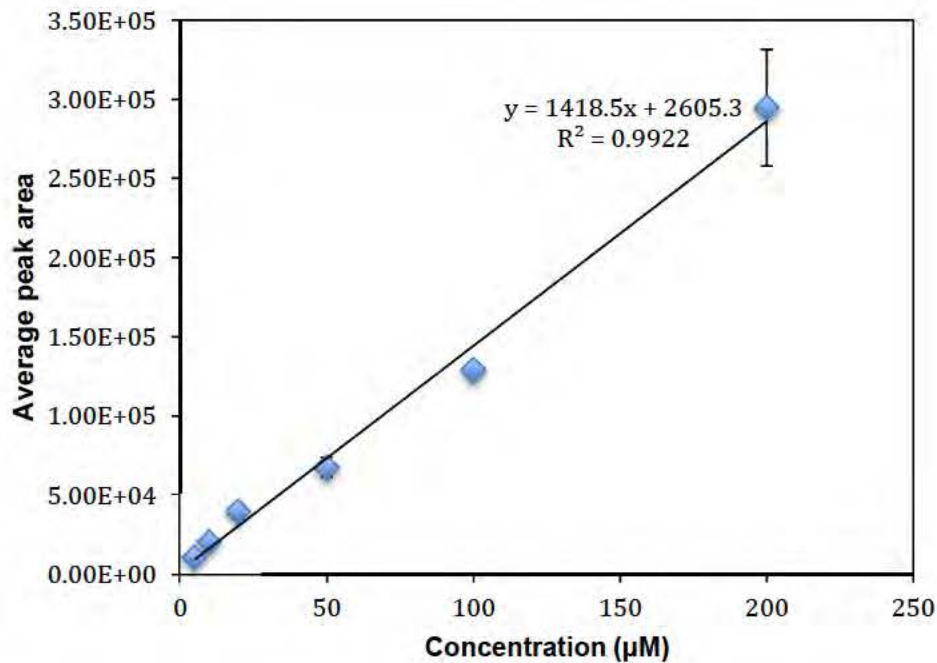


Figure III.11.3. Calibration curve for Cbi(CN)₂ spiked in rabbit plasma.

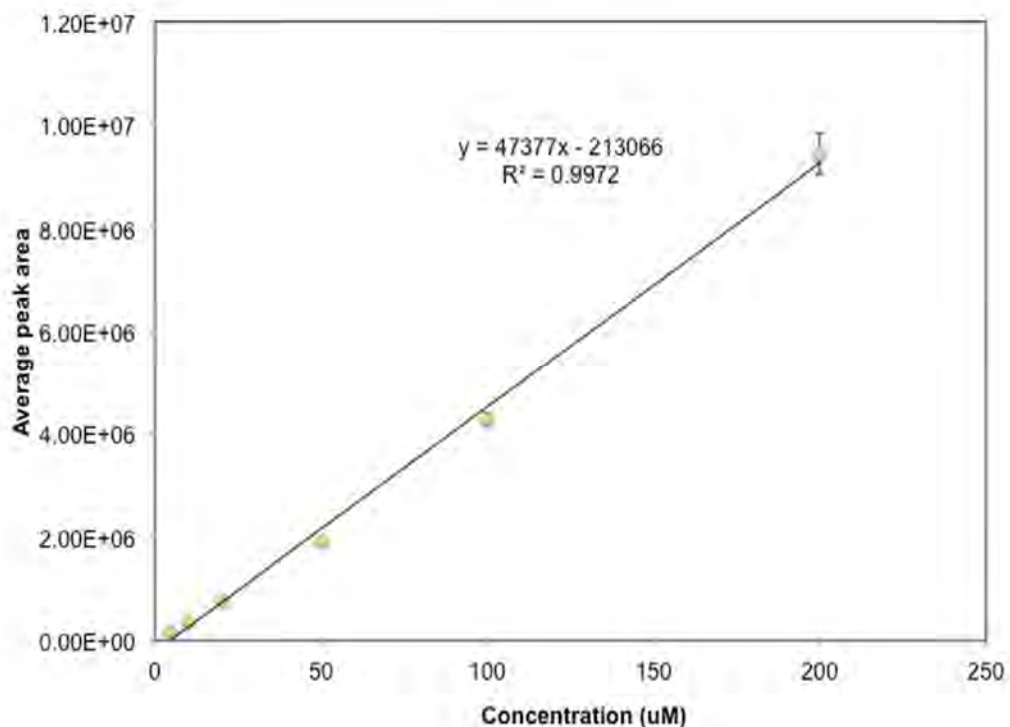


Figure III.13.2. Calibration curve for Cbi(CN) spiked in rabbit plasma.

III.13.3.2. *Detection of Dinitrocobinamide*

For the determination of dinitrocobinamide, MRMs (1104.9 → 1058.9, 1035.9 → 989.9, and 989.9 → 916.9 m/z) were found by LC-MS-MS. Even though excess nitrite was added and MRMs for Cbi(NO₂)₂ were previously found, dinitrocobinamide ions were difficult to observe (Figure III.13.5) because multiple ligands compete with relatively poor affinity for nitrite ions. The main chromatographic peaks observed are only Cbi (1035.9 → 989.9 and 989.9 → 916.9 m/z). Therefore, it was determined to derivative Cbi to only one species with a compound that has strong affinity to the cobalt.

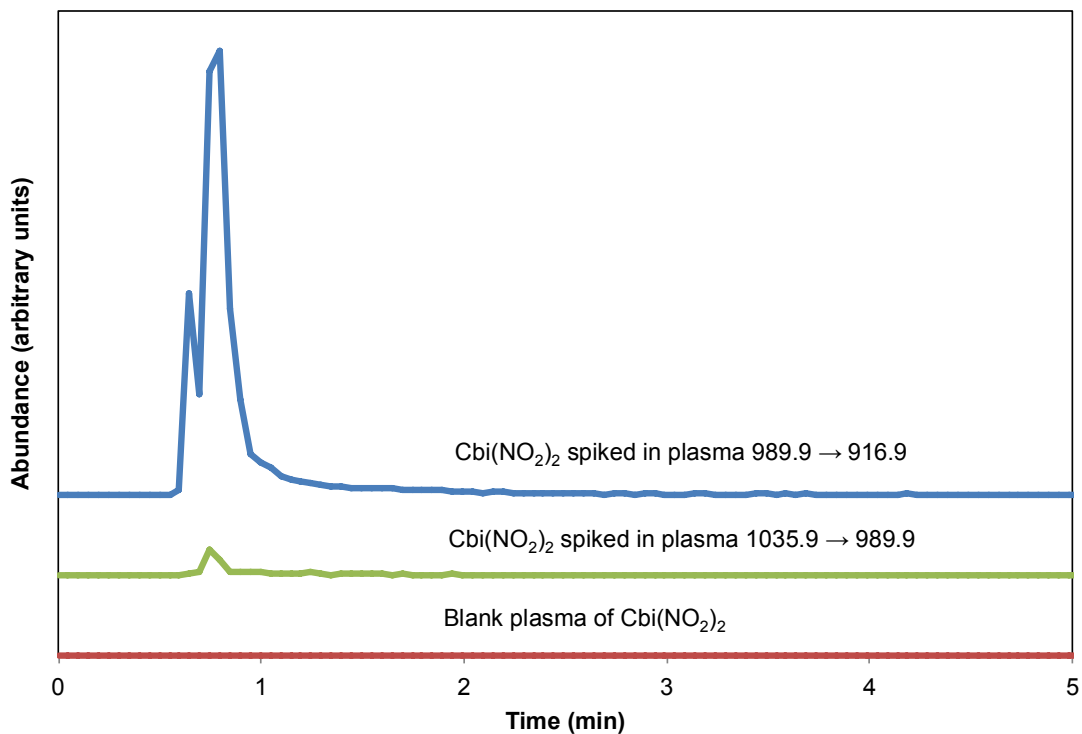


Figure III.13.5. Chromatograms of Cbi(NO₂)₂ eluting at 0.75 min, and Cbi eluting at 0.8 min spiked in swine plasma. The chromatograms represent the signal response of the MRM transitions of Cbi(NO₂)⁺ 1035.9 → 989.9 and Cbi 989.0 → 916.9 *m/z* and total ion chromatograph of the blank.

III.13.3.3. Determination of Total Cobinamide

Due to difficulty in detecting dinitrocobinamide, determination of the total concentration of cobinamide was attempted by adding excess cyanide. The excess cyanide should compete with other Cbi ligands and create one form of cobinamide (Cbi(CN)₂). Due to the strong affinity cyanide has for the cobalt atom of Cbi. Using the 3-MP and Cbi(CN)₂ MRMs, it was determined that both 3-MP and Cbi(CN)₂ can be detected simultaneously in rabbit plasma when excess cyanide is present (Figure III.13.6).

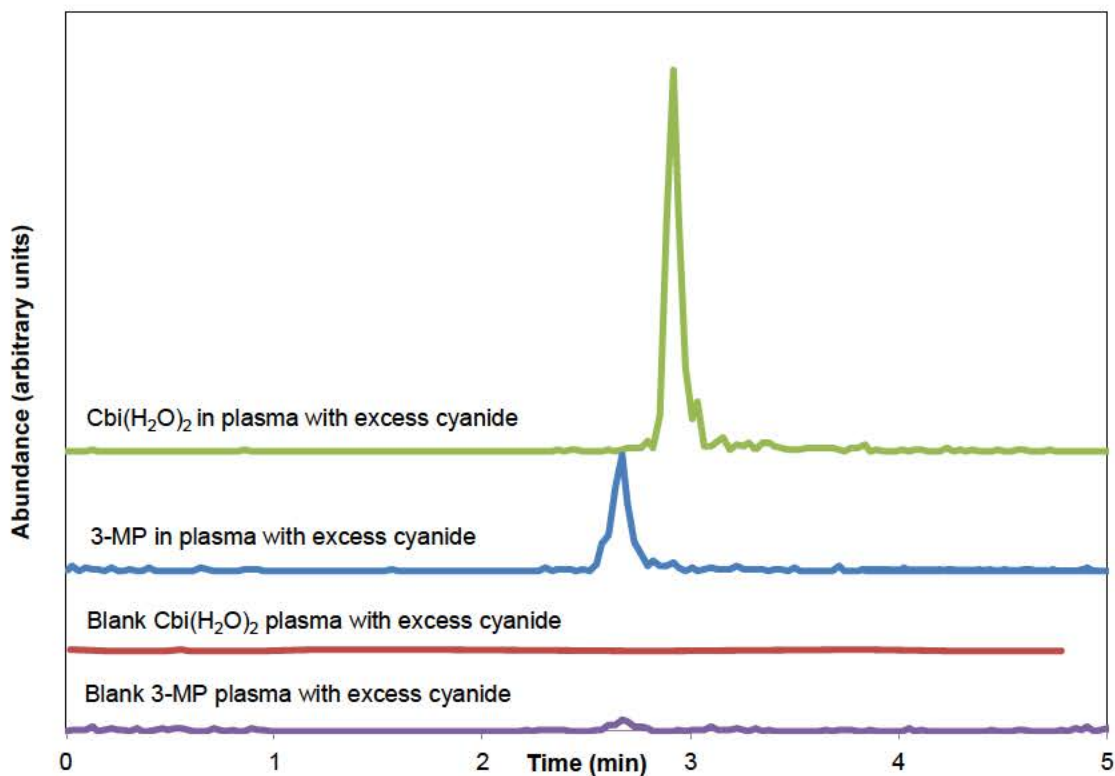


Figure III.13.6. Chromatograms of Cbi(CN)₂ eluting at 2.9 min and 3-MPB eluting at 2.67 min, in swine plasma. The chromatograms represent the signal response of the MRM transitions of Cbi(CN)₂ 1015.9-930.9 and 3-MP 311.0 → 223.1 *m/z*.

III.13.3.4. Determination of Total Cbi from Different Species of Cbi

For the determination of dicyanocobinamide, MRMs (1015.0 → 930.5 and 1015.9 → 988.9 *m/z*) were found by LC-MS-MS. Due to difficulty in detecting dinitrocobinamide, determination of the total concentration of cobinamide was attempted by adding excess cyanide. The excess cyanide should compete with other Cbi ligands and create one form of cobinamide (Cbi(CN)₂), due to the strong affinity cyanide has for the cobalt atom of Cbi. Using the 3-MP and Cbi(CN)₂ MRMs, it was determined that both 3-MP and Cbi(CN)₂ can be detected simultaneously in rabbit plasma when excess cyanide is present.

When 3x excess cyanide was added, a conversion ratio was determined by spiking $\text{Cbi}(\text{CN})_2$, $\text{Cbi}(\text{NO}_2)_2$, $\text{Cbi}(\text{H}_2\text{O})_2^{2+}$, or mix (1:1:1, $\text{Cbi}(\text{CN})_2:\text{Cbi}(\text{NO}_2)_2:\text{Cbi}(\text{H}_2\text{O})_2^{2+}$) (100 μL , 100 μM) into swine plasma. The cyanide was then added to convert all the species to $\text{Cbi}(\text{CN})_2$ (Figure III.13.7). When Cbi species were compared with $\text{Cbi}(\text{CN})_2$ standard, it was found that $\text{Cbi}(\text{NO}_2)_2$ had a 60% conversion, $\text{Cbi}(\text{H}_2\text{O})_2^{2+}$ had ~30% and mix ~90% conversion. Therefore, greater concentrations (10x) of cyanide were prepared.

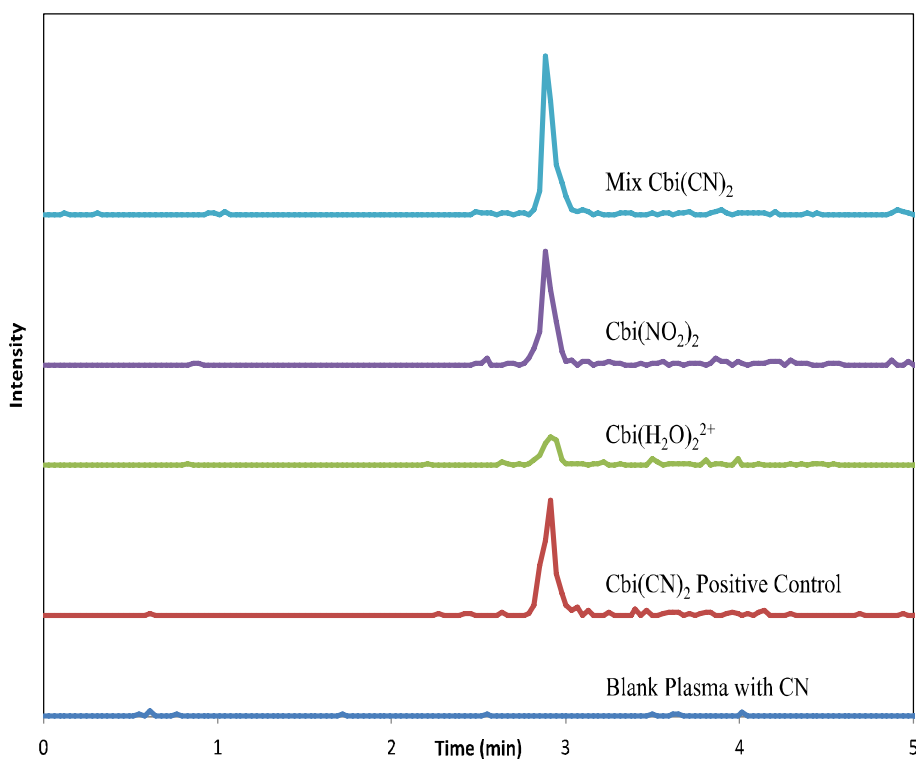


Figure III.13.7. Chromatograms of $\text{Cbi}(\text{CN})_2$ eluting at 2.95 min spiked in swine plasma.

With 10x cyanide, $\text{Cbi}(\text{NO}_2)_2$ conversion was ~100% and $\text{Cbi}(\text{H}_2\text{O})_2^{2+}$ was ~70%. Next, 3-MP stability was determined with Cbi species in the presence of excess cyanide. It was found that 3-MP did not degrade with excess cyanide when compared to 3-MP samples with no cyanide; all 3-MP samples were

100±15% when compared to the 3-MP standard (Figure III.13.8). Also, the conversion of Cbi's with 3-MP and excess cyanide for $\text{Cbi}(\text{NO}_2)_2$ was found to be ~100% and $\text{Cbi}(\text{H}_2\text{O})_2^{2+}$ at ~60%. The chromatograms of Cbi's being converted to $\text{Cbi}(\text{CN})_2$ with 3-MP are observed in Figure III.13.9. The lack of conversion for $\text{Cbi}(\text{H}_2\text{O})_2^{2+}$ indicates that a higher concentration of cyanide could bind to Cbi and release it from proteins increasing the conversion to $\text{Cbi}(\text{CN})_2$.

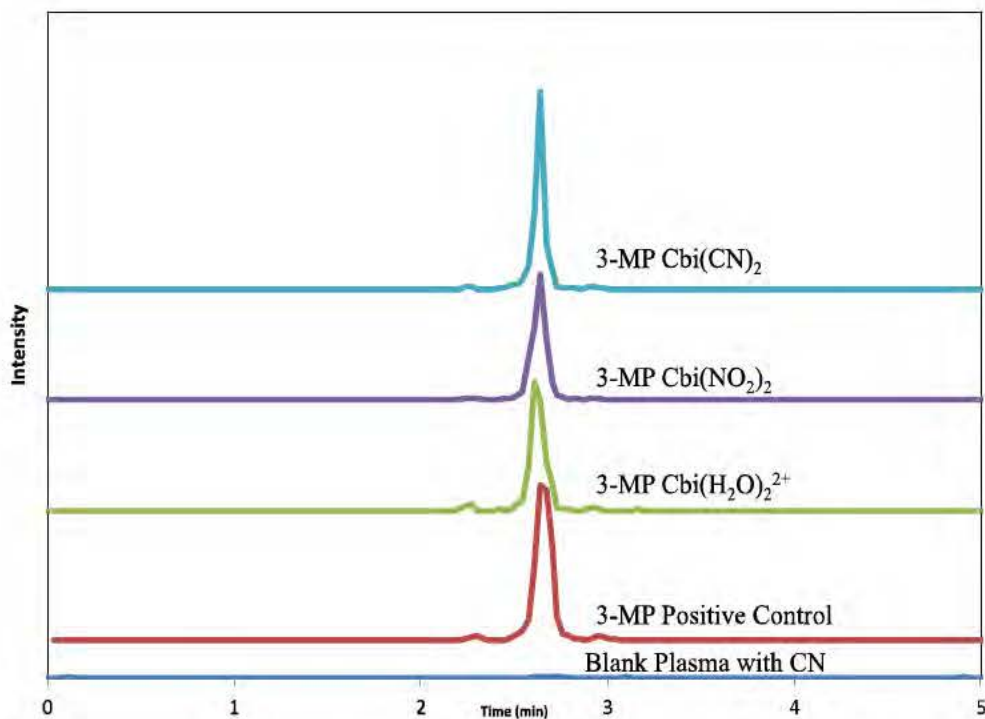


Figure III.13.8. The chromatograms represent the signal response of 3-MP, eluting at 2.67 min, in plasma with varying Cbi species and excess cyanide. The MRM transitions observed are 311-223 *m/z*.

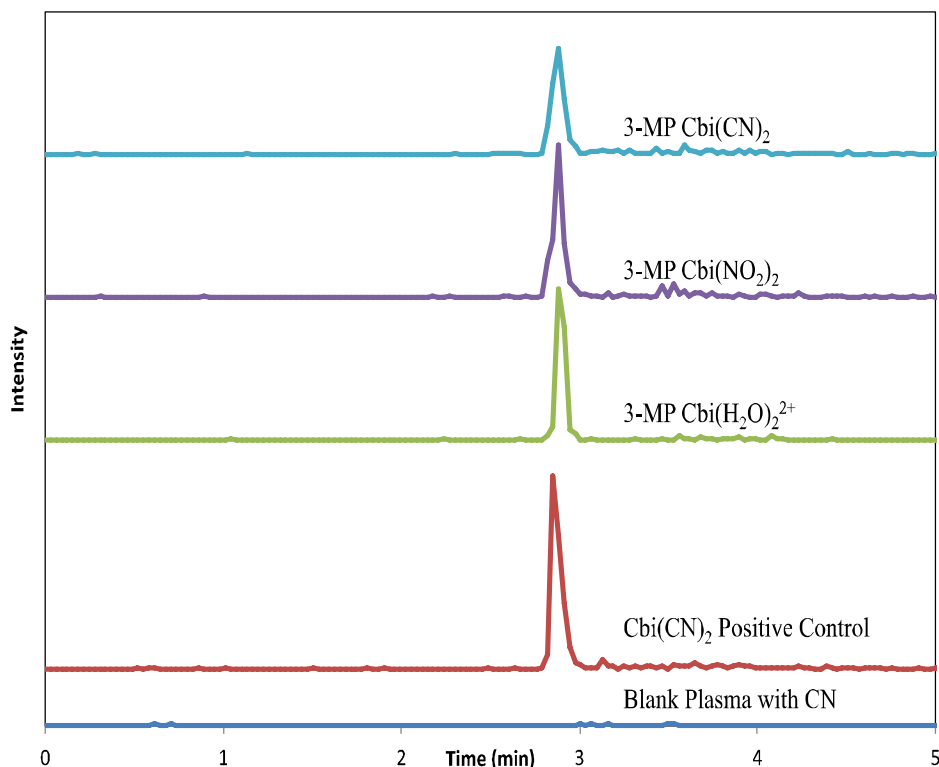


Figure III.13.9. Chromatograms of varying species of Cbi with 3-MP and excess cyanide after conversion to $\text{Cbi}(\text{CN})_2$ eluting at 2.9 min. The chromatograms represent the signal response of the MRM transitions of $\text{Cbi}(\text{CN})_2$ 1015.9-930.9 m/z.

III.13.4. Conclusion

A simple and robust analytical method to simultaneously determine Cbi and 3-MP is being developed. Both 3-MP and Cbi can be detected with high concentrations of cyanide. Various species of Cbi were found to be converted to $\text{Cbi}(\text{CN})_2$ for a total Cbi concentration.

III.13.5. Future Work

Synthesizing and determining the mass spec fragmentations of dinitrocobinamide ($\text{Cbi}(\text{NO}_2)_2$) and monocyano-mononitro-cobinamide ($\text{Cbi}(\text{NO}_2)(\text{CN})$) will be added to the method. The stability of aqueous and plasma

samples $\text{Cbi}(\text{NO}_2)_2$ and $\text{Cbi}(\text{NO}_2)(\text{CN})$ will need to be determined. Then the method can be fully validated.

III.13.6. References

1. Isom, G. E.; Borowitz, J. L.; Mukhopadhyay, S., Sulfurtransferase Enzymes Involved in Cyanide Metabolism. In *Comprehensive Toxicology*, McQueen, C., Ed. 2010; Vol. 4, pp 485-500.
2. Nagasawa, H. T.; Goon, D. J. W.; Crankshaw, D. L.; Vince, R.; Patterson, S. E., Novel, orally effective cyanide antidotes. *Journal of Medicinal Chemistry* **2007**, *50*, 6462-6464.
3. Brenner, M.; Kim, J. G.; Lee, J.; Mahon, S. B.; Lemor, D.; Ahdout, R.; Boss, G. R.; Blackledge, W.; Jann, L.; Nagasawa, H. T.; Patterson, S. E., Sulfanegen sodium treatment in a rabbit model of sub-lethal cyanide toxicity. *Toxicology and applied pharmacology* **2010**, *248* (3), 269-76.
4. Brenner, M.; Mahon, S. B.; Lee, J.; Kim, J.; Mukai, D.; Goodman, S.; Kreuter, K. A.; Ahdout, R.; Mohammad, O.; Sharma, V. S.; Blackledge, W.; Boss, G. R., Comparison of cobinamide to hydroxocobalamin in reversing cyanide physiologic effects in rabbits using diffuse optical spectroscopy monitoring. *Journal of Biomedical Optics* **2010**, *15* (1), 017001-017001.
5. Chan, A.; Balasubramanian, M.; Blackledge, W.; Mohammad, O. M.; Alvarez, L.; Boss, G. R.; Bigby, T. D., Cobinamide is superior to other treatments in a mouse model of cyanide poisoning. *Clinical Toxicology* **2010**, *48*, 709-717.

6. Chan, A.; Crankshaw, D. L.; Monteil, A.; Patterson, S. E.; Nagasawa, H. T.; Briggs, J. E.; Kozocas, J. A.; Mahon, S. B.; Brenner, M.; Pilz, R. B.; Bigby, T. D.; Boss, G. R., The combination of cobinamide and sulfanegen is highly effective in mouse models of cyanide poisoning. *Clinical Toxicology* **2011**, *49*, 366-373.
7. *Food and Drug Administration Guidance for industry bioanalytical method validation*. Rockville, MD, 2001.
8. Stutelberg, M. W.; Vinnakota, C. V.; Mitchell, B. L.; Monteil, A. R.; Patterson, S. E.; Logue, B. A., Determination of 3-mercaptopyruvate in rabbit plasma by high performance liquid chromatography tandem mass spectrometry. *Journal of Chromatography B* **2014**, *949-950*, 94-98.
9. Corley, J., Methods for defining LOD and LOQ. In *Handbook of Residue Analytical Methods for Agrochemicals*, John Wiley & Sons: 2002; Vol. 1 pp 63-71.

CHAPTER 14

DETERMINATION OF COBINAMIDE SULFITE AND ITS CYANO AND AQUO DERIVATIVES BY RP-HPLC-ESI-MS-MS.

Joseph K. Dzisam and Brian A. Logue

III.14.1. Introduction

Current treatments for cyanide exposure include three general classes of agents: methemoglobin generators (sodium nitrite, amyl nitrite, and dimethyl aminophenol), sulfur donors (sodium thiosulfate and glutathione), and direct binding agents (hydroxocobalamin and dicobalt edetate)³. While each type of treatment has been effective at countering the toxic effects of cyanide, each has major limitations, especially during mass casualty situations.

Methemoglobin generators oxidize hemoglobin in the red blood cells to produce methemoglobin¹⁰, a complex with high affinity for cyanide¹¹. However, production of methemoglobin leads to methemoglobinemia, which reduces oxygen transport in the erythrocytes and tissues¹². This is especially dangerous when smoke inhalation has occurred, causing carboxyhemoglobinemia concurrently with methemoglobinemia³. Sulfur donor antidotes detoxify cyanide by converting cyanide to thiocyanate with the help of sulfurtransferase enzymes (e.g., rhodanese and 3-mercaptopyruvate sulfurtransferase)¹³. However, sulfur donors are limited due to variable subcellular distribution of sulfurtransferase enzymes¹³. For example, rhodanese is concentrated in the mitochondrial matrix of the liver and kidney, but is not prevalent in the central nervous system³.

Thiosulfate, the only U.S. FDA-approved sulfur donor cyanide antidote, also has a disadvantage of slow uptake into cells. Other compounds, including 3-mercaptopyruvate, have been suggested as more efficient sulfur donors for cyanide therapy^{3,11,14,15}. Binding agents sequester cyanide from cytochrome c oxidase to effectively reduce the toxicity of cyanide. Hydroxocobalamin (Cob), the only U.S. FDA-approved binding agent^{16,17}, is relatively safe and effective³, but binds only one cyanide ion per molecule, and is a very high molecular weight molecule. Therefore, it requires large doses (i.e., approximately 4 to 5 g) and intravenous administration to be effective, limiting its use in mass casualty situations^{3,14}. Cobinamide (Cbi), the penultimate precursor in the hydroxocobalamin biosynthetic pathway^{3,18}, has been suggested as an effective cyanide binding agent. To date, studies have shown that Cbi is superior to other treatments, mainly due to its flexible administration and therapeutic index advantages^{19,20}. The greater effectiveness of Cbi is due to its extremely high affinity for cyanide [$K_{F, \text{overall}} = 10^{22} \text{ M}^{-1}$;^{14,18,20}], its ability to directly bind two cyanide ions, and its relatively high solubility^{14,18}. Depending on the pH and ligands present, cobinamide can exist in several forms in aqueous solution, such as diaquocobinamide, $[\text{Cbi}(\text{H}_2\text{O})_2]^{2+}$, hydroxo-aquocobinamide, $[\text{Cbi}(\text{OH})(\text{H}_2\text{O})]^+$ and dihydroxocobinamide, $[\text{Cbi}(\text{OH})_2]^0$ ²¹. Cobinamide itself exists predominantly as $[\text{Cbi}(\text{OH})(\text{H}_2\text{O})]^+$ at neutral pH, as $[\text{Cbi}(\text{H}_2\text{O})_2]^{2+}$ under acidic conditions, and as $[\text{CN}(\text{OH})_2]^0$ under basic conditions²². In the presence of cyanide, either the aquo or hydroxo ligands are replaced to produce

$[\text{Cbi}(\text{CN})(\text{H}_2\text{O})]^+$, $[\text{Cbi}(\text{CN})(\text{OH})]^0$, or $[\text{Cbi}(\text{CN})_2]^0$ ^{21,22} depending on the CN concentration and reaction time.

The multiple species of Cbi exhibit disparate kinetic, thermodynamic, and biological behavior. For example, the aquo and hydroxo forms of Cbi significantly bind to transcobalamin protein (TC), haptocorrin (HC), and intrinsic factors (IF), thereby substantially affecting their distribution ²³⁻²⁵. Several methods have been developed for the determination of the aqueous Cbi-cyanide system, including electrochemical, spectrophotometric, and chromatographic methods ^{14,18,21,26}. However, these methods lack the ability to simultaneously differentiate between all the species of Cbi of interest. Therefore, the development of a highly selective method for each Cbi species of interest with the appropriate sensitivity for biological analysis is necessary for the determination and elucidation of pharmacokinetic parameters, such as apparent volume of distribution, clearance, and bioavailability for each Cbi species. Such a method may help in the identification of more effective formulations of Cbi for treatment of cyanide poisoning, and toxicity induced by other small molecules (e.g., H_2S).

The objective of this project is to develop a single analytical method for the determination of multiple forms of cobinamide from biological fluids, to include $[\text{Cbi}(\text{H}_2\text{O})_2]^{2+}$, $[\text{Cbi}(\text{OH})_2]^0$, $[\text{Cbi}(\text{SO}_3)\text{Na}]^+$, $[\text{Cbi}(\text{CN})_2\text{Na}]^+$, $[\text{Cbi}(\text{CN})(\text{H}_2\text{O})]^+$, and $[\text{Cbi}(\text{NO}_2)_2]^0$.

III.14.2. MATERIALS AND METHODS

III.14.2.1. Materials

All reagents were LC grade, unless otherwise noted. Potassium cyanide, sodium cyanide, sodium sulfite, methanol, and ammonium hydroxide were all obtained from Fisher Scientific (Hanover Park, IL, USA). Sodium hydrosulfide hydrate and ammonium formate were supplied by Sigma-Aldrich (St. Louis, MO, USA). Formic acid was obtained from Thermo Scientific (Rockford, IL, USA). Water was purified to 18 mΩ-cm using a *Water PRO PS* system of purification (Labconco, Kansas City, KS, USA).

Aquohydroxocobinamide (pH = 6.18) was obtained from Dr. Gerry Boss, MD (Department of Medicine, University of California, San Diego, La Jolla, USA). A stock solution of 1 mM of the aquohydroxocobinamide was prepared by dissolving 99 mg into 100 mL of de-ionized water (0.99 mg/mL) in an amber bottle and stored at about 10 °C. Working solutions were obtained via serial dilution to the desired concentration.

III.14.2.2. Synthesis of cobinamide species

Monocyanocobinamide ($[\text{Cbi}(\text{CN})(\text{H}_2\text{O})]^+$ or $[\text{Cbi}(\text{CN})(\text{OH})]^0$) was prepared by reacting equi-molar amounts of the prepared cobinamide solution (1 mL, 1 mM) with potassium cyanide (51.3 mM, 19.5 μL). The dicyanocobinamide adduct ($[\text{Cbi}(\text{CN})_2]^0$) was formed when two-equivalents of KCN or NaCN was added to hydroxo-aquocobinamide at room temperature. To determine if a non-adducted $\text{Cbi}(\text{CN})_2$ could be analyzed by ESI-MS-MS, (i.e., the sodium or potassium molecular ion predominates when NaCN or KCN, respectively, are used to

synthesize $\text{Cbi}(\text{CN})_2$, a cyanide-capturing apparatus with two chambers separated by a hydrophobic porous frit (Figure II.4.1) was used to produce $\text{Cbi}(\text{CN})_2$ in the absence of potassium and sodium. Cobinamide sulfite was prepared by combining an equi-molar solution of sodium sulfite (4 mM, 125 μL) with cobinamide (500 mM, 1 mL), producing a final pH of 6.4. Additionally, cobinamide dihydrogensulfide, $\text{CbiS}(\text{S})_2$ was synthesized by reacting two and half equivalent moles of NaSH (50 mM, 50 μL) with 1 mole of cobinamide (1 mM, 1 mL).

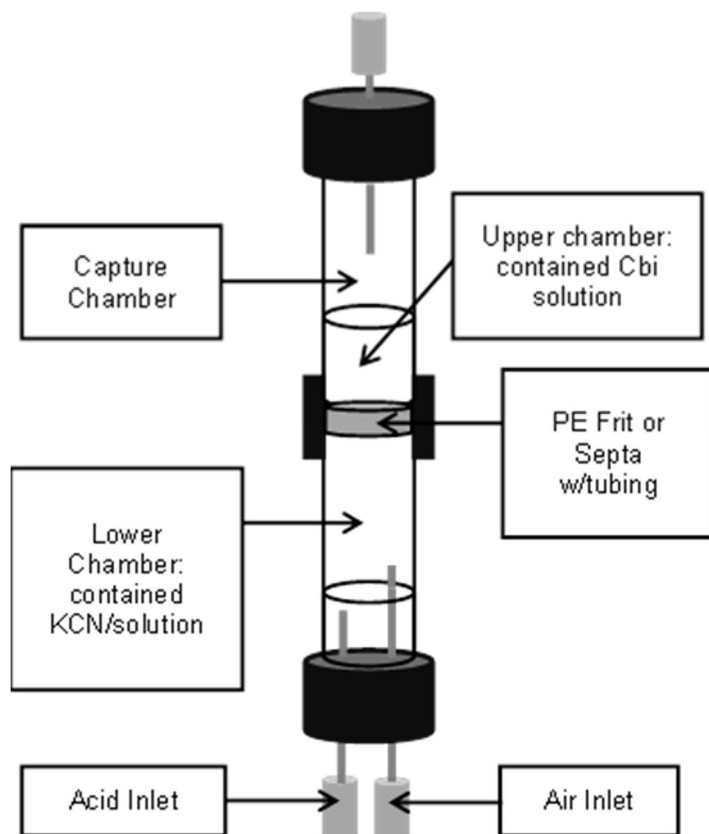


Figure III.14.1. Schematic of the cyanide apparatus used to create sodium- and potassium-free Cbi-cyanide species. The lower chamber contained KCN solution to which acid was added to generate HCN(g). Air was bubbled through the lower chamber via the air injection syringe to deliver HCN(g) to cobinamide solution in the upper chamber.

III.14.3.3. Differentiation of the aquo-hydroxo cobinamide species

To verify the assignment of molecular ions of $[\text{Cbi}(\text{H}_2\text{O})_2]^{2+}$, $[\text{Cbi}(\text{OH})(\text{H}_2\text{O})]^+$, and $[\text{Cbi}(\text{OH})_2]^0$ species, a cobinamide solution was prepared at different pHs and mass spectra of the resulting solutions were gathered to identify the major species at each pH. Solutions of Cbi (55 μM) with pHs from 2 to 12 were prepared by titration. Acid solutions were prepared with formic acid, and basic solutions were titrated with ammonium hydroxide. The species were then analyzed by MS-MS in positive mode. The trend of intensities of each solution was analyzed for one day, three days, and five days.

III.14.3.4. Sample preparation of Cbi species for HPLC-MS-MS analysis

Aqueous Cbi standards were prepared, and to each 1 mL, 300 μL of acetone was added. The mixture was then centrifuged for 30 minutes at 13,100 rpm (16,500 \times g). The supernatant (250 μL of it) was pipetted into a 4 ml vial and dried with N_2 gas. Dried samples were reconstituted with 100 μL of 10%

methanol and 90% 5 mM aqueous ammonium formate and filtered through a 0.22 µm filter prior to HPLC-MS-MS analysis. Plasma samples were spiked with a 1:10 aqueous analyte to plasma matrix ratio, and were prepared by the processes enumerated above.

III.14.3.5. Initial MS-MS analysis

All mass spectrometric analysis was performed by an AB Sciex Q-Trap 5500 MS (Applied Biosystems, Foster City, CA, USA) with electrospray ionization in positive mode. Mass spectra were acquired by direct infusion of aqueous Cbi solutions (10 µL/ min) with scans of MS1 from 200-1200 Da over 1.6 minutes. Product ion scans were completed using both MS1 and MS3. The entrance orifice potential was 180 Volts, and curtain gas 1 and ion source gas 1 were operated at 14 and 20 psi, respectively. The ion spray voltage was 4500 V with a temperature of 500 K. Optimized MRM parameters are presented in Table III.14.1.

Table III.14.1. MRM ions and associated parameters corresponding to some Cbi forms of interest.

Compound	MS1(m/z Da)	MS3(m/z Da)	CE(Volts)	DP(Volts)
[CbiSO ₃ Na] ⁺	1092.8	989.9	65.01	71.22
	1092.8	930.9	96.67	234.01
[Cbi(CN) ₂ Na] ⁺	1064.9	1010.8	49.43	266.54
	1064.9	930.8	97.47	263.1
[Cbi(OH)(CN)] ⁰ /	1031.6	946.7	79.38	65.01
[Cbi(CN)(H ₂ O)] ⁺	1031.6	875.6	80.91	180.95
[Cbi(H ₂ O) ₂] ²⁺	1024.5	930.8	74.58	36.54
	1024.5	949.7	66.03	198.59
	1025.8	931.7	70.71	261.64
[Cbi(OH) ₂] ⁰	1022.7	961.8	65.16	201.56
	1022.7	946.8	72.02	229.81
[Cbi(S) ₂] ⁰	1053.6	989.7	57.32	193.4
	1053.6	930.7	86.91	172.63
	1053.6	916.7	95.62	186.09
[Cbi(S)(OH)] ⁰	1037.8	989.7	58.55	194.21
	1037.8	930.7	95.98	170.92
	1037.8	916.7	83.23	182.78

III.14.3.6. HPLC-MS-MS analysis

High-performance liquid chromatography-tandem mass spectrometry (HPLC-MS-MS) was conducted on a Shimadzu HPLC (LC-20AD, Shimadzu Corp., Kyoto, Japan) coupled to the AB Sciex Q-Trap 5500 MS. Samples were separated on a Synergi 4 μ RP-Max (2.00 x 50mm) reversed-phase column (Phenomenex, Torrance, CA, USA). Mobile phase A contained 10% methanol and 90% 5 mM ammonium formate, and mobile phase B contained 10% 5 mM aqueous ammonium formate in 90 % methanol, gradient elution was used with the initial mobile phase (0% B) linearly increased to 100% B over 3 minutes, held constant for 0.5 minutes, and linearly decreased to 0% over 1.5 minutes at a flow rate of 0.25 mL/minutes.

III.14.3.7. Data analysis section: limit of detection of [Cbi(OH)₂]⁰

From the pH studies, Cbi species of pH 11 with concentrations 0.5, 1, 5, 10, 20, 50, and 100 μ M, respectively, were prepared, allowed to stabilize for 3 days before HPLC-MS-MS analysis was conducted. The resultant data from the chromatograms (depicted in Figure II.3.4.6) were used to estimate the limit of detection at S/N = 3.

III.14.3.8. Synthesis of cobinamide species

Monocyanocobinamide ([Cbi(CN)(H₂O)]⁺ or [Cbi(CN)(OH)]⁰) was prepared by reacting equi-molar amounts of the prepared cobinamide solution (1 mL, 1 mM) with potassium cyanide (51.3 mM, 19.5 μ L). The dicyanocobinamide adduct ([Cbi(CN)₂]⁰) was formed when two molar-equivalents of KCN or NaCN

was added to hydroxoaquocobinamide at room temperature. To determine if a non-adducted Cbi(CN)₂ could be analyzed by ESI-MS-MS, (i.e., the sodium or potassium molecular ion predominates when NaCN or KCN, respectively, are used to synthesize Cbi(CN)₂), a cyanide-capturing apparatus with two chambers separated by a hydrophobic porous frit was used to produce Cbi(CN)₂ in the absence of potassium and sodium. Cobinamide sulfite was prepared by combining an equi-molar solution of sodium sulfite (4 mM, 125 μL) with cobinamide (500 mM, 1 mL), producing a final pH of 6.4. Additionally, cobinamide dihydrogensulfide, CbiS(S)₂, was synthesized by reacting two and half molar equivalent of NaSH (50 mM, 50 μL) with 1 mole of cobinamide (1 mM, 1 mL).

III.14.3.9. Sample preparation of Cbi species for HPLC-MS-MS analysis

Aqueous Cbi standards were prepared, and to each 1 mL, 300 μL of acetone was added. The mixture was then centrifuged for 30 minutes at 13,100 rpm (16,500 x g). The supernatant (250 μL) was pipetted into a 4 ml vial and dried with N₂ gas. Dried samples were reconstituted with 100 μL of 10% methanol and 90% 5 mM aqueous ammonium formate and filtered through a 0.22 μm filter prior to HPLC-MS-MS analysis. Plasma samples were spiked with a 1:10 aqueous analyte to plasma matrix ratio, and were prepared by the processes enumerated above.

III.14.3.10. Data analysis section: limit of detection of [Cbi(OH)₂]⁰

From the pH studies, Cbi species at pH 11 with concentrations of 0.5, 1, 5, 10, 20, 50, and 100 μM , respectively, were prepared and allowed to stabilize for 3 days before HPLC-MS-MS analysis was conducted. The resultant chromatogram in Figure II.3.4-1 was used to estimate the limit of detection.

III.14.3.11. Synthesis of Cobinamide Species

Monocyanocobinamide ($[\text{Cbi}(\text{CN})(\text{H}_2\text{O})]^+$ or $[\text{Cbi}(\text{CN})(\text{OH})]^0$) was prepared by reacting equi-molar amounts of the prepared cobinamide solution (1 mL, 1 mM) with potassium cyanide (51.3 mM, 19.5 μL). The dicyanocobinamide adduct ($[\text{Cbi}(\text{CN})_2]^0$) was formed when two molar-equivalents of KCN or NaCN was added to hydroxo-aquocobinamide at room temperature. To determine if a non-adducted $\text{Cbi}(\text{CN})_2$ could be analyzed by ESI-MS-MS, (i.e., the sodium or potassium molecular ion predominates when NaCN or KCN, respectively, are used to synthesize $\text{Cbi}(\text{CN})_2$), a cyanide-capturing apparatus with two chambers separated by a hydrophobic porous frit was used to produce $\text{Cbi}(\text{CN})_2$ in the absence of potassium and sodium. Cobinamide sulfite was prepared by combining an equi-molar solution of sodium sulfite (4 mM, 125 μL) with cobinamide (500 mM, 1 mL), producing a final pH of 6.4. Additionally, cobinamide dihydrogensulfide, $\text{Cbi}(\text{S})_2$, was synthesized by reacting two and half molar equivalents of NaSH (50 mM, 50 μL) with 1 mole of cobinamide (1 mM, 1 mL). Dinitrocobinamides were synthesized by reacting four molar equivalents of sodium nitrate (4 mM, 1 mL) with 1 mole of cobinamide (1 mM, 1 mL).

III.14.3.12. Synthesis of Internal Standard

Three molar equivalents of isotopically labelled $K^{13}C^{15}N$ dissolved in 10 mM NaOH was reacted with cobinamide to form $[Cbi(^{13}C^{15}N)_2]$, for use as an internal standard. The integrity of the internal standard was verified using solid phase extraction (SPE) and subsequent fluorometric analysis to determine the concentration of 'free' cyanide in the internal standard. A hydrophobic lipophilic balance (HLB) column (1 ml) was used for SPE with 100% methanol as the elution solvent. A Flouromax-4 spectrofluorometer (Horiba Scientific, USA) was used for the spectrofluorometric determination with NDA/Taurine as reagents. A tube volume each of 100 % water and methanol was used for conditioning the SPE column prior to the introduction of the 100 μ M of the analyte (the internal standard). The 'load' was collected, and the equivalent tube volume of water was used for first and second washes respectively. A tube volume of 100 % methanol was used for elution. For the flourometric analysis, 100 μ M of NaCN dissolved in 10 mM NaOH was used as the 'standard' whiles the blank was 0.01 M of NaOH. Aliquots (300 μ L each) of NDA (4 mM) and taurine (50 mM) were added to 100 μ L of the standard, blank, load, washes (1 and 2), and elution. One mL of 0.1M NaOH was subsequently added to each aliquot. The excitation wavelength was set at 410 nm with a 3 nm slit window while the emission was scanned from 425 nm to 600 nm, also with a slit window at 3 nm. The maximum emission was 481 nm.

III.14.3.13. HPLC-MS-MS Analysis at 40% B

High-performance liquid chromatography-tandem mass spectrometry (HPLC-MS-MS) was conducted on a Shimadzu HPLC (LC-20AD, Shimadzu Corp., Kyoto, Japan) coupled to the AB Sciex Q-Trap 5500 MS. Samples were separated on a Synergi 4 μ RP-Max (2.00 x 50mm) reversed-phase column (Phenomenex, Torrance, CA, USA). Mobile Phase A contained 10% methanol and 90% 5 mM ammonium formate, and Mobile Phase B contained 10% 5 mM aqueous ammonium formate in 90% methanol. Gradient elution was used with the initial mobile phase (40% B) linearly increased to 100% B over 3 minutes, held constant for 0.5 minutes, and linearly decreased to 40% over 1.5 minutes at a flow rate of 0.25 mL/min.

III.14.3.14. Determination of limit of detection of [Cbi(NO₂)₂]

In order to determine the limit of detection of [Cbi(NO₂)₂], a solution of the analyte with concentrations of 0.5, 2, 5, 10, and 20 μ M were prepared and analyzed via the method outline below.

III.14.3.15. Investigation of peaks in blank plasma, and stability of analyte in pH medium

In order to verify the origin of the peaks in the blank, we put forth two hypotheses: that it could be due to a contaminant or an interferent or both. If the plasma were to be 'contaminated' with cobinamide, then addition of cyanide to the plasma should yield cyanide derivatives of cobinamide. Blank plasma and CN (8 mM, 100 μ L) spiked in plasma were run in triplicates to verify the presence

of cyanide derivative. A positive control of the cyanide analogues of cobinamide, $[\text{Cbi}(\text{CN})(\text{NO}_2)]^0$ and $[\text{Cbi}(\text{CN})_2]^0$ were also prepared in triplicates and analyze alongside with that of the blanks. Also, the stability of $[\text{Cbi}(\text{NO}_2)_2]$ in different pH media were also verified by preparing various solutions of $[\text{Cbi}(\text{NO}_2)_2]$ (80 μM) in a neutral medium, basic medium (using ammonium hydroxide, pH 9.56) and acidic medium (formic acid used, final pH 3.68). The analyte at the various pH solutions were analysed immediately and after 1 hour, so as to verify their stability.

III.14.3.16. Sample preparation of Cbi species for HPLC-MS-MS analysis for 40%B

Plasma samples were spiked with a 1:10 aqueous analyte to plasma matrix ratio, and were prepared by adding 100 μL of the aqueous Cbi standards and 900 μL of plasma. To each 100 μL of spiked plasma samples, 300 μL of acetone was added to precipitate the proteins in the plasma. The mixture was then centrifuged for 20 minutes at 13,100 rpm (16,500 x g). The supernatant (150 μL) was pipetted into a 4 mL vial and dried with N_2 gas. Dried samples were reconstituted with 100 μL of 40% Mobile phase B and 60 % Mobile phase A, and filtered through a 0.22 μm filter prior to HPLC-MS-MS analysis.

III.14.4. RESULTS AND DISCUSSION

III.14.4.1. MS analysis of Cbi species

Table III.14.1 shows the masses, collision energies and declustering potentials of the MRM transitions of some cobinamide species of interest, and Figure III.14.2 shows an example mass spectrum of cobinamide-sulfite. The transition for cobinamide-sulfite was not present, but the sodium adduct, $[\text{CbiSO}_3\text{Na}]^+$, was easily seen at 1092.5. The molecular ion of the sodium adduct was used to identify transitions of interest for MS-MS. The appearance of a sodium adduct was not surprising, considering analysis of hydroxocobalamin by LCMSMS also utilized a sodium adduct ²⁷.

Transitions for each of the other Cbi species of interest were determined and optimized in a similar fashion. The identified molecular ion at 1031.6 m/z (Table III.14.1), representing $[\text{Cbi}(\text{OH})(\text{CN})]^0$ or $[\text{Cbi}(\text{CN})(\text{H}_2\text{O})]^+$, was not initially identified in a 1:1 molar solution of Cbi and CN^- . After the solution was allowed to stand for four weeks, the monocyano-Cbi species was identified. The most probable explanation for this observation is facile kinetic formation of $[\text{Cbi}(\text{CN})_2]^0$, but ultimate thermodynamically favorable formation of $[\text{Cbi}(\text{OH})(\text{CN})]^0$ and/or $[\text{Cbi}(\text{CN})(\text{H}_2\text{O})]^+$ ^{21,22}.

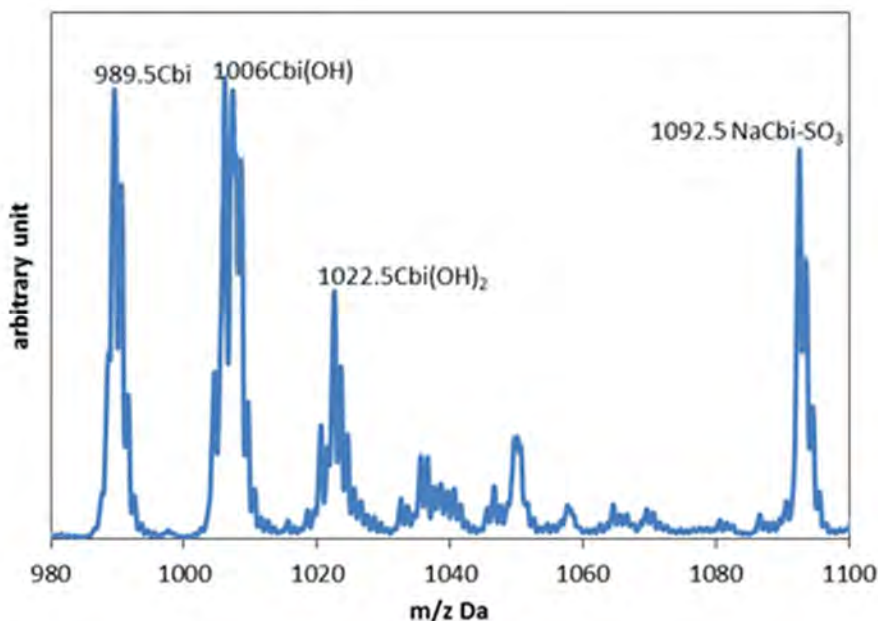


Figure III.14.2. Mass spectrum of cobinamide-sulfite. The sodium adduct, $[\text{CbiSO}_3\text{Na}]^+$, is clearly observed at 1092.5 m/z.

III.14.4.2. Differentiation of aquo and hydroxo Cbi Species

Because the Cbi aquo-hydroxo species, $[\text{Cbi}(\text{OH})(\text{H}_2\text{O})]^+$, $[\text{Cbi}(\text{H}_2\text{O})]^{2+}$, and $[\text{Cbi}(\text{OH})_2]^0$, differ by only 3 mass units, abundant stable isotopes of these species may be mistakenly assigned to different Cbi species (Figure III.14.3). Because the mass spectral peaks cannot be definitely assigned by mass alone, the mass spectral behavior of the 1022-1027 region was analyzed at multiple pH values. Figure III.14.4 shows a plot of fraction of the MS intensities versus the pH of cobinamide solutions prepared at pH 2-12. The figure shows a strong correlation between 1024.5, 1025.5 and 1026.5 over the pH range studied, suggesting that these ions are isotopic forms of the $[\text{Cbi}(\text{H}_2\text{O})]^{2+}$ species. A similar correlation was seen for ions 1022.5 and 1023.5, which were assigned to

$[\text{Cbi}(\text{OH})_2]^0$. Also, the results show that the Cbi solutions in the pH media are thermodynamically stable three days after preparation (i.e., Day 3).

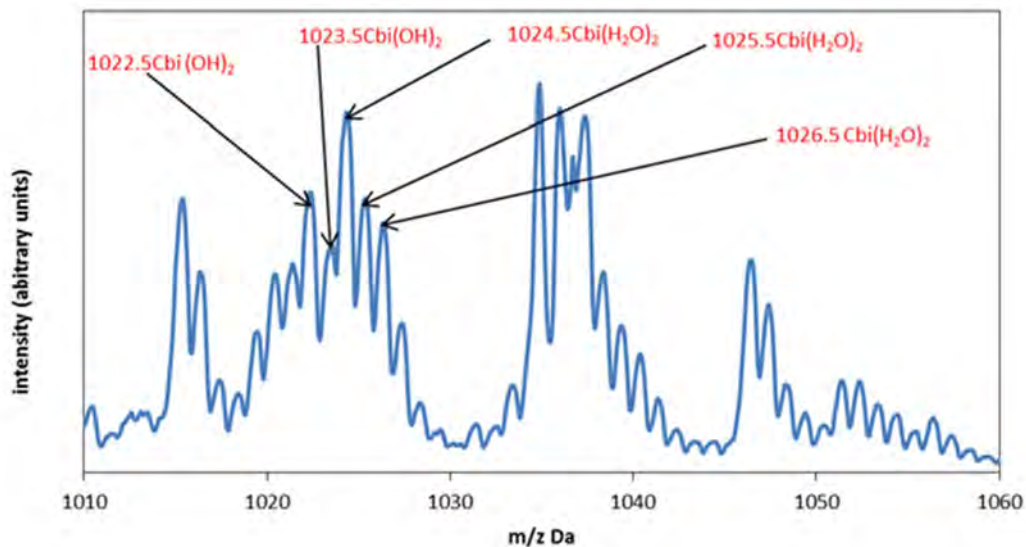
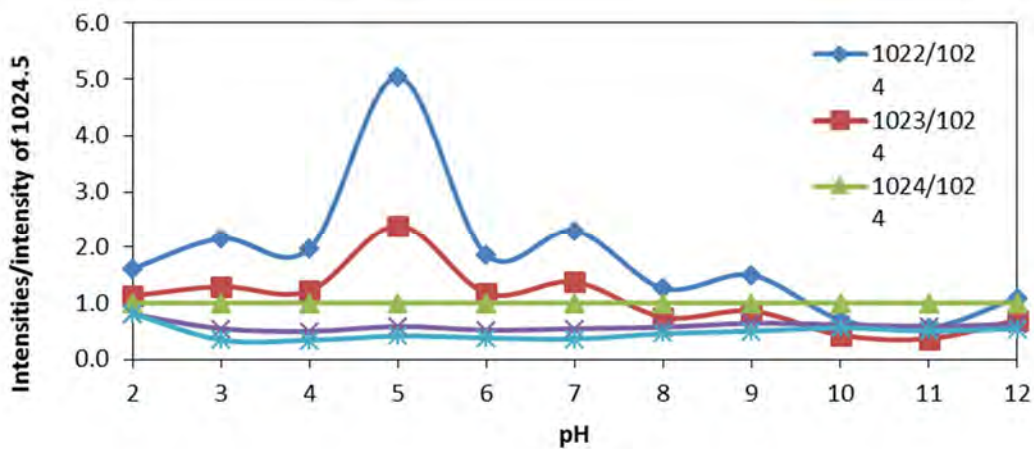


Figure III.14.3. Mass spectra of aquo- and hydroxo- Cbi species with tentative assignment of the peaks at 1022.5-1026.5.



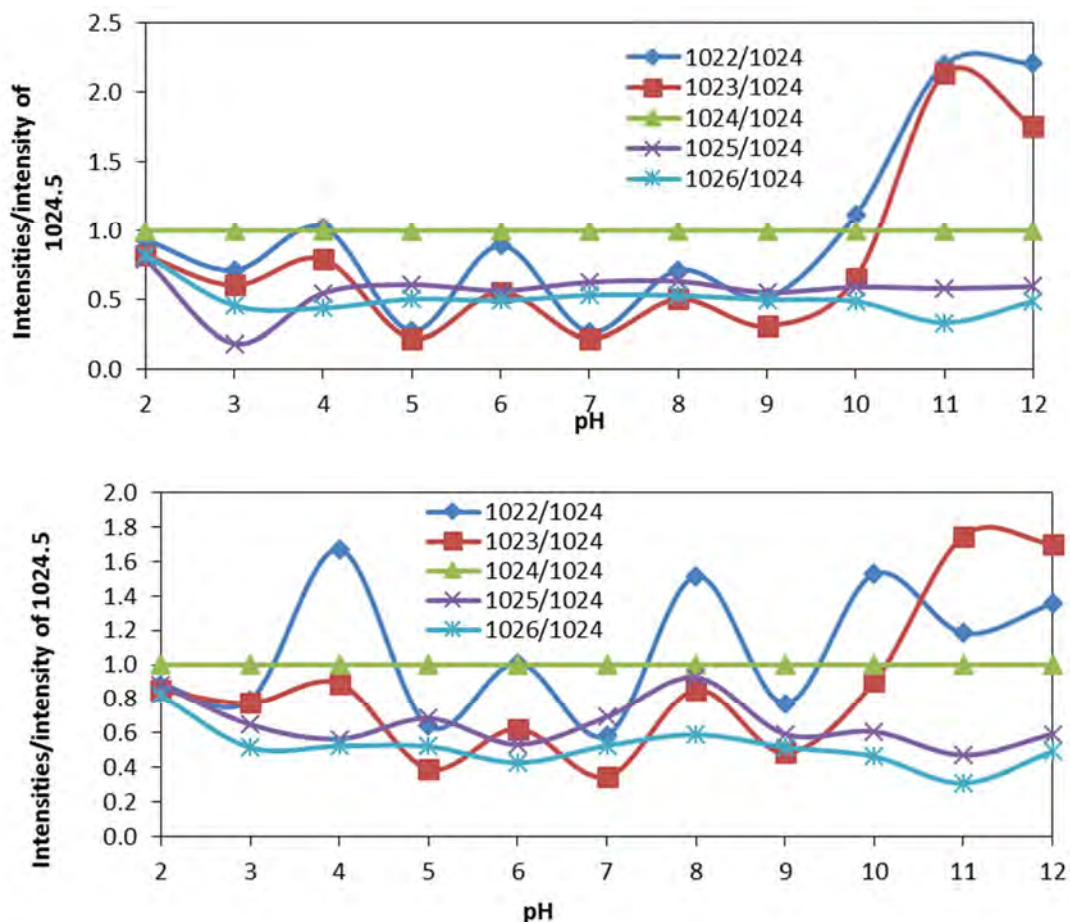


Figure III.14.4. Plots of intensities of 1022.5, 1023.5, 1024.5, 1025.5 and 1026.5 divided by the intensity of 1024.5. **A, B and C** were conducted in Days 1, 3 and 5, respectively. The trend reveals a direct correlation between 1024.5 (green), 1025.5 (purple) and 1026.5 (light blue). Similarly, 1022.5 (deep blue) and 1023.5 (red) are also correlated. The correlation shows isotopic relations. Day 1 and 5 solutions were not thermodynamically stable, but Day 3 solutions were very stable, as they showed the trends of the Cbi species at the expected pH values.

III.14.4.3. HPLC-MS-MS analysis

Initially, $[\text{Cbi}(\text{H}_2\text{O})_2]^{2+}$ was separated via the HPLC both in aqueous solution and in plasma, eluting at around 2.80 minutes (Figure III.14.5). The chromatogram shown in the lower portion (blue) in Figure III.14.5 is the Cbi sample in aqueous solution (100 μM), and the upper chromatogram (red) shows Cbi solution spiked into plasma matrix at a ratio of 1:10 (100 μM).

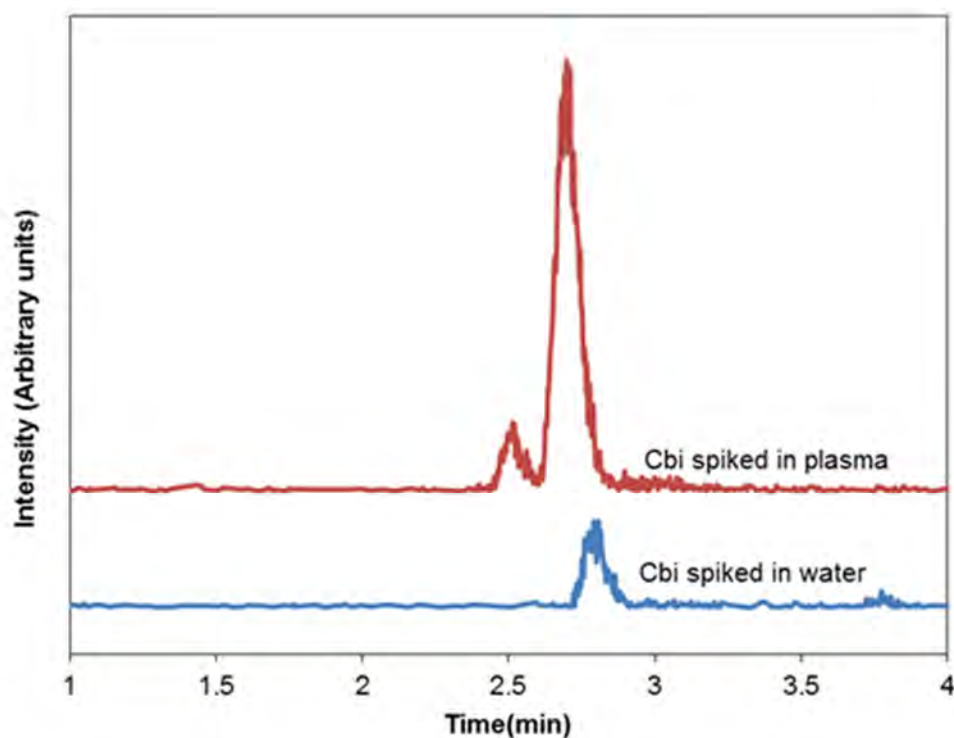


Figure III.14.5. Chromatograms showing the elution of diaquocobinamide(100 μM) from the LC column in water (blue) and in plasma (red). LC conditions: mobile phase A ; 90 % 5 mM ammonium formate and 10 % methanol, mobile phase B has 90% methanol and 10% ammonium formate (5 mM). MS transition: 1024.4 \rightarrow 930.5.

From the pH studies, Cbi species of pH 11 with concentrations 0.5, 1, 5 10, 20, 50, and 100 μM , respectively, were prepared, allowed to stabilize for 3 days, and the detection limit of $[\text{Cbi}(\text{OH})_2]^0$ was determined to be 5 μM (Figure III.14.6).

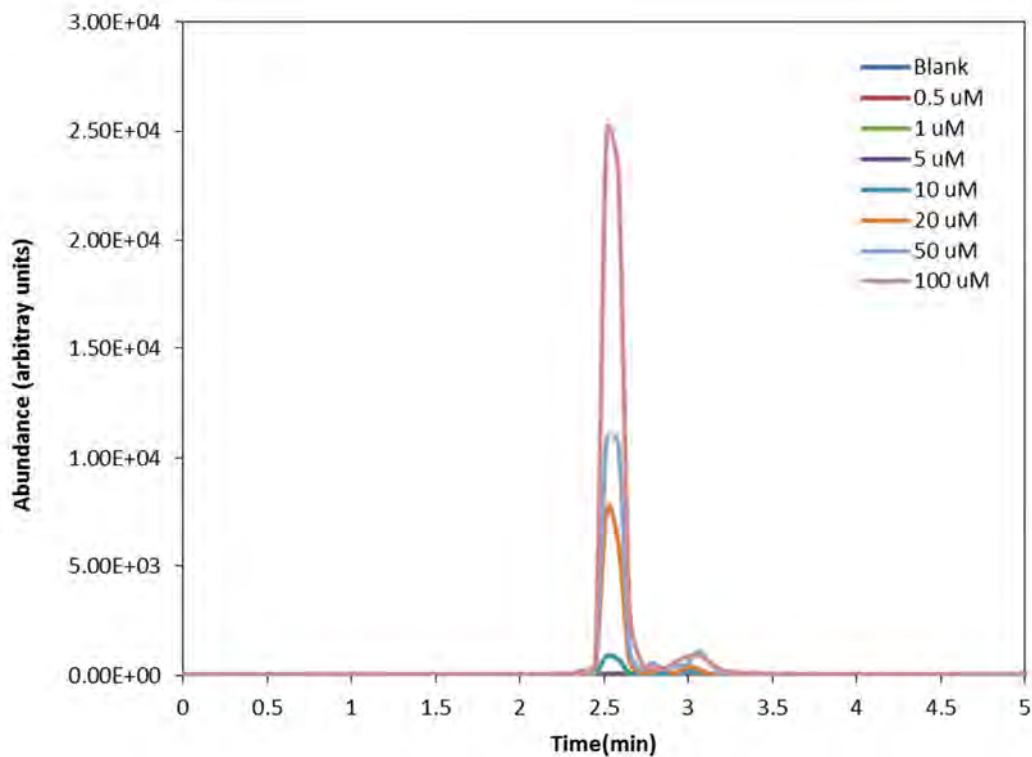


Figure III.14.6. Chromatogram of Cbi species prepared at pH 11 after 3 days. LC conditions were as described earlier. MS transition: 1022.7 → 946.8.

Similarly, $[\text{Cbi}(\text{S})_2]^0$ and $[\text{Cbi}(\text{S})(\text{OH})_2]^0$ were also seen to exhibit thermodynamic stability after 24 hours of preparation. Determination of the limits of detection of the $[\text{Cbi}(\text{S})_2]^0$ and $[\text{Cbi}(\text{S})(\text{OH})_2]^0$ were not readily quantifiable by signal-to-noise ratio of 3 (Figure III.14.7). Another procedure involving the use of root mean square error, RMSE²⁸ will be used to find the detection limits of $[\text{Cbi}(\text{S})_2]^0$ and $[\text{Cbi}(\text{S})(\text{OH})_2]^0$.

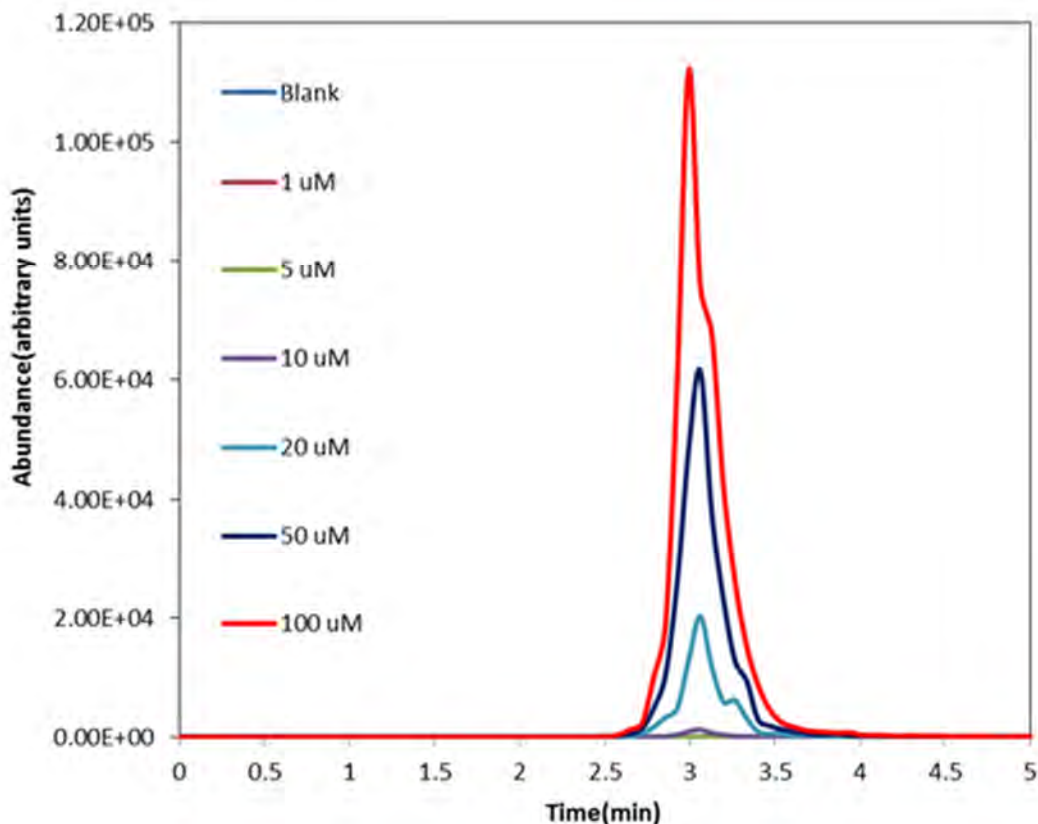


Figure III.14.7. Chromatogram of $[\text{Cbi}(\text{S})_2]^0$ transition $1053 \rightarrow 916$. LC Conditions were as described above.

III.14.4.4. MS analysis of Cbi species

Table III.14.2 shows the masses, collision energies, and declustering potentials of the MRM transitions of some cobinamide species of interest. The identified molecular ion at 1031.6 m/z (Table III.14.2), representing $[\text{Cbi}(\text{OH})(\text{CN})]^0$ or $[\text{Cbi}(\text{CN})(\text{H}_2\text{O})]^+$, was not initially identified in a 1:1 molar solution of Cbi and CN^- . After the solution was allowed to stand for four weeks, the monocyano-Cbi species was identified. The most probable explanation for this observation is facile kinetic formation of $[\text{Cbi}(\text{CN})_2]^0$, but ultimate

thermodynamically favorable formation of $[\text{Cbi}(\text{OH})(\text{CN})]^0$ and/or $[\text{Cbi}(\text{CN})(\text{H}_2\text{O})]^+$

21,22

III.14.4.5. Detection limit of $[\text{Cbi}(\text{OH})_2]^0$

Figure III.14.8 shows the overlaid chromatograms of $[\text{Cbi}(\text{OH})_2]^0$ at pH 11 at concentrations of 0.5, 1, 5, 10, 20, 50, and 100 μM . The detection limit was 10 μM (purple color) with an elution time of 2.58 minutes.

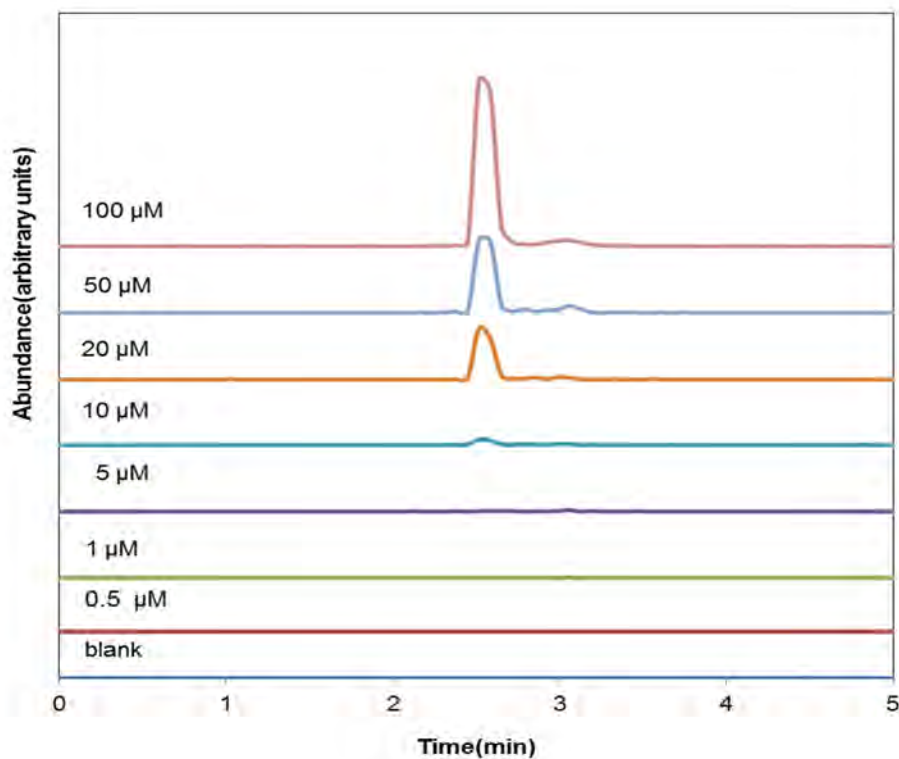


Figure III.14.8. Overlaid chromatograms of Cbi species prepared at pH 11 after 3 days. LC conditions were as described earlier. MS transition: $m/z = 1022.7 \rightarrow 946.8$.

III.14.4.6. Detection limit of $[\text{Cbi}(\text{S})_2]^0$

The detection limit of $[\text{Cbi}(\text{S})_2]^0$ was not easily quantified by signal-to-noise ratio of 3 (Figure III.14.4.8). The method of the root mean square error, RMSE²⁹, was used to determine the detection limit of $[\text{Cbi}(\text{S})_2]^0$ in aqueous solution as 6 μM . The $[\text{Cbi}(\text{S})_2]^0$ solutions were seen to be thermodynamically stable within 24 hours of preparation (Figure III.14.4.9).

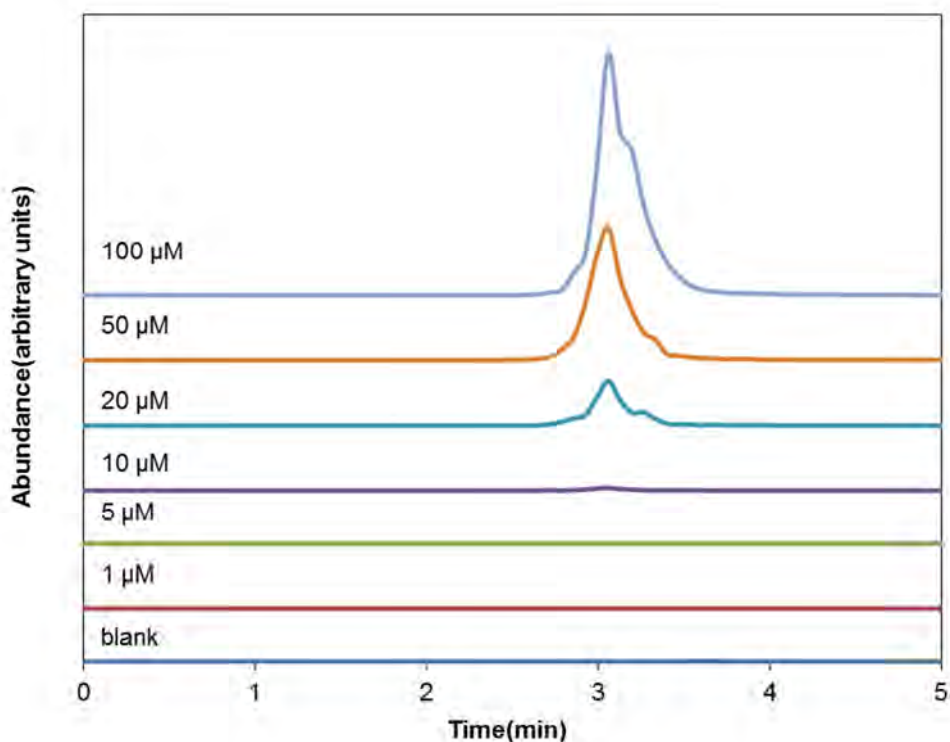


Figure III.14.9. Overlaid chromatograms of $[\text{Cbi}(\text{S})_2]^0$ at transition $m/z = 1053 \rightarrow 916$. LC conditions were as described above.

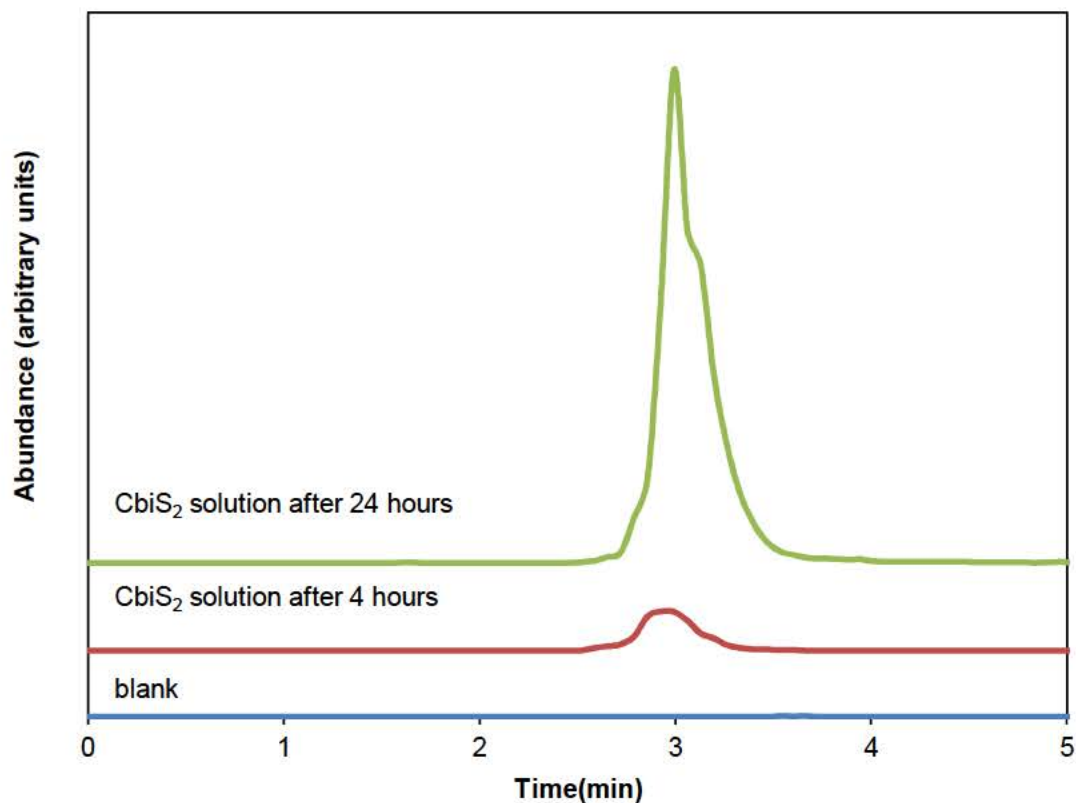


Figure III.14.10. Overlaid chromatograms of [CbiS₂]. The solution prepared in aqueous medium (100 μM) became thermodynamically stable within 24 hours (blue chromatogram is blank). The intensity for the solution prepared within 4 hours (red) was not as much as that for the 24 hour period (green).

Validation of the method for the detection of [CbiS₂] was initially performed in aqueous medium, but results from swine plasma suggest the need for further clean-up steps to refine the shape of peaks and transitions observed, as peaks for the transitions of $m/z = 1053 \rightarrow 916$, $1053 \rightarrow 930$, and $1053 \rightarrow 989$ were not easily resolved. However, peaks for the transition $m/z = 1092 \rightarrow 989$ were conspicuously seen as being resolved (Figure III.14.4.10). Further investigation is on-going to verify the chemical identity of the species, as well as the correlation(s) with the transitions $m/z = 1053 \rightarrow 989$ and $1092 \rightarrow 989$, if any.

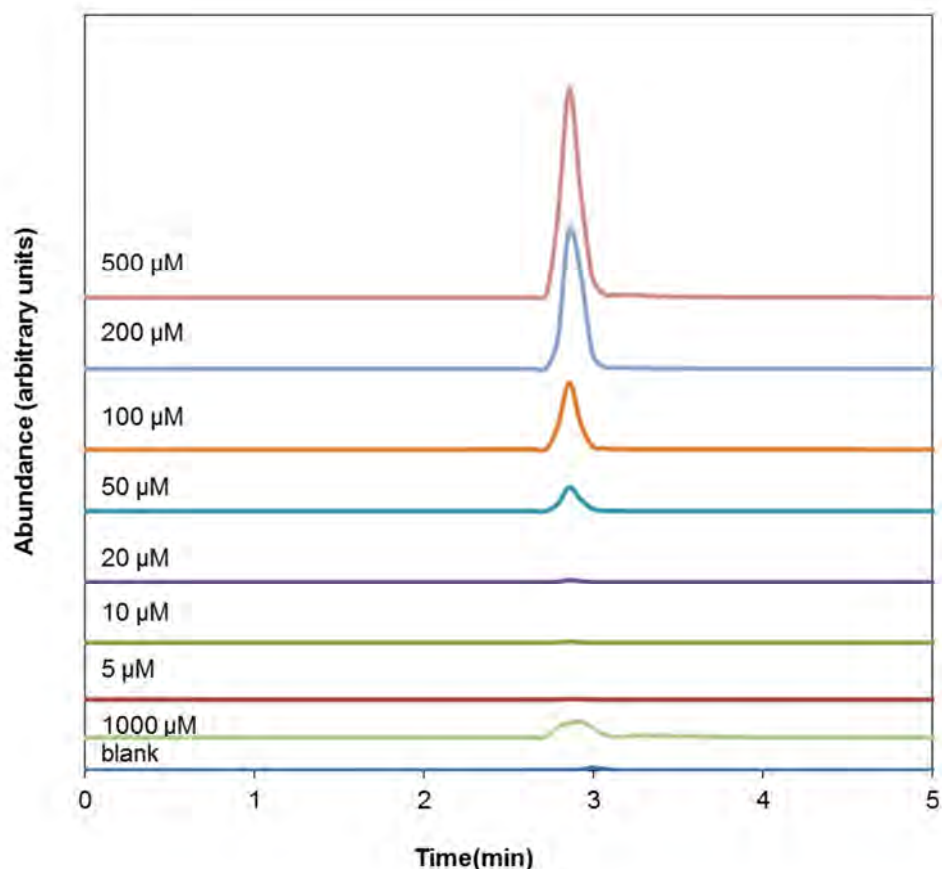


Figure III.14.11. Overlaid chromatograms from $[\text{CbiS}_2]^0$ swine plasma. The transitions shown here is $m/z = 1092 \rightarrow 989$. The $m/z = 1053 \rightarrow 989$ transitions (not shown) were unresolved.

III.14.4.7. MS Analysis of Cbi Species

Table III.14.2 shows the masses, collision energies, and declustering potentials of the MRM transitions of some cobinamide species of interest. The transitions for the dinitrocobinamide and the internal standard are also listed in the table. The transition for dinitrocobinamide was not present, but the sodium adduct, $[\text{Cbi}(\text{NO}_2)_2\text{Na}]^+$, was easily seen at 1104.5 (Figure III.14.12). The

molecular ion of the sodium adduct was used to identify transitions of interest for MS-MS. The appearance of a sodium adduct was not surprising, considering analysis of hydroxocobalamin by LC-MS-MS also utilized a sodium adduct ²⁷.

Transitions for each of the other Cbi species of interest were determined and optimized in a similar fashion. The internal standard was identified with the molecular ion at 1068.5 m/z (Table III.14.2), as [Cbi(¹³C¹⁵N)]⁰. Figure III.14.13 shows how spectrofluorometric spectral data that confirms the 'integrity of the internal standard after it was synthesized and subsequently subjected to analytical further scrutiny (tests) including chromatography.

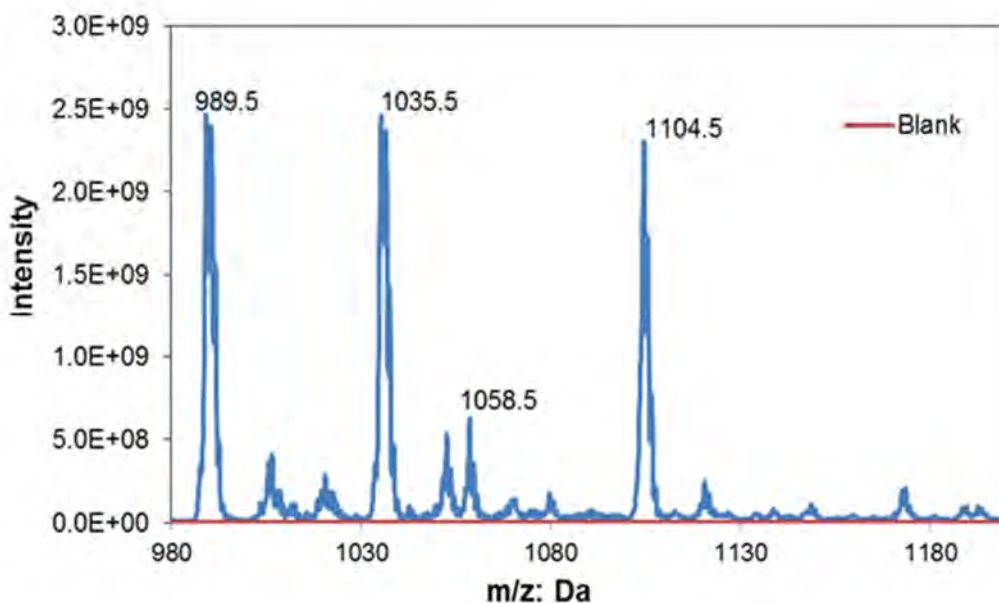


Figure III.14.12. Mass spectrum (MS1) showing the dinitrocobinamide with the sodium adduct, [Cbi(NO₂)₂Na]⁺ with m/z=1104.5, mononitrocobinamide with sodium adduct, [Cbi(NO₂)Na]²⁺, m/z=1058.5, mononitrocobinamide with no sodium adduct, [Cbi(NO₂)]⁺, m/z=1035, and the cobinamide (Cbi) with no ligands at m/z=989.5.

Table III.14.2. MRM ions and associated parameters corresponding to some Cbi forms of interest.

Compound	MS1(m/z Da)	MS3(m/z Da)	CE(Volts)	DP(Volts)
[CbiSO ₃ Na] ⁺	1092.8	989.9	65.01	71.22
	1092.8	930.9	96.67	234.01
[Cbi(CN) ₂ Na] ⁺	1064.9	1010.8	49.43	266.54
	1064.9	930.8	97.47	263.1
[Cbi(OH)(CN)] ^{0/}	1031.6	946.7	79.38	65.01
[Cbi(CN)(H ₂ O)] ⁺	1031.6	875.6	80.91	180.95
[Cbi(H ₂ O) ₂] ²⁺	1024.5	930.8	74.58	36.54
	1024.5	949.7	66.03	198.59
	1025.8	931.7	70.71	261.64
[Cbi(OH) ₂] ⁰	1022.7	961.8	65.16	201.56
	1022.7	946.8	72.02	229.81
[Cbi(S) ₂] ⁰	1053.6	989.7	57.32	193.4
	1053.6	930.7	86.91	172.63
	1053.6	916.7	95.62	186.09
[Cbi(S)(OH)] ⁰	1037.8	989.7	58.55	194.21
	1037.8	930.7	95.98	170.92
	1037.8	916.7	83.23	182.78
[Cbi(NO ₂) ₂ Na] ⁺	1104.5	1058.8	231.72	24.42
	1104.5	1013.8	182.00	34.15
[Cbi(¹³ C ¹⁵ N) ₂ Na] ⁺	1068.5	1010.7	265.54	49.43
	1068.5	930.5	263.10	97.47

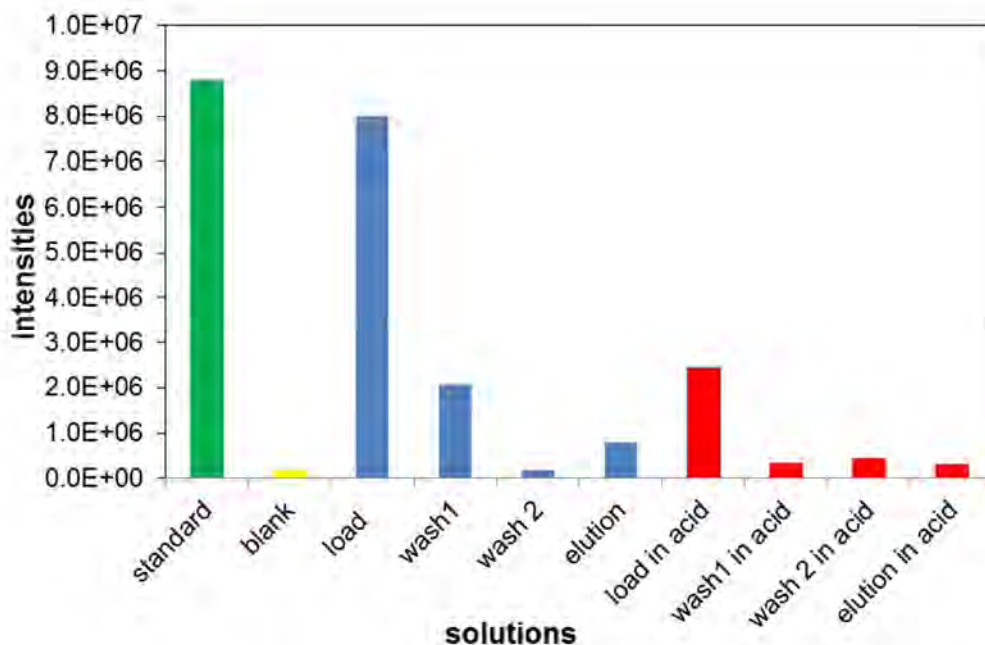


Figure III.14.13. SPE of $[\text{Cbi}({}^{13}\text{C}{}^{15}\text{N})_2]^0$. Spectral intensities of 'free' cyanide in acidified solution (red) and non-acidified solution containing the internal standard (blue). The standard cyanide spectra intensity is shown in green, and the blank is shown in yellow. The concentration of cyanide verified (standard and free) with NDA/ Taurine reagent was 100 μM .

Figure III.14.14 shows the bar chart for the intensities from the 'standard', blank, and the load, washes and elution from the internal standard after SPE. The intensity of the load in the non-acidified solution was about the same as the intensity in the standard, indicating that almost all 'free' cyanide was eliminated from the solution after SPE. The residual free cyanide was removed after the first and second wash. For the acidified solution, it is evident that the 1 M H_2SO_4 converted almost all the cyanide in solution into $\text{HCN}(g)$. Figure III.14.4.13 also shows the chromatogram of the internal standard (non-acidified) after SPE. The elution time on the Max RP column was 0.92 minutes.

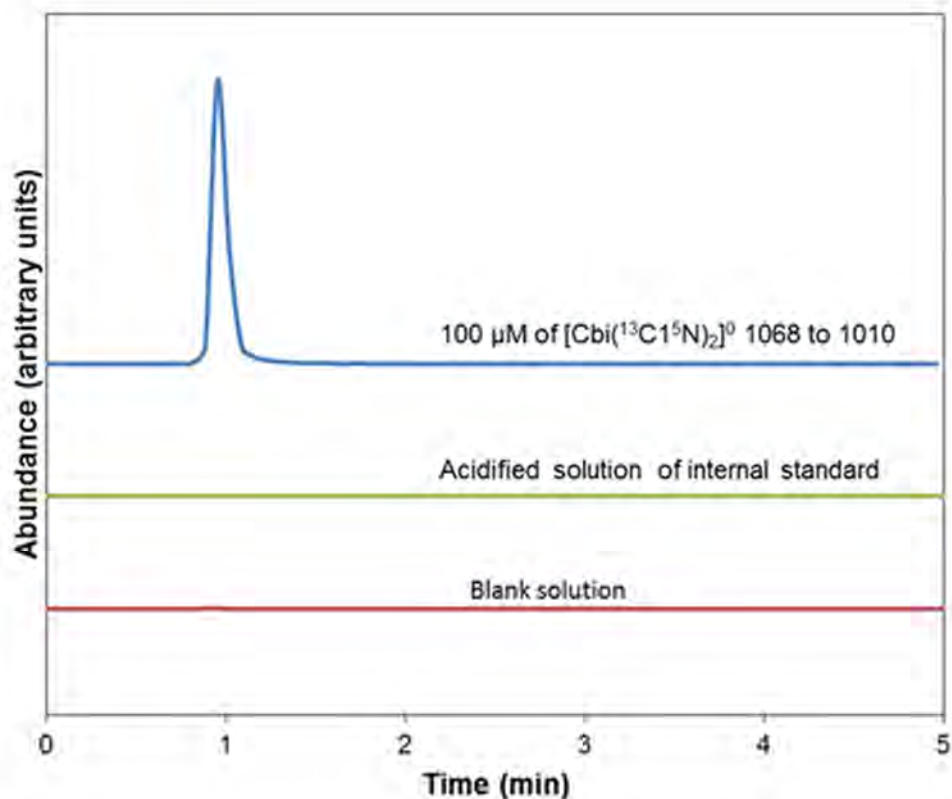


Figure III.14.14. Chromatograms showing the elution of isotopically-labelled dicyanocobinamide, the internal standard, spiked into swine plasma. MS transition: $m/z = 1068.5 \rightarrow 1010.7$. There is no evidence of peak in the blank (red) and the acidified solution (green).

III.14.4.8. Chromatographic Behavior of $[\text{Cbi}(\text{NO}_2)_2]^0$

Preliminary chromatograms of $[\text{Cbi}(\text{NO}_2)_2]^0$ are shown in Figure III.14.15, which reveals a significant and a conspicuous peak with the transition $1104 \rightarrow 1058$ in plasma but not in aqueous medium, suggesting that $[\text{Cbi}(\text{NO}_2)_2]^0$ can be found in plasma but not in aqueous medium. Further analysis of the chromatograms (not shown) of the analogues of cobinamides for the same run are enumerated in Table III.14.3. A plausible deduction from Table III.14.3 and Figure III.14.4.14 is that $[\text{Cbi}(\text{NO}_2)_2]^0$ is quite stable in plasma but not stable in

aqueous medium, and that $[\text{Cbi}(\text{NO}_2)_2]^0$ breaks down to form other species as shown in Table III.14.3 (probably due to an increase in pH as a result of the release of the conjugate base, NO_2^-). Subsequent chromatography of blank plasma (without $[\text{Cbi}(\text{NO}_2)_2]^0$) showed a significant peak at the 1104 \rightarrow 1058 transition. Investigation is on-going to elucidate this observation.

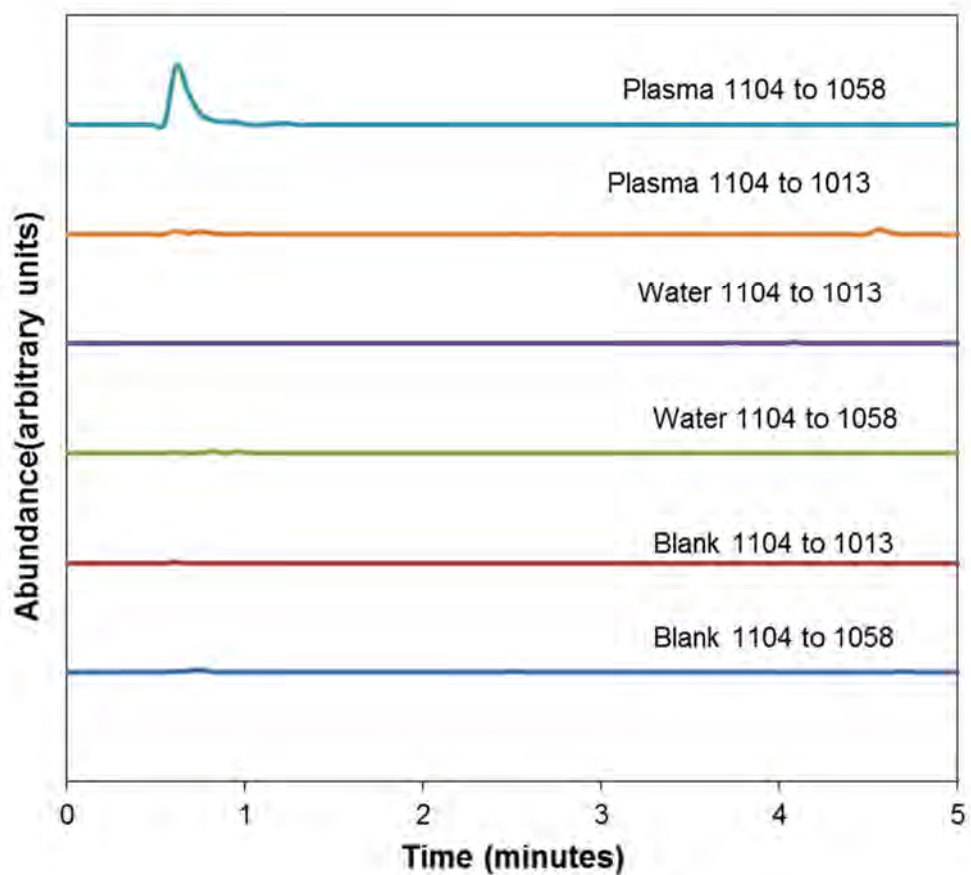


Figure III.14.15. Overlaid chromatograms of $[\text{Cbi}(\text{NO}_2)_2]^0$ at transition $m/z = 1104.5 \rightarrow 1058.8$ and $1104.5 \rightarrow 1013.8$, respectively, in water and plasma. LC conditions were as described above.

Table II.4.3. The occurrence of various transitions of cobinamide analogues in plasma and aqueous medium (water).

Species/mass (Da)	Aqueous	Plasma	Remarks
[Cbi(NO ₂) ₂ Na] ⁺ 1104	no	yes	1104 to 1058 significant: 1104 to 1013 very tiny
[Cbi(NO ₂)Na] ²⁺ 1058	no	yes	1058 to 1011 very little :1058 to 989 not visible
[Cbi(NO ₂)] ⁰ 1035	yes	yes	1035 to 989 very large in water than in plasma
[Cbi(H ₂ O) ₂] ²⁺ 1024	yes	no	1024 to 930 seen in water, other transition not seen
[Cbi(OH) ₂] ⁰ 1022	yes	yes	both transitions, 1022 to 946 and 1022 to 961 are significant in plasma. However, only 1022 to 961 seen in water
[Cbi] ²⁺ 989	yes	yes	All transitions visible in plasma and in water with the same abundance, indicating that Cbi recovery is high

III.14.4.9. Limit of detection (LOD)

The chromatograms for the determination of LOD are shown in Figure III.14.16. The figure shows an elution time of about 0.68 minutes and a concentration dependence with signal. The LOD could be estimated as signal to noise ratio of 3, since there is a significant peak intensity in the blank. This observation of peak in the blank swine plasma could be due to an interferent and or a contaminant. Several attempts were made to unravel the occurrence of peaks of the 1104 →1058 transitions.

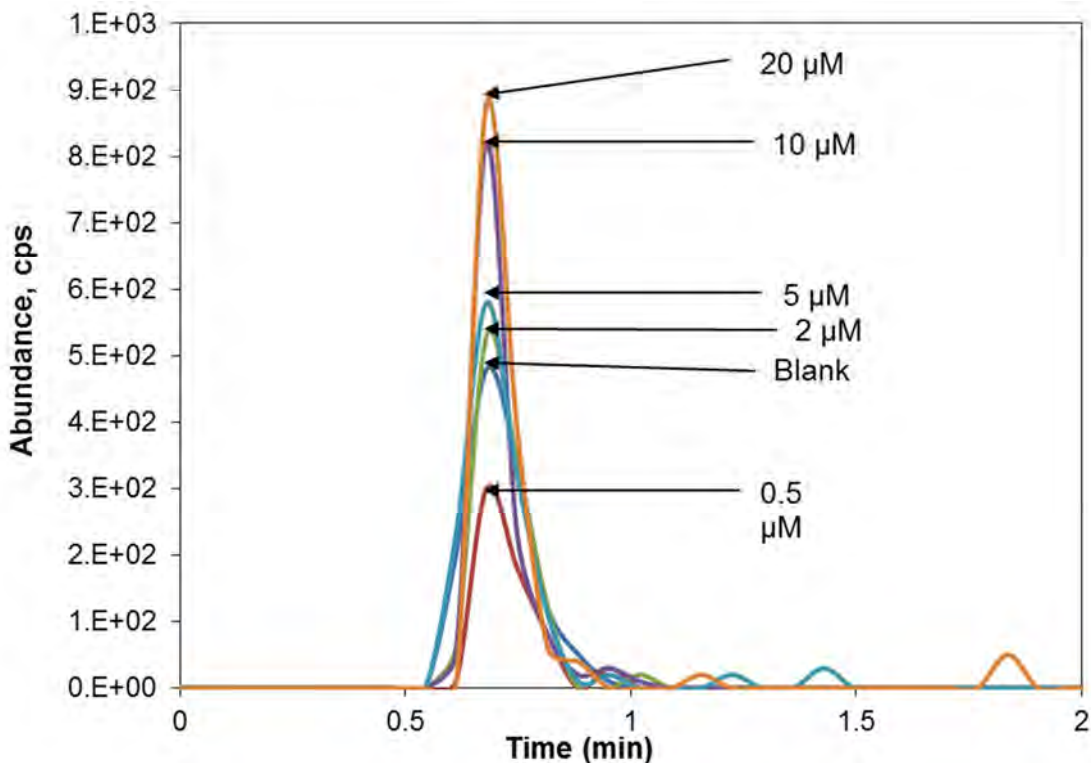


Figure III.14.16. Overlaid chromatograms of $[\text{Cbi}(\text{NO}_2)_2]^0$ in swine plasma at different concentrations. The peak intensity for the blank (deep blue) is significant and more conspicuous than the $0.5 \mu\text{M}$ (red). Transitions monitored were $1104 \rightarrow 1058$.

III.14.4.10. Origin of $1104 \rightarrow 1058$ transitions in blank plasma

Chromatograms of blank plasma and spiked CN plasma and positive control of $[\text{Cbi}(\text{NO}_2)_2]^0$ are shown in Figure III.14.17. The positive control is the $1104 \rightarrow 1058$ transition in $[\text{Cbi}(\text{NO}_2)_2]^0$. It is evident from Figure III.14.17. that all the $1104 \rightarrow 1058$ transitions were visible in the positive control (labelled as 'DN' for dinitrocobinamide), spiked mononitromonoyano cobinamide (designated as 'CN(NO₂)') spiked cyanide into the blank plasma (labelled as 'spiked CN), and dicyanocobinamide, labelled as 'diCN. If there were any 'free cobinamide' (with either aquo or hydroxo ligands) in the plasma, then, it should be converted to the cyanide derivatives, monocyano mononitro or dicyano cobinamides, and

consequently, the peak for the blank spiked CN plasma should not have any conspicuous 1104 →1058 transitions. However, there were 1104 →1058 transitions in all the samples prepared, as in the positive control, including the blank. This observation is likely to be due to an interferent in the plasma, and not the presence of cobinamide in the plasma itself (directly). The observation that the 1104 →1058 transitions could most likely emanate from an interferent is further collaborated by analyzing other transitions of the cyanide derivatives from the same species prepared, as shown in Figures III.14.18 and III.14.19.

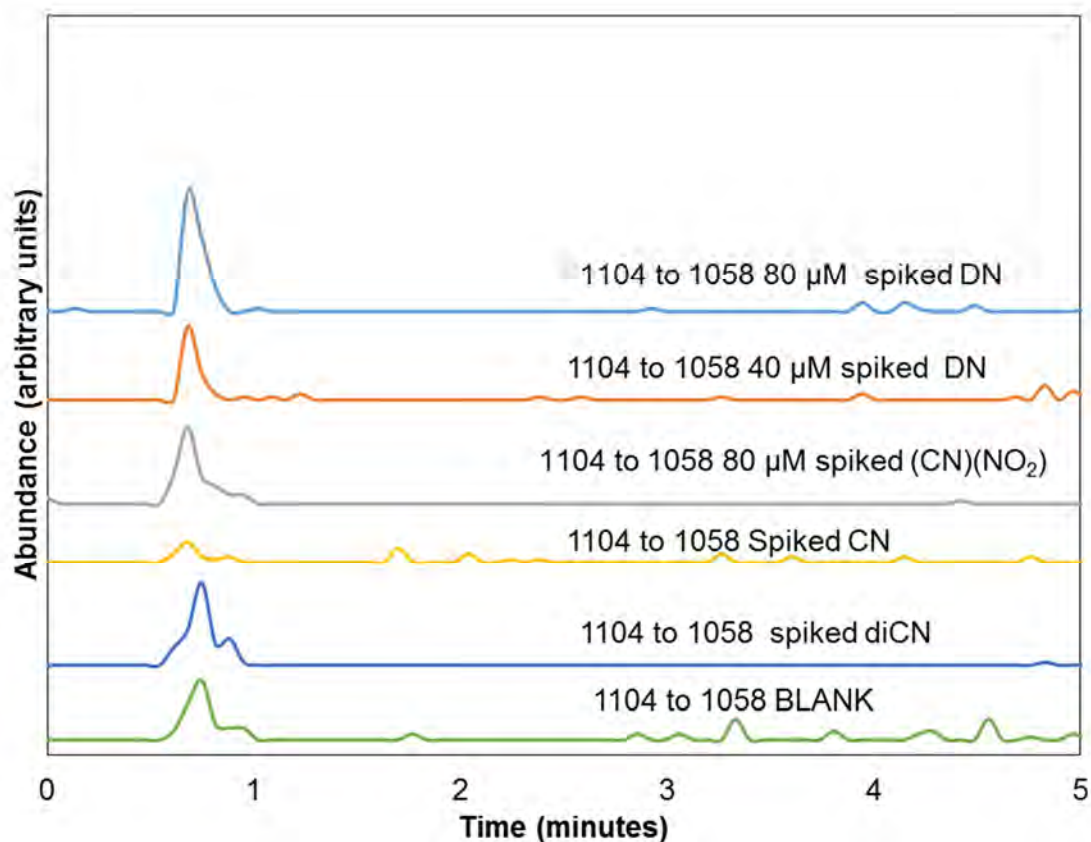


Figure III.14.17. Overlaid chromatograms of 1104 →1058 transitions for the positive controls (shown in red and grey,) spiked mononitromonocyano (yellow) and dicyano (blue) derivatives of cobinamide. The blank is shown in green with a

significant peak for the 1104 →1058 transitions. The presence of 1104 →1058 transitions in all the samples prepared could be due to an interferent in the plasma, and may not be due to a residual or contaminant of the aquo or hydroxo forms or other derivatives of the cobinamides.

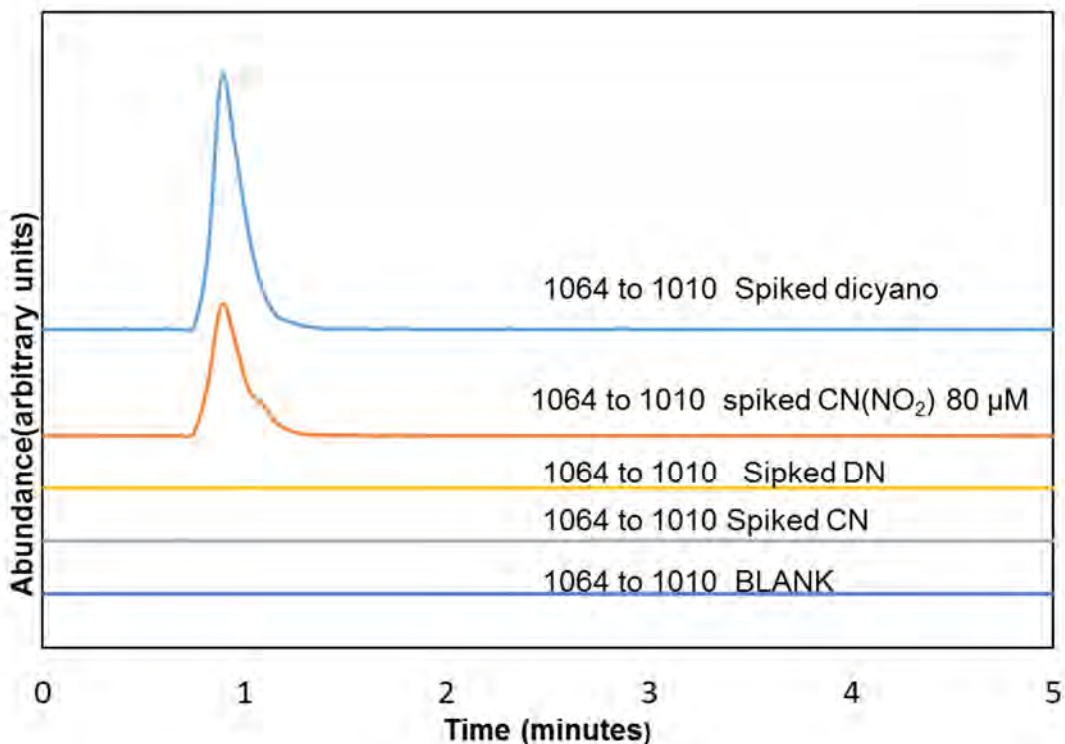


Figure III.14.18. Overlaid chromatograms 1064.5 → 1010.8 transitions. The positive control is spiked dicyano cobinamide (blue). The red is mononitromonocyanocobinamide spiked in plasma; the large intensity seen could be due to the presence of dicyanocobinamide formed after cyanide was added to the dinitrocobinamide. Cyanide spiked into blank plasma is shown in yellow; any free cobinamide in the blank plasma should have converted to dicyanocobinamide so that the 1064.5 → 1010.8 transitions could be seen. The absence of a peak for the transition 1064.5 → 1010.8 in the spiked -CN blank plasma suggests that there is no form of cobinamide in the unspiked plasma (similar to results in Figure II.4.3 -2. above).

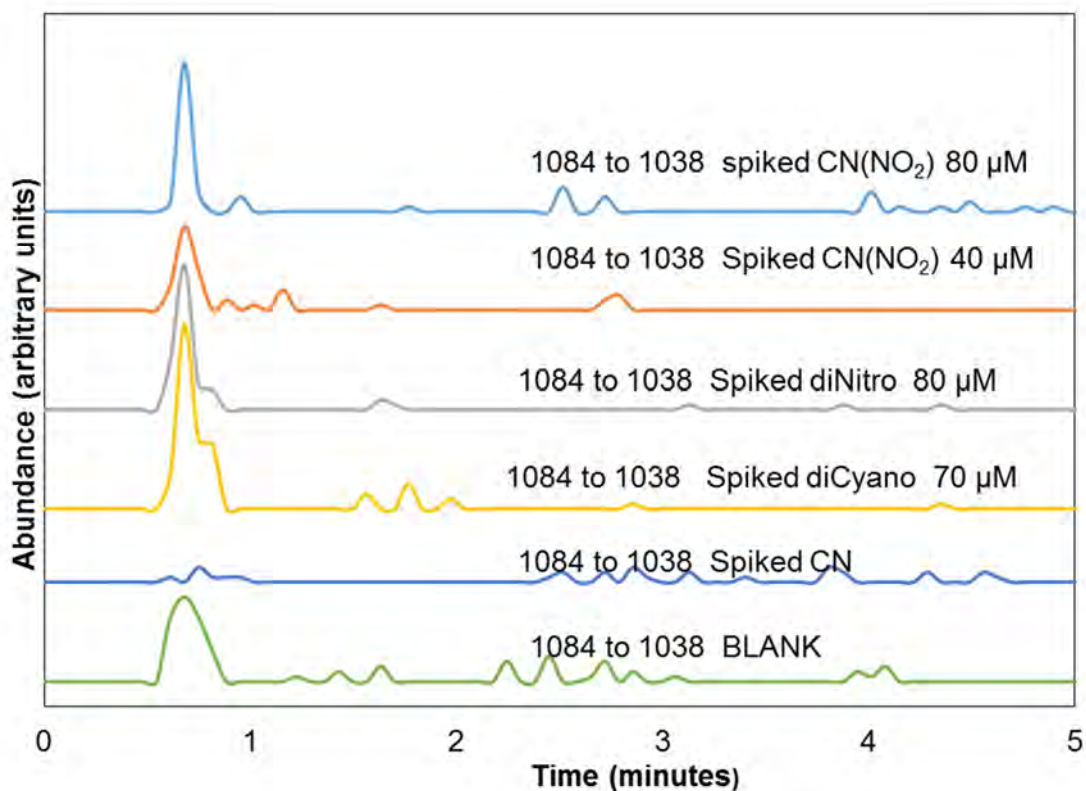


Figure III.14.19. Overlaid chromatograms 1084.5 →1038 transitions. The positive control is spiked mononitromonocyanocobinamide (blue and red). The grey peak is spiked dinitrocobinamide spiked in plasma. The yellow represents spiked dicyanocobinamide, and the deep blue (tiny) is the peak for spiked CN into the blank plasma. By the same analogy described earlier any free cobinamide in the unspiked plasma should have been converted to cyanide derivatives when the CN was spiked into it. The absence of any conspicuous peaks for the spiked-CN plasma could be an indication of lack of any cobinamide in the blank plasma. The large peak seen for this transition in the blank (green) could possibly be an interferent or a contamination that is not in the plasma but probably from other sources such as the injector of the LC.

The stability of the dinitrocobinamide species in pH media were also studied in the blank plasma, as shown in Figures III.14.20, III.14.21, and III.14.22. For the neutral plasma, the intensity for the 1104 →1058 transitions increased significantly with time (after 1 hour), while the spiked dinitrocobinamide, DN, remained about the same.

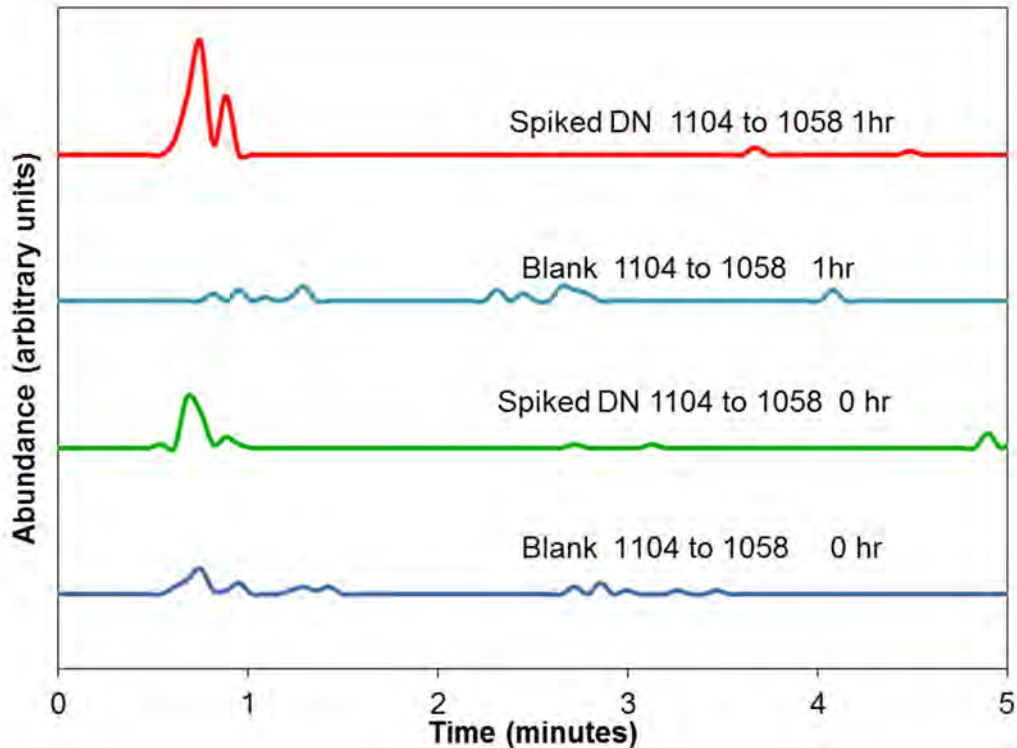


Figure III.14.20. Stacked chromatogram for 'neutral' spiked and unspiked plasma (blank) prepared at 0 hour and 1 hour, respectively, prior to analysis. The intensity for the blank plasma (light blue) analyzed after 1 hour is very much higher than that for 0 hour (deep blue). 'DN' is spiked dinitrocobinamide into the plasma at 1 hour (red) or 0 hour (green). The intensities for the spiked DN samples were almost the same.

In similar fashion, the trends for acidified and alkalinized spiked and unspiked plasma were analyzed.

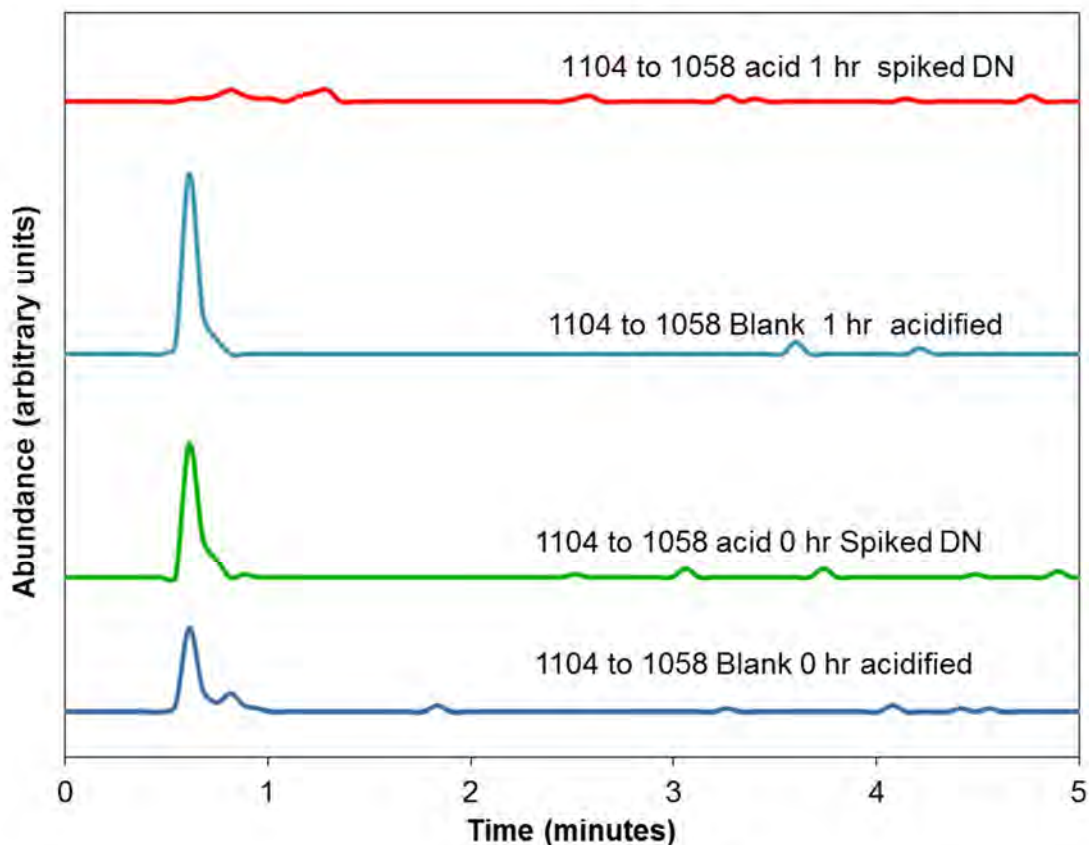


Figure III.14.21. Stacked chromatogram for ‘acidified’ spiked and unspiked plasma (blank) prepared at 0 hour and 1 hour, respectively, prior to analysis. The intensity for the acidified blank plasma (light blue) analyzed after 1 hour is very much higher than that for 0 hour (deep blue). ‘DN’ is spiked dinitrocobinamide into the plasma at 1 hour (red) or 0 hour (green). The intensity for the spiked DN analyzed after 1 hour diminished almost to undetectable limits, as compared to all other peaks.

The intensity for the acidified blank was much higher because there could be an interferent in the plasma that ‘reacted’ with the plasma and hence enhanced the intensity. Similarly, the analyte in the spiked DN could have reacted with the formic acid and so the intensity got attenuated.

The alkalized medium was quite different from the neutral and the acidic media. For the 1 hour elapsed time, the signal for the spiked DN was significantly enhanced, while the signal for the alkalized blanks was attenuated.

There could be an interferent in the blank plasma that probably 'reacted' with the ammonium hydroxide.

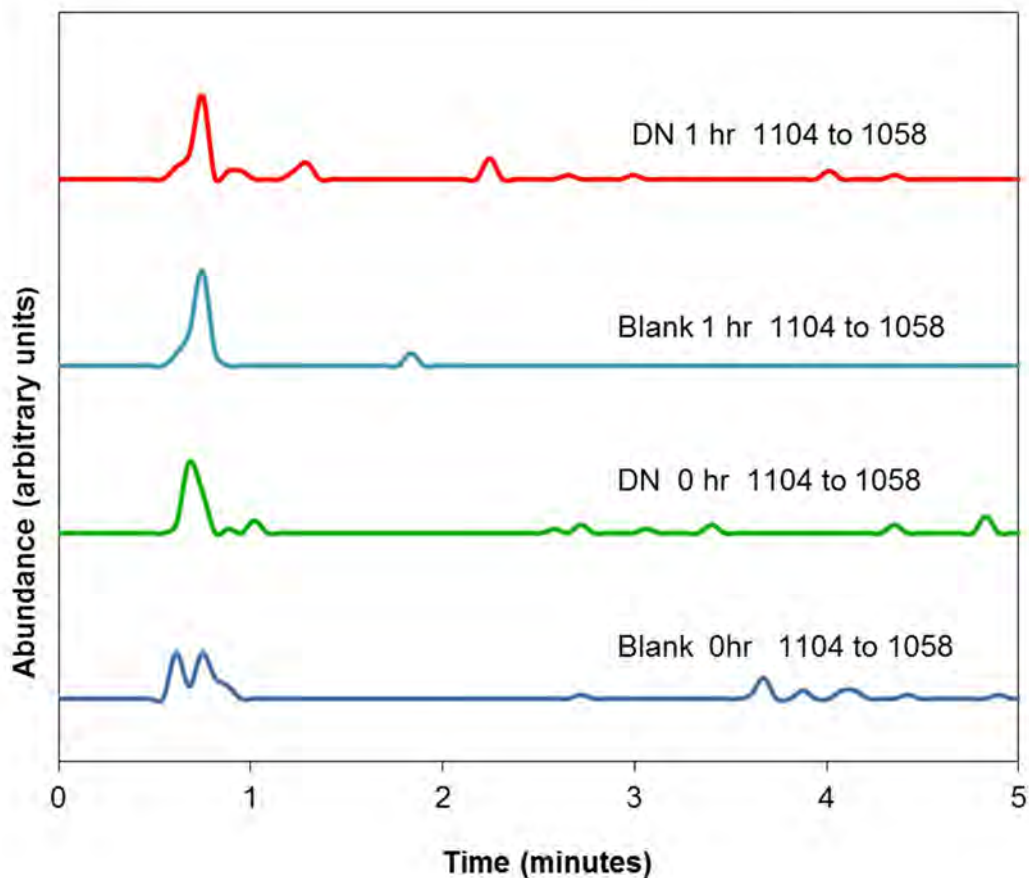


Figure III.14.22. Overlaid chromatogram for 'alkalinized' spiked and unspiked plasma (blank) prepared at 0 hour and 1 hour, respectively, prior to analysis. The intensity for the alkalinized blank plasma (light blue) analyzed after 1 hour is very much lower than that for 0 hour (dark blue). 'DN' is spiked dinitrocobinamide into the plasma at 1 hour (red) or 0 hour (green). The intensity for the spiked DN analyzed after 1 hour was significantly enhanced.

III.14.5. Conclusions

Cbi forms of interest were successfully synthesized, masses assigned, and the associated MRM parameters were optimized. A suitable method was

developed for the analysis of the Cbi species of interest. The detection limit of $[\text{Cbi}(\text{OH})_2]^0$ was determined to be 5 μM , and the detection limit for $[\text{CbiS}_2]^0$ was 6 μM . The detection limit of $[\text{Cbi}(\text{OH})_2]^0$ was determined to be 5 μM . $[\text{Cbi}(\text{H}_2\text{O})_2]^{2+}$ and $[\text{Cbi}(\text{OH})_2]^0$ shows thermodynamic stability at three days at acidic and basic pH medium, respectively. The Identity of $[\text{Cbi}(\text{OH})(\text{H}_2\text{O})]^+$ could not be confirmed. The thermodynamic stability of $[\text{CbiS}_2]^0$ was within 24 hours after sample preparation. Correlation between the transitions $m/z = 1053 \rightarrow 989$ and $1092 \rightarrow 989$ is yet to be investigated. An internal standard will be incorporated in the sample preparation (procedure) for the analysis of $[\text{CbiS}_2]^0$.

Nitrocobinamides were successfully synthesized, associated MRM parameters optimized, and a suitable method was developed for its analysis. Similarly, an internal standard was synthesized and verified to be suitable for the Cbi analogue analysis in swine plasma. The presence of a significant peak in the blank (neutral) plasma could be due to an interferent, of which its signal was attenuated by ammonium hydroxide. The Nitrocobinamide specie appears to be thermodynamically stable in alkalinized medium.

III.14.6. References

1. Brenner, M.; Kim, J. G.; Lee, J.; Mahon, S. B.; Lemor, D.; Ahdout, R.; Boss, G. R.; Blackledge, W.; Jann, L.; Nagasawa, H. T.; Patterson, S. E., Sulfanegen sodium treatment in a rabbit model of sub-lethal cyanide toxicity. *Toxicol. Appl. Pharmacol.* **2010**, *248* (3), 269-76.
2. Rehman, H. U., Methemoglobinemia. *West. J. Med.* **2001**, *175* (3), 193-6.

3. Chan, A.; Crankshaw, D. L.; Monteil, A.; Patterson, S. E.; Nagasawa, H. T.; Briggs, J. E.; Kozocas, J. A.; Mahon, S. B.; Brenner, M.; Pilz, R. B.; Bigby, T. D.; Boss, G. R., The combination of cobinamide and sulfanegen is highly effective in mouse models of cyanide poisoning. *Clin. Toxicol. (Phila.)* **2011**, *49* (5), 366-73.
4. Stepuro, T. L.; Zinchuk, V. V., Nitric oxide effect on the hemoglobin-oxygen affinity. *J. Physiol. Pharmacol.* **2006**, *57* (1), 29-38.
5. Isom, G. E.; Borowitz, J. L.; Mukhopadhyay, S., Sulfurtransferase Enzymes Involved In Cyanide Metabolism. In *Elsevier Ltd*, Purdue University, W. L., IN,, Ed. Elsevier Ltd: 2010; pp 486-498.
6. Broderick, K. E.; Potluri, P.; Zhuang, S.; Scheffler, I. E.; Sharma, V. S.; Pilz, R. B.; Boss, G. R., Cyanide detoxification by the cobalamin precursor cobinamide. *Exp. Biol. Med. (Maywood)* **2006**, *231* (5), 641-9.
7. E.Patterson, S.; R.Monteil, A.; Cohen, J. F.; L.Crankshaw, D.; Vince, R.; Nagasawa, H. T., Cyanide antidotes for mass casualties: water-soluble salts of the dithiane (sulfanegen) from 3-mercaptopyruvate for intramuscular administration. *J. Med. Chem.* **2013**, *56* (3), 1346-1349.
8. Hamel, J., A review of acute cyanide poisoning with a treatment update. *Crit. Care Nurse* **2011**, *31* (1), 72-81; quiz 82.
9. Hall, A. H.; Saiers, J.; Baud, F., Which cyanide antidote? *Crit. Rev. Toxicol.* **2009**, *39* (7), 541-52.
10. Broderick, K. E.; Balasubramanian, M.; Chan, A.; Potluri, P.; Feala, J.; Belke, D. D.; McCulloch, A.; Sharma, V. S.; Pilz, R. B.; Bigby, T. D.; Boss, G. R.,

The Cobalamin Precursor Cobinamide Detoxifies Nitropruside-Generated Cyanide. *Exp. Biol. Med. (Maywood)* **2007**, 232 (6), 789-798.

11. Brenner, M.; Kim, J. G.; Mahon, S. B.; Lee, J.; Kreuter, K. A.; Blackledge, W.; Mukai, D.; Patterson, S.; Mohammad, O.; Sharma, V. S.; Boss, G. R., Intramuscular cobinamide sulfite in a rabbit model of sublethal cyanide toxicity. *Ann. Emerg. Med.* **2010**, 55 (4), 352-63.

12. Chan, A.; Balasubramanian, M.; Blackledge, W.; Mohammad, O. M.; Alvarez, L.; Boss, G. R.; Bigby, T. D., Cobinamide is superior to other treatments in a mouse model of cyanide poisoning. *Clin. Toxicol. (Phila.)* **2010**, 48 (7), 709-17.

13. Ma, J.; Dasgupta, P. K.; Zelder, F. H.; Boss, G. R., Cobinamide chemistries for photometric cyanide determination. A merging zone liquid core waveguide cyanide analyzer using cyanoaquacobinamide. *Anal. Chim. Acta* **2012**, 736, 78-84.

14. Boss, G.; Sharma, V.; Brenner, M.; Dasgupta, P. K.; Blackledge, W. C., Rapid Method to measure cyanide in biological samples. *Patent Application Publication Pub.No.: US 2013/0005044A1* **2013**, PCT No.: PCT/US 2011/028542 CO7F15/06(2006.01) US cl. 436/109,540/145.

15. Fedosov, S. N.; Petersen, T. E.; Nexø, E., Binding of cobalamin and cobinamide to transcobalamin from bovine milk. *Biochemistry* **1995**, 34 (49), 16082-7.

16. Fedosov, S. N.; Berglund, L.; Fedosova, N. U.; E, N.; Petersen, T. E., Comparative analysis of cobalamin binding kinetics and ligand protection for

intrinsic factor, transcobalamin, and haptocorrin. *J. Biol. Chem.* **2002**, 277 (12), 9989-96.

17. Fedosov, S. N.; Fedosova, N. U.; Kraütler, B.; Nexø, E.; Petersen, T. E., Mechanisms of Discrimination between Cobalamins and Their Natural Analogues during Their Binding to the Specific B12-Transporting Proteins. *Biochemistry* **2007**, 46, 6446-6458.

18. Blackledge, W. C.; Blackledge, C. W.; Griesel, A.; Mahon, S. B.; Brenner, M.; Pilz, R. B.; Boss, G. R., New facile method to measure cyanide in blood. *Anal. Chem.* **2010**, 82 (10), 4216-21.

19. Kruve, A.; Kaupmees, K.; Liigand, J.; Oss, M.; Leito, I., Sodium adduct formation efficiency in ESI source. *J. Mass Spectrom.* **2013**, 48 (6), 695-702.

20. Corley, J., Best Practices in Establishing Detection and Quantification limits for Pesticides in Foods Rutgers, T. S. U. o. N. J., North Brunswick, NJ.USA, Ed. October 24 2002; Vol. 15:54.

21. Corley, J., Best Practices in Establishing Detection and Quantification limits for Pesticides in Foods Rutgers, T. S. U. o. N. J., North Brunswick, NJ.USA, Ed. 2002; Vol. 15:54.

KEY RESEARCH ACCOMPLISHMENTS

- Multiple cyanide sensors have been developed that rapidly detect cyanide in biological fluids
- Methods to detect various cyanide metabolites have been published using various instruments
- Toxicokinetic studies have been completed on cyanide metabolites
- Novel methods are being developed to detect next generation cyanide therapeutics.

REPORTABLE OUTCOMES

Presentations

M.W. Stutelberg, C.V. Vinnakota, B.L. Mitchell, A.R. Monteil, S.E. Patterson, and B.A. Logue (2013) Determination of 3-mercaptopyruvate in rabbit plasma by high performance liquid chromatography tandem mass spectrometry. 48th Midwest Regional Meeting, Springfield, MO, October 16-19, Analytical Oral Session I-343.

J.K. Dzisam, G.A. Rockwood, and B.A. Logue (2013) Determination of sulfite, cyanide, and aquo derivatives of cobinamide by HPLC-MS-MS. 48th Midwest Regional Meeting, Springfield, MO, October 16-19, Analytical Oral Session I-347.

W.H. Zhou, R.P. Oda, I. Petrikovics, G.A. Rockwood, and B.A. Logue (2013) Analysis of CNA5 in blood by gas chromatography mass-spectrometry. 48th Midwest Regional Meeting, Springfield, MO, October 16-19, Analytical Poster Session I-328.

B.A. Logue (2014) Cyanide: History, Effects, and Analysis. Sewry Colloquium Invited Speaker based on Research Excellence, South Dakota State University, February 18.

J.D. Downey, I. Petrikovics, B.A. Logue, M. Brenner, G.R. Boss, S.B. Mahon, M.R. DeFreytas, D.M. Hildenberger, A.R. Allen, and G.A. Rockwood (2013) In vivo efficacy and optimization of novel cyanide countermeasures [IAA AOD12060-001-0000/A120-B.P2012-01]. NIH CounterACT 8th Annual Network Research Symposium, Denver, CO, USA, June 16-19, Cyanide session 3A, Platform presentation and poster.

B.A. Logue, R.K. Bhandari, R.P. Oda, and R.E. Jackson (2014). Diagnosis of cyanide exposure and analysis of novel cyanide antidotes. Bioscience Review 2014: Advances in Medical Chemical Defense, Hunt Valley, MD, May 11-15, Platform presentation.

I. Petrikovics, D. DeSilva, E. Miller, B.A. Logue, M. Budai, K. Kovacs, C. Chou, S. Lee and D. Thompson (2014) Cyanide as an Environmental Contaminant and Protecting Against its Toxic Effects. Society of Environmental Toxicology and Chemistry (SETAC) Europe 24th Annual Meeting, Basel, Switzerland, 11-15 May 2014, Poster session.

Manuscripts published

Bhandari B.K., Oda R.O., Youso S.L., Petrikovics I., Bebarta V.S., Rockwood G.A., Logue B.A. Simultaneous determination of cyanide and thiocyanate in plasma by chemical ionization gas chromatography mass-spectrometry (CI-GC-MS). (2012) *Analytical and Bioanalytical Chemistry*. 404. 2287-2294.

Mitchell B.L., Rockwood G.A., Logue B.A. (2013) Quantification of A-ketoglutarate cyanohydrin in swine plasma by hultra-high performance liquid chromatography tandem mass spectrometry. *Journal of Chromatography B*. 934. 60-65.

Mitchell B.L., Bhandari R.K. Bebarta V.S., Rockwood G.A., Boss G.R., Logue B.A. (2013) Toxicokinetic profiles of A-ketoglutarate cyanohydrin, a cyanide detoxification product, following exposure to potassium cyanide. *Toxicology Letters*. 222. 83-89.

Bhandari, R. K., Manandhar, E., Oda, R. P., Rockwood, G. A., and Logue, B. A. (2013). Simultaneous high-performance liquid chromatography-tandem mass spectrometry (HPLC-MS-MS) analysis of cyanide and thiocyanate from plasma. *Analytical and Bioanalytical Chemistry*.

Bhandari, R. K., Oda, R. P., Petrikovics, I., Thompson, D. E., Brenner, M., Mohan, S. B., Bebarta, V. S., Rockwood, G. A., and Logue, B. A. (2014). Cyanide toxicokinetics: The behavior of cyanide, thiocyanate and 2-amino-2-thiazoline-4-carboxylic acid in multiple animal models. *J Anal Toxicol*. 38. 218-225.

Stutelberg M.W., Vinnakota C.V., Mitchell B.L., Monteil A.R., Patterson S.E., and Logue B.A. (2014) Determination of 3-mercaptopyruvate in plasma by high performance liquid chromatography tandem mass spectrometry. *Journal of Chromatography B*. 949-950. 94-98.

Jackson, R., Oda, R., Bhandari, R., Mahon, S., Brenner, M., Rockwood, G., and Logue, B. The development of a fluorescence-based sensor for rapid diagnosis of cyanide exposure. (2014). *Anal. Chem*. 86, 1845-1852.

Manuscripts in preparation

Stutelberg M. W., Dzisam J. K., Monteil A. R., Boss G. R., Patterson S. E., and Logue B. A. (2014) Simultaneous determination of cobinamide and 3-mercaptopyruvate in swine plasma by liquid chromatography-tandem mass spectrometry. *Analytical and Bioanalytical Chemistry*, In Preparation.

Zhou W.H., Oda R.P., Stutelberg M.W., Petrikovics I., and Logue B.A. (2014) Determination of dimethyl trisulfide from whole blood using dynamic headspace gas chromatography-mass spectrometry. *Journal of Chromatography B*, In Preparation.

Dzisam J.K., Stutelberg M.W., Boss G.R., and Logue B.A. (2014) Simultaneous Determination of Aquo, Cyano, and Nitro-Cobinamide Derivatives by Liquid Chromatography Tandem Mass Spectrometry. *Analytical and Bioanalytical Chemistry*, In Preparation.

CONCLUSIONS

Multiple sensors to rapidly detect cyanide concentrations in biological fluids have been developed. Methods were developed to detect cyanide and cyanide metabolites in biological fluids by various methods. These methods featured simple sample preparation with excellent accuracy and precision enabling a large sample analysis in a small amount of time. A new cyanide metabolite (α -ketoglutarate cyanohydrin) was determined as well as a toxicokinetic profiles completed on various cyanide metabolites. Methods for next generation cyanide therapeutics were also developed.

References

Introduction

1. *Strategic Plan and Research Agenda for Medical Countermeasures Against Chemical Threats* (August, 2007), http://www.ninds.nih.gov/research/counterterrorism/counterACT_home.htm. Accessed 8/29/2012.2.
2. Youso, S. L.; Rockwood, G. A.; Lee, J. P.; Logue, B. A. 2010. *Anal Chim Acta* 677 24-28.
3. Logue, B. A.; Hinkens, D. M.; Baskin, S. I.; Rockwood, G. A. 2010. *Crit Rev Anal Chem* 44 122-147.

Chapter 7

1. Meister, A. and Anderson, M. E., 1983. Glutathione. *Ann Rev Biochem* 52, 711-760.
2. Jose, C. J., Jacob, R. H., Gardner, G. E., Pethick, D. W., and Liu, S. M., 2010. Selenium supplementation and increased muscle glutathione concentration do not improve the color stability of lamb meat. *J Agric Food Sci* 58 (12), 7389-7393.

3. Serru, V., Baudin, B., Ziegler, F., David, J-P., Cals, M-J., Vaubourdolle, M., and Mario, N., 2001. Quantification of reduced and oxidized glutathione in whole blood samples by capillary electrophoresis. *Clin Chem* 47 (7), 1321-1324.
4. Michelet, F., Gueguen, R., Leroy, P., Wellman, M., Nicolas, A., and Siest, G., 1995. Blood and plasma glutathione measured in healthy subjects by HPLC: Relation to sex, aging, biological variables, and life habits. *Clin Chem* 41 (10), 1509-1517.
5. Hatch, R. C., Laflamme, D. P., and Jain, A. V., 1990. Effects of various known and potential cyanide antagonists and a glutathione depletor on acute toxicity of cyanide in mice. *Vet Human Toxicol* 32 (1), 9-16.
6. Catsimpoolas, N., and Wood, J. L., 1964. The reaction of cyanide with bovine serum albumin. *J Biol Chem* 239 (12), 4132-4137.
7. Youso, S. L., Rockwood, G. A., Lee, J. P., Logue, B. A., 2010. Determination of cyanide exposure by gas chromatography-mass spectrometry analysis of cyanide-exposed plasma proteins. *Anal Chim Acta* 677 (1), 24-28.
8. Nagasawa, H. T., Cummings, S. E., and Baskin, S. I., 2004. The structure of "ITCA", a urinary metabolite of cyanide. *Organic Prep and Proc Int'l* 36 (2), 178-182.

9. Ellman, G. L., 1959. Tissue sulfhydryl groups. *Arch Biochem Biophys* 82, 70-77.

10. Habeeb, A. F. S. A., 1972. Reaction of protein sulfhydryl groups with Ellman's reagent. *Methods Enzymol.* 25 (part B), 457-464.

Chapter 10

1. Petrikovics I, Kuzmitcheva G, Budai M, Haines D, Nagy A, Rockwood GA, Way JL (2010) Encapsulated rhodanese with two new sulfur donors in cyanide antagonism. In *XII International Congress of Toxicology*. Barcelona, Spain.

2. Frankenberg L (1980) Enzyme therapy in cyanide poisoning: effect of rhodanese and sulfur compounds. *Arch Toxicol* 45: 315-323.

3. Iciek M, Wlodek L (2001) Biosynthesis and biological properties of compounds containing highly reactive, reduced sulfane sulfur. *Pol J Pharmacol* 53: 215-225.

4. Petrikovics I, Pei L, McGuinn W, Cannon E, Way J (1994) Encapsulation of rhodanese and organic thiosulfonates by mouse erythrocytes. *Fund and Appl Toxicol* 23: 70-75.

Chapter 11

2. Petrikovics I, Kuzmitcheva G, Budai M, Haines D, Nagy A, Rockwood GA, Way JL (2010) Encapsulated rhodanese with two new sulfur donors in cyanide antagonism. In *XII International Congress of Toxicology*. Barcelona, Spain.

2. Frankenberg L (1980) Enzyme therapy in cyanide poisoning: effect of rhodanese and sulfur compounds. *ArchToxicol* **45**: 315-323.

3. Iciek M, Wlodek L (2001) Biosynthesis and biological properties of compounds containing highly reactive, reduced sulfane sulfur. *Pol J Pharmacol* **53**: 215-225.

4. Petrikovics I, Pei L, McGuinn W, Cannon E, Way J (1994) Encapsulation of rhodanese and organic thiosulfonates by mouse erythrocytes. *Fund and Appl Toxicol* **23**: 70-75.

4. Golchoubian, H.; Hosseinpoor, F., Effective oxidation of sulfides to sulfoxides with hydrogen peroxide under transition-metal-free conditions. *Molecules* **2007**, *12* (3), 304-311.

Chapter 13

1. Isom, G. E.; Borowitz, J. L.; Mukhopadhyay, S., Sulfurtransferase Enzymes Involved in Cyanide Metabolism. In *Comprehensive Toxicology*, McQueen, C., Ed. 2010; Vol. 4, pp 485-500.
2. Nagasawa, H. T.; Goon, D. J. W.; Crankshaw, D. L.; Vince, R.; Patterson, S. E., Novel, orally effective cyanide antidotes. *Journal of Medicinal Chemistry* **2007**, *50*, 6462-6464.
3. Brenner, M.; Kim, J. G.; Lee, J.; Mahon, S. B.; Lemor, D.; Ahdout, R.; Boss, G. R.; Blackledge, W.; Jann, L.; Nagasawa, H. T.; Patterson, S. E., Sulfanegen sodium treatment in a rabbit model of sub-lethal cyanide toxicity. *Toxicology and applied pharmacology* **2010**, *248* (3), 269-76.
4. Brenner, M.; Mahon, S. B.; Lee, J.; Kim, J.; Mukai, D.; Goodman, S.; Kreuter, K. A.; Ahdout, R.; Mohammad, O.; Sharma, V. S.; Blackledge, W.; Boss, G. R., Comparison of cobinamide to hydroxocobalamin in reversing cyanide physiologic effects in rabbits using diffuse optical spectroscopy monitoring. *Journal of Biomedical Optics* **2010**, *15* (1), 017001-017001.
5. Chan, A.; Balasubramanian, M.; Blackledge, W.; Mohammad, O. M.; Alvarez, L.; Boss, G. R.; Bigby, T. D., Cobinamide is superior to other treatments in a mouse model of cyanide poisoning. *Clinical Toxicology* **2010**, *48*, 709-717.
6. Chan, A.; Crankshaw, D. L.; Monteil, A.; Patterson, S. E.; Nagasawa, H. T.; Briggs, J. E.; Kozocas, J. A.; Mahon, S. B.; Brenner, M.; Pilz, R. B.; Bigby, T. D.; Boss, G. R., The combination of cobinamide and sulfanegen is highly effective in mouse models of cyanide poisoning. *Clinical Toxicology* **2011**, *49*, 366-373.

7. *Food and Drug Administration Guidance for industry bioanalytical method validation*. Rockville, MD, 2001.
8. Stutelberg, M. W.; Vinnakota, C. V.; Mitchell, B. L.; Monteil, A. R.; Patterson, S. E.; Logue, B. A., Determination of 3-mercaptopyruvate in rabbit plasma by high performance liquid chromatography tandem mass spectrometry. *Journal of Chromatography B* **2014**, 949-950, 94-98.
9. Corley, J., Methods for defining LOD and LOQ. In *Handbook of Residue Analytical Methods for Agrochemicals*, John Wiley & Sons: 2002; Vol. 1 pp 63-71.

Chapter 14

1. Isom, G. E.; Borowitz, J. L.; Mukhopadhyay, S., Sulfurtransferase Enzymes Involved in Cyanide Metabolism. In *Comprehensive Toxicology*, McQueen, C., Ed. 2010; Vol. 4, pp 485-500.
2. Nagasawa, H. T.; Goon, D. J. W.; Crankshaw, D. L.; Vince, R.; Patterson, S. E., Novel, orally effective cyanide antidotes. *Journal of Medicinal Chemistry* **2007**, 50, 6462-6464.
3. Brenner, M.; Kim, J. G.; Lee, J.; Mahon, S. B.; Lemor, D.; Ahdout, R.; Boss, G. R.; Blackledge, W.; Jann, L.; Nagasawa, H. T.; Patterson, S. E., Sulfanegen sodium treatment in a rabbit model of sub-lethal cyanide toxicity. *Toxicol. Appl. Pharmacol.* **2010**, 248 (3), 269-76.
4. Brenner, M.; Mahon, S. B.; Lee, J.; Kim, J.; Mukai, D.; Goodman, S.; Kreuter, K. A.; Ahdout, R.; Mohammad, O.; Sharma, V. S.; Blackledge, W.; Boss,

G. R., Comparison of cobinamide to hydroxocobalamin in reversing cyanide physiologic effects in rabbits using diffuse optical spectroscopy monitoring.

Journal of Biomedical Optics **2010**, *15* (1), 017001-017001.

5. Chan, A.; Balasubramanian, M.; Blackledge, W.; Mohammad, O. M.; Alvarez, L.; Boss, G. R.; Bigby, T. D., Cobinamide is superior to other treatments in a mouse model of cyanide poisoning. *Clinical Toxicology* **2010**, *48*, 709-717.

6. Chan, A.; Crankshaw, D. L.; Monteil, A.; Patterson, S. E.; Nagasawa, H. T.; Briggs, J. E.; Kozocas, J. A.; Mahon, S. B.; Brenner, M.; Pilz, R. B.; Bigby, T. D.; Boss, G. R., The combination of cobinamide and sulfanegen is highly effective in mouse models of cyanide poisoning. *Clinical Toxicology* **2011**, *49*, 366-373.

7. *Food and Drug Administration Guidance for industry bioanalytical method validation*. Rockville, MD, 2001.

8. Stutelberg, M. W.; Vinnakota, C. V.; Mitchell, B. L.; Monteil, A. R.; Patterson, S. E.; Logue, B. A., Determination of 3-mercaptopyruvate in rabbit plasma by high performance liquid chromatography tandem mass spectrometry. *Journal of Chromatography B* **2014**, *949-950*, 94-98.

9. Corley, J., Methods for defining LOD and LOQ. In *Handbook of Residue Analytical Methods for Agrochemicals*, John Wiley & Sons: 2002; Vol. 1 pp 63-71.

10. Rehman, H. U., Methemoglobinemia. *West. J. Med.* **2001**, *175* (3), 193-6.

11. Chan, A.; Crankshaw, D. L.; Monteil, A.; Patterson, S. E.; Nagasawa, H. T.; Briggs, J. E.; Kozocas, J. A.; Mahon, S. B.; Brenner, M.; Pilz, R. B.; Bigby, T.

- D.; Boss, G. R., The combination of cobinamide and sulfanegen is highly effective in mouse models of cyanide poisoning. *Clin. Toxicol. (Phila.)* **2011**, *49* (5), 366-73.
12. Stepuro, T. L.; Zinchuk, V. V., Nitric oxide effect on the hemoglobin-oxygen affinity. *J. Physiol. Pharmacol.* **2006**, *57* (1), 29-38.
13. Isom, G. E.; Borowitz, J. L.; Mukhopadhyay, S., Sulfurtransferase Enzymes Involved In Cyanide Metabolism. In *Elsevier Ltd*, Purdue University, W. L., IN,, Ed. Elsevier Ltd: 2010; pp 486-498.
14. Broderick, K. E.; Potluri, P.; Zhuang, S.; Scheffler, I. E.; Sharma, V. S.; Pilz, R. B.; Boss, G. R., Cyanide detoxification by the cobalamin precursor cobinamide. *Exp. Biol. Med. (Maywood)* **2006**, *231* (5), 641-9.
15. E.Patterson, S.; R.Monteil, A.; Cohen, J. F.; L.Crankshaw, D.; Vince, R.; Nagasawa, H. T., Cyanide antidotes for mass casualties: water-soluble salts of the dithiane (sulfanegen) from 3-mercaptopyruvate for intramuscular administration. *J. Med. Chem.* **2013**, *56* (3), 1346-1349.
16. Hamel, J., A review of acute cyanide poisoning with a treatment update. *Crit. Care Nurse* **2011**, *31* (1), 72-81; quiz 82.
17. Hall, A. H.; Sainers, J.; Baud, F., Which cyanide antidote? *Crit. Rev. Toxicol.* **2009**, *39* (7), 541-52.
18. Broderick, K. E.; Balasubramanian, M.; Chan, A.; Potluri, P.; Feala, J.; Belke, D. D.; McCulloch, A.; Sharma, V. S.; Pilz, R. B.; Bigby, T. D.; Boss, G. R., The Cobalamin Precursor Cobinamide Detoxifies Nitropruside-Generated Cyanide. *Exp. Biol. Med. (Maywood)* **2007**, *232* (6), 789-798.

19. Brenner, M.; Kim, J. G.; Mahon, S. B.; Lee, J.; Kreuter, K. A.; Blackledge, W.; Mukai, D.; Patterson, S.; Mohammad, O.; Sharma, V. S.; Boss, G. R., Intramuscular cobinamide sulfite in a rabbit model of sublethal cyanide toxicity. *Ann. Emerg. Med.* **2010**, *55* (4), 352-63.
20. Chan, A.; Balasubramanian, M.; Blackledge, W.; Mohammad, O. M.; Alvarez, L.; Boss, G. R.; Bigby, T. D., Cobinamide is superior to other treatments in a mouse model of cyanide poisoning. *Clin. Toxicol. (Phila.)* **2010**, *48* (7), 709-17.
21. Ma, J.; Dasgupta, P. K.; Zelder, F. H.; Boss, G. R., Cobinamide chemistries for photometric cyanide determination. A merging zone liquid core waveguide cyanide analyzer using cyanoaquacobinamide. *Anal. Chim. Acta* **2012**, *736*, 78-84.
22. Boss, G.; Sharma, V.; Brenner, M.; Dasgupta, P. K.; Blackledge, W. C., Rapid Method to measure cyanide in biological samples. *Patent Application Publication Pub.No.: US 2013/0005044A1* **2013**, *PCT No.: PCT/US 2011/028542 CO7F15/06(2006.01)* US cl. 436/109,540/145.
23. Fedosov, S. N.; Petersen, T. E.; Nexø, E., Binding of cobalamin and cobinamide to transcobalamin from bovine milk. *Biochemistry* **1995**, *34* (49), 16082-7.
24. Fedosov, S. N.; Berglund, L.; Fedosova, N. U.; E, N.; Petersen, T. E., Comparative analysis of cobalamin binding kinetics and ligand protection for intrinsic factor, transcobalamin, and haptocorrin. *J. Biol. Chem.* **2002**, *277* (12), 9989-96.

25. Fedosov, S. N.; Fedosova, N. U.; Krautler, B.; Nexø, E.; Petersen, T. E., Mechanisms of Discrimination between Cobalamins and Their Natural Analogues during Their Binding to the Specific B12-Transporting Proteins. *Biochemistry* **2007**, *46*, 6446-6458.
26. Blackledge, W. C.; Blackledge, C. W.; Griesel, A.; Mahon, S. B.; Brenner, M.; Pilz, R. B.; Boss, G. R., New facile method to measure cyanide in blood. *Anal. Chem.* **2010**, *82* (10), 4216-21.
27. Krueve, A.; Kaupmees, K.; Liigand, J.; Oss, M.; Leito, I., Sodium adduct formation efficiency in ESI source. *J. Mass Spectrom.* **2013**, *48* (6), 695-702.
28. Corley, J., Best Practices in Establishing Detection and Quantification limits for Pesticides in Foods Rutgers, T. S. U. o. N. J., North Brunswick, NJ.USA, Ed. October 24 2002; Vol. 15:54.
29. Corley, J., Best Practices in Establishing Detection and Quantification limits for Pesticides in Foods Rutgers, T. S. U. o. N. J., North Brunswick, NJ.USA, Ed. 2002; Vol. 15:54.

APPENDICES

APPENDIX I

Development of a Fluorescence-Based Sensor for Rapid Diagnosis of Cyanide Exposure

Randy Jackson,[†] Robert P. Oda,[†] Raj K. Bhandari,[†] Sari B. Mahon,[‡] Matthew Brenner,^{‡,§} Gary A. Rockwood,^{||} and Brian A. Logue^{*†,¶}

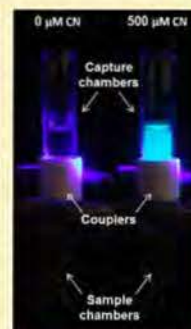
[†]Department of Chemistry and Biochemistry, South Dakota State University, Box 2202, Brookings, South Dakota 57007, United States

[‡]Beckman Laser Institute and Medical Clinic, University of California, Irvine, California 92612, United States

[§]Division of Pulmonary and Critical Care Medicine, Department of Medicine, University of California, Irvine, California 92868, United States

^{||}Analytical Toxicology Division, United States Army Medical Research Institute of Chemical Defense, 3100 Ricketts Point Road, Aberdeen Proving Ground, Maryland 21010, United States

ABSTRACT: Although commonly known as a highly toxic chemical, cyanide is also an essential reagent for many industrial processes in areas such as mining, electroplating, and synthetic fiber production. The "heavy" use of cyanide in these industries, along with its necessary transportation, increases the possibility of human exposure. Because the onset of cyanide toxicity is fast, a rapid, sensitive, and accurate method for the diagnosis of cyanide exposure is necessary. Therefore, a field sensor for the diagnosis of cyanide exposure was developed based on the reaction of naphthalene dialdehyde, taurine, and cyanide, yielding a fluorescent β -isoindole. An integrated cyanide capture "apparatus", consisting of sample and cyanide capture chambers, allowed rapid separation of cyanide from blood samples. Rabbit whole blood was added to the sample chamber, acidified, and the HCN gas evolved was actively transferred through a stainless steel channel to the capture chamber containing a basic solution of naphthalene dialdehyde (NDA) and taurine. The overall analysis time (including the addition of the sample) was <3 min, the linear range was 3.13–200 μM , and the limit of detection was 0.78 μM . None of the potential interferents investigated (NaHS, NH_4OH , NaSCN, and human serum albumin) produced a signal that could be interpreted as a false positive or a false negative for cyanide exposure. Most importantly, the sensor was 100% accurate in diagnosing cyanide poisoning for acutely exposed rabbits.



Cyanide (HCN or CN^- , inclusively represented as CN) is commonly known as a poison and a chemical warfare agent (CWA). However, the industrial need for CN in many chemical processes, such as mineral extraction, electroplating, and the fabrication of synthetic fibers,¹ drives cyanide production for industrial use to over 1.1 million tons per year.² Therefore, industrial use of mass quantities of cyanide, with its associated transportation through highly populated areas, drastically increases the risk of exposure. Cyanide exposure may also occur through diet, smoke inhalation (fire or cigarette smoke), or exposure from illicit use.^{3,4} Illicit use can be targeted at a single individual (i.e., poisoning), a small group of targeted individuals (e.g., mass suicides), or a large group of people (e.g., terrorist attacks). Some of the more recent incidents of illicit cyanide use are the Tylenol Poisonings in 1982,⁵ the use of cyanide-gas-producing devices in Tokyo subway and railway station restrooms in 1995,⁶ ingestion of cyanide tablets by Michael Marin upon receipt of a guilty verdict for arson in June 2012,⁷ and the death of Urooj Khan, a lottery winner, in Chicago in July 2012.⁸ Another illicit, relatively little-known, use of cyanide is to stun exotic fish for

easy capture, with an estimated 90% of the exotic fish originating from the Philippines captured in this manner.⁹

Whether the route of cyanide exposure is accidental or deliberate, the mechanism of cyanide toxicity is similar. Cyanide causes cellular death by blocking adenosine triphosphate (ATP) production through the binding of cytochrome c oxidase.¹⁰ The onset of cyanide toxicity is rapid, and toxic levels in blood can be observed at concentrations of approximately 19 μM ^{11,12} while death can be observed at concentrations as low as 115 μM .^{12,13} Although CN is highly toxic, it is endogenously present in animals due to normal amino acid metabolism, dietary intake, and tobacco consumption.^{3,14} Because CN and its major metabolites, thiocyanate (SCN^-) and 2-aminothiazoline-4-carboxylic acid (ATCA), have each been used as markers for cyanide exposure in biofluids,^{14–16} endogenous concentrations may complicate the diagnosis of cyanide exposure if not fully understood. Table 1 lists the ranges of endogenous

Received: November 26, 2013

Accepted: January 3, 2014

Published: January 3, 2014

concentrations of CN and its major metabolites, each of which are highly variable.

Table 1. Endogenous Levels of Cyanide Thiocyanate and ATCA in the Blood of Smokers and Non-Smokers

marker of CN exposure	typical biological matrix analyzed	nonsmoker (μM)	smoker (μM)	refs
cyanide	whole blood or RBCs	$0.02-10^4$	$0.03-10$	1, ^a 16, and 17
thiocyanate	plasma	4.6–130	1.7–290	1, ^b 16, and 17
ATCA	urine or plasma	0.08–0.27	0.12–0.45	1 ^c and 16

^aConcentrations compiled for nonsmokers ranged from 0.02 to 3 μM for Logue et al.¹ and 3–10 μM for Minalata et al.¹⁷ ^bLogue et al.¹ compiled endogenous concentrations of cyanide, thiocyanate, and ATCA for smokers and nonsmokers from studies prior to 2010.

Thiocyanate is the most common indirect marker of cyanide exposure because it is the major metabolite of cyanide, accounting for 80% of cyanide metabolism.¹⁸ ATCA has only recently been suggested for use as a biomarker, but it accounts for up to 20% of cyanide metabolism, with an increase in ATCA production as cyanide dose increases.^{3,19} Although SCN^- is a valuable marker of cyanide exposure, metabolism of cyanide to thiocyanate is enzymatically rate limited²⁰ and maximum thiocyanate concentrations can lag maximum cyanide concentrations by approximately 20 min to 6 h.²¹ Although ATCA mirrors the behavior of cyanide,¹⁹ its concentration in plasma has been found to be relatively low, necessitating an extremely sensitive diagnostic analysis.

Because of the rapid onset of toxic effects from cyanide poisoning and the difficulty in developing a rapid and sensitive analysis for ATCA, the most appropriate target for diagnosis of acute cyanide exposure is the direct analysis of cyanide as soon after exposure as possible. Although the detection of cyanide may be accomplished by several methods, including chromatography, mass spectrometry, fluorescence, and chemiluminescence,²² five recent methods for cyanide analysis from biological matrices have been proposed (Table 2) that focus on rapid analysis and/or portable technology. Three of these methods are based on a change in the absorbance of

cobinamide (hydroxoquocobinamide^{23,24} or hydroxycyanocobinamide²⁵) in the presence of cyanide. The remaining two are based on fluorescence detection of cyanide upon its interaction with copper(II) cubic mesoporous graphitic carbon nitride (Cu^{2+} -c-mpg- C_3N_4)²⁶ or 1-(4'-nitrophenyl) benzimidazolium.²⁷ Additionally, there have been a number of fluorometric and colorimetric probes developed in recent years for cyanide analysis,²⁸ but these probes have yet to be integrated into sensor technology. Table 2 lists the analysis time and limits of detection (LODs) for the proposed sensors, along with potential issues associated with each technology. Although some of the listed CN detection techniques have LODs reaching concentrations into the nanomolar range, endogenous levels of CN in humans range from 0.02 to 10 μM (see Table 1). Furthermore, the toxic effects of CN appear at blood concentrations around 19 μM .²² Therefore, an LOD of 3 μM or less, as achieved by each technology listed in Table 2, is likely sufficient for diagnosis of CN exposure (i.e., an LOD of 3 μM is typically associated with a lower limit of quantification of around 10 μM). Considering this, the other characteristics listed in Table 2 are likely more important in comparing these diagnostic technologies. For the techniques proposed, large sample volumes (1 mL),²³ interference from hydrogen sulfide,^{23,24} long analysis times,^{26,27} and unconfirmed ability to diagnose CN exposure,^{26,27} limit their application for diagnosis.

Considering limitations of the currently proposed rapid/portable CN detection techniques, there is a critical need for a rapid point-of-care diagnostic to confirm cyanide exposure and inform the administration of antidotes. The objective of this study was to develop a rapid and sensitive sensor for the accurate diagnosis of acute, toxic cyanide exposure.

EXPERIMENTAL SECTION

Materials. All materials used were HPLC grade unless otherwise indicated. Sodium hydroxide, sulfuric acid, sodium cyanide, KH_2PO_4 , K_2HPO_4 , and NH_4OH were purchased from Fisher Scientific (Hanover Park, IL). 2,3-Naphthalene dialdehyde (NDA) was obtained from TCI America (Portland, OR). Taurine (2-aminoethane sulfonic acid) and $\text{NaBO}_2 \cdot 4\text{H}_2\text{O}$ were purchased from Alfa Aesar (Ward Hill, MA). NaSCN was purchased from Acros Organics (Morris Plains, NJ). Human

Table 2. Comparison of Recently Proposed Rapid Analysis Methods and/or Portable Technologies for the Diagnosis of Cyanide Exposure

investigator	core technology	sample prep method	analysis time (min)	LOD ^a (μM)	notes
Ma et al., 2011 ²³	hydroxoquocobinamide	microdiffusion	~2	0.5 ^{b,c}	H_2S is an interferent.
Ma and Dasgupta, 2010 ²⁴	hydroxoquocobinamide	microdiffusion	~1.5	0.030 ^b	H_2S is an interferent, and the NaOH mobile phase is necessary. ^d
Tian et al., 2013 ²⁵	hydroxycyanocobinamide	microdiffusion	<4	2.2 ^{b,c}	Potential interferents were not evaluated, but H_2S likely interferes.
Lee et al., 2012 ²⁶	turn on fluorescence Cu^{2+} -c-mpg- C_3N_4 ^e	isolate serum. Follow on sample prep not described.	40 ^f	0.080 ^b	The analysis time reported (10 min) likely did not include the time needed to clot blood and separate the serum. ^{h,i}
Kumar et al., 2013 ²⁷	fluorescence of 1-(4'-nitrophenyl) benzimidazolium	isolate serum then add HEPES buffer and DMSO solution.	31 ^f	0.030 ^b	The analysis time reported (<60 s) did not include the time needed to clot blood and separate serum. ^{h,i}

^aLOD, limit of detection. ^bThe listed LODs are for rabbit whole blood. ^cThese techniques were verified using CN exposed rabbits. ^dMethod not verified in an animal model. ^ec-mpg- C_3N_4 is cubic mesoporous graphitic carbon nitride. ^fThirty minutes was added to the reported analysis time to account for the estimated time necessary to clot blood and separate serum from blood. ^gThe listed LODs are for human blood serum. ^hThe sample preparation to obtain serum from blood requires extra equipment.

serum albumin (HSA) and NaHS were purchased from Sigma-Aldrich (St. Louis, MO).

Phosphate (0.1 M)/borate (0.05 M) buffer and stock solutions of sodium hydroxide (1 M), sulfuric acid (1 M), and NaSCN (1 mM) were prepared in deionized water. Sodium cyanide standards and NaHS were obtained by dilution from 1.8 mM and 1 M stock solutions, respectively, with 10 mM NaOH. NH_4OH was prepared by diluting the original aqueous solution (29% by weight or 14.5 M) to 30 μM in deionized water. The NDA (2 mM) stock solution was prepared in phosphate/borate buffer and 40% methanol. A taurine (50 mM) solution was prepared in phosphate/borate buffer. A standard HSA solution was obtained by dissolving 3.3 mg of HSA per mL of deionized water.

Biological Samples. Rabbit whole blood samples were obtained from two sources: (1) nonsterile whole blood with 2.5% EDTA from young rabbits was purchased from Pel-Freez Biologicals (Rogers, AR) and (2) whole blood from cyanide exposed, New Zealand White rabbits (*Oryctolagus cuniculus*, male, 3.5–4.5 kg) was obtained from the University of California, Irvine. Rabbits ($n = 6$) were administered lethal doses of 6.8 mM NaCN in 0.9% NaCl (1 mL/min continuous intravenous infusion) and blood was drawn prior to and 15, 25, and 35 min following the initiation of cyanide infusion. The blood samples were placed in EDTA tubes to prevent coagulation, frozen, and shipped on ice (overnight) to South Dakota State University for analysis of cyanide. Upon receipt, the blood was stored at -80°C until cyanide analysis was performed.

All rabbits were cared for in compliance with the "Principles of Laboratory Animal Care" formulated by the National Society for Medical Research and the "Guide for the Care and Use of Laboratory Animals" prepared by the National Academy of Sciences and published by the National Institutes of Health.²⁹ All studies involving rabbits were reviewed and approved by the Institutional Animal Care and Use Committee (IACUC).

Fluorometric Analysis of Cyanide. Microdiffusion was used to prepare cyanide for analysis. The microdiffusion of CN was accomplished via a stacked cyanide capture apparatus. A schematic of the stacked cyanide capture apparatus can be seen in Figure 1 with a lower chamber, called the sample chamber, used to contain cyanide standards, swabs, whole blood samples, or other sample matrices, and an upper chamber called the capture chamber, containing a capture solution of 0.5 mM NDA:12.5 mM taurine:0.1 M NaOH (1:1:1 by volume). These

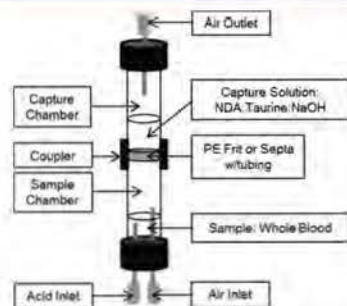


Figure 1. Schematic of the stacked cyanide capture apparatus.

two chambers [8 (i.d.) \times 50 mm long] were separated by a hydrophobic 10 micron porous polyethylene (PE) frit or a 1.5 mm thick silicone septum pierced with a 2 mm long, 28 gauge forward flow tube. The frit/septum was sandwiched between the sample and capture chamber using a 1.8 cm long piece of threaded (13 \times 425) PVC tubing with a 1.6 cm external diameter as a coupler. A needle at the top of the capture chamber served as an outlet for the carrier gas. The sample chamber septum was pierced with two inlet needles (at the bottom of Figure 1), one for the injection of acid and one for introduction of air. Attempts to combine the acid and air introduction failed due to large viscosity fluctuation between the solution and the air, resulting in difficulty in controlling the rate of air flow through the chamber.

For the separation of CN from the biological matrix, the sample was placed in the sample chamber and acidified with sulfuric acid (300 μL of 1 M) and air (20 mL for the PE frit, 20 and 50 mL for the silicone septum were evaluated) was forced over the sample headspace to a capture solution where HCN gas was trapped in the capture chamber using strong base to convert HCN to nonvolatile CN^- . The captured CN^- was then reacted with NDA and taurine in the capture solution, resulting in a fluorescent β -isoindole product (Figure 2, Scheme A \rightarrow B).³⁰ The cyanide capture apparatus fit within the detector chamber so that the portion of the capture chamber containing the capture solution was in alignment with the LED and a photodiode or optic fiber connected to a spectrophotometric detector. Sample analysis time, beginning at sample introduction through fluorescence detection, was less than 3 min. During this study, the cyanide capture apparatus was cleaned with deionized water between analyses, but washing the air and acid inlets and the air outlet (Figure 1) was unnecessary [i.e., no carryover was observed except when using the PE frit and high concentrations of cyanide ($>500 \mu\text{M}$), likely due to HCN partitioning into the PE material; note that the PE material was not used for the majority of the study]. Although the cyanide capture apparatus was reused in this study, it could easily be designed to be disposable, eliminating the need for washing and the potential for carryover.

Fluorometric analysis was performed using one of two configurations. Fluorometric Configuration 1 (FC1) utilized a 420 nm light emitting diode (LED, TT Electronics, Weybridge, Surrey, KT13 9XB, England) positioned at a 90° angle from a 400–650 nm light sensitive photodiode (Avago Technologies, Ft. Collins, CO) and produced digital signals ranging from 0 to 218. Fluorometric Configuration 2 (FC2) consisted of a 410 nm high-powered LED (LED Engin, Inc., San Jose, CA) irradiated through a focusing lens and directed toward the sample. A second focusing lens positioned 90° from the irradiation path was used to direct the fluorescent light to a 600 μm optical fiber connected to a USB2000+ spectrophotometric detector. The signal at 500 nm was used to quantify the amount of cyanide in the sample. The focusing lenses, the optical fiber, and the spectrophotometric detector were purchased from Ocean Optics (Dunedin, FL). Since the detection limit for FC1 was not within the biologically relevant range desired, fluorometric analysis was performed using FC2, unless otherwise noted.

The field sensor dimensions were 15 \times 20 \times 30 cm (1 \times w \times h). Housed within the sensor was an acid reservoir, cyanide capture apparatus chamber, a USB2000+ spectrophotometer (connected to a laptop computer), a valve switching mechanism, a 1 mL syringe with a 30 mm stroke linear

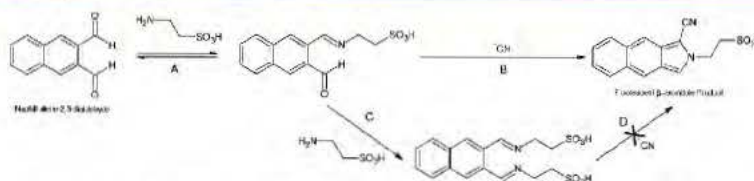


Figure 2. The proposed reaction schemes for the possible reactions of NDA, taurine, and cyanide. Pathways A \rightarrow B and A \rightarrow C both yield H_2O as a byproduct.

actuator, and a 50 mL syringe with a 100 mm stroke linear actuator (each linear actuator served as a syringe pump). NDA and taurine were stored separately and added to the capture chamber prior to analysis.

Reagent Stability. The stability of capture solution reagents was an important factor pertaining to the field portability of the sensor. Three different capture solution storage scenarios were investigated. In scenario 1, all the capture solution reagents (NDA, taurine, and NaOH) were mixed together and stored as one solution. In scenario 2, NDA and taurine were mixed and stored as one solution, while the NaOH solution was added at the time of analysis. In scenario 3, all the capture solution reagents were stored individually and mixed at the time of analysis. All solutions were stored in amber vials at room temperature for the duration of the stability study and cyanide analysis was accomplished using FC1. A cyanide stock solution (200 μM) was analyzed for all scenarios. The stock solutions for scenarios 1 and 2 were analyzed from 0 to 60 min, with samples for scenario 3 analyzed up to 70 days.

Analysis of Possible Interferents. Potentially interfering compounds, NH_4OH (30 μM), NaSCN (0.5 mM), HSA (3.3 mg/mL), and NaHS (110 μM), were evaluated alone (for false positive evaluation) and spiked with 20 μM NaCN (for false negative evaluation). The compounds of interest were evaluated at concentrations likely found in biological matrices during cyanide poisoning (i.e., the naturally occurring concentration of NH_4OH as ammonia gas,³¹ thiocyanate in excess of the highest levels seen in smokers,^{16,32} the amount of HSA present in blood,³¹ and the highest concentration of H_2S found in the blood of sulfide poisoning fatalities³³). Multiple mixtures of the interferent solutions were used to evaluate additive effects to include (1) equal parts NaHS and NH_4OH solutions, (2) equal parts NaSCN and NH_4OH solutions, (3) equal parts NaSCN, NaHS, NH_4OH , and HSA solutions, (4) equal parts NaSCN and HSA solutions, and (5) equal parts of NaHS, NH_4OH , and HSA solutions.

Analysis of Cyanide from Rabbit Whole Blood. The analysis of cyanide from rabbit whole blood was optimized to include sample volume (50 and 100 μL), acid injection volume (200–500 μL), and acid concentration (0.25 to 2 M). Once the optimum conditions were determined, a calibration curve was created with 0.25 to 200 μM cyanide spiked rabbit blood calibrators analyzed in triplicate. Prior to each analysis, a 10 μM quality control (QC) standard (cyanide spiked rabbit whole blood) was analyzed to represent the concentration threshold, above which, a subject was said to be “exposed”. This concentration was chosen because it is the highest cyanide concentration that has been previously observed in the blood of human smokers.¹ Cyanide exposed rabbit blood samples (from U. C., Irvine) were analyzed in triplicate for time points 0 (baseline), 15, 25, and 35 min. As a measure to verify the

performance of the sensor, the rabbit blood samples were also analyzed using the LC-MS/MS analysis method for cyanide described by Bhandari et al. 2013.³⁴

Data Analysis. The limit of detection (LOD) was determined as the analyte concentration that produced a signal-to-noise ratio (S/N) of 3, with the noise measured as the standard deviation of the blank. The lower limit of quantification (LLOQ) was defined as the analyte concentration that produced a S/N of at least 10, a measured concentration, calculated from the calibration curve, that was within 20% of the nominal concentration as a measure of accuracy, and a percent relative standard deviation (%RSD) of $\leq 20\%$ as a measure of precision. For inclusion of calibrators in the linear range of the sensor, replicate calibration standards were required to produce a precision of $\leq 20\%$ RSD and accuracy of $100 \pm 20\%$. The upper limit of quantification (ULOQ) was defined as the highest analyte concentration that produced a measured concentration, that was within 20% of the nominal concentration as a measure of accuracy with a precision of $\leq 20\%$ RSD. It should be noted that the spectrophotometer limited the maximum signal to $\approx 63,000$ cps, which limited the ULOQ for both aqueous and blood samples. All quantitative analytical values (i.e., concentration, mean, standard deviation, etc.) were calculated using Microsoft Office Excel 2010 (Redmond, WA).

Caution. Cyanide is toxic and hazardous to humans at blood concentrations of $\approx 20 \mu\text{M}$.³² HCN is produced from aqueous cyanide containing solutions near or below a pH of 9.2. Therefore, all aqueous cyanide standards were prepared in 10 mM NaOH and handled in a well-ventilated hood. HCN gas was produced during the acidification process in the sample chamber and then captured and derivatized in a basic solution containing NDA and taurine in the capture chamber. The fluorescent β -indole product was disposed of with organic waste. The proper use of personal protective equipment (i.e., gloves, lab coat, etc.), laboratory equipment (i.e., ventilation hood), and proper waste disposal must be followed to prevent the possibility of exposure.

RESULTS AND DISCUSSION

Development of a Cyanide Sample Preparation Apparatus. Two barrier materials were evaluated to separate the sample and capture chambers of the cyanide microdiffusion apparatus (Figure 1): (1) a silicone septa with stainless steel tubing and (2) a 10 micron porous PE frit. Figure 3 shows the calibration curves achieved with each barrier material. When the PE frit was used as the barrier, the signals observed for the lowest and highest concentrations tested were nonlinearly related to the cyanide concentration, and attempts to describe the calibration data with a linear fit produced nonzero intercepts. The PE frit produced an LOD of 3.13 μM and a

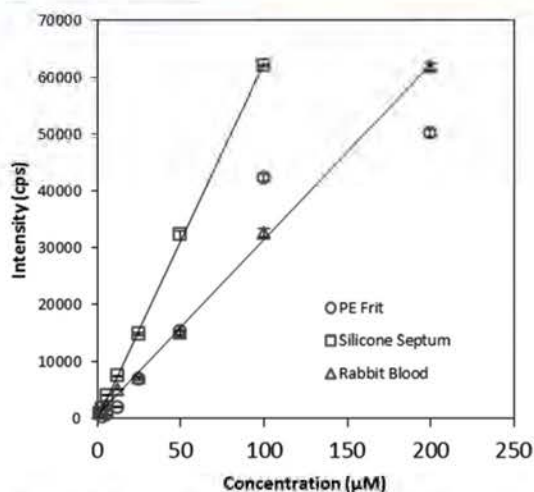


Figure 3. Calibration curves obtained for the PE frit (20 mL of air), the silicone septa with forward flow tubing (50 mL of air shown), and rabbit whole blood (50 mL of air). Aqueous standards were used for the PE frit (○) and the silicone septa (□). A silicone septa, with forward flow tubing as the chamber separation material, was used for analysis of rabbit whole blood (△). Error bars represent standard deviation.

linear range of 25–100 μM . When using the silicone septa, linear behavior was produced throughout the calibration range. When a low volume of air (20 mL) was used to carry HCN from the sample to the capture chamber, the linear range was 1.5–200 μM with a detection limit of 0.5 μM (data not shown). When using 50 mL of air, the LOD decreased to 0.25 μM , the sensitivity increased 2.4 \times (from 263 to 626 μM^{-1}), and the linear range changed to 1.5–100 μM . (Note: with this larger air volume, the 200 μM cyanide standard produced a signal that saturated the detector, resulting in the reduced upper limit of quantification.) Linear least-squares treatment of the calibration data for both air volumes resulted in correlation coefficients of 0.999. The linear behavior of the silicon septa compared to the nonlinear behavior of the PE frit was likely due to nonequilibrium partitioning of HCN into the PE.

Aside from the analytical performance of the two barrier materials, foaming of the sample was a major practical issue. If heavy foaming occurred, it forced the capture solution out of the air outlet (Figure 1) and required lower flow rates and longer analysis times to ensure conservation of the capture solution. Separation of the sample and capture chamber with a polyethylene frit produced very small bubbles, resulting in heavy sample foaming due to minimal surface tension stress lengthening the time needed for the bubbles to burst. To avoid the loss of capture solution, the time necessary to deliver the air through the sample and capture chamber significantly increased. Conversely, when air was forced through the silicone septa, relatively large bubbles with uniform size and shape were produced, which significantly limited foaming and allowed a faster flow of air from the sample to the capture chamber. Moreover, the larger bubbles did not appear to hinder the transfer of HCN to the capture solution. Therefore, the silicone septum was preferred both practically and analytically.

Reagent Stability. Reagent stability is crucial when developing a portable sensor, especially in locations where there is a lack of refrigeration and/or climate control. Figure 4

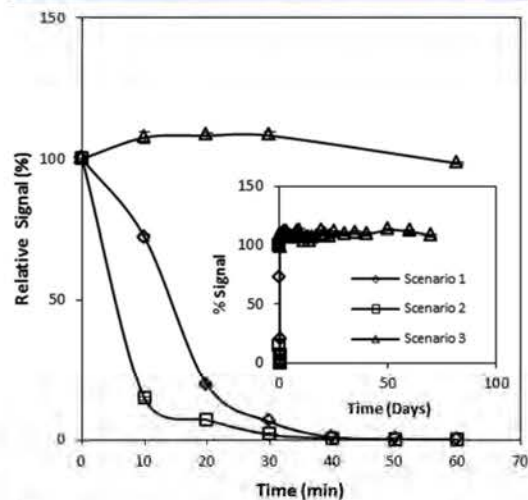


Figure 4. Assessment of the short- and long-term stability of the capture solution reagents. The long-term stability of the reagents (up to 70 days) is presented in the inset. Error bars represent standard deviation.

shows that under the storage conditions where the NDA and taurine were stored together (scenarios 1 and 2), extremely unstable mixtures resulted. Conversely, NDA and taurine stored separately (scenario 3) resulted in stable reagents for all time periods tested. The behavior of scenarios 1 and 2 was similar, where the initial fluorescent signal rapidly decreased until the fluorescence was essentially eliminated by 40 min. Visually, the solutions for scenarios 1 and 2 were initially clear but quickly became faintly yellow and orange, respectively, each also containing a small amount of black precipitate. Over time, these solutions became darker until the black precipitate pervaded. This color change was a visual indication that NDA and taurine were likely reacting together, potentially yielding an NDA–ditaurine complex (see Figure 2, pathway A \rightarrow C \rightarrow D). Since taurine was in excess, it is likely that by 40 min, the main component of the solutions was an NDA–ditaurine complex, which was incapable of producing the fluorescent β -isoindeole product.

Although more stringent storage conditions should be tested (e.g., larger variations in temperature to account for extremes the sensor may encounter), the stability of the capture solution reagents, when stored separately, is encouraging for use in a cyanide field sensor. In accordance with Figure 4, the reagents would not need special storage conditions when stored separately (i.e., the only special storage condition was the use of amber bottles). It should be noted that the day-to-day variations observed from storage scenario 3 were likely due to fluctuations in the temperature of the room and the electrical current produced from the sensor's power source (i.e., dual 9 V batteries) and were not reflective of variability in the chemical or sample preparation strategies associated with the analysis.

Analysis of Possible Interferents. The evaluation of potential interferents was undertaken to assess the possibility of

false positive or negative diagnosis of cyanide poisoning from common components of blood. Figure 5 shows that none of

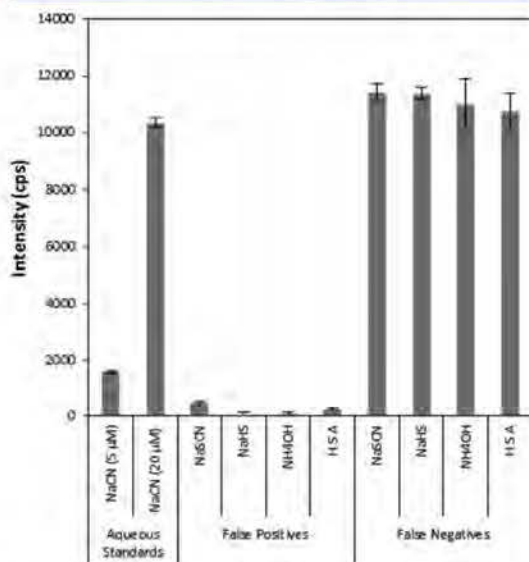


Figure 5. Assessment of potential interferences to the sensor technology present in cyanide spiked blood. Error bars represent standard deviation.

the compounds investigated produced false positive signals (i.e., above the 5 μM cyanide standard) and that all individually tested samples containing 20 μM NaCN produced signals within ±10% of the standard (i.e., no false negatives were observed). Similarly, none of the mixtures tested produced signals that could be interpreted as false positives or negatives (data not shown). The specificity of the current sensor is

encouraging, considering H₂S has been noted as a potential interferent for other methods of cyanide analysis. For example, the EPA ion chromatography method notes H₂S (evolved when NaHS is acidified) as an interferent, masking the presence of cyanide³⁵ and the cobinamide-based cyanide detection methods by Ma and Dasgupta also note H₂S as a potential interferent.^{23,24}

Samples containing thiocyanate and HSA did produce a slightly elevated signal compared to the aqueous blank, but below the 5 μM NaCN aqueous standard. In 1971, Chung and Wood³⁶ showed that thiocyanate produced cyanide under acidic conditions in the presence of hydrogen peroxide as an oxidizing agent. Since the sample chamber was under acidic conditions, oxygen bubbled through the sample chamber likely acted as an oxidizing agent, causing a small amount of cyanide to form. For HSA, the elevated fluorescence may have been due to the release of cyanide from cyanide–HSA adducts under acidic conditions.³⁷

Analysis of Cyanide from Rabbit Whole Blood. The analysis of cyanide from whole blood required modification of the method used for aqueous solutions, with 100 μL of sample and 300 μL of 1.5 M H₂SO₄ found to be optimum conditions for the microdiffusion of cyanide. Because the surface-area-to-volume ratio of the sample chamber limited the amount of HCN gas evolved, lower volumes of acid were used and the concentration of acid became very important, with higher concentrations increasing the amount of HCN evolved. The linear range for cyanide quantification in whole blood was found to be 3.13–200 μM with a detection limit of 0.78 μM, a slope of 310 μM⁻¹, and a correlation coefficient of 0.999 (Figure 3). Even with optimization, the recovery of cyanide was low (39% and 34% for 5 and 75 μM QC standards, respectively). The inefficient recovery of cyanide was likely caused upon addition to whole blood by its rapid transformation to volatile HCN gas at pH values below its pK_a of 9.2,¹⁴ enzyme-catalyzed conversion to SCN⁻ in the presence of

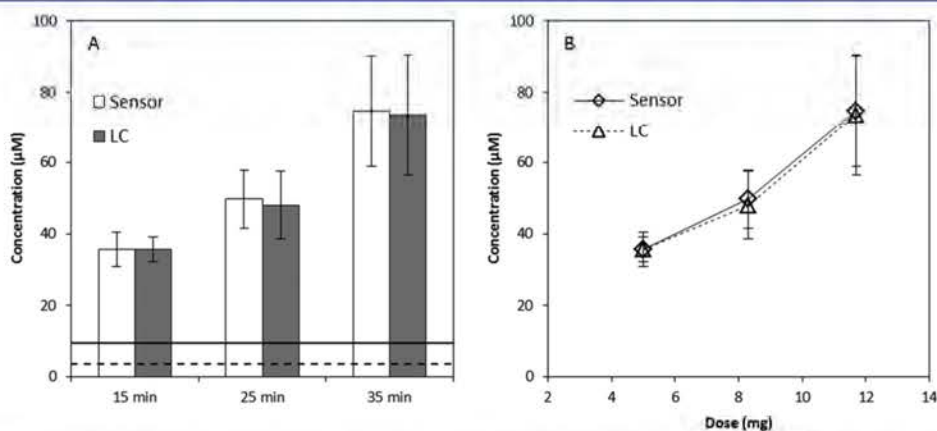


Figure 6. (A) Comparison of the cyanide concentrations found in the whole blood of cyanide exposed rabbits at 15, 25, and 35 min into the infusion period (5, 8.3, and 11.7 mg NaCN exposure, respectively). The dashed line represents the LLOQ (3.12 μM) and the solid line represents 10 μM cyanide, the threshold considered “cyanide exposure” for this study. Standard deviation values (±3 s) for the lines were not presented because they were negligible compared to the scale of the x axis. Note that for the 15 min time point $n = 3$ because three animals did not have blood drawn at that time interval. (B) Dose–response curves for three different doses of NaCN (5, 8.3, and 11.7 mg) intravenously administered to rabbits. Error bars represent standard deviation.

a sulfur donor,⁴ and binding to blood components, including hemoglobin (Hb), methemoglobin (metHb), and albumin.³

Diagnosis of Cyanide Exposure in Rabbits. The described sensor was used to verify cyanide exposure in rabbits (Figure 6). Rabbit blood drawn prior to exposure produced a small amount of fluorescence due to endogenous cyanide concentrations,^{19,38} but it was below the LOD. Rabbit blood drawn at 15, 25, and 35 min into the infusion period produced cyanide concentrations of 35.6 ± 4.8 , 49.7 ± 8.2 , and $74.6 \pm 15.6 \mu\text{M}$, respectively, as measured by the sensor. These concentrations deviated by less than 3.5% of the concentrations found by LC-MS/MS (Figure 6A). Similar to observations of Bhandari et al.,¹⁹ blood cyanide concentrations exhibited a linear response to increasing doses of cyanide (Figure 6B). Each rabbit that could be considered "exposed" (i.e., CN concentration levels above $10 \mu\text{M}$) was correctly diagnosed from the analysis of whole blood by the sensor. Moreover, each sample was analyzed for exposure in under 3 min, and triplicate analysis of individual rabbits produced measured cyanide concentrations with a %RSD of $\leq 12\%$ for all time points. The interanimal variability observed was expected due to varying physiological characteristics of individual rabbits (e.g., animal size, levels of rhodanese present, etc.). Overall, the sensor was 100% accurate in diagnosing cyanide poisoning for acutely exposed rabbits.

CONCLUSIONS

A rapid and sensitive cyanide field sensor was developed based on the detection of a fluorescent β -isoindole product produced by the reaction of NDA, taurine, and cyanide. The optimized sensor consists of a cyanide capture apparatus with two chambers separated by silicone septa punctured with small bore stainless steel tubing. This configuration produced a linear range of $1.5\text{--}100 \mu\text{M}$ with a detection limit of $0.25 \mu\text{M}$ for aqueous cyanide and a linear range of $3.13\text{--}200 \mu\text{M}$ with a detection limit of $0.78 \mu\text{M}$ for rabbit whole blood. None of the potential interferents produced a signal that could be considered a false positive or negative for cyanide exposure, and the excellent storage stability of the capture solution reagents make the described cyanide sensor highly applicable to field use. Compared to the rapid and/or portable sensors shown in Table 2, the described sensor has a rapid analysis time, a biologically relevant detection limit, and no known interferents. Although the analysis time for this sensor is short, rapid diagnosis of cyanide may be limited by the collection of blood (i.e., a finger prick with a lancet and collection of venous blood by trained personnel would require a significant amount of time). Studies are underway to link the salivary concentrations of cyanide with cyanide exposure, eliminating the need for invasive and potentially lengthy blood collection.

The performance of the sensor, most importantly the 100% accurate and rapid (<3 min) diagnosis of cyanide exposure in rabbits, is promising for the development of a highly robust field-portable sensor for the accurate diagnosis of cyanide exposure. Further sensor development, specifically focused on more rapid analysis and miniaturization, is currently underway.

AUTHOR INFORMATION

Corresponding Author

*E-mail: brian.logue@sdsstate.edu. Tel: +1 605 688 6698.

Notes

The authors declare no competing financial interest.

ACKNOWLEDGMENTS

The research was supported by the CounterACT Program, National Institutes of Health Office of the Director, and the National Institute of Allergy and Infectious Diseases, Interagency Agreement Numbers Y1-OD-0690-01/A-120-B.P2010-01, Y1-OD-1561-01/A120-B.P2011-01, AOD12060-001-00000/A120-B.P2012-01 and the USAMRICD under the auspices of the U.S. Army Research Office of Scientific Services Program Contract W911NF-11-D-0001 administered by Battelle (Delivery order 0079, Contract TCN 11077), USAMRMC W81XWH-12-2-0098, and NIH U54 NS079201. We gratefully acknowledge funding from the Oak Ridge Institute for Science and Education (ORISE). We thank the National Science Foundation Major Research Instrumentation Program (Grant CHE-0922816) for funding the AB SCIEX QTRAP 5500 LC-MS/MS. The LC-MS/MS instrumentation was housed in the South Dakota State University Campus Mass Spectrometry Facility, which was supported by the National Science Foundation/EPSCoR Grant 0091948 and the State of South Dakota. The opinions or assertions contained herein are the private views of the authors and are not to be construed as official or as reflecting the views of the Department of the Army, the National Institutes of Health, the National Science Foundation, or the Department of Defense. The authors declare that there are no conflicts of interest. The authors alone are responsible for the content and writing of the paper.

REFERENCES

- (1) Logue, B. A.; Hinkens, D. M.; Baskin, S. I.; Rockwood, G. A. *Crit. Rev. Anal. Chem.* **2010**, *40*, 122–147.
- (2) Mudder, T. I.; Botz, M. M. *Eur. J. Miner. Process. Environ. Prot.* **2004**, *4*, 62–74.
- (3) Baskin, S.; Brewer, T. In *Medical Aspects of Chemical and Biological Warfare*; Sidell, F.; Takafuji, E.; Franz, D., Eds.; Office of the Surgeon General, Department of the Army: Falls Church, VA, 1997; pp 271–286; Baskin, S. I.; Kelly, J. B.; Maliner, B. I.; Rockwood, G. A.; Zoltani, C. K. In *Medical Aspects of Chemical Warfare*; Tuorinsky, S. D., Ed.; Office of the Surgeon General, Department of the Army: Falls Church, VA, 2008; pp 371–410.
- (4) Moriya, F.; Hashimoto, Y. *J. Forensic Sci.* **2001**, *46*, 1421–5.
- (5) Douglas, J. E.; Olshaker, M. *The Anatomy Of Motive: The FBI's Legendary Mindhunter Explores The Key To Understanding And Catching Violent Criminals*; Scribner: New York City, 1999.
- (6) Okumuru, T.; Ninomiya, N.; Ohta, M. *Prehosp. Disaster Med.* **2003**, *18*, 189–192.
- (7) Davenport, P. Michael Marin, Ex-Wall Street Trader, Took Cyanide after Guilty Arson Verdict. *Huffington Post* (www.huffingtonpost.com), July 27, 2012.
- (8) Keyser, J. Urooj Khan, Chicago Lottery Winner's Cyanide Death Under Investigation. *Huffington Post* (www.huffingtonpost.com), January 8, 2013.
- (9) McManus, J. W.; Reyes, R. B.; Nanola, C. L. *J. Environ. Manage.* **1997**, *21*, 69–78; Barber, C. V.; Pratt, R. V. *Environment* **1998**, *40*, 5–34; Wabritz, C.; Taylor, M.; Green, E.; Razak, T., *From Ocean to Aquarium*; Cambridge, U.K., 2003.
- (10) Cooper, C. E.; Brown, G. C. *J. Bienerg. Biomembr.* **2008**, *40*, 533–539.
- (11) Cherian, M. A.; Richmond, I. *J. Clin. Pathol.* **2000**, *53*, 794–795.
- (12) Toxicology Profile for Cyanide. Agency for Toxic Substances and Disease Registry, U.S. Department of Health and Human Services: Washington, D.C., 2006.
- (13) Laforge, M.; Gourlain, H.; Fompeydie, D.; Buneaux, F.; Borron, S. W.; Galliot-Guilley, M. *J. Toxicol. Clin. Toxicol.* **1999**, *37*, 337–340.
- (14) Logue, B. A.; Kirschten, N. P.; Petrikovics, I.; Moser, M. A.; Rockwood, G. A.; Baskin, S. I. *J. Chromatogr., B: Anal. Technol. Biomed. Life Sci.* **2005**, *819*, 237–44.

- (15) Jackson, R.; Petrikovics, I.; Latic, E. P. C.; Yu, J. C. C. *Anal. Methods* **2010**, *2*, 552–557.
- (16) Vinnakota, C. V.; Peetha, N. S.; Perrizo, M. G.; Ferris, D. G.; Oda, R. P.; Rockwood, G. A.; Logue, B. A. *Biomarkers* **2012**, *17*, 625–633.
- (17) Minakata, K.; Nozawa, H.; Gonnori, K.; Yamagishi, I.; Suzuki, M.; Hasegawa, K.; Watanabe, K.; Suzuki, O. *Anal. Bioanal. Chem.* **2011**, *400*, 1945–1951.
- (18) Baskin, S. I.; Petrikovics, I.; Platoff, G. E.; Rockwood, G. A.; Logue, B. A. *Toxicol. Mech. Methods* **2006**, *16*, 339–45. Baskin, S. I.; Petrikovics, I.; Kurche, J. S.; Nicholson, J. D.; Logue, B. A.; Maliner, B.; Rockwood, G. A. In *Pharmacological Perspectives of Toxic Chemicals and Their Antidotes*; Flora, S. J. S., Jr., Romano, J. A., Baskin, S. I., Sekhar, K., Eds.; Narosa Publishing House: New Delhi, India, 2004, p 105; Baskin, S. I.; Isom, G. E. In *Comprehensive Toxicology*; Sipes, I. G., McQueen, C. A., Gaudolfi, A. J., Eds.; Elsevier Science: New York, NY, 1997, pp 477–488.
- (19) Bhandari, R. K.; Oda, R. P.; Petrikovics, I.; Thompson, D. E.; Brenner, M.; Mohan, S. B.; Beberta, V. S.; Rockwood, G. A.; Logue, B. A., *J. Anal. Toxicol.* **2014**, in press.
- (20) Sylvester, D. M.; Hayton, W. L.; Morgan, R. L.; Way, J. L. *Toxicol. Appl. Pharmacol.* **1983**, *69*, 265–271.
- (21) Sousa, A. B.; Manzano, H.; Soto-Blanco, B.; Gorniak, S. L. *Arch. Toxicol.* **2003**, *77*, 330–334.
- (22) Ma, J.; Dasgupta, P. K. *Anal. Chim. Acta* **2010**, *673*, 117–125.
- (23) Ma, J.; Ohira, S.-I.; Mishra, S. K.; Puanngam, M.; Dasgupta, P. K.; Mahon, S. B.; Brenner, M.; Blackledge, W.; Boss, G. R. *Anal. Chem.* **2011**, *83*, 4319–4324.
- (24) Ma, J.; Dasgupta, P. K.; Blackledge, W.; Boss, G. R. *Anal. Chem.* **2010**, *82*, 6244–6250.
- (25) Tian, Y.; Dasgupta, P. K.; Mahon, S. B.; Ma, J.; Brenner, M.; Wang, Jian-Hua; Boss, G. R. *Anal. Chim. Acta* **2013**, *768*, 129–135.
- (26) Lee, E. Z.; Lee, S. U.; Heo, N.-S.; Stucky, G. D.; Jun, Y.-S.; Hong, W. H. *Chem. Commun.* **2012**, *48*, 3942–3944.
- (27) Kumar, S.; Singh, P.; Hundal, G.; Hunda, M. S.; Kumar, S. *Chem. Commun.* **2013**, *49*, 2667–2669.
- (28) Niu, H.-T.; Su, D.; Jiang, X.; Yang, W.; Yin, Z.; Hea, J.; Cheng, J.-P. *Org. Biomol. Chem.* **2008**, *6*, 3038–3040. Niu, H.-T.; Jiang, X.; He, J.; Cheng, J.-P. *Tetrahedron Lett.* **2008**, *49*, 6521–6524. Lv, X.; Liu, J.; Liu, Y.; Zhao, Y.; Chen, M.; Wang, P.; Guo, W. *Org. Biomol. Chem.* **2011**, *9*, 4954–4958. Li, H.; Li, B.; Jin, L.-Y.; Kan, Y.; Yin, B. *Tetrahedron.* **2011**, *67*, 7348–7353. Kumari, N.; Jha, S.; Bhattacharya, S. *J. Org. Chem.* **2011**, *76*, 8215–8222.
- (29) *Guide for the Care and Use of Laboratory Animals*, 8th ed.; The National Academic Press: Washington, D.C., 2011.
- (30) Carlson, R. G.; Srinivasachar, K.; Givens, R. S.; Matuszewski, B. K. *J. Org. Chem.* **1986**, *51*, 3978–3983. Sano, A.; Takezawa, M.; Takitani, S. *Anal. Chim. Acta* **1989**, *225*, 351–358.
- (31) Diem, K. *Documenta Geigy: Scientific Tables*, 7th ed.; Wiley: Basel, Switzerland, 1970.
- (32) Tsuge, K.; Kataoka, M.; Seto, Y. *J. Health Sci.* **2000**, *46*, 343–350.
- (33) *Air Quality Guidelines*; Theakston, F., Ed.; WHO Regional Office for Europe: Copenhagen, Denmark, 2000.
- (34) Bhandari, R. K.; Manandhar, E.; Oda, R. P.; Rockwood, G. A.; Logue, B. A. *Anal. Bioanal. Chem.*, **2014**, in press.
- (35) *Other Test Method 29, Sampling and Analysis for Hydrogen Cyanide Emissions from Stationary Sources*; U. S. Environmental Protection Agency: Atlanta, GA, 2011.
- (36) Chung, J.; Wood, J. L. *J. Biol. Chem.* **1971**, *246*, 555–560.
- (37) Fasco, M. J.; Hauer, C. R., III; Stack, R. F.; O’Hehir, C.; Barry, J. R.; Eadon, G. A. *Chem. Res. Toxicol.* **2007**, *20*, 677–684.
- (38) Lundquist, P.; Rosling, H.; Sorbo, B. *Clin. Chem.* **1985**, *31*, 591–595. Takeda, S.; Inada, Y.; Tomaru, T.; Ikeda, T.; Tashiro, N.; Morimoto, F.; Shibata, F. *Masui* **1990**, *39*, 701–707.

APPENDIX II

Anal Bioanal Chem (2012) 404:2287–2294
DOI 10.1007/s00216-012-6360-5

ORIGINAL PAPER

Simultaneous determination of cyanide and thiocyanate in plasma by chemical ionization gas chromatography mass-spectrometry (CI-GC-MS)

Raj K. Bhandari · Robert P. Oda · Stephanie L. Youso ·
Ilona Petrikovics · Vikhyat S. Bebarta ·
Gary A. Rockwood · Brian A. Logue

Received: 15 May 2012 / Revised: 30 July 2012 / Accepted: 14 August 2012 / Published online: 4 September 2012
© Springer-Verlag 2012

Abstract An analytical method utilizing chemical ionization gas chromatography-mass spectrometry was developed for the simultaneous determination of cyanide and thiocyanate in plasma. Sample preparation for this analysis required essentially one-step by combining the reaction of cyanide and thiocyanate with pentafluorobenzyl bromide and simultaneous extraction of the product into ethyl acetate facilitated by a phase-transfer catalyst, tetrabutylammonium sulfate. The limits of detection for cyanide and thiocyanate were 1 μM and 50 nM, respectively. The linear dynamic range was from 10 μM to 20 mM for cyanide and from 500 nM to 200 μM for thiocyanate with correlation coefficients higher than 0.999 for both cyanide and thiocyanate. The precision, as measured by %RSD, was below 9 %, and the accuracy was within 15 % of the nominal concentration for all quality

control standards analyzed. The gross recoveries of cyanide and thiocyanate from plasma were over 90 %. Using this method, the toxicokinetic behavior of cyanide and thiocyanate in swine plasma was assessed following cyanide exposure.

Keywords Cyanide · Thiocyanate · Method development · Chemical-ionization gas-chromatography mass-spectrometry

Introduction

Cyanide, as HCN or CN^- , is a deadly chemical that can be introduced into living organisms by a number of means, such as ingestion of edible plants (e.g., cassava, spinach), inhalation of smoke from cigarettes or fires, or accidental exposure during industrial operations (e.g., pesticide production) [1–3]. Once cyanide is introduced into cells, it inhibits cytochrome c oxidase, which subsequently causes cellular hypoxia, cytotoxic anoxia, and may eventually result in death [4]. Several literature sources have reported that the half-life of CN^- is less than one hour in mammalian species (e.g., humans, rats, pigs), which makes confirmation of cyanide exposure via direct analysis difficult if a significant amount of time has elapsed between exposure and analysis [3, 5–8]. Therefore, other markers of cyanide exposure have been proposed. One such marker is thiocyanate (SCN^-), the major metabolite of cyanide. In the presence of a sulfur donor (e.g., thiosulfate), about 80 % of cyanide is metabolized to thiocyanate through an enzyme catalyzed reaction (Fig. 1) [7–9].

Numerous procedures have been developed for the individual analysis of either cyanide or thiocyanate by gas-chromatography (GC) [2, 10–18]. While cyanide, as HCN,

R. K. Bhandari · R. P. Oda · S. L. Youso · B. A. Logue (✉)
Department of Chemistry and Biochemistry,
South Dakota State University,
Avera Health and Science Center 131, Box 2202,
Brookings, SD 57007, USA
e-mail: brian.logue@sdsu.edu

I. Petrikovics
Department of Chemistry, Sam Houston State University,
P.O. Box 2117, Huntsville, TX 77341, USA

V. S. Bebarta
Medical Toxicology, San Antonio Military Medical Center,
United States Air Force,
San Antonio, TX 78229, USA
e-mail: Vikhyat.bebarta@us.af.mil

G. A. Rockwood
Analytical Toxicology Division,
US Army Medical Research Institute of Chemical Defense,
3100 Ricketts Point Road,
Aberdeen Proving Ground, MD 21010-5400, USA

 Springer

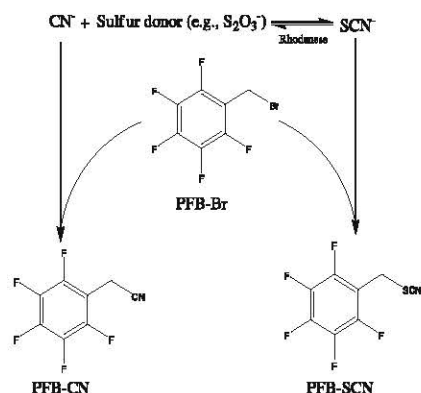


Fig. 1 The conversion of cyanide to thiocyanate and reaction of these cyanide exposure markers with pentafluorobenzyl bromide (PFB-Br)

is volatile and may be analyzed by head-space GC [11–13], thiocyanate is not volatile. Therefore, SCN^- must be chemically modified to a semi-volatile compound for analysis by GC. Methylation to methyl thiocyanate with dimethyl sulfate [15], conversion to cyanogen chloride by chloramine-T [18, 19], and alkylation with pentafluorobenzyl bromide (PFB-Br) [2, 10, 20] are among the methods that have been reported for analysis of SCN^- by GC. After GC separation, CN^- and SCN^- have been detected using electron capture [21–23], nitrogen-phosphorus detection [24–26], and mass spectrometry (MS) [2, 10, 27]. Although each detector has advantages and disadvantages, MS detectors have several advantages, including extreme sensitivity and the ability to perform stable isotope dilution, which greatly increases the precision of most bioanalytical methods. Therefore, MS detectors are well-suited for detection of trace amounts of chemical substances from biological samples. For a recent review of methods for the analysis of cyanide and thiocyanate, refer to Logue et al. [3].

Within the last decade, there has been a single report of the simultaneous analysis of CN^- and SCN^- from biological fluids by GC-MS [10]. PFB-Br was used to yield volatile adducts of CN^- and SCN^- (Fig. 1) from saliva samples, and analysis was performed using electron ionization GC-MS. Although the extraction and analysis of CN^- and SCN^- were simple, the chemical modification of cyanide and thiocyanate was only 55–65 % efficient, the internal standard did not correct for variations in the derivatization reaction, and the method was only tested with saliva. The detection limits for the method were 1 μM for cyanide and 5 μM for thiocyanate. In addition, attempts to simultaneously analyze plasma CN^- and SCN^- using the Paul and Smith [10] method in our laboratory resulted in the inability to analyze low concentrations of CN^- because of an unresolved interfering species. Therefore, although SCN^- was

easily analyzed from plasma by Paul and Smith [10] method, a novel method was necessary for simultaneous analysis of CN^- and SCN^- from plasma.

In the current report, a simple and sensitive chemical ionization-gas chromatography-mass spectrometry (CI-GC-MS) method for the simultaneous detection of cyanide and thiocyanate from plasma is presented. This method was used to determine cyanide and thiocyanate concentrations in swine plasma following cyanide exposure.

Experimental

Reagents and standards

Sodium cyanide (NaCN), sodium tetraborate decahydrate, sodium hydroxide (NaOH), and all solvents (HPLC-grade or higher) were purchased from Fisher Scientific (Fair Lawn, NJ, USA). Sodium thiocyanate (NaSCN) was purchased from Acros Organics (Morris Plains, USA). PFB-Br was obtained from Thermo Scientific (Hanover Park, IL, USA). The phase transfer catalyst, tetrabutylammonium sulfate (TBAS; 50 % w/w solution in water) was acquired from Sigma-Aldrich (St. Louis, MO, USA). Isotopically labeled internal standards, $\text{NaS}^{13}\text{C}^{15}\text{N}$ (99 % ^{13}C , 98 % ^{15}N) and $\text{Na}^{13}\text{C}^{15}\text{N}$ (99 % ^{13}C , 98 % ^{15}N), were acquired from Isotech (Miamisburg, OH, USA). HPLC-grade water was used to prepare all aqueous solutions. Single cyanide and thiocyanate stock solutions (1 mM each) were prepared and diluted to the desired working concentrations for all experiments. *Note: Cyanide is toxic and is released as HCN in acid solutions. Therefore, all solutions were prepared in a well-ventilated hood, and aqueous standards were prepared in 10 mM NaOH.*

Biological fluids

Swine (*Sus scrofa*) plasma was acquired from three sources: (1) plasma with EDTA anti-coagulant was purchased from Pelfreeze Biological (Rogers, AR, USA), (2) citrate anti-coagulated plasma was obtained through the Veterinary Science Department at South Dakota State University, and (3) cyanide-exposed plasma was acquired from Wilford Hall Medical Center (Lackland Air Force Base, TX). Upon receipt, the plasma was frozen and stored at $-80\text{ }^\circ\text{C}$ until utilized for optimizing analytical methodologies for sample analysis.

Four swine (about 50 kg each) were injected (intramuscularly) with different doses ranging from 7.5 to 15 mg/kg of potassium cyanide. Arterial blood samples were drawn, and plasma was taken from those blood samples at 13 different time points, including a baseline, 15 min, apnea

(around 9 min), and ten additional time points post-apnea (2, 4, 6, 8, 10, 20, 30, 40, 50, and 60 min). The plasma samples were then shipped on ice to SDSU for analysis for CN^- and SCN^- . The swine study was conducted in accordance with the guidelines stated in "The Guide for the Care and Use of Laboratory Animals" in an AALAS (American Association for Laboratory Animal Science) accredited facility and were approved by the appropriate institutional review boards.

Sample preparation

Spiked and non-spiked biological samples (100 μL) were added to 2 mL micro-centrifuge vials. Aliquots (100 μL each) of $\text{Na}^{13}\text{C}^{15}\text{N}$ (200 μM) and $\text{NaS}^{13}\text{C}^{15}\text{N}$ (100 μM) were added to the sample vials as internal standards along with TBAS (800 μL of 10 mM TBAS in a saturated solution of sodium tetraborate decahydrate, pH 9.5) and PFB-Br (500 μL of a 20 mM solution in ethyl acetate). The solution was vortexed for 2 min, heated at 70 $^{\circ}\text{C}$ in a heating block for 1 h, and centrifuged for 4 min (room temperature) at 10,000 rpm (9,300 \times g) to separate the organic and aqueous layers. An aliquot (200 μL) of the supernatant organic layer was then transferred into a GC-MS autosampler vial fitted with a 200 μL glass insert for subsequent GC-MS analysis. The total sample preparation time was around 1.5 h and was essentially one step.

Gas chromatography-mass spectrometry

Prepared samples were analyzed for PFB-CN and PFB-SCN using an Agilent Technologies 6890 N gas chromatograph and a 5975B inert XL electron ionization/chemical ionization mass selective detector in CI mode with a 7683 B series autosampler. An 80 % dimethyl-20 % diphenyl polysiloxane capillary column (30 m \times 0.25 mm ID, 0.5 μm film thickness; Restek, Bellefonte, PA) was used with helium as the carrier gas at a flow rate of 1 mL/min and a column head pressure of 8.10 psi. The injection (splitless, split delay 1 min) volume was 1 μL , and the injection port was held at 210 $^{\circ}\text{C}$. The GC oven was initially heated to 60 $^{\circ}\text{C}$. Upon injection, the temperature was increased to 165 $^{\circ}\text{C}$ at 7 $^{\circ}\text{C}/\text{min}$ and then elevated to 270 $^{\circ}\text{C}$ at a rate of 50 $^{\circ}\text{C}/\text{min}$, where it was held for 1 min. The overall analysis time was 18.10 min with PFB-CN and PFB-SCN eluting at approximately 8.3 and 12.1 min, respectively. It is to be noted that the internal standards co-elute with the native species, thus, they all have same retention time as that of the native species. Attempts were made to shorten the overall run time, but the resolution and/or symmetry of the analyte peaks became unacceptable. The MS source and MS quad temperatures were 250 $^{\circ}\text{C}$ and 150 $^{\circ}\text{C}$, respectively. Methane was used as a reagent gas for positive ion CI with electron energy of 150 eV. The abundant ions of PFB-CN [m/z ,

208 (95 %) and 209 (5 %)], PFB- $^{13}\text{C}^{15}\text{N}$ [m/z , 210 (91 %) and 211 (9 %)], PFB-SCN [m/z , 240 (93 %) and 241 (7 %)], and PFB-S $^{13}\text{C}^{15}\text{N}$ [m/z , 242 (91 %) and 243 (9 %)] were monitored with selected ion monitoring (SIM). It should be noted that the internal standards used only differed by two mass units. Therefore, mass carryover, (i.e., potential overlap between naturally occurring stable isotopes of the target analyte and the labeled internal standard) must be considered, especially at high analyte concentrations (e.g., a significant concentration of stable isotopes from the analyte at may contribute to the internal standard signal causing an overestimation of the internal standard). Therefore, a relatively large concentration of internal standard was used throughout the study.

Calibration, quantification, and limit of detection

Bioanalytical method validation was accomplished by generally following the Food and Drug Administration guidelines [28]. Aqueous cyanide and thiocyanate stock solutions (1 mM each) were used for preparing calibration and quality control (QC) standards. From the stock solutions, calibration standards for CN^- (10, 20, 50, 100, 200, 500, and 1,000 μM) and SCN^- (0.5, 1, 2, 5, 10, 20, 50, 100, and 200 μM) were prepared in swine plasma. To obtain a calibration equation, the average signal ratios from analyses (i.e., peak-area ratio of the analyte to the internal standard) were plotted as a function of CN^- or SCN^- concentration. Peak integration was performed manually from baseline to baseline in ChemStation software (Agilent Technologies, Santa Clara, CA). A non-weighted and a weighted ($1/x^2$) least-squares linear fit were used for cyanide and thiocyanate, respectively. The best model for each analyte was determined by a weighted sum-of-squares analysis.

For determining the upper limit of quantification (ULOQ) and lower limit of quantification (LLOQ), a percent relative standard deviation (%RSD) of <10 % (as a measure of precision) and a percent deviation within ± 20 % back-calculated from the nominal concentration of each calibration standard (as a measure of accuracy) were used as inclusion criteria for the calibration standards. QC standards ($N=5$) were prepared in swine plasma at three different concentrations—15 (low QC standard), 75 (medium QC standard), and 350 μM (high QC standard) for cyanide and 1.5 (low QC standard), 15 (medium QC standard), and 150 μM (high QC standard) for thiocyanate. The QC standards were analyzed in quintuplicate each day for 3 days and were run in parallel with the calibration standards. *Intra-assay* precision and accuracy were calculated from each day's analysis, and *inter-assay* precision and accuracy were calculated from the comparison of the data gathered from three separate days. It should be noted that the *inter-assay* and *intra-assay* studies were conducted within 1 week.

The limit of detection (LOD) was found by analyzing multiple concentrations of CN^- and SCN^- below the LLOQ and determining the lowest concentration with a signal-to-noise ratio (peak-to-peak) of at least 3.

Selectivity, stability, and recovery

The assay selectivity was defined as the ability to differentiate and quantify the analytes (i.e., PFB-CN and PFB-SCN) in the presence of other components in the sample. Selectivity was determined by comparing three blank samples of swine plasma with spiked swine plasma (350 μM cyanide and 150 μM of thiocyanate) and determining if chemical components in the plasma interfered with the ability to quantify PFB-CN and PFB-SCN. The peak asymmetry (A_s) was calculated by dividing the front half-width by the back half-width at 10 % peak height [29].

For evaluating the stability of cyanide and thiocyanate, swine plasma was spiked with high and low QC concentrations of each analyte. These samples were then stored under multiple conditions (-80°C , -20°C , 4°C , and room temperature (RT)) and analyzed over multiple storage times. Cyanide and thiocyanate were considered to be stable under the conditions tested, if the calculated concentration of the stored sample was within 10 % of the initial concentration. For the long-term stability of cyanide and thiocyanate, three aliquots of spiked plasma were stored and analyzed (each in triplicate) on the day of preparation and after 1, 2, 5, 10, and 30 days of storage at the temperatures indicated. Freeze-thaw stability of CN^- and SCN^- and autosampler stability of PFB-modified CN^- and SCN^- were also evaluated. For freeze-thaw stability, three aliquots each of the high and low QC standards of both cyanide and thiocyanate were initially analyzed and then stored at -80°C for 24 h. The samples were then thawed unassisted at room temperature. One set of samples was analyzed, and the non-analyzed samples were refrozen for 24 h at -80°C . This process was repeated two more times. At the time of each analysis, internal standards were added to correct for variations due to sample preparation and instrumental errors. To determine the autosampler stability of PFB-modified CN^- and SCN^- , the cyanide and thiocyanate spiked plasma samples were reacted with PFB-Br, placed in the autosampler, and analyzed at approximately 1, 2, 6, 12, and 24 h.

For recovery experiments, three aliquots of high, medium, and low aqueous QC standards of cyanide and thiocyanate were analyzed and compared with plasma samples spiked with equivalent concentrations of cyanide and thiocyanate. The recoveries of cyanide and thiocyanate were calculated as a percentage by dividing the recovered analyte concentration by the calculated concentration of the appropriate aqueous QC standards.

Results and discussion

GC-MS analysis and selectivity

For simultaneous analysis of cyanide and thiocyanate by GC-MS, CN^- and SCN^- were reacted with PFB-Br to create semi-volatile species, PFB-CN and PFB-SCN (Fig. 1). Representative selected ion chromatograms (SIM) (i.e., $m/z=208$ for PFB-CN and $m/z=210$ for PFB-SCN) of non-spiked and spiked swine plasma and spiked water sample can be seen in Figs. 2 and 3. PFB-CN and PFB-SCN elute at 8.3 and 12.1 min, respectively. The peak shape for PFB-CN was sharp and symmetrical ($A_s=1.14$) while the peak for PFB-SCN showed some tailing ($A_s=2.40$). The method showed excellent selectivity for CN^- and SCN^- in the presence of other sample constituents. PFB-CN showed no interfering background signal (Fig. 2), and although a small PFB-SCN peak (8.3 μM) does elute from non-spiked swine plasma (Fig. 3, lower trace), this was attributed to endogenous thiocyanate in the plasma as confirmed by MS fragmentation [10, 18]. Multiple studies have shown the presence of SCN^- in biological fluids (e.g., plasma, saliva, urine) from subjects not exposed to cyanide. This SCN^- likely comes from multiple sources, such as foods (e.g., cheese, milk, cabbage family) [30–32]. The endogenous swine plasma SCN^- concentrations for the swine plasma tested in our lab ranged from 8.2–46.6 μM . For comparison, the endogenous plasma SCN^- concentrations from humans (non-smokers) range from 4.83–87.5 μM [33–35]. If the peak at 12.1 min is considered endogenous plasma SCN^- , both analyte peaks were well-resolved from any interfering peaks ($R_s=15$ from the

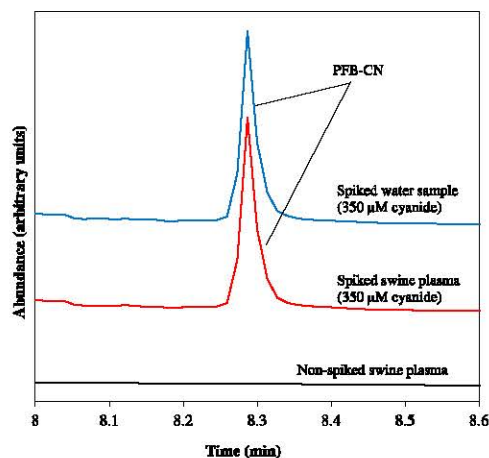


Fig. 2 GC-MS chromatograms of PFB-CN in spiked (350 μM , upper trace) and non-spiked (lower trace) swine plasma monitored in SIM mode ($m/z=208$)

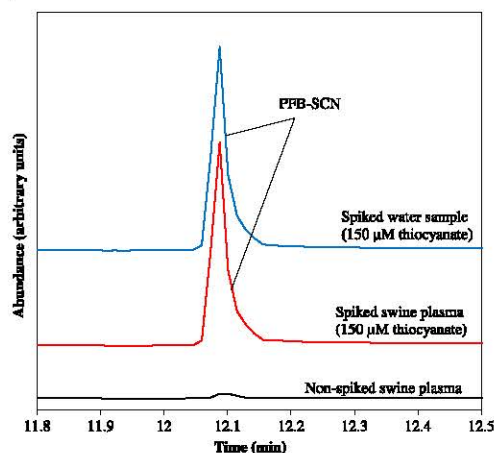


Fig. 3 GC-MS chromatographs of PFB-SCN in spiked (150 μM , upper trace) and non-spiked (lower trace) swine plasma monitored in SIM mode ($m/z=240$)

nearest peak at 7.7 min for CN^- (not shown) and $R_s=4$ from the nearest visible peak at 11.8 min for SCN^-).

Detection limit, calibration, and linearity

The LODs (signal-to-noise-ratios greater than 3:1) for cyanide and thiocyanate were found to be 1 μM and 50 nM, respectively. These limits of detection easily allow quantification of typical biological concentrations of both cyanide and thiocyanate and compare favorably with other similar methods [3]. Kage et al. [2] reported the detection limits for a similar GC-MS method to monitor cyanide and thiocyanate separately in whole blood to be 10 and 3 μM , respectively. Paul and Smith [10] reported limits of detection to be 1 μM for cyanide and 5 μM for thiocyanate from saliva samples.

Using the current method, both calibration curves for cyanide (unweighted) and thiocyanate (weighted, $1/x^2$) were found to be linear with correlation coefficients of 0.9999. The calibration curves and the regression equation of both cyanide and thiocyanate in plasma samples are listed in Table 1. The LLOQ was found to be 10 μM for cyanide and 0.5 μM for thiocyanate. The ULOQ was 20 mM for cyanide and 200 μM for thiocyanate. The linear ranges for CN^- and SCN^- are also presented in Table 1. It is interesting to note that, while the typical linear ranges for GC-MS methods span two orders of magnitude [36–38], the linear range of CN^- for this method, spanning over three orders of magnitude, is extraordinarily large. The linear range of SCN^- is also excellent, although it does not cover a full

Table 1 LOD and linearity of cyanide and thiocyanate in swine plasma samples

Analyte	LOD (μM)	Linearity (μM)	Regression equations
Cyanide	1	10–20,000	$y=0.0020x-0.0012$ (day 1)
			$y=0.0022x+0.0000$ (day 2)
			$y=0.0019x+0.0022$ (day 3)
Thiocyanate	0.05	0.5–200	$y=-0.017x+0.034$ (day 1)
			$y=-0.017x+0.057$ (day 2)
			$y=-0.016x+0.072$ (day 3)

three orders of magnitude. The stability of the calibration curve during the interday study was excellent as evident by the stability of the slope—0.0019–0.0022 for CN^- and 0.016–0.017 for SCN^- . LLOQs and ULOQs were not reported by Kage et al. [2] or Paul and Smith [10].

Accuracy and precision

The accuracy and precision of the method were determined by quintuplicate analysis of three different QC standards (15, 75, and 350 μM for cyanide; 1.5, 15, and 150 μM for thiocyanate) on three different days (Table 2). The precision of the method was excellent, with both the *intra-assay* and *inter-assay* precisions below 9 % RSD. The accuracy for *intra-assay* and *inter-assay* analyses was also excellent (± 9 % of nominal concentrations). Full accuracy and precision values were not reported for the Kage et al. [2] and Paul and Smith [10] methods, although for a single sample analyzed in quintuplicate, Paul and Smith [10] reported a %RSD of 11.6 % for CN^- and 4.3 % for SCN^- .

Assay recovery, stability, and robustness

Assay recoveries for cyanide and thiocyanate are reported in Table 3. The recoveries for both cyanide and thiocyanate were excellent at high, medium, and low analyte concentrations. The recovery of cyanide ranged from 91–99 % while the recovery for thiocyanate ranged from 92–93 %. These recoveries are greater than the 80 % recoveries reported by Kage et al. [2] and 55–65 % recoveries reported by Paul and Smith [10].

Cyanide and thiocyanate stabilities were evaluated in spiked plasma at -80 , -20 , 4 $^{\circ}\text{C}$, or RT, and for three freeze–thaw (FT) cycles. Cyanide was stable for 2 days at -80 , -20 , and 4 $^{\circ}\text{C}$ and was quickly removed from plasma at RT (<1 h). For the freeze–thaw stability experiment, the concentrations of cyanide and

Table 2 The accuracy and precision of cyanide and thiocyanate analysis from spiked swine plasma by CI-GC-MS

Analyte	Concentration (μM)	Intrassay		Interassay	
		Accuracy (%) ^a	Precision (%RSD) ^a	Accuracy (%) ^b	Precision (%RSD) ^b
Cyanide	15	104.7	2.2	107.1	5.2
	75	100.4	2.1	101.3	2.5
	350	102.8	1.7	101.5	1.1
Thiocyanate	1.5	100.1	5.8	98.4	8.4
	15	102.8	2.6	103.0	3.6
	150	92.1	0.8	92.1	1.6

^aQC method validation ($N=5$) for day 3

^bMean of three different days of QC method validation ($N=15$)

thiocyanate after one FT cycle were within 10 % of the original concentration for both high and low QC standards (approximately 92 % for cyanide and 97 % for thiocyanate). For FT cycles 2 and 3, the concentrations of cyanide and thiocyanate were below 10 % of the initial concentration for both the high and low QC standards. The concentrations of cyanide and thiocyanate fell after each consecutive FT cycle but, for both cycles 2 and 3, the stability was near 80 % (± 6 %) of the original concentration for both the high and low QC standards. Thus, FT experiments suggest that CN^- and SCN^- are stable for no more than 1 cycle. Low temperatures do increase the stability of CN^- as compared with RT, presumably because microbial growth and the rate of enzymatic reactions for cyanide conversion are reduced [39]. Although this is the case, cyanide has been found to be generally unstable at low temperatures compared with other markers of cyanide exposure [40, 41].

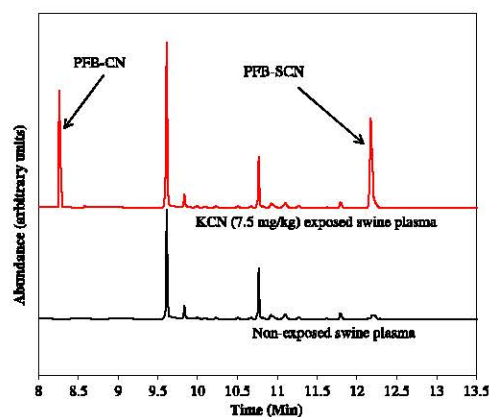
The instability of CN^- in biological samples was expected because HCN is volatile and is quickly lost from biological samples at pH values below 7–8 (HCN $\text{pK}_a=9.2$). CN^- is also nucleophilic and may react with sulfur-containing compounds, aldehydes, or ketones to form cyano-adducts [42]. Previous studies have found that cyanide can convert to SCN^- under common storage conditions [3]. Analysis of SCN^- concentrations during the stability study shows that this was not the case. Alternatively, cyanide can also be produced from biological samples under certain storage conditions [42]. Many micro-organisms

produce cyanide as a result of putrefaction or single-carbon metabolism [43–45], and non-specific oxidative reactions may produce cyanide from organic compounds. The loss of cyanide during the stability experiments indicate that cyanide generation does not occur or is only a minor process. Although it has been found that additives may help reduce cyanide loss or production (e.g., addition of silver ions can help stabilize CN^- under storage and active oxygen-scavenging reagents, such as ascorbic acid, reduce cyanide production [40, 43]), the use of additives was not evaluated in this study.

Thiocyanate was stable for up to 5 days at -80 , -20 , or 4 °C and 1 day at RT. It has been found that SCN^- can be converted to cyanide in the presence of erythrocytes [46], or oxidizing agents such as nitrite and hydrogen peroxide in samples under storage or during analysis [45, 47]. Our observations suggest that this mechanism is not a major loss mechanism in this study as no increase in cyanide occurred in the samples as thiocyanate levels decreased. Thiocyanate has also been found to bind to albumin or other proteins

Table 3 Recovery (expressed as percentage) of cyanide and thiocyanate from spiked swine plasma samples

Analyte	Concentration (μM)	Recovery (%)
Cyanide	15	91
	75	99
	350	95
Thiocyanate	1.5	92
	15	92
	150	93

**Fig. 4** GC-MS total ion chromatographs (TIC) of potassium cyanide (7.5 mg/kg) exposed swine plasma and non-exposed swine plasma (lower trace), both without internal standard

which may result in a decrease of free thiocyanate concentrations [48].

Derivatized cyanide and thiocyanate stabilities were evaluated in spiked plasma at approximately 1, 2, 6, 12, and 24 h after placement in an autosampler. The calculated concentrations of both cyanide and thiocyanate were within 10 % of the initial concentration at all times tested. Thus, both derivatized cyanide and thiocyanate were stable for at least 24 h when placed in an autosampler.

Application of the method

The method described in this paper was used to analyze plasma cyanide and thiocyanate concentrations in a toxicokinetics study of acute cyanide exposure in pigs. Figure 4 shows GC-MS total ion chromatographs (TIC) of plasma samples of potassium cyanide (7.5 mg/kg) exposed (upper trace) and non-exposed (lower trace) swine. The peaks of derivatized cyanide (i.e., PFB-CN) and derivatized thiocyanate (i.e., PFB-SCN) are observed at around 8.3 and 12.1 min, respectively. The method presented here performed very well in this study. The simple sample preparation allowed quick analysis of the large number of samples and standards generated from the study and the low LOQs allowed quantification of CN^- and SCN^- in all plasma samples. The full results of this toxicokinetic study will be published in the near future.

Conclusions

A simple analytical method for the simultaneous determination of cyanide and its major metabolite, thiocyanate, was developed using CI-GC-MS. The described analytical method includes one-step sample preparation and is sensitive, accurate, and precise with high recoveries. In addition, the method described yielded excellent detection limits for both CN^- and SCN^- , and large linear ranges for CN^- and SCN^- were observed. Sample preparation was minimal and only lasted approximately 1.5 h for single samples, and within a 24-h period, approximately 70 parallel samples were processed and analyzed. The ability to detect both cyanide and thiocyanate simultaneously provides efficiency and economy of samples and reagents, as well as a reduction in labor cost. The method presented was able to identify cyanide-exposed swine in a pig plasma samples in a toxicokinetics study through analysis of CN^- and its major metabolite, SCN^- .

Acknowledgments The research was supported by the CounterACT Program, National Institutes of Health Office of the Director, and the National Institute of Allergy and Infectious Diseases, Inter Agency Agreement Number Y1-OD-0690-01/A-120-B.P2010-01, Y1-OD-1561-01/A120-B.P2011-01, and the USAMRICD under the auspices of the US Army Research Office of Scientific Services Program

Contract No. W911NF-11-D-0001 administered by Battelle (delivery order 0079, contract no TCN 11077). We gratefully acknowledge the funding from the Oak Ridge Institute for Science and Education (ORISE). The authors would also like to acknowledge Dr. George Perry, Associate Professor, Animal and Range Science of South Dakota State University, for making arrangements to provide swine plasma. The authors are thankful to Susan M. Boudreau, RN, BSN, Maria G. Castaneda, MS, Toni E. Vargas, PA-C, MHS, and Patricia Dixon, MHS, from the Clinical Research Division, Wilford Medical Center, Lackland A F B, TX, for providing cyanide exposed swine plasma samples for these studies. The opinions or assertions contained herein are the private views of the authors and are not to be construed as official or as reflecting the views of the Department of the Army, the National Institutes of Health, or the Department of Defense.

References

1. Baskin SI, Petrikovics I, Kurcha JS, Nicholson JD., Logue BA, Maliner BJ, Rockwood GA (2004) Insights on cyanide toxicity and methods of treatment. In: Flora SJS, Romano JA Jr, Baskin SI, Shekhar K (eds) *Pharmacological perspectives of toxic chemicals and their antidotes*. New Delhi, India: Narosa Publishing House
2. Kage S, Nagata T, Kudo K (1996) Determination of cyanide and thiocyanate in blood by gas chromatography and gas chromatography-mass spectrometry. *J Chromatogr B Biomed Appl* 675(1):27–32
3. Logue BA, Hinkens DM, Baskin SI, Rockwood GA (2010) The analysis of cyanide and its breakdown products in biological samples. *Crit Rev Anal Chem* 40(2):122–147. doi:10.1080/10408340903535315
4. Conn EE (1978) Cyanogenesis, the production of cyanide, by plants. In: Keeler RF, Van Kampen KR, James LF (eds) *Effects of poisons in plants on livestock*. Academic Press, San Diego, pp 301–310
5. Ballantyne B (1976) Changes in blood cyanide as a function of storage time and temperature. *J Forensic Sci Soc* 16(4):305–310
6. Isom GE, Baskin SI (1997) Enzymes involved in cyanide metabolism. In: Sipes IG, McQueen CA, Gandolfi AJ (eds) *Comprehensive toxicology*. Elsevier Science, New York, NY
7. Sousa AB, Manzano H, Soto-Blanco B, Gorniak SL (2003) Toxicokinetics of cyanide in rats, pigs and goats after oral dosing with potassium cyanide. *Arch Toxicol* 77(6):330–334. doi:10.1007/s00204-003-0446-y
8. Wood JL, Cooley SL (1956) Detoxication of cyanide by cystine. *J Biol Chem* 218(1):449–457
9. Ansell M, Lewis FA (1970) A review of cyanide concentrations found in human organs. a survey of literature concerning cyanide metabolism, 'normal', non-fatal, and fatal body cyanide levels. *J Forensic Med* 17(4):148–155
10. Paul BD, Smith ML (2006) Cyanide and thiocyanate in human saliva by gas chromatography-mass spectrometry. *J Anal Toxicol* 30(8):511–515
11. Calafat AM, Stanfil SB (2002) Rapid quantitation of cyanide in whole blood by automated headspace gas chromatography. *J Chromatogr B* 772:131–137
12. Dumas P, Gingras G, LeBlanc A (2005) Isotope dilution-mass spectrometry determination of blood cyanide by headspace gas chromatography. *J Anal Toxicol* 29(1):71–75
13. Felby S (2009) Determination of cyanide in blood by reaction head-space gas chromatography. *Forensic Sci Med Pathol* 5(1):39–43. doi:10.1007/s12024-008-9069-1
14. Odoul M, Fouillet B, Nouri B, Chambon R, Chambon P (1994) Specific determination of cyanide in blood by headspace gas chromatography. *J Anal Toxicol* 18(4):205–207

15. Funazo K, Tanaka M, Shono T (1981) Determination of cyanide or thiocyanate at trace levels by derivatization and gas chromatography with flame thermionic detection. *Anal Chem* 53:1377–1380
16. Funazo K, Kusano K, Wu HL, Tanaka M, Shono T (1982) Trace determination of cyanide by derivatization and flame thermionic gas chromatography. *J Chromatogr* 245:93–100
17. Liu G, Liu J, Hara K, Wang Y, Yu Y, Gao L, Li L (2009) Rapid determination of cyanide in human plasma and urine by gas chromatography-mass spectrometry with two-step derivatization. *J Chromatogr B Anal Technol Biomed Life Sci* 877(27):3054–3058. doi:10.1016/j.jchromb.2009.07.029
18. Thomson I, Anderson RA (1980) Determination of cyanide and thiocyanate in biological fluids by gas chromatography-mass spectrometry. *J Chromatogr* 188(2):357–362
19. Segal HS (1962) The microdiffusion separation and determination of microgram quantities of thiocyanate in corn. *J Agric Food Chem* 10:10–12. doi:10.1021/jf60119a004
20. Youso SL, Rockwood GA, Lee JP, Logue BA (2010) Determination of cyanide exposure by gas chromatography-mass spectrometry analysis of cyanide-exposed plasma proteins. *Anal Chim Acta* 677(1):24–28. doi:10.1016/j.aca.2010.01.028
21. Maseda C, Matsubara K, Shiono H (1989) Improved gas chromatography with electron-capture detection using a reaction pre-column for the determination of blood cyanide: a higher content in the left ventricle of fire victims. *J Chromatogr* 490(2):319–327
22. Chen SH, Wu SM, Kou HS, Wu HL (1994) Electron-capture gas chromatographic determination of cyanide, iodide, nitrite, sulfide, and thiocyanate anions by phase-transfer-catalyzed derivatization with pentafluorobenzyl bromide. *J Anal Toxicol* 18(2):81–85
23. de Brabander HF, Verbeke R (1977) Determination of thiocyanate in tissues and body fluids of animals by gas chromatography with electron-capture detection. *J Chromatogr* 138(1):131–142
24. Takekawa K, Oya M, Kido A, Suzuki O (1998) Analysis of cyanide in blood by headspace solid-phase microextraction (SPME) and capillary gas chromatography. *Chromatographia* 47(209–214)
25. Zamecnik J, Tam J (1987) Cyanide in blood by gas chromatography with NP detector and acetomitrile as internal standard. Application on air accident fire victims. *J Anal Toxicol* 11(1):47–48
26. Boadas-Vaello P, Jover E, Llorens J, Bayona JM (2008) Determination of cyanide and volatile alkylnitriles in whole blood by headspace solid-phase microextraction and gas chromatography with nitrogen phosphorus detection. *J Chromatogr B Anal Technol Biomed Life Sci* 870(1):17–21. doi:10.1016/j.jchromb.2008.05.031
27. Frison G, Zancanaro F, Favretto D, Ferrara SD (2006) An improved method for cyanide determination in blood using solid-phase microextraction and gas chromatography/mass spectrometry. *Rapid Commun Mass Spectrom* 20(19):2932–2938. doi:10.1002/rcm.2689
28. Food and Drug Administration (2001) Guidance for industry bio-analytical method validation. US Department of Health and Human Services, FDA, Rockville, MD
29. Foley JP, Dorsey JG (1984) A review of the exponentially modified Gaussian (EMG) function: evaluation and subsequent calculation of universal data. *J Chromatogr Sci* 22:40–46
30. Levine MS, Radford EP (1978) Occupational exposures to cyanide in Baltimore fire fighters. *J Occup Med* 20(1):53–56
31. Dalferes ER Jr, Webber LS, Radhakrishnamurthy B, Berenson GS (1980) Continuous-flow (autoanalyzer I) analysis for plasma thiocyanate as an index to tobacco smoking. *Clin Chem* 26(3):493–495
32. Connolly D, Barron L, Paull B (2002) Determination of urinary thiocyanate and nitrate using fast ion-interaction chromatography. *J Chromatogr B Anal Technol Biomed Life Sci* 767(1):175–180
33. Pettigrew AR, Fell GS (1973) Microdiffusion method for estimation of cyanide in whole blood and its application to the study of conversion of cyanide to thiocyanate. *Clin Chem* 19(5):466–471
34. Hasuike Y, Nakanishi T, Moriguchi R, Otaki Y, Namami M, Hama Y, Naka M, Miyagawa K, Izumi M, Takamitsu Y (2004) Accumulation of cyanide and thiocyanate in haemodialysis patients. *Nephrology, Dialysis, Transplantation: Official Publication of the European Dialysis and Transplant Association-European Renal Association* 19(6):1474–1479. doi:10.1093/ndt/gfh076
35. Glatz Z, Novakova S, Sterbova H (2001) Analysis of thiocyanate in biological fluids by capillary zone electrophoresis. *J chromatogr A* 916(1–2):273–277
36. Logue BA, Kirshen NP, Petrikovics I, Moser MA, Rockwood GA, Baskin SI (2005) Determination of the cyanide metabolite 2-aminothiazoline-4-carboxylic acid in urine and plasma by gas chromatography-mass spectrometry. *J Chromatogr B Anal Technol Biomed Life Sci* 819(2):237–244. doi:10.1016/j.jchromb.2005.01.045
37. Panchal JG, Patel RV, Menon SK (2011) Development and validation of GC/MS method for determination of pramipexole in rat plasma. *Biomol Chromatogr* 25:524–530
38. Gerace E, Salomone A, Fasano F, Costa R, Boschi D, Di Stilo A, Vincenti M (2011) Validation of a GC/MS method for the detection of two quinoline-derived selective androgen receptor modulators in doping control analysis. *Anal Bioanal Chem* 400(1):137–144. doi:10.1007/s00216-010-4569-8
39. Cipollone R, Ascenzi P, Tomao P, Imperi F, Visca P (2008) Enzymatic detoxification of cyanide: clues from *Pseudomonas aeruginosa* Rhodanese. *J Mol Microbiol Biotechnol* 15(2–3):199–211. doi:10.1159/000121331
40. Lundquist P, Rosling H, Sorbo B (1985) Determination of cyanide in whole blood, erythrocytes, and plasma. *Clin Chem* 31(4):591–595
41. Seto Y (2002) False cyanide detection. *Anal Chem* 74(5):134A–141A
42. Askeland RA, Morrison SM (1983) Cyanide production by *Pseudomonas fluorescens* and *Pseudomonas aeruginosa*. *Appl Environ Microbiol* 45(6):1802–1807
43. Knowles CJ (1976) Microorganisms and cyanide. *Bacteriol Rev* 40(3):652–680
44. Seto Y (1995) Oxidative conversion of thiocyanate to cyanide by oxyhemoglobin during acid denaturation. *Arch Biochem Biophys* 321(1):245–254. doi:10.1006/abbi.1995.1392
45. Seto Y (1996) Determination of physiological levels of blood cyanide without interference by thiocyanate. *Jpn J Toxicol Environ Health* 42:319–325
46. Seto Y, Tsunoda N, Ohta H, Shinohara T (1993) Determination of blood cyanide by headspace gas chromatography with nitrogen-phosphorus detection and using a megabore capillary column. *Anal Chim Acta* 276:247–259
47. Vessey CJ, Wilson J (1978) Red cell cyanide. *J Pharm Pharmacol* 30:20–26
48. Pollay M, Stevens A, Davis C Jr (1966) Determination of plasma-thiocyanate binding and the Donnan ratio under simulated physiological conditions. *Anal Biochem* 17(2):192–200

APPENDIX III

Journal of Analytical Toxicology 2014,38:218–225
doi:10.1093/jat/tku020

Article

Cyanide Toxicokinetics: The Behavior of Cyanide, Thiocyanate and 2-Amino-2-Thiazoline-4-Carboxylic Acid in Multiple Animal Models

Raj K. Bhandari^{1*}, Robert P. Oda¹, Ilona Petrikovics², David E. Thompson², Matthew Brenner^{3,4}, Sari B. Mahon⁵, Vikhyat S. Beberta⁵, Gary A. Rockwood⁶ and Brian A. Logue¹

¹Department of Chemistry and Biochemistry, South Dakota State University, Avera Health Science Center (SAV) 131, PO Box 2202, Brookings, SD 57007, USA, ²Department of Chemistry, Sam Houston State University, PO Box 2117, Huntsville, TX 77341, USA, ³Beckman Laser Institute and Medical Clinic, University of California, Irvine, CA 92612, USA, ⁴Division of Pulmonary and Critical Care Medicine, Department of Medicine, University of California, Irvine, CA 92868, USA, ⁵Division of Medical Toxicology, Department of Emergency Medicine, San Antonio Military Medical Center, San Antonio, TX 78234, USA, and ⁶Analytical Toxicology Division, US Army Medical Research Institute of Chemical Defense, 3100 Ricketts Point Road, Aberdeen Proving Ground, MD 21010, USA

*Author to whom correspondence should be addressed. Email: brian.logue@sdstate.edu

Cyanide causes toxic effects by inhibiting cytochrome *c* oxidase, resulting in cellular hypoxia and cytotoxic anoxia, and can eventually lead to death. Cyanide exposure can be verified by direct analysis of cyanide concentrations or analyzing its metabolites, including thiocyanate (SCN⁻) and 2-amino-2-thiazoline-4-carboxylic acid (ATCA) in blood. To determine the behavior of these markers following cyanide exposure, a toxicokinetics study was performed in three animal models: (i) rats (250–300 g), (ii) rabbits (3.5–4.2 kg) and (iii) swine (47–54 kg). Cyanide reached a maximum in blood and declined rapidly in each animal model as it was absorbed, distributed, metabolized and eliminated. Thiocyanate concentrations rose more slowly as cyanide was enzymatically converted to SCN⁻. Concentrations of ATCA did not rise significantly above the baseline in the rat model, but rose quickly in rabbits (up to a 40-fold increase) and swine (up to a 3-fold increase) and then fell rapidly, generally following the relative behavior of cyanide. Rats were administered cyanide subcutaneously and the apparent half-life ($t_{1/2}$) was determined to be 1,510 min. Rabbits were administered cyanide intravenously and the $t_{1/2}$ was determined to be 177 min. Swine were administered cyanide intravenously and the $t_{1/2}$ was determined to be 26.9 min. The SCN⁻ $t_{1/2}$ in rats was 3,010 min, but was not calculated in rabbits and swine because SCN⁻ concentrations did not reach a maximum. The $t_{1/2}$ of ATCA was 40.7 and 13.9 min in rabbits and swine, respectively, while it could not be determined in rats with confidence. The current study suggests that cyanide exposure may be verified shortly after exposure by determining significantly elevated cyanide and SCN⁻ in each animal model and ATCA may be used when the ATCA detoxification pathway is significant.

Introduction

Cyanide (as HCN or CN⁻, represented inclusively as CN) is a rapidly acting, toxic chemical that can be readily absorbed by inhalation, ingestion or dermally. After CN is absorbed, it is rapidly distributed throughout the body, causing toxic effects by mechanisms that include inhibiting cytochrome *c* oxidase, resulting in cellular hypoxia and cytotoxic anoxia, and can eventually result in death (1). Cyanide is volatile and reactive leading to a short half-life ($t_{1/2}$). It is difficult to determine cyanide exposure by direct CN analysis if significant time has elapsed (2–5). Thus, indirect biomarkers, including thiocyanate (SCN⁻) and 2-amino-2-thiazoline-4-carboxylic acid (ATCA), are necessary in certain situations for the verification of cyanide poisoning.

In the presence of a sulfur donor (e.g. thiosulfate) and a sulfur transferase enzyme (e.g. rhodanese), ~80% of a dose of CN is metabolized to SCN⁻ (2–4, 6). Although SCN⁻ has been used as the main indirect cyanide exposure marker, it can be difficult to establish definitive CN exposure due to large endogenous SCN⁻ concentrations in biological fluids (7–9). Cyanide can also react with L-cystine through a proposed intermediate, β -thiocyanoalanine, where it is subsequently transformed into ATCA. ATCA is a minor metabolite of CN, and it has been suggested that it accounts for ~15–20% of cyanide metabolism (6, 10). ATCA may be useful as an alternative for determination of CN exposure because it does not metabolize further (6, 11, 12), and it is a chemically stable metabolite under most storage conditions (13, 14). Although it is a promising marker of CN exposure, there are relatively few studies on the behavior of ATCA following cyanide exposure, and the direct relationship between CN exposure and elevated ATCA concentrations has only tenuously been established (4, 14–17).

The objective of the current study was to simultaneously determine the toxicokinetic behavior of CN, SCN⁻ and ATCA, providing a direct evaluation of the relationship between these biomarkers. In addition, the ability of CN and its detoxification products to serve as cyanide exposure biomarkers was evaluated and a comparison between multiple mammalian species was performed.

Materials and Methods

Chemicals and samples

All chemicals used were at least HPLC grade or higher. Potassium thiocyanate (KSCN), sodium cyanide (NaCN), sodium tetraborate decahydrate and sodium hydroxide (NaOH) were all purchased from Fisher Scientific (Fair Lawn, NJ, USA). Tetrabutylammonium sulfate (TBAS; 50% w/w, solution in water), used as a phase transfer catalyst, was purchased from Sigma-Aldrich (St. Louis, MO, USA). Pentafluorobenzyl bromide (PFBB-Br) was obtained from Thermo Scientific (Hanover Park, IL, USA). Isotopically labeled internal standards (Na¹³C¹⁵N and Na¹³C¹⁵N) were acquired from Isotech (Miamisburg, OH, USA). Solid-phase extraction (SPE) MCX (mixed-mode cation exchange) columns were acquired from Waters[®] Corporation (Milford, MA, USA). Deuterated ATCA (ATCA-d₂) was prepared by reaction of deuterated L-cysteine (3,3-d₂) with cyanamide (18) and provided by the Department of Veterans Affairs Medical Center, Minneapolis, MN, USA.

© The Author 2014. Published by Oxford University Press. All rights reserved. For Permissions, please email: journals.permissions@oup.com

N-Methyl-*N*-trimethylsilyltrifluoroacetamide (MSTFA) was purchased from Pierce Chemical Company (Rockford, IL, USA).

Animals

Three different animal models were used in this study: (i) Sprague-Dawley rats (*Rattus norvegicus*), (ii) New Zealand White rabbits (*Oryctolagus cuniculus*) and (iii) Yorkshire swine (*Sus scrofa*). Male Sprague-Dawley rats weighing 250–300 g (Charles River Breeding Laboratories, Inc., Wilmington, MA, USA) with catheters implanted were kept in temperature and light-controlled rooms ($22 \pm 2^\circ\text{C}$, 12 h light/dark cycle), fed Teklad Rodent Diet (W) 8604 (Teklad HSD, Inc., WI, USA) and provided with water at Sam Houston State University (Huntsville, TX, USA). Rabbits weighing 3.5–4.5 kg (Western Oregon Rabbit Supply, Philomath, OR, USA) were housed individually in the Animal Resource Facility (ARF) of the College of Medicine at the University of California, Irvine, CA, USA, fed Purina Pro-lab (St. Louis, MO, USA) and provided with water. Swine (47–54 kg) were purchased from the local USDA licensed breeder (John Albert, Cibola, TX, USA, USDA #74-A-1246) and were housed in paddocks (outdoor fenced pastures) and moved into indoor pens before the experiments. They were furnished with Purina Pro-Lab's (St. Louis, MO, USA) mini-pig-breeder diet (5082) and provided with water.

All animals were cared for in compliance with the "Principles of Laboratory Animal Care" formulated by the National Society for Medical Research and the "Guide for the Care and Use of Laboratory Animals" prepared by the National Academy of Sciences and published by the National Institutes of Health (NIH Publication #86-23, revised 1978). All studies involving rats, rabbits or swine were reviewed and approved by the Institutional Animal Care and Use Committee (IACUC) at the appropriate institutions.

Experimental design

Rats ($N = 9$) were injected with sub-lethal doses ($N = 3$) of potassium cyanide (KCN) solution subcutaneously [2 mg/kg (25% LD₅₀), 4 mg/kg (50% LD₅₀) or 6 mg/kg (75% LD₅₀)]. In order to establish a baseline, blood was drawn prior to injection for a "zero" time point. Blood samples (320 μL) were also drawn at 5, 15, 30, 60 min, and 2, 4, 6, 12, 15 and 50.5 h post-injection. These blood samples were placed in heparinized tubes to prevent coagulation. The tubes were then centrifuged to separate the plasma from the red blood cells (RBCs). A portion of plasma was removed for ATCA analysis (50 μL) and the rest was hemolyzed to produce whole blood for simultaneous CN and SCN⁻ analysis. The baseline concentration for CN, SCN⁻ and ATCA in saline-treated rats showed no significant change in the concentration over the duration of the experiment.

New Zealand White rabbits ($N = 8$) were anesthetized with an intramuscular injection of a 2:1 ratio of ketamine HCl (100 mg/mL, Ketaject, Phoenix Pharmaceutical Inc., St. Joseph, MI, USA): xylazine (20 mg/mL, Anased, Lloyd Laboratories, Shenandoah, IA, USA) at a dose of 0.75 cc/kg. After the intramuscular injection, a catheter was placed in the animals' marginal ear vein to administer continuous IV ketamine/xylazine anesthesia. The animals were intubated and were mechanically ventilated (dual phase control respirator, model 32A4BEPM-5R, Harvard Apparatus, Chicago, IL, USA) at a respiratory rate of 32 min⁻¹, a tidal volume

of 50 cc, and FIO₂ of 100%. Blunt dissection was performed to isolate the femoral artery and vein on the left thigh for cyanide infusion and blood sampling. Sodium cyanide (10 mg) dissolved in 60 mL of 0.9% NaCl was administered intravenously through the femoral line over 60 min. Blood samples (300 μL) were drawn at 11 different time points, including a baseline (time "zero"), 20, 40 and 55 min during CN infusion. After the cyanide infusion was completed, seven additional time points over the next 90 min at 60, 65, 75, 90, 105, 120 and 150 min from the start of the experiment were drawn. Arterial blood samples were collected in heparinized tubes kept on ice and centrifuged to separate the plasma. The plasma samples (150 μL) were then immediately frozen and shipped on ice to South Dakota State University (SDSU) for analysis of CN, SCN⁻ and ATCA. The baseline concentration for CN, SCN⁻ and ATCA in control saline-treated rabbits showed no significant change over the duration of the experiment. At the completion of the experiment, the animals were euthanized with an intravenous injection of 1.0 cc Euthasol (390 mg pento-barbital sodium, 50 mg phenytoin sodium; Vibrac AH, Inc, Fort Worth, TX, USA) administered through the marginal ear vein.

Swine ($N = 11$) were infused intravenously with approximately (or an average of) 1.7 mg/kg potassium cyanide until apnea occurred. The animals were then observed for an additional 60 min. Arterial blood (20 mL) was sampled prior to cyanide exposure (considered baseline or time "zero"), 5 min after the start of the cyanide infusion, 5 min into cyanide administration, at apnea and every 2 min for the first 10 min after apnea, and then every 10 min until 60 min postapnea. Blood (4 mL) was placed in an EDTA tube and centrifuged to separate the plasma. The plasma samples (500 μL) were then frozen and shipped on ice to SDSU for analysis of CN, SCN⁻ and ATCA.

CN and SCN⁻ analysis

The whole blood samples from rats and plasma samples from rabbits and swine were simultaneously analyzed for CN and SCN⁻ by chemical-ionization (CI) GC-MS after chemical modification based on a method previously reported (19). Briefly, blood samples (100 μL) were added to 2 mL microcentrifuge vials. Internal standards (100 μL) of Na¹³C¹⁵N (200 μM) and NaS¹³C¹⁵N (100 μM) were added to the sample vials along with TBAS (800 μL of 10 mM TBAS in a saturated solution of sodium tetraborate decahydrate, pH 9.5) and PFB-Hr (500 μL of a 20-mM solution in ethyl acetate) and vortexed for 2 min. Samples were then heated at 70°C for 1 h, and centrifuged for 4 min at 10,000 rpm (9,300 $\times g$) to separate the organic and aqueous layers. The organic layer (200 μL) was collected and analyzed using CI-GC-MS. The concentrations for both CN and SCN⁻ were well above the detection limit of the analytical method (~1 μM for CN and 50 nM for SCN⁻) for all samples analyzed.

ATCA analysis

Rat, rabbit and swine plasma samples (50 μL) were analyzed for ATCA according to a slightly modified procedure previously reported (20). Briefly, plasma samples (80 μL), internal standard (ATCA-d₂; 120 μL of 100 ng/mL) and 300 μL of 1% HCl in acetone were added to a 2-mL microcentrifuge vial, vortexed for 2 min and centrifuged for 4 min (room temperature) at 10,000 rpm (9,300 $\times g$). The supernatant was transferred to a clean microcentrifuge tube, 1.0 mL of 0.1 M HCl was added,

and the sample was aspirated through a prepared mixed-mode cation-exchange solid-phase extraction column (1 mL). The ATCA was eluted from the column into a 2-mL microcentrifuge tube using 1 mL of a water:methanol:ammonium hydroxide solution (25:50:25, by volume). Hydrochloric acid (200 μ L of 0.1 M) was added to the microcentrifuge tube to decrease the pH of the sample (pH < 11) and the sample was dried. The dried samples were reacted with 200 μ L of 30% MSTFA in hexane for 60 min at 50 °C in capped centrifuge tubes. The samples were then analyzed using electron-ionization GC-MS. The concentrations for ATCA were well above the detection limit of the analytical method (~170 nM) for each plasma sample tested.

Toxicokinetic analysis

The blood and plasma concentration-time data after subcutaneous or intravenous administration were analyzed using a one-compartment toxicokinetic model which was determined according to the methods previously described (21, 22). Concentration-time curves were used to obtain the maximum concentration (C_{max}) of CN, SCN^- and ATCA in blood and plasma, elimination constants (K_{el}) and terminal elimination half-life ($t_{1/2}$), with interpolation. A linear trapezoidal method was used to calculate the area under the curve (AUC) for cyanide and ATCA. The parameters such as C_{max} , K_{el} , $t_{1/2}$ and AUC were not calculated for thiocyanate in rabbit and swine models because there was no elimination observed from these experimental subjects throughout the duration of the experiments. The data presented is normalized to the baseline concentration of each compound to allow variation in concentrations of the analytes evaluated (CN, SCN^- and ATCA) to be observed on the same

figure, such that direct comparison of the relative behavior can more easily be observed.

Results

Behavior of CN, SCN^- and ATCA following cyanide exposure in Rats

Figure 1 shows the normalized CN, SCN^- and ATCA concentrations (i.e., normalized to the baseline concentration of the each compound, listed in Table II) from rats dosed at 6 mg/kg KCN. The baseline concentrations were determined to be 9.95, 38.6 and 0.282 μ M for CN, SCN^- and ATCA, respectively. As seen in Figure 1, the blood CN concentrations increased rapidly upon subcutaneous injection of KCN to a maximum at ~30 min and then declined rapidly as cyanide was distributed and metabolized. The CN concentrations then leveled off at ~100 min post-exposure and slowly declined. Thiocyanate concentrations rose at a slower rate compared with CN and then declined slowly at a rate similar to that of cyanide after reaching a maximum at ~120 min postexposure. Thiocyanate concentrations remained well above baseline for the duration of the experiment. Considering the variability of the data, ATCA concentrations changed only slightly when compared with the baseline concentration. Similar trends for all markers were observed for each dose of cyanide.

Dose-concentration behavior

The dose-blood concentration relationship for CN and SCN^- in rats with the C_{max} plotted for each dose is shown in Figure 2. As the dose of KCN increased, there was an expected increase in

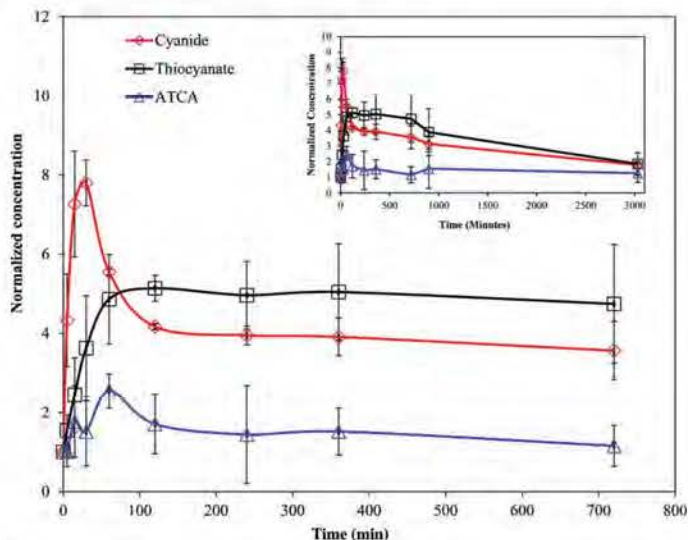


Figure 1. Whole blood CN, SCN^- and plasma ATCA normalized concentrations after cyanide exposure (6 mg/kg body weight KCN injection subcutaneously to rats). Error bars are plotted as standard error of mean (SEM) ($N = 3$). Inset: Full time course up to 50.5 h post-injection of KCN.

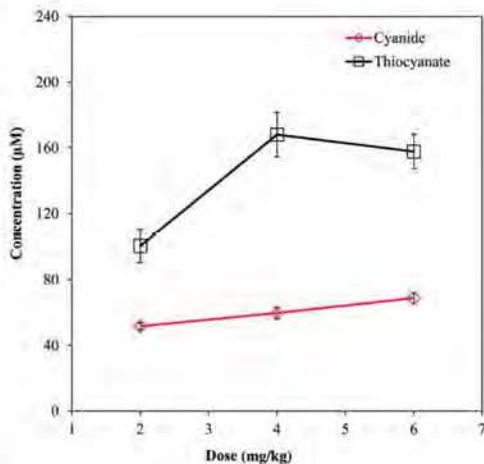


Figure 2. Dose–concentration curve for three different doses of KCN (2, 4 and 6 mg/kg) injected subcutaneously to rats. Error bars are plotted as standard error of mean (SEM) ($N = 3$).

the concentrations of CN and SCN^- . Cyanide concentrations showed a linear response to increasing CN dose, whereas the dose–response of thiocyanate was non-linear, leveling off at $\sim 160 \mu\text{M}$, with the 4 mg/kg dose and remaining at that level for the 6 mg/kg dose. The dose response of ATCA was not meaningful because of the large interanimal variability of plasma ATCA concentrations combined with the minor increase in C_{max} compared with baseline concentrations.

Behavior of CN, SCN^- and ATCA in rabbits after cyanide exposure

Figure 3 shows the normalized plasma concentrations of CN, SCN^- and ATCA from rabbits ($N = 8$) over 150 min. The baseline concentrations were determined to be 5.66, 9.99 and $0.227 \mu\text{M}$ for CN, SCN^- and ATCA, respectively. Plasma CN and ATCA concentrations reached a maximum at 55 min (14.7 and $9.1 \mu\text{M}$ for CN and ATCA, respectively) and then declined after CN administration was stopped. Plasma SCN^- rose slowly throughout the duration of the experiment (150 min). CN, SCN^- and ATCA were measurable throughout the study. ATCA concentrations clearly rose above the baseline by a larger ratio than the CN or SCN^- .

Behavior of CN, SCN^- and ATCA after cyanide exposure in swine

Figure 4 shows the normalized CN, SCN^- and ATCA concentrations from swine ($N = 11$) over 40 min. The baseline concentrations were determined to be 3.87, 5.45 and $0.175 \mu\text{M}$ for CN, SCN^- and ATCA, respectively. Plasma CN and ATCA concentrations reached a maximum at apnea (i.e., the 10-min time point) and then declined. The concentrations of each metabolite normalized to the baseline are very similar until 4 min postapnea (i.e., the 14 min time point in Figure 4) where the CN and

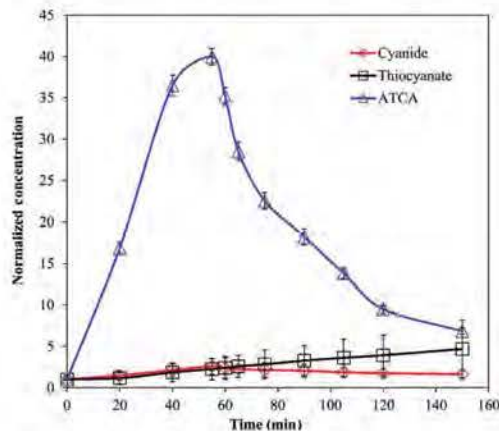


Figure 3. Plasma CN, SCN^- and ATCA normalized concentrations after 10 mg NaCN infusion to rabbits. Error bars are plotted as standard error of mean (SEM) ($N = 8$).

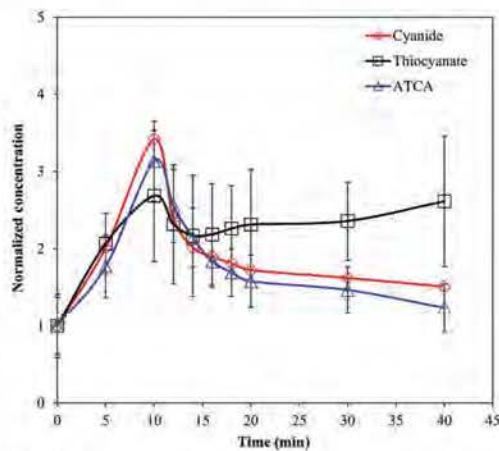


Figure 4. Swine plasma CN, SCN^- and ATCA normalized concentrations during and after intravenous dose (0.17 mg/kg/min until apnea; $\sim 10 \text{ min}$). Error bars are plotted as standard error of mean (SEM) ($N = 11$).

ATCA continue to decrease, but the SCN^- rises slowly through the completion of the experiment (40 min).

Toxicokinetics of CN, SCN^- and ATCA

A summary of the toxicokinetic parameters for rats, rabbits and swine is presented in Table 1. The AUC, C_{max} and $t_{1/2}$ were calculated for all three markers of cyanide exposure with the exception of SCN^- in rabbits and swine because it did not reach a maximum, and ATCA in rats because of considerable variability at each time point and the very low concentrations of ATCA measured. In rats, the AUC ranged from 6.53×10^4 to 7.74×10^4 and

Table 1

The Toxicokinetic Parameters of Cyanide, Thiocyanate and ATCA in Different Animal Models

Animals	Analyte	Matrix	CN dose (mg/kg)		C _{max} (μM)		t _{1/2} (min)	
			Current study	Previous study	Current study	Previous study	Current study	Previous study
Rats	Cyanide	Blood	2 ^a , 4 ^b , 6 ^c	1.0 (23), 3.0 (3)	51.7 ^a , 59.8 ^b , 68.8 ^c	25 (23), 89.0 (3)	1200 ^a , 1370 ^b , 1510 ^c	14.1(23), 39.4(3)
	Thiocyanate	Plasma		1.0 (23), 3.0 (3)	100 ^a , 160 ^b , 150 ^c	877 (23), 58.1 (3)	2530 ^a , 2880 ^b , 3010 ^c	348 (3)
	ATCA	Plasma		N/A (16), 10.0 (17)	N/A ^d	4.91 (16), 2.82 (17)	N/A ^d	150 (16)
Pigs	Cyanide	Blood/plasma ^e	1.7	3.0 (3)	30.2	57.5 (3)	26.8	32.4 (3)
	Thiocyanate	Plasma		3.0 (3)	N/A ^d	42.8 (3)	N/A ^d	297 (3)
	ATCA	Plasma		—	4.70	—	13.9	—
Rabbits	Cyanide	Plasma	2.5	—	14.7	—	177	—
	Thiocyanate	Plasma		—	N/A ^d	—	N/A ^d	—
	ATCA	Plasma		—	9.10	—	40.7	—
Goats	Cyanide	Blood	—	3.0 (3)	—	83.5 (3)	—	78.8 (3)
	Thiocyanate	Plasma	—	3.0 (3)	—	55.2 (3)	—	634 (3)
	ATCA	Plasma	—	—	—	—	—	20–60 (2, 27)
Humans	Cyanide	Blood	—	—	—	—	—	1440–3640 (26, 26, 28, 28)
	Thiocyanate	Plasma	—	—	—	—	—	—
	ATCA	Plasma	—	—	—	—	—	—

^aResults obtained from 2 mg/kg CN dose (11).

^bResults obtained from 4 mg/kg CN dose.

^cResults obtained from 6 mg/kg CN dose.

^dATCA could not be evaluated due to interanimal variability.

^ePlasma was used for cyanide analysis in our study.

^fSCN⁻ did not reach maximum value in our study.

Table 2

Endogenous blood CN or plasma SCN⁻ and ATCA concentrations from humans, rats, rabbits and swine models

Analyte	Humans (μM)	Rats (μM)		Rabbits (μM)		Swine (μM)	
		Current study	Previous studies	Current study	Previous studies	Current study	Previous studies
CN ^f	0.02–2.9 (4), 0.03–10 (5)	10.79	0.19 (28, 40), 3.27 (29, 41)	5.81	3.64 (39)	8.82	N/A
SCN ^{-h}	4.83–87.5 (4)	42.61	53.9 (23), 20.9 (3)	8.84	N/A	8.17	17.1 (8), 41.1 (9)
ATCA ^b	0.08–0.122 (4)	0.84	0.95 (16), 1.29 (17)	0.23	N/A	1.51	N/A

^fCN analyzed from whole blood.

^hSCN⁻ and ATCA were commonly analyzed from plasma.

2.27 × 10⁴ to 3.07 × 10⁴ μM min for cyanide and thiocyanate, respectively. For rabbits, the AUC was found to be 0.33 × 10⁴ and 548 μM min for cyanide and ATCA, respectively. The AUC for swine was determined to be 0.05 × 10⁴ and 75.4 μM min for cyanide and ATCA, respectively.

Discussion

The toxicokinetic parameters found for CN, SCN⁻ and ATCA in this study are presented in Table 1, alongside similar studies for comparison. Previously, cyanide has been found to be rapidly absorbed, distributed and subsequently quickly eliminated (2, 3, 23, 24), with a t_{1/2} ranging from 14 to 60 min. Rapid distribution of CN was also seen in our study for each model tested (Figures 1, 3 and 4). For the rabbits and swine, CN was also rapidly eliminated, with t_{1/2} values of ~27 and 178 min, which is in general agreement with similar studies (Table 1). Conversely, rats produced a much longer mean elimination half-life. The difference may be due to the duration of our study, 50.5 h post cyanide-exposure versus 1 and 24 h in the Leuschner *et al.*

(23) and Sousa *et al.* (3) studies, respectively. If the three distribution/elimination time points in our study (i.e., 30, 60 and 120 min) are used, the half-life obtained (t_{1/2} = 103 min) is comparable with that seen by Sousa *et al.* (3), and perhaps is more reflective of cyanide distribution than elimination. In addition, the other studies used oral dosing versus subcutaneous injection in the rat model for our study. Subcutaneous injection could potentially cause a rapid absorption and distribution of CN, versus a slower uptake of CN through the digestive tract. If a large dose of cyanide was rapidly absorbed into the erythrocytes, as suggested by Lundquist *et al.* (25), our data would suggest that the sequestered CN is only slowly released back into rat plasma for transport to tissues to be metabolized. Whole blood concentrations were also measured in multiple samples from each individual animal for the duration of the current study versus multiple animals at each time point in previous studies (3, 23). The fluid volume removed from an individual rat was ~10% of the total body fluid volume. Thus, by the end of the experiment, despite being provided with food and water *ad lib*, our experimental subjects could have become dehydrated, causing their hematocrit to be elevated, potentially resulting in a higher level of CN to be measured at later time points. Further investigations would need to be conducted in the rat model to verify the prolonged half-life seen in this study. If verified, the long half-life may indicate the ability of rats to tolerate elevated levels of CN over long periods of time, perhaps due to a relatively large pool of sequestering agents (e.g., methemoglobin). A relatively large pool of sequestering agents may reduce the free CN, thereby not overwhelming normal detoxification pathways leading to increased tolerance of CN.

Thiocyanate in the swine and rabbits increased at about the same rate as CN, while the formation of SCN⁻ in rats was markedly slower, which could be due to the method of CN administration, subcutaneous versus intravenous. At each dose, the maximum concentration of thiocyanate in rats occurred at around 1 h after cyanide exposure and stayed relatively consistent for several hours before it began to decrease. The extended

consistent SCN^- concentrations could be interpreted as having reached a steady-state between formation and elimination of thiocyanate. The mean elimination half-life of SCN^- in rats ranged from 2530 to 3010 min, and was much longer than that was found in the Sousa *et al.* (2003) study, possibly due to the reasons previously presented. That being said, the half-life of SCN^- in rats did fall within the range of human SCN^- $t_{1/2}$ (Table I).

Thiocyanate concentrations were still increasing at the end of the rabbit and swine studies, and would be expected to peak and decline as observed in rats if these studies were lengthened. It is interesting to note that SCN^- declined immediately after apnea in swine (i.e., after KCN administration was stopped), and then started to rise slowly after the 6-min postapnea time point and continued to rise for the duration of the study (Figure 3). This behavior, which is atypical compared with other similar studies, is likely influenced by several factors. Initially, plasma SCN^- levels rose at about the same rate as the infused cyanide levels, reaching a maximum at apnea, suggesting a direct correlation between cyanide and thiocyanate levels. Then the plasma SCN^- declined abruptly, possibly due to reduced cardiac output leading to lower cyanide delivery to the detoxification sites and reduced export of thiocyanate due to lack of blood flow in tissues. After several minutes of reduced SCN^- production and transport, the levels of SCN^- increased, until the end of the experiment, albeit at a slower rate than initially. The secondary rise in thiocyanate production would suggest that once the initial shock of apnea passes, the SCN^- detoxification pathway is reinitiated, although the slower rate of SCN^- production might suggest some impairment in this process. If any portion of the CN transport or biotransformation is energy-dependent, the pathway might become partially disabled by undergoing apnea. If the swine study were to be lengthened in time, the SCN^- concentrations should reach a maximum and decline, as observed in the rat study.

Compared with cyanide and thiocyanate, ATCA had the lowest mean elimination half-life in rabbit and swine models, resulting in shorter residence time in the plasma (Table I). In the rabbit and swine models, ATCA generally mimicked the behavior of CN, but appears to be a minor metabolic pathway for cyanide detoxification, especially in rats. Although the general behavior of CN and ATCA in each model is similar, the difference in the behavior of normalized ATCA concentrations in rabbits (i.e., the 40-fold increase above baseline), compared with swine and rats (i.e., only a 4-fold increase), is striking.

To investigate the likelihood of a minimized sulfur-donor cyanide detoxification pathway causing increased production of ATCA in rabbits, species-dependent rhodanese concentrations in multiple animal tissues (e.g., liver, kidney, lung, brain, stomach and muscle) were evaluated from literature sources. Among all the tissues, kidney contains relatively large amounts of rhodanese: 6.69, 24.9, 10.44–110.8 and 6.20–7.69 mg/g tissue in humans, swine, rats and rabbits, respectively (6, 26, 30, 31). The lower rhodanese concentrations in humans and rabbits suggest that the sulfur donor pathway for cyanide detoxification may be less active when compared with swine and rats, potentially leading to increased ATCA formation. L-Cystine concentrations were also evaluated with only a few studies reporting liver concentrations ranging from 22 to 77 and 20 to 300 nmol/g tissue in humans and rats, respectively (32, 33). Because the ranges of L-cystine from these studies are similar, it is unclear as to if

L-cystine concentrations play a role in the formation of ATCA as opposed to thiocyanate. Further characterization of L-cystine levels may shed some light on this hypothesized explanation of elevated ATCA in rabbits.

As seen in Figure 2, cyanide exhibited a linear relationship between the cyanide dose and blood concentrations under the conditions tested, which fundamentally implies that cyanide has rapid and complete distribution, with first-order kinetic behavior. For SCN^- , the dose–concentration behavior was non-linear and as the dose of cyanide was increased, the plasma concentration of SCN^- initially increased to 4 mg/kg where it remained essentially constant. This is likely due to saturation of the sulfur-donor pathway for cyanide detoxification. As mentioned here previously, the ATCA concentration–dose behavior was not evaluated due to the large interanimal variability of plasma ATCA concentrations in rats. This is an area of potential future study likely best investigated in rabbits.

The percentage of cyanide converted to ATCA in this study was estimated for rats, rabbits and swine. Cyanide conversion to ATCA was calculated as a percentage by dividing the maximum concentration of ATCA in each model over the total maximum concentration of cyanide, thiocyanate and ATCA. Considering that cyanide is distributed in the range of 70–96% in the red blood cells, with the remainder in the plasma (25, 34), it was estimated that ~0.10–0.78%, 2.46–9.19% and 0.60–3.7% of the cyanide dose was converted to ATCA in rats, rabbits and swine, respectively. Although the calculation of the percentage of cyanide conversion to ATCA from the current study is meant to be a rough estimate and further studies should be undertaken to accurately determine the amount of cyanide converted to ATCA, our calculations are significantly lower than previously reported estimates of 15–20% (6) and are likely even overestimated for swine and rabbits, due to SCN^- failing to reach a maximum. This difference is likely due to differences in experimental protocols, where Wood and Cooley (6) initially administered 20 mg of L-cystine- S^{35} via tail vein, and after 15 and 25 min, 1 mg of NaCN was subcutaneously administered. The added L-cystine potentially artificially increased the amount of ATCA generated.

It is well known that all biological samples contain endogenous concentrations of cyanide and its metabolites (4, 35–38). Therefore, these concentrations were measured in each animal prior to cyanide exposure and are reported in Table II, alongside previous applicable work. In comparing the endogenous concentrations of CN, SCN^- and ATCA, the concentrations found in rabbits are closer to those found in humans than the rats and swine.

Conclusion

If kidney rhodanese and endogenous cyanide concentrations are indicators of similarity between human and animal cyanide metabolism, the rabbits would be more similar to humans than rat and swine. If the rabbit model approximates human behavior, ATCA appears to be a promising candidate for early diagnosis of cyanide poisoning. Specifically, ATCA shows similar behavior relative to cyanide, it increases 40-fold above baseline concentrations, does not metabolize further (11, 14, 39) and it is exceedingly stable during storage of plasma samples (14, 20), something that is a serious issue for CN and SCN^- (4, 19). Although the rabbit model appears to be the closest to humans in a number of indirect measurements, future work should address the absorption,

distribution and elimination of ATCA in humans (e.g., from nitroprusside patients) in parallel with rabbits in order to confirm applicability of the rabbit to investigate human cyanide metabolism.

Acknowledgments

The authors acknowledge Susan M. Boudreau, RN, BSN, Maria G. Castaneda, MS, Toni E. Vargas, PA-C, MHS and Patricia Dixon, MHS, from the Clinical Research Division, Wilford Hall Medical Center, Lackland AFB, TX, for providing potassium cyanide exposed swine plasma samples for these studies. The opinions or assertions contained herein are the private views of the authors and are not to be construed as official or as reflecting the views of the Department of the Army, the National Institutes of Health or the Department of Defense.

Funding

The research was supported by the CounterACT Program, National Institutes of Health Office of the Director and the National Institute of Allergy and Infectious Diseases, Interagency Agreement Numbers Y1-OD-0690-01/A-120-BP2010-01, Y1-OD-1561-01/A120-BP2011-01 and the USAMRICD under the auspices of the US Army Research Office of Scientific Services Program Contract No. W911NF-11-D-0001 administered by Battelle (Delivery order 0079, Contract No TCN 11077) and AMRMC W81XWH-12-2-0098. We also gratefully acknowledge funding from the Oak Ridge Institute for Science and Education (ORISE).

References

1. Conn, EE. *Cyanogenesis, the Production of Cyanide, by Plants. Effects of Poisons Plants on Livestock*. Academic Press: San Diego, 1978, 301–310.
2. Ansell, M., Lewis, FA. (1970) A review of cyanide concentrations found in human organs. A survey of literature concerning cyanide metabolism, 'normal', non-fatal, and fatal body cyanide levels. *Journal of Forensic Medicine*, 17, 148–155.
3. Sousa, AB, Manzano, H, Soto-Blanco, B, Gorniak, SL. (2003) Toxicokinetics of cyanide in rats, pigs and goats after oral dosing with potassium cyanide. *Archives of Toxicology*, 77, 330–334. doi:10.1007/s00204-003-0446-y.
4. Logue, BA, Hinkens, DM, Baskin, SI, Rockwood, GA. (2010) The analysis of cyanide and its breakdown products in biological samples. *Critical Reviews in Analytical Chemistry*, 40, 122–147.
5. Minakata, K., Nozawa, H., Gonmori, K., Yamagishi, I., Suzuki, M., Hasegawa, K. et al. (2011) Determination of cyanide in blood by electrospray ionization tandem mass spectrometry after direct injection of dicyanogold. *Analytical and Bioanalytical Chemistry*, 400, 1943–1951. doi:10.1007/s00216-011-4824-7.
6. Wood, JL, Cooley, SL. (1956) Detoxication of cyanide by cystine. *The Journal of Biological Chemistry*, 218, 449–457.
7. Hasuike, Y., Nakanishi, T., Moriguchi, R., Otaki, Y., Nanami, M., Hana, Y. et al. (2004) Accumulation of cyanide and thiocyanate in haemodialysis patients. *Nephrology, Dialysis, Transplantation: Official Publication of the European Dialysis and Transplant Association – European Renal Association*, 19, 1474–1479. doi:10.1093/ndt/gth076.
8. Pettigrew, AR, Fell, GS. (1973) Microdiffusion method for estimation of cyanide in whole blood and its application to the study of conversion of cyanide to thiocyanate. *Clinical Chemistry*, 19, 466–471.
9. Murray, S, Lake, RG, Gray, S, Edwards, AJ, Springall, C, Bowry, EA. et al. (2001) Effect of cruciferous vegetable consumption on heterocyclic aromatic amine metabolism in man. *Carcinogenesis*, 22, 1413–1420.
10. Baskin, SI, Brewer, TG. Textbook of Military Medicine. In: Zajtcuk, R., Bellamy, RF. (ed). TMM Publications, 1997, pp271–286. Office of the Surgeon General.
11. Baskin, SI, Petrikovics, I, Kurche, JS, Nicholson, JD, Logue, BA, Maliner, BJ. et al. Insights on cyanide toxicity and methods of treatment. In: Flora, SJ, Romano, JA, Jr, Baskin, SI, Shekhar, K. (eds). *Pharmacological Perspectives of Toxic Chemicals and Their Antidotes*. Narosa Publishing House, New Delhi, India, 2004, pp105–146, Ch. 9.
12. Weuffen, W, Jess, G, Julich, WD, Bernhardt, D. (1980) Studies on the relationship between 2-iminothiazolidine-4-carboxylic acid and the thiocyanate metabolism in the guinea-pig (author's transl). *Pharmazie*, 35, 221–223.
13. Bradham, LS, Catsimopoulos, N, Wood, JL. (1965) Determination of 2-iminothiazolidine-4-carboxylic acid. *Analytical Biochemistry*, 11, 230–237.
14. Lundquist, P, Kagedal, B, Nilsson, L, Rosling, H. (1995) Analysis of the cyanide metabolite 2-aminothiazoline-4-carboxylic acid in urine by high-performance liquid chromatography. *Analytical Biochemistry*, 228, 27–34. doi:10.1006/abio.1995.1310.
15. Logue, BA, Maserek, WK, Rockwood, GA, Keebaugh, MW, Baskin, SI. (2009) The analysis of 2-amino-2-thiazoline-4-carboxylic acid in the plasma of smokers and non-smokers. *Toxicology Mechanisms and Methods*, 19, 202–208. doi:10.1080/15376510802488165.
16. Petrikovics, I, Yu, JC, Thompson, DE, Jayanna, P, Logue, BA, Nasr, J. et al. (2012) Plasma persistence of 2-aminothiazoline-4-carboxylic acid in rat system determined by liquid chromatography tandem mass spectrometry. *Journal of Chromatography B, Analytical Technologies in the Biomedical and Life Sciences*, 891–892: 81–84. doi:10.1016/j.jchromb.2012.01.024.
17. Yu, JC, Martin, S, Nasr, J, Stafford, K, Thompson, DE, Petrikovics, I. (2012) LC-MS/MS analysis of 2-aminothiazoline-4-carboxylic acid as a forensic biomarker for cyanide poisoning. *The World Journal of Methodology*, 2, 33–41.
18. Nagasawa, HT, Cummings, SE, Baskin, SI. (2004) The structure of "ITCA", a urinary metabolite of cyanide. *Organic Preparations and Procedures International*, 36, 178–182. doi:10.1080/00304940409355393.
19. Bhandari, RK, Oda, RP, Youso, SL, Petrikovics, I, Beharta, VS, Rockwood, GA. et al. (2012) Simultaneous determination of cyanide and thiocyanate in plasma by chemical ionization gas chromatography mass spectrometry (CI-GC-MS). *Analytical and Bioanalytical Chemistry*, 404, 2287–2294. doi:10.1007/s00216-012-6360-5.
20. Logue, BA, Kirschten, NP, Petrikovics, I, Moser, MA, Rockwood, GA, Baskin, SI. (2005) Determination of the cyanide metabolite 2-aminothiazoline-4-carboxylic acid in urine and plasma by gas chromatography-mass spectrometry. *Journal of Chromatography B, Analytical Technologies in the Biomedical and Life Sciences*, 819, 237–244. doi:10.1016/j.jchromb.2005.01.045.
21. Shargel, L, Wu Pong, S, Yu, ABC. One-compartment open model: intravenous bolus administration. In: *Applied Biopharmaceuticals and Pharmacokinetics*. 6th edition, McGraw Hill: New York, 2005.
22. Welling, PG. Pharmacokinetic principles. In: *Drug Toxicokinetics*. Welling, P G, De La Iglesia, FA. (eds). Marcel Dekker, Inc.: New York, 1993.
23. Leuschner, J, Winkler, A, Leuschner, F. (1991) Toxicokinetic aspects of chronic cyanide exposure in the rat. *Toxicology Letters*, 57, 195–201. doi: 10.1016/0378-4274(91)90146-W.
24. Agency for Toxic Substances and Disease Registry (2006) *Toxicological Profile for Cyanide*. US Department of Health and Human Services: Atlanta, USA, 2006.

25. Lundquist, P., Rosling, H., Sorbo, B. (1985) Determination of cyanide in whole blood, erythrocytes, and plasma. *Clinical Chemistry*, 31, 591–595.
26. Hinwrich, W.A., Saunders, J.P. (1948) Enzymatic conversion of cyanide to thiocyanate. *American Journal of Physiology*, 153, 348–354.
27. Hartung, R. Cyanides and nitriles. In: Clayton, G.D., Clayton, F.E. (eds). *Patty's Industrial Hygiene*. 3rd edition. John Wiley & Sons, Inc.: New York, 1982. 4845–4900.
28. Schub, V., Bonn, R., Kindler, J. (1979) Kinetics of elimination of thiocyanate in 7 healthy subjects and in 8 subjects with renal failure. *Klinische Wochenschrift*, 57, 243–247.
29. Junge, B. (1985) Changes in serum thiocyanate concentration on stopping smoking. *British Medical Journal*, 291, 22.
30. Westley, J. (1981) Thiosulfate: cyanide sulfurtransferase (rhodanese). *Methods in Enzymology*, 77, 285–291.
31. Aminlari, M., Malekhusseini, A., Akrami, F., Ebrahimnejad, H. (2007) Cyanide-metabolizing enzyme rhodanese in human tissues: comparison with domestic animals. *Comparative Clinical Pathology*, 16, 47–51.
32. Lee, J.I., Londono, M., Hirschberger, L.L., Stipanuk, M.H. (2004) Regulation of cysteine dioxygenase and gamma-glutamylcysteine synthetase is associated with hepatic cysteine level. *The Journal of Nutritional Biochemistry*, 15, 112–122. doi:10.1016/j.jnutbio.2003.10.005.
33. Stipanuk, M.H., Dornay, J.E., Jr, Lee, J.I., Coloso, R.M. (2006) Mammalian cysteine metabolism: new insights into regulation of cysteine metabolism. *The Journal of Nutrition*, 136, (6 Suppl.) 1652S–1659S.
34. Baar, S. (1966) The micro determination of cyanide: its application to the analysis of whole blood. *The Analyst*, 91, 268–272.
35. Manzano, H., de Sousa, A.B., Soto-Blanco, B., Guerra, J.L., Malorica, P.C., Gornlak, S.L. (2007) Effects of long-term cyanide ingestion by pigs. *Veterinary Research Communications*, 31, 93–104. doi:10.1007/s11259-006-3361-x.
36. Shen, X., Wang, P., Hu, S., Yang, Z., Ma, H., Gao, W. et al (2011) Simultaneous determination of oxygen, nitrogen and hydrogen in metals by pulse heating and time of flight mass spectrometric method. *Talanta*, 84, 1057–1062. doi:10.1016/j.talanta.2011.03.007.
37. Takeda, S., Inada, Y., Tomaru, T., Ikeda, T., Tashiro, N., Morimoto, F. et al (1990) Plasma and red blood cell cyanide concentrations during hypotension induced by sodium nitroprusside or by a nitroprusside-trimetaphan mixture in rabbits. *Masui The Japanese Journal of Anesthesiology*, 39, 701–707.
38. Toida, T., Togawa, T., Tanabe, S., Imanari, T. (1984) Determination of cyanide and thiocyanate in blood plasma and red cells by high-performance liquid chromatography with fluorometric detection. *Journal of Chromatography*, 308, 133–141.
39. Weuffen, W., Jess, G., Jölich, W.D., Bernhardt, D. (1980) Studies on the relationship between 2-iminothiazolidine-4-carboxylic acid and the thiocyanate metabolism in the guinea-pig (author's transl). *Die Pharmazie*, 35, 221–223.
40. Shibata, M., Inoue, K., Yoshimura, Y., Nakazawa, H., Seto, Y. (2004) Simultaneous determination of hydrogen cyanide and volatile aliphatic nitriles by headspace gas chromatography, and its application to an in vivo study of the metabolism of acrylonitrile in the rat. *Archives of Toxicology*, 78, 301–305. doi:10.1007/s00204-004-0545-4.
41. Tor-Agbidye, J., Palmer, V.S., Sabri, M.J., Craig, A.M., Blythe, L.L., Spencer, P.S. (1998) Dietary deficiency of cystine and methionine in rats alters thiol homeostasis required for cyanide detoxification. *Journal of Toxicology and Environmental Health Part A*, 55, 583–595. doi:10.1080/009841098158269.

APPENDIX IV

Author's personal copy

Anal Bioanal Chem
DOI 10.1007/s00216-013-7536-3

RESEARCH PAPER

Simultaneous high-performance liquid chromatography-tandem mass spectrometry (HPLC-MS-MS) analysis of cyanide and thiocyanate from swine plasma

Raj K. Bhandari & Erica Manandhar & Robert P. Oda & Gary A. Rockwood & Brian A. Logue

Received: 23 July 2013 / Revised: 19 November 2013 / Accepted: 26 November 2013
Springer-Verlag Berlin Heidelberg 2013

Abstract An analytical procedure for the simultaneous determination of cyanide and thiocyanate in swine plasma was developed and validated. Cyanide and thiocyanate were simultaneously analyzed by high-performance liquid chromatography tandem mass spectrometry in negative ionization mode after rapid and simple sample preparation. Isotopically labeled internal standards, Na¹³C¹⁵N and NaS¹³C¹⁵N, were mixed with swine plasma (spiked and nonspiked), proteins were precipitated with acetone, the samples were centrifuged, and the supernatant was removed and dried. The dried samples were reconstituted in 10 mM ammonium formate. Cyanide was reacted with naphthalene-2,3-dicarboxaldehyde and taurine to form N-substituted 1-cyano[f]benzoinidole, while thiocyanate was chemically modified with monobromobimane to form an SCN-bimane product. The method produced dynamic ranges of 0.1–50 and 0.2–50 μM for cyanide and thiocyanate, respectively, with limits of detection of 10 nM for cyanide and 50 nM for thiocyanate. For quality control standards, the precision, as measured by percent relative standard deviation, was below 8 %, and the accuracy was within ±10 % of the nominal

concentration. Following validation, the analytical procedure successfully detected cyanide and thiocyanate simultaneously from the plasma of cyanide-exposed swine.

Keywords Bioanalysis · Method validation · Chemical warfare agent · Monobromobimane · Naphthalene-2,3-dicarboxaldehyde

Introduction

The analysis of cyanide (as HCN or CN⁻, inclusively represented as CN) in biological fluids is of forensic relevance because cyanide is a highly toxic chemical which blocks terminal electron transfer by binding to cytochrome c oxidase, resulting in cyanide-mediated histotoxic anoxia [1–3]. Cyanide is enzymatically metabolized in vivo to thiocyanate (SCN⁻), in the presence of a sulfur donor (e.g., thiosulfate) [2, 3], as the major metabolic pathway.

Several analytical techniques have been successfully performed for the individual analysis of cyanide and thiocyanate from biological fluids, including spectrophotometry [4–6], gas chromatography–mass spectrometry (GC-MS) [7–9] and liquid chromatography [10–12]. While analysis of CN and SCN⁻ can be performed separately, considering the large number of samples produced for therapeutic and other studies involving cyanide, there is a need for a rapid, accurate, and reliable method which can simultaneously determine cyanide and thiocyanate. Such an analytical method should simplify analysis and significantly reduce labor costs. Although many

R. K. Bhandari · E. Manandhar · R. P. Oda · B. A. Logue (*)
Department of Chemistry and Biochemistry, South Dakota State University, Avera Health and Science Center 131, Box 2202, Brookings, SD 57007, USA
e-mail: brian.logue@sdsstate.edu

G. A. Rockwood
Analytical Toxicology Division, US Army Medical Research Institute of Chemical Defense, 3100 Ricketts Point Road, Aberdeen Proving Ground, MD 21010, USA

Published online: 12 December 2013

 Springer

Table 1 Comparison of some important features of available methods for simultaneous cyanide and thiocyanate analysis from biological fluids

Study	Analytical technique	LOD (μM)		Time		Biofluid(s)
		CN	SCN ⁻	Total ^a (h)	Analysis ^b (min)	
Imanari et al. [14]	HPLC-UV	0.2	0.2	1.0	30	Urine
Toida et al. [15]	HPLC-FLD	0.02	0.02	7.0	24	RBC/plasma
Chinaka et al. [16]	IC-UV-FLD	0.0038	0.006	1.5	30	Blood
Paul and Smith [17]	GC-MS	1.0	5.0	0.9	6	Saliva
Bhandari et al. [13]	GC-MS	1.0	0.05	1.8	18	Plasma

^aTotal estimated time including sample preparation and final analysis

^bTime necessary for completion of the analytical technique (not including sample preparation)

methods exist for the individual analysis of CN and SCN⁻ [3], few methods have been developed for their simultaneous determination in biological fluids [13–17]. These methods are summarized in Table 1. Imanari, Toida and co-workers [14, 15] reported high-performance liquid chromatography (HPLC) methods based on the König reaction [18, 19] for analysis of CN and SCN⁻ in urine with spectrophotometric detection [14] and blood with fluorometric detection [15]. For both methods, CN and SCN⁻ were separated using a strong-base anion exchange column and subsequently reacted with chloramine-T, pyridine, and barbituric acid. Although the Imanari et al. [14] method only required 1 h to complete, a much longer sample preparation time, 7 h, was necessary for the modification of this method for blood samples [15]. In 1998, Chinaka et al. [16] reported an ion chromatographic method for the simultaneous determination of CN and SCN⁻ in blood, where CN was derivatized with naphthalene-2,3-dicarboxaldehyde (NDA) and taurine for fluorometric detection, while unreacted SCN⁻ was detected spectrophotometrically. While this method produced excellent limits of detection (LODs) for CN and SCN⁻, the baseline found for SCN⁻ was high, other anions common to blood were found to interfere with SCN⁻ analysis, and the method took 1.5 h to complete. In 2006, Paul and Smith [17] reported a method for simultaneous analysis of CN and SCN⁻ using GC-MS after reaction of both anions with pentafluorobenzyl bromide (PFB-Br). The method had a number of disadvantages, including relatively high LODs, the method was only applicable to human saliva, and the internal standard used did not correct for variations in the derivatization reaction. Recently, we developed a similar method for the simultaneous analysis of CN and SCN⁻ in swine plasma using PFB-Br with GC-MS analysis [13]. The method featured excellent accuracy, precision, and LODs. However, the analysis time was long with an overall analysis time (sample preparation and GC-MS analysis) of approximately 2 h.

The goal of the work presented here was to develop a rapid and robust HPLC-MS-MS method for the simultaneous determination of CN and SCN⁻ as a complementary method to those already established, with anticipated advantages including rapid analysis time, low LODs, and high selectivity. The

developed method was applied to simultaneously determine CN and SCN⁻ in the plasma of cyanide-exposed swine.

Experimental

Materials

Reagents and standards

Sodium cyanide, sodium hydroxide (NaOH), and all solvents (HPLC-grade or higher) were purchased from Fisher Scientific (Fair Lawn, NJ, USA). Sodium thiocyanate was purchased from Acros Organics (Morris Plains, NJ, USA). NDA was obtained from Tokyo Chemical Industry, America (Portland, OR, USA). Taurine was acquired from Alfa Aesar (Ward Hill, MA, USA). Monobombimane (MBB) was purchased from Fluka Analytical through Sigma-Aldrich (St. Louis, MO, USA). Ellman's reagent (5,5'-dithiobis 2-nitrobenzoic acid) was obtained from Thermo Scientific (Hanover Park, IL, USA). Isotopically labeled internal standards, NaS¹³C¹⁵N and Na¹³C¹⁵N, were acquired from Isotech (Miami, OH, USA). Ammonium formate was purchased from Sigma-Aldrich (St. Louis, MO, USA).

Single cyanide and thiocyanate stock solutions (1 mM each) were prepared and diluted to the desired working concentrations for all experiments. Stock solutions of NDA (4 mM) and taurine (50 mM) were prepared in methanol and deionized water, respectively. Ellman's reagent (10 mM) was prepared in phosphate buffer (0.01 M, pH 7). A MBB solution (4 mM) was prepared in 0.1 M borate buffer (pH 8.0). The NDA, taurine, Ellman's reagent, and MBB solutions were stored at 4 °C in the dark. (Note: Cyanide is released as HCN from solutions with pH values near or below the pK_a of HCN (pK_a = 9.2). Thus, all aqueous standards containing cyanide were prepared in 10 mM NaOH and handled in a well-ventilated hood).

Biological fluids

Citrate anti-coagulated swine (*Sus scrofa*) plasma was obtained through the Veterinary Science Department at South

Dakota State University and plasma from cyanide-exposed swine was obtained from the laboratory of Dr. Vikhyat S. Bebartha at Wilford Hall Medical Center (Lackland Air Force Base, TX). For the cyanide-exposed swine, 11 swine (about 50 kg each) were intramuscularly injected with 1.7 mg/kg potassium cyanide. Blood samples were collected (4 mL), placed in EDTA tubes, and centrifuged to separate the plasma. The plasma samples (500 μ L) were then frozen and shipped on ice to South Dakota State University. Upon receipt, all plasma samples were stored at -80°C until analyzed. All animal procedures were conducted with the guidelines stated in "The Guide for the Care and Use of Laboratory Animals" (National Academic Press, 1996). The research facility where the plasma was gathered was AALAS (American Association for Laboratory Animal Science) accredited and all the animal protocols were approved by the appropriate institutional review board.

Methods

Sample preparation

Plasma (spiked or non-spiked, 200 μ L) was added to a 2 mL micro-centrifuge vial along with 50 μ L each of 100 μM $\text{NaS}^{13}\text{C}^{15}\text{N}$ and $\text{Na}^{13}\text{C}^{15}\text{N}$. Acetone (400 μ L) was added to the sample to precipitate plasma proteins and the vial was vortexed for 2 min and then centrifuged for 5 min at 13,200 rpm (16,200 \times g; Thermo Scientific Legend Micro 21R Centrifuge, Waltham, MA, USA). An aliquot (500 μ L) of the supernatant was then transferred to a 4-mL glass screw-top vial and dried under $\text{N}_2(\text{g})$ for 15 min at room temperature (RT) (Reacti-vap III, Pierce, Rockford, IL, USA). After drying, the sample was reconstituted with 200 μ L of 10 mM aqueous ammonium formate. NDA and taurine (50 μ L each) were added and mixed thoroughly to produce an N-substituted 1-cyano[f]benzoinsole (CBI) (Fig. 1). An

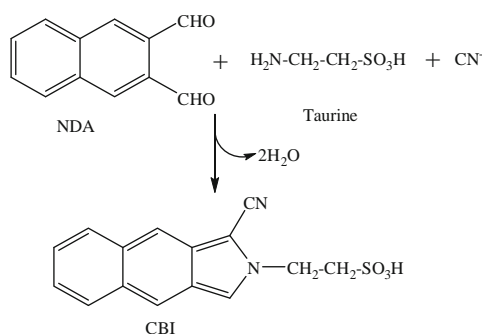


Fig. 1 Schematic representation of the reaction of NDA and taurine in the presence of cyanide to form an N-substituted 1-cyano[f]benzoinsole (CBI) complex

aliquot (100 μ L) of Ellman's reagent was added to react with free thiols in solution and vortex-mixed (1 min). MBB (100 μ L) was then added to produce the SCN-bimane complex shown in Fig. 2. The sample was heated on a block heater (VWR International, Radnor, PA, USA) at 70°C for 15 min. After filtration with a 0.22 μm tetrafluoropolyethylene membrane syringe filter, an aliquot of the prepared sample (100 μ L) was transferred into a screw-top autosampler vial (2 mL) with a 150- μ L glass insert for subsequent HPLC-MS-MS analysis. The analysis of cyanide through reaction with NDA to form CBI was originally suggested by Sano et al. [20]. To our knowledge, the analysis of SCN^- using MBB to produce an SCN-bimane product is first suggested here. In previous studies, it was thought that MBB reacts with free thiols only [21, 22].

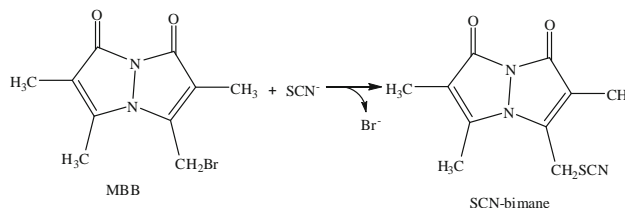
HPLC-MS-MS analysis

Prepared samples were simultaneously analyzed for CBI and SCN-bimane (Figs. 1 and 2) using a Shimadzu HPLC (LC-20AD, Shimadzu Corp., Kyoto, Japan) with a Phenomenex Kinetex XB-C18 RP column (50 \times 2.10 mm, 2.6 μ , 100 \AA) protected by a Synergi 2.5 μ Fusion-RP 100 \AA C18 (both Phenomenex, Torrance, CA, USA) guard cartridge (10 \times 200 mm, i.d.). Each chromatographic analysis was carried out with mobile phase components of aqueous 10 mM ammonium formate (mobile phase A) and 10 mM ammonium formate in methanol (mobile phase B). An aliquot (10 μ L) of the prepared sample was separated by gradient flow at 0.25 mL/min and 40°C . The concentration of B, initially 50 %, was increased linearly to 100 % over 3 min, held at 100 % for 1 min, decreased linearly to 50 % over 1 min, and held constant for 2 min to re-equilibrate the column between samples. An AB Sciex Q-trap 5500 MS-MS (Applied Biosystems, Foster City, CA, USA) with multiple reaction monitoring (MRM) was used to detect CBI and SCN-bimane using electrospray ionization (ESI)-MS-MS operated in negative polarity. Nitrogen gas (30 psi) was used as the curtain and nebulization gas. The dwell time was 100 ms for all MRM transitions. The ion source was operated at $-4,500\text{ V}$ and 500°C with nebulizer (GS1) and heater (GS2) gas pressures at 40.0 and 60.0 psi, respectively. The collision cell was operated with an entrance potential of -5.0 V and a cell potential of -7.4 V , with a medium collision gas pressure.

Calibration, quantification, and LOD

The calibration and quality control (QC) standards were prepared from aqueous cyanide and thiocyanate stock solutions (200 μM each). All the calibration standards for CN (0.01, 0.02, 0.05, 0.1, 0.2, 0.5, 1, 2, 5, 10, 20, 50, and 100 μM) and SCN^- (0.01, 0.02, 0.05, 0.1, 0.2, 0.5, 1, 2, 5, 10, 20, 50 and 100 μM) were prepared in swine plasma. The peak area signal

Fig. 2 Schematic representation of the MBB thiocyanate reaction to form a SCN-bimane product



ratios (i.e., the peak area of the analyte transition divided by the peak area of the internal standard transition) were plotted as a function of calibrator concentration. Both nonweighted and weighted ($1/x$ and $1/x^2$) linear calibration curves were prepared by least squares and a nonweighted linear fit was found to best describe the calibration data for cyanide, with a $1/x^2$ weighted linear fit used for thiocyanate. A computer workstation running Analyst™ software 1.4.1. (Farmingham, MA, USA) was used for data acquisition and peak integration.

The upper limit of quantification (ULOQ) and the lower limit of quantification (LLOQ) were defined by investigation of calibrators which satisfied the following inclusion criteria: (1) a percent relative standard deviation of <10 % (as a measure of precision) and (2) a percent deviation within ± 20 % back-calculated from the nominal concentration of each calibration standard (as a measure of accuracy). Three QC standard concentrations were prepared in swine plasma for CN (0.3, 3 and 15 μM as low, medium, and high, respectively) and SCN⁻ (0.7, 4, and 15 μM as low, medium, and high, respectively) and were analyzed in quintuplicate ($N=5$) each day for 3 days. These QC standards were analyzed in parallel with the calibration standards. Intra-assay precision and accuracy of the method was assessed by analyzing replicates of the QC standards from each day's analysis. Inter-assay precision and accuracy of the method were calculated by comparing the QC standards from three separate days. The intra- and inter-assay investigations were performed within seven calendar days.

The LODs were estimated by analysis of multiple concentrations of CN and SCN⁻ below their respective LLOQ. The LOD was defined as the lowest analyte concentration reproducibly producing a signal-to-noise ratio of 3 which contained both MRM transitions. Noise was calculated as the peak-to-peak noise directly adjacent to the analyte peak.

Selectivity, stability, and recovery

The ability to differentiate and quantify CBI and SCN-bimane in the presence of other plasma components (assay selectivity) was determined by comparing blank swine plasma (triplicate) with spiked swine plasma (15 μM , triplicate) by the procedure described earlier. Matrix effects were also investigated by

creating a calibration curve in aqueous solution and one in plasma and evaluating the similarity of the curves. There was no significant difference between the two curves, indicating that matrix effects were not important. Symmetry of the chromatographic peaks, as measured by peak asymmetry (A_s), was evaluated by dividing the front-width by the back-width at 10 % peak height [23].

The short- and long- term storage stability of cyanide and thiocyanate was evaluated using swine plasma spiked with high and low QC concentrations of each analyte. For short-term stability, both the low and high QC samples were evaluated in the autosampler, on the bench-top, and under multiple freeze-thaw (FT) conditions. The autosampler stability of CBI and SCN-bimane was evaluated for prepared cyanide and thiocyanate QC standards (both high and low) after placing the QC standards in the LC autosampler at 15 °C and analyzing at approximately 0, 1, 2, 4, 8, 12, and 24 h. The bench-top stability of CBI and SCN-bimane was evaluated using QC standards which were allowed to stand at room temperature (RT) for 0, 1, 2, 4, 8, 12, and 24 h prior to analysis. FT stability was evaluated by initially analyzing three aliquots each of the high and low QC concentrations (i.e., the same day of sample preparation) and then freezing and storing all standards at -80 °C for 24 h. The standards were then thawed unassisted at RT, analyzed and compared with the initial analysis. The remaining standards were again frozen, thawed, and analyzed. In total, this process was performed for three FT cycles. It should be noted that internal standards were added to the QCs directly prior to sample preparation, exclusive of autosampler stability, to correct for variations due to sample preparation and instrumental errors.

Both low and high QC standards were also used for long-term stability studies. The QC standards were stored at -80 °C, -20 °C, 4 °C, and RT. These standards were analyzed in triplicate on the day they were prepared, and after 1, 2, 5, 10, 20, and 30 days. Cyanide and thiocyanate were considered stable if the calculated concentrations were within ± 10 % of the original concentration.

The assay recovery of each compound was determined from spiked swine plasma and spiked aqueous samples at low, medium, and high QC concentrations. Recoveries of cyanide and thiocyanate were determined as a percentage by comparing peak areas obtained from the spiked swine plasma

with spiked aqueous samples at the same concentrations. All recovery experiments were performed in triplicate.

Results and discussion

HPLC-MS-MS analysis of CN and SCN⁻

The method presented includes the chemical modification of CN and SCN⁻ with a mixture of NDA/taurine and monobromobimane (MBB), respectively (Figs. 1 and 2), in a one-pot sample preparation method. The mass spectra of cyanide (as CBI) and thiocyanate (as SCN-bimane) produced by ESI(-)-MS are shown in Fig. 3a, b, respectively, with the major abundant ions identified. The *m/z* ratios of 298.6 and

248.0 correspond to the molecular ion of the CBI complex and SCN-bimane product of cyanide and thiocyanate, respectively ([M-H]⁻). For cyanide, the 298.6 → 190.7 and 298.6 → 80.9 transitions were selected as the quantification and identification transitions, respectively, using the corresponding transitions for isotopically labeled cyanide as internal standard signals, 300.6 → 192.7 and 300.6 → 80.9. For thiocyanate, the 248.0 → 111.0 and 248.0 → 124.1 transitions were selected as the quantification and identification transitions, respectively, while the corresponding transitions for labeled thiocyanate internal standard were 250.0 → 111.0 and 250.0 → 126.1. The optimized declustering potentials (DPs) and collision energies (CEs) for the detection of CBI were -70 and -25 V, respectively. For SCN-bimane, the optimized DPs and CEs were -185 and -19 V, respectively. Identical DPs and CEs were used for the applicable isotopically labeled internal standards.

Representative HPLC-MS-MS chromatograms of cyanide and thiocyanate, as CBI and SCN-bimane, are depicted in Fig. 4. Initially, the analysis of SCN⁻ following MBB addition was not possible because MBB reacted with abundant thiol groups present in plasma, which competed with the MBB-SCN reaction [21, 22]. Thus, Ellman's reagent was added in excess to react with the free thiols in plasma, prior to MBB addition, to allow increased production of the SCN-bimane complex. As seen in Fig. 4, the peak shapes for both thiocyanate (1.7 min) and cyanide (2.1 min) were sharp and symmetrical with peak asymmetries of 1.0 and 1.1, respectively.

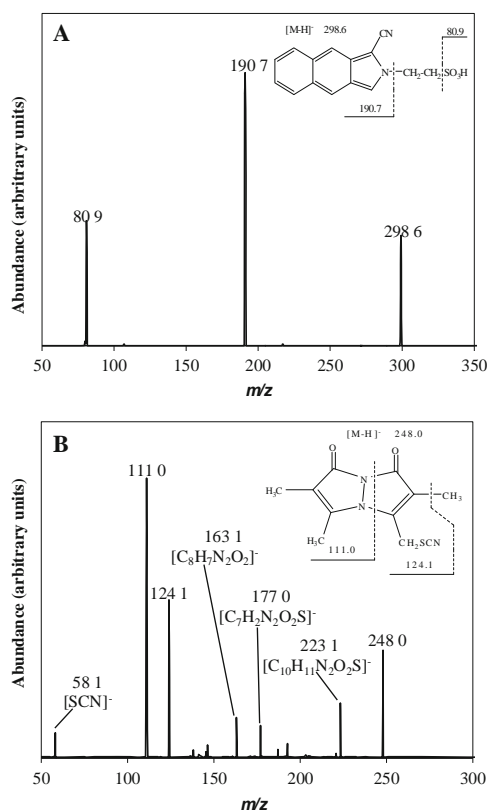


Fig. 3 ESI(-) product ion mass spectra of CBI (a) and SCN-bimane (b) with identification of the abundant ions. Molecular ions of CBI and SCN-bimane [M-H]⁻ correspond to 298.6 and 248.0, respectively. Insets, structures of CBI (a) and SCN-bimane (b) with abundant fragments indicated

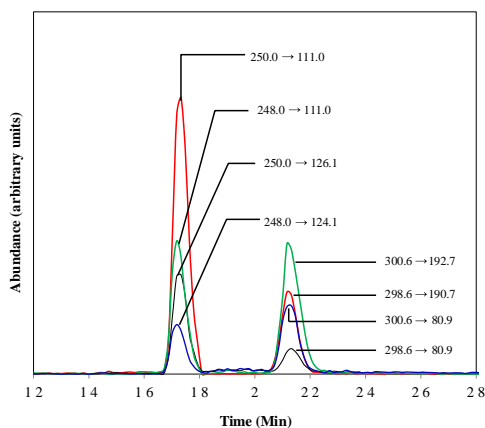


Fig. 4 HPLC-MS-MS chromatograms of 10 μM cyanide and 20 μM thiocyanate spiked into swine plasma with internal standard (50 μM each). The chromatograms represent signal response to the MRM transitions of cyanide (298.6 → 190.7, 298.6 → 80.9, 300.6 → 192.7, and 300.6 → 80.9) and thiocyanate (248.0 → 111.0, 248.0 → 124.1, 250.0 → 111.0, and 250.0 → 126.1). Thiocyanate and cyanide (as SCN-bimane and CBI) eluted from the column at approximately 1.7 and 2.1 min, respectively

Table 2 Comparison of the stability of the slope, R^2 , accuracy and precision for cyanide, and thiocyanate analysis from spiked swine plasma over 3 days

Analyte	Day	R^2	Slope	Accuracy (%)	Precision (%RSD)
CN	1	0.9997	0.019	100±8.5	<7.5
	2	0.9999	0.018	100±8.4	<5.4
	3	0.9996	0.019	100±8.8	<6.5
SCN ⁻	1	0.9994	0.022	100±5.9	<5.6
	2	0.9997	0.021	100±5.3	<6.8
	3	0.9998	0.020	100±6.1	<7.3

Overall, the sample preparation and analysis was rapid and simple. The duration of sample preparation was approximately 40 min, with the chromatographic analysis lasting approximately 8 min (including equilibrium for the following sample), for a total analysis time of approximately 50 min. Therefore, using conservative estimates, it is estimated that approximately 170 parallel samples could be processed and analyzed within a 24-h period. The duration of analysis for this method is shorter than previous methods for simultaneous analysis of CN and SCN⁻ (Table 1), and although the duration of the Imanari et al. [14] and Paul and Smith [17] methods are certainly comparable, these two methods were not used for the analysis of plasma or blood.

Calibration and quantification

Calibration curves for cyanide and thiocyanate were constructed in the range of 0.01–100 μM in swine plasma. For cyanide, calibration standards at 0.01, 0.02, 0.05, and 100 μM were found to be outside the LLOQ or ULOQ, while calibration standards at 0.01, 0.02, 0.05, 0.1, and 100 μM were found to be outside the LLOQ or ULOQ for thiocyanate, resulting in linear dynamic ranges from 0.1 to 50 to 0.2 to 50 μM , for cyanide and thiocyanate, respectively. The linear ranges for both cyanide and thiocyanate are comparable to typical bioanalytical LC-MS-MS methods, which generally span at least two orders of magnitude [24–26]. For both cyanide and thiocyanate, the

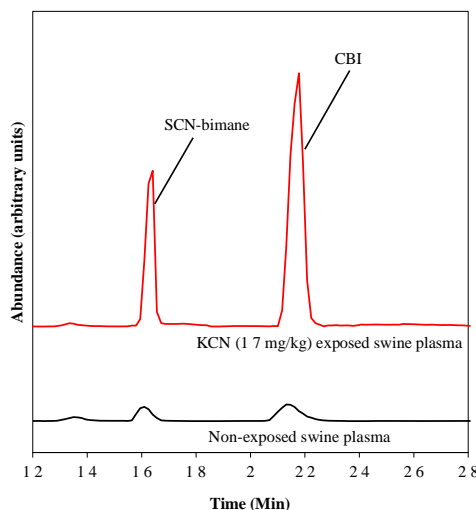


Fig. 5 Chromatograms of potassium cyanide-exposed (1.7 mg/kg) swine plasma (upper trace) and nonexposed swine plasma (lower trace), both without internal standard. The chromatograms represent the signal response of the MRM transition 298.6→190.7 and 248.0→111.0 m/z transition for CBI and SCN-bimane, respectively

calibration curves were found to be highly stable over 3 days in terms of slopes and correlation coefficients (Table 2).

LOD, accuracy, and precision

The accuracy, precision, and LOD for CN and SCN⁻ are reported in Table 3. The LODs found for cyanide and thiocyanate are in the nM range; lower than methods previously reported for simultaneous analysis of CN and SCN⁻ (Table 1). While the significantly lower LODs for cyanide and thiocyanate in plasma are not necessarily essential (i.e., significant endogenous CN and SCN⁻ concentrations mitigate the need for extremely low LODs), they should allow for quantification of cyanide and thiocyanate concentrations in other biological matrices where they may be present at extremely low levels.

Table 3 The accuracy, precision, LOD, and recovery of cyanide and thiocyanate analysis from spiked swine plasma by HPLC-MS-MS

Analyte	LOD (μM)	QC Concentration (μM)	Recovery (%)	Intraassay		Interassay	
				Accuracy (%) ^a	Precision (%RSD) ^a	Accuracy (%) ^b	Precision (%RSD) ^b
CN	0.01	0.3	72.9	100±7.5	1.1	100±7.2	1.5
		3	81.6	100±8.4	7.3	100±9.4	5.4
		15	83.1	100±7.3	2.2	100±4.2	4.1
SCN ⁻	0.05	0.7	73.1	100±4.4	4.2	100±5.3	6.8
		4	78.6	100±5.9	3.4	100±5.9	3.4
		15	80.8	100±1.9	5.6	100±1.9	3.9

^aQC method validation (N=5) for day 3

^bMean of three different days of QC method validation (N=15)

Our method produced excellent accuracy and precision for all the conditions tested. The accuracy and precision reported in Table 2 is the aggregate of all QC standards for 3 days. The accuracy was within 8.8 and 6.1 % of the nominal concentration for CN and SCN⁻, respectively, and the precision was not higher than 7.5 % relative standard deviation (RSD) for either CN or SCN⁻. Moreover, the absolute values of the accuracy and precision were very consistent for each analyte. The accuracy and precision reported in Table 3 was calculated in aggregate for low, medium, and high QC standards analyzed on three different days. The intra- and inter-assay precision and accuracy were below 8 % RSD and within ± 10 % of the nominal concentrations for all intra- and inter-assay analyses.

Stability and recovery

The short-term stabilities of cyanide and thiocyanate in swine plasma were evaluated in the autosampler and on the bench-top over 24 h. In the autosampler, both cyanide and thiocyanate demonstrated excellent stability for prepared samples, with the measured concentrations within 10 % of the initial concentration at all times tested. On the bench-top, cyanide and thiocyanate concentrations were stable for up to 1 and 8 h, respectively. In addition, the concentrations of cyanide and thiocyanate were within 10 % of the original concentration for both low and high QC standards for only one FT cycle.

For long-term stability investigations, both cyanide and thiocyanate were evaluated for 1 month at -80, -20, and 4 °C. Cyanide was stable for 2 days at -80 and -20 °C but was quickly eliminated from plasma at 4 °C for both the low and high QC standards. Thiocyanate was stable for 5 days at -80 and -20 °C, and for 2 days at 4 °C. The results from investigations of long-term stability suggest that both cyanide and thiocyanate should be analyzed immediately. If this cannot be done, the plasma samples should be frozen and analyzed within 2 days.

The limited stability of cyanide under typical storage conditions may be due to its volatile nature with rapid loss of hydrocyanic acid from biological samples at pH values below 7–8 (HCN pK_a=9.2). Alternatively, cyanide can be produced or utilized through single-carbon metabolism [27, 28]. Other studies have implicated microbial metabolism for alteration in CN levels [29–31]. It has been suggested that additives, such as addition of silver ions or ascorbic acid, may increase the stability of cyanide [29, 32], which may be an area of future investigation. The instability of SCN⁻ could be due to thiocyanate protein binding, resulting in the loss of free thiocyanate in plasma samples [8, 33].

The recoveries of cyanide and thiocyanate are reported in Table 3 and ranged from 72 to 83 % for cyanide and 73–81 % for thiocyanate. The recoveries for this method are similar to previous reports [16, 17, 34].

Application of the method

Potassium cyanide-exposed swine plasma samples were collected and analyzed for plasma cyanide and thiocyanate using the method presented here. Figure 5 shows representative chromatograms of potassium cyanide-exposed (1.7 mg/kg; upper trace) and non-exposed (lower trace) swine. The peaks for thiocyanate and cyanide were observed around 1.7 and 2.1 min, respectively, with the presence of endogenous concentrations detected in the nonexposed swine. In Fig. 5, the non-spiked swine plasma contained small amounts of cyanide (3.58 μ M) and thiocyanate (4.35 μ M). These levels were attributed to endogenous concentrations which likely come from multiple sources, such as diet [3, 13, 35, 36]. The assignment of endogenous CN and SCN⁻ was verified by identical retention times as compared with spiked plasma possessing the quantitation and identification ions. Overall, the method performed well for the diagnosis of cyanide exposure in swine.

Conclusions

A highly selective method featuring simple sample preparation with excellent accuracy and precision was developed and validated in swine plasma. The reported method has the ability to simultaneously detect cyanide and thiocyanate at low concentrations and proved useful for their detection from the plasma of cyanide-exposed swine. To our knowledge, this is the first description of an HPLC-MS-MS method for the simultaneous analysis of cyanide and thiocyanate from any matrix.

Acknowledgments The research was supported by the CounterACT Program, National Institutes of Health Office of the Director, and the National Institute of Allergy and Infectious Diseases, Interagency agreement numbers Y1-OD-0690-01/A-120-B.P2010-01, Y1-OD-1561-01/A-120-B.P2011-01, and AOD12060-001-00000/A-120-B.P2012-01 and the US Army Medical Research Institute of Chemical Defense (USAMRICD) under the auspices of the US Army Research Office of Scientific Services program contract no. W911NF-11-D-0001 administered by Battelle (Delivery order 0079, contract no. TCN 11077). We thank the National Science Foundation Major Research Instrumentation Program (grant no. CHE-0922816) and the State of South Dakota for funding the purchase of the AB SCIEX QTRAP 5500 LC-MS-MS. The LC-MS-MS instrumentation was housed in the South Dakota State University Campus Mass Spectrometry Facility which was supported by the National Science Foundation/EPSCoR grant no. 0091948 and the State of South Dakota. The authors would also like to acknowledge Dr. George Perry, Animal and Range Science (South Dakota State University) for providing swine plasma. Furthermore, the authors are thankful to Dr. Vikhyat Bebartha, Susan M. Boudreau, RN, BSN, Maria G. Castaneda, MS, Toni E. Vargas, PA-C, MHS, and Patricia Dixon, MHS from the Clinical Research Division, Wilford Hall Medical Center (Lackland Air Force Base, San Antonio, TX) for providing potassium cyanide-exposed swine plasma. The opinions or assertions contained herein are the private views of the authors and are not to be construed as official or as reflecting the views of the Department of the Army, the National Institutes of Health, the Department of Defense, the National Science Foundation, or the State of South Dakota.

References

- Conn EE (1978) Cyanogenesis, the production of cyanide, by plants. In: Keeler RF, Van Kampen KR, James LF (eds) Effects of poisons plants on livestock. Academic, San Diego, pp 301–310
- Baskin SI, Petrikovics I, Kurche JS, Nicholson JD, Logue BA, Maliner BJ, Rockwood GA (2004) Insights of cyanide toxicity and methods of treatment. In: Flora SJS, Romano JA Jr, Baskin SI, Shekhar K (eds) Pharmacological perspectives of toxic chemicals and their antidotes. Narosa Publishing House, New Delhi, pp 105–146, Ch. 9
- Logue BA, Hinkens DM, Baskin SI, Rockwood GA (2010) The analysis of cyanide and its breakdown products in biological samples. *Crit Rev Anal Chem* 40(2):122–147
- Kaur P, Upadhyay S, Gupta VK (1987) Spectrophotometric determination of hydrogen cyanide in air and biological fluids. *Analyst* 112(12):1681–1683
- Naik RM, Kumar B, Asthana A (2010) Kinetic spectrophotometric method for trace determination of thiocyanate based on its inhibitory effect. *Spectrochimica acta Part A, Molecular and Biomolecular Spectroscopy* 75(3):1152–1158. doi:10.1016/j.saa.2009.12.078
- Hanza A, Bashammakh AS, Al-Sibaai AA, Al-Saidi HM, El-Shahawi MS (2010) Dual-wavelength beta-correction spectrophotometric determination of trace concentrations of cyanide ions based on the nucleophilic addition of cyanide to imine group of the new reagent 4-hydroxy-3-(2-oxoindolin-3-ylideneamino)-2-thioxo-2H-1,3-thiazin-6(3H)-one. *Analytica chimica acta* 657(1) 69–74. doi:10.1016/j.aca.2009.10.025
- Youso SL, Rockwood GA, Lee JP, Logue BA (2010) Determination of cyanide exposure by gas chromatography–mass spectrometry analysis of cyanide-exposed plasma proteins. *Analytica chimica acta* 677(1):24–28. doi:10.1016/j.aca.2010.01.028
- Youso SL, Rockwood GA, Logue BA (2012) The analysis of protein-bound thiocyanate in plasma of smokers and non-smokers as a marker of cyanide exposure. *Journal of analytical toxicology* 36(4): 265–269. doi:10.1093/jat/bks017
- Frison G, Zancanaro F, Favretto D, Ferrara SD (2006) An improved method for cyanide determination in blood using solid-phase microextraction and gas chromatography/mass spectrometry. *Rapid communications in mass spectrometry* : RCM 20(19):2932–2938. doi:10.1002/rcm.2689
- Sano A, Takimoto N, Takitani S (1992) High-performance liquid chromatographic determination of cyanide in human red blood cells by pre-column fluorescence derivatization. *J Chromatogr* 582(1–2): 131–135
- Traquai A, Raul JS, Geraut A, Berthelon L, Ludes B (2002) Determination of blood cyanide by HPLC-MS. *J Anal Toxicol* 26(3):144–148
- Chen SH, Yang ZY, Wu HL, Kou HS, Lin SJ (1996) Determination of thiocyanate anion by high-performance liquid chromatography with fluorimetric detection. *J Anal Toxicol* 20(1):38–42
- Bhandari RK, Oda RP, Youso SL, Petrikovics I, Bebarat VS, Rockwood GA, Logue BA (2012) Simultaneous determination of cyanide and thiocyanate in plasma by chemical ionization gas chromatography mass-spectrometry (CI-GC-MS). *Anal Bioanalytical Chem* 404(8):2287–2294. doi:10.1007/s00216-012-6360-5
- Imanari T, Tanabe S, Toida T (1982) Simultaneous determination of cyanide and thiocyanate by high performance liquid chromatography. *Chem Pharm Bull* 30(10):3800–3802
- Toida T, Togawa T, Tanabe S, Imanari T (1984) Determination of cyanide and thiocyanate in blood plasma and red cells by high-performance liquid chromatography with fluorometric detection. *J Chromatogr* 308:133–141
- Chinaka S, Takayama N, Michigami Y, Ueda K (1998) Simultaneous determination of cyanide and thiocyanate in blood by ion chromatography with fluorescence and ultraviolet detection. *J Chromatogr B, Biomed Sci appl* 713(2) 353–359
- Paul BD, Smith ML (2006) Cyanide and thiocyanate in human saliva by gas chromatography–mass spectrometry. *J Anal Toxicol* 30(8): 511–515
- König W (1904) Über eine neue, vom Pyridine derivierende Klasse vom Farbstoffen. *Zeitschrift für Praktische Chemie* 69(1):105–137
- Bark LS, Higson HG (1963) A review of the methods available for the detection and determination of small amounts of cyanide. *Analyst* 88:751–760
- Sano A, Takezawa M, Takitani S (1989) Spectrofluorimetric determination of cyanide in blood and urine with naphthalene-2,3-dialdehyde and taurine. *Anal Chim Acta* 225 351–358
- Kosower NS, Kosower EM (1987) Thiol labeling with bromobimanes. *Methods Enzymol* 143:76–84
- Guan X, Hoffman B, Dwivedi C, Matthes DP (2003) A simultaneous liquid chromatography/mass spectrometric assay of glutathione, cysteine, homocysteine and their disulfides in biological samples. *J Pharm Biomed Anal* 31(2):251–261
- Foley JP, Dorsey JG (1984) A review of the exponentially modified Gaussian (EMG) function: evaluation and subsequent calculation of universal data. *J Chromatogr Sci* 22:40–46
- Garofolo F (2004) LC-MS instrument calibration. In: Chan CC, Lam H, Lee YC, Zhang X-M (eds) Analytical method validation and instrument performance verification. Wiley, Hoboken, NJ, pp 197–220
- Whitmire M, Ammerman J, de Liso P, Killmer J, Kyle D, Mainstore E, Porter L, Zhang T (2011) LC-MS/MS bioanalysis method development, validation and sample analysis: points to consider when conducting nonclinical and clinical studies according with current regulatory guidances. *J Anal Bioanal Techniques* S4:001
- Van Eeckhaut A, Lanckmans K, Sarre S, Smolders I, Michotte Y (2009) Validation of bioanalytical LC-MS/MS assays: evaluation of matrix effects. *J Chromatogr B Anal Technol Biomed Life Sci* 877(23):2198–2207. doi:10.1016/j.jchromb.2009.01.003
- Smith MR, Lequerica JL, Hart MR (1985) Inhibition of methanogenesis and carbon metabolism in *Methanosarcina* sp. by cyanide. *J Bacteriol* 162(1):67–71
- Boxer GE, Rickards JC (1952) Studies on the metabolism of the carbon of cyanide and thiocyanate. *Arch Biochem Biophys* 39(1):7–26
- Knowles CJ (1976) Microorganisms and cyanide. *Bacteriol Rev* 40(3):652–680
- Seto Y (1995) Oxidative conversion of thiocyanate to cyanide by oxyhemoglobin during acid denaturation. *Arch Biochem Biophys* 321(1):245–254. doi:10.1006/abbi.1995.1392
- Seto Y (1996) Determination of physiological levels of blood cyanide without interference by thiocyanate. *Jpn J Tox Env Health* 42(4): 319–325
- Lundquist P, Rosling H, Sorbo B (1985) Determination of cyanide in whole blood, erythrocytes, and plasma. *Clin chemistry* 31(4):591–595
- Pollay M, Stevens A, Davis C Jr (1966) Determination of plasma-thiocyanate binding and the Donnan ratio under simulated physiological conditions. *Anal Biochem* 17(2):192–200
- Kage S, Nagata T, Kudo K (1996) Determination of cyanide and thiocyanate in blood by gas chromatography and gas chromatography–mass spectrometry. *J Chromatography B, Biom Appl* 675(1): 27–32
- Daferes ER Jr, Webber LS, Radhakrishnamurthy B, Berenson GS (1980) Continuous-flow (Autoanalyzer I) analysis for plasma thiocyanate as an index to tobacco smoking. *Clin Chem* 26(3):493–495
- Connolly D, Barron L, Paul B (2002) Determination of urinary thiocyanate and nitrate using fast ion-interaction chromatography. *J Chromatogr B, An Technol Biomed Sci* 767(1):175–180

APPENDIX V

Journal of Chromatography B, 934 (2013) 60–65



Contents lists available at SciVerse ScienceDirect

Journal of Chromatography B

journal homepage: www.elsevier.com/locate/chromb



Quantification of α -ketoglutarate cyanohydrin in swine plasma by ultra-high performance liquid chromatography tandem mass spectrometry



Brendan L. Mitchell^a, Gary A. Rockwood^b, Brian A. Logue^{a,*}

^a Department of Chemistry and Biochemistry, South Dakota State University, Brookings, SD 57007, USA

^b Analytical Toxicology Division, US Army Medical Research Institute of Chemical Defense, Aberdeen Proving Ground, MD 21010, USA

ARTICLE INFO

Article history:

Received 5 February 2013

Received in revised form 17 June 2013

Accepted 27 June 2013

Available online xxx

Keywords:

α -Ketoglutarate cyanohydrin

Liquid chromatography tandem

mass spectrometry

Cyanide

Method development

Biomarkers

ABSTRACT

Determination of exposure to cyanide can be accomplished by direct cyanide analysis or indirectly by analysis of cyanide detoxification products, such as thiocyanate and 2-amino-2-thiazoline-4-carboxylic acid. A potentially important marker and detoxification product of cyanide exposure, α -ketoglutarate cyanohydrin (α -KgCN), is produced by the reaction of cyanide and α -ketoglutarate. Therefore, an ultra high-performance liquid chromatography tandem mass spectrometry method to determine α -KgCN in plasma was developed. Swine plasma was spiked with α -KgCN and α -KgCN- d_4 (internal standard) and proteins were precipitated with 1% formic acid in acetonitrile. After centrifugation, the supernatant was dried, reconstituted, separated by reversed phase high performance liquid chromatography and analyzed by tandem mass spectrometry. The method produced a dynamic range of 0.3–50 μ M and a detection limit of 200 nM for α -KgCN. Furthermore, the method produced a %RSD of less than 13% for all intra- and inter-assay analyses. The stability of α -KgCN was poor for most storage conditions tested, except for -80°C , which produced stable concentrations of α -KgCN for the 30 days tested. The validated method was tested by analysis of α -KgCN in the plasma of cyanide-exposed swine. α -KgCN was not detected pre-exposure, but was detected in all post-exposure plasma samples tested. To our knowledge, this method is the first reported analytical method for detecting α -KgCN in any matrix.

© 2013 Elsevier B.V. All rights reserved.

1. Introduction

Cyanide exposure can occur in a variety of ways, including accidental, suicidal, or homicidal. General population exposure can occur through smoke inhalation from cigarettes or fires, consuming cyanogenic glycosides found in foods, and working in industrial facilities that use cyanide [1]. Furthermore, cyanide exposure can also occur by the use of cyanide as a chemical warfare agent [2]. Once in the body, the toxicity of cyanide stems from its ability to inhibit cytochrome c oxidase, thereby disrupting oxygen transport to mitochondria [3]. Therefore, the confirmation of cyanide exposure is important to administer treatment in a timely fashion and monitor health conditions after exposure. The direct analysis of cyanide to confirm exposure has serious limitations, due to cyanide's volatility, reactivity, and short half-life in biological fluids [4–6]. Cyanide exists as both hydrogen cyanide (HCN) and the cyanide ion (CN^-) which are in rapid equilibrium with each

other. Under normal biological conditions, cyanide exists mainly as HCN, which is extremely volatile and rapidly eliminated from biological matrices [4]. If cyanide exists as CN^- , it is nucleophilic and will rapidly react with various species in biological matrices, thereby eliminating free cyanide from the sample [7]. These limitations have led to the exploration of biomarker analysis for indirect determination of cyanide exposure.

Indirect analysis of cyanide has mainly focused around thiocyanate and 2-amino-2-thiazoline-4-carboxylic acid (ATCA), the major products of cyanide detoxification. Thiocyanate has shown promise as a marker of cyanide exposure and various methods exist for the analysis of thiocyanate in biological fluids [6]. However, disadvantages of thiocyanate analysis for cyanide exposure have been reported. Ballantyne reported that thiocyanate concentrations fluctuated during various sample storage conditions and recovery of thiocyanate from whole blood was low [8]. Furthermore, thiocyanate can be formed from metabolism of other compounds besides cyanide [9]. ATCA has also shown promise as an alternative marker of cyanide exposure and a few methods have been developed for the analysis of ATCA in biological fluids [7,10–12]. Although there is limited information on its relevance as a biomarker for cyanide exposure, Petrikovics et al. suggested that

* Corresponding author at: SDSU, Box 2202, Brookings, SD 57007, USA.
Tel.: +1 605 688 6698; fax: +1 605 688 6364.
E-mail address: brian.logue@sdstate.edu (B.A. Logue).

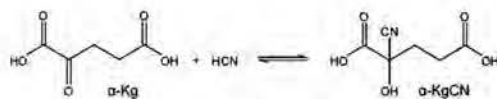


Fig. 1. Proposed reaction pathway for the conversion of α -Kg into α -KgCN.

plasma ATCA might not be a good biomarker for cyanide exposure based on a toxicokinetic study in rats [13]. Conversely, ATCA has been suggested as an advantageous marker of long-term low-level cyanide exposure [7,10–12]. Other markers of cyanide exposure include cyanide-protein adducts [3,14,15] and cyanocobalamin [16–18]. Cyanide-protein adducts may serve as excellent long-term markers of cyanide exposure, but the utility of this marker for rapid analysis has not been assessed, and the synthesis of the standards for this technique can be costly and demanding [19]. Although cyanocobalamin is a potential marker, hydroxocobalamin, which sequesters cyanide to form cyanocobalamin, is a treatment for cyanide exposure [20–22]. Therefore, the use of hydroxocobalamin as a treatment would convolute the use of cyanocobalamin as a biomarker. Furthermore, detection of cyanocobalamin for cyanide exposure is limited due to photodegradation [23,24]. Considering the limitations concerning current biomarkers of cyanide exposure, novel markers should be considered.

Cyanide is known to react with carbonyl compounds to form cyanohydrins [25]. In biological systems, cyanide is converted to α -ketoglutarate cyanohydrin (α -KgCN) through an equilibrium reaction with α -ketoglutarate (α -Kg) (Fig. 1) [6]. Because α -Kg resides in the plasma [26], the ability to determine concentrations of α -KgCN may allow for verification of cyanide exposure. Therefore, the objective of this project was to develop an analytical method to determine cyanide exposure by detection of α -KgCN in plasma. Because oral dosing of α -Kg has been shown to mitigate the toxicity of cyanide exposure [25,27–30], this method should also be beneficial in aiding studies of α -Kg as a therapeutic treatment for CN⁻ poisoning.

2. Experimental

2.1. Reagents and materials

All reagents were at least HPLC grade. Sodium cyanide (NaCN) and all solvents were purchased from Fisher Scientific (Fair Lawn, NJ, USA). α -Kg and α -ketoglutarate acid- d_6 (α -Kg- d_6) were purchased from Sigma-Aldrich (St. Louis, MO, USA). LC/MS grade formic acid was purchased from Thermo Scientific (Rockford, IL, USA). Swine (*Sus scrofa*) plasma (non-sterile with sodium citrate anti-coagulant) was acquired from the Veterinary Science Department at South Dakota State University. Cyanide-exposed swine plasma was received from Wilford Hall Medical Center (Lackland Air Force Base, TX). One animal (about 50 kg) was sedated, endotracheally intubated, and maintained under anesthesia with inhaled isoflurane. After acclimation, KCN (4 mg/mL) was infused intravenously (0.17 mg/kg/min) until apnea. Arterial blood was sampled at baseline, 5 min into cyanide infusion, at apnea, every 2 min after apnea for 10 min, and then every 10 min for 60 min. Whole blood (20 mL) was withdrawn from the animal at each time point. The blood (4 mL) was then placed into EDTA tubes and centrifuged to separate the plasma from the red blood cells, resulting in a final plasma volume of 1 mL for each sample. The plasma was shipped overnight on dry ice to South Dakota State University, where it was immediately frozen upon arrival and stored at -80 °C until needed.

2.2. Synthesis of α -KgCN and α -KgCN- d_4

α -KgCN was synthesized according to an adapted procedure of Green and Williamson [31], by first adding α -Kg and an equimolar amount of NaCN to water and stirring at room temperature for 30 min. The resulting solution was filtered and the solvent was removed by rotary evaporation to afford a white, sticky product. Characterization was achieved by 13 C NMR, along with ESI-MS operated in negative polarity mode. 13 C NMR (CD_3OD , 400 MHz): δ 178, 120, 70. ESI(-)-MS: m/z 172.0, 144.7, 101.0, 44.8. An isotopically-labeled internal standard, α -KgCN- d_4 was synthesized and characterized as described above for α -KgCN, with α -Kg- d_6 replacing α -Kg. 13 C NMR (CD_3OD , 400 MHz): δ 178, 172, 122, 73. ESI(-)-MS: m/z 176.1, 149.1, 105.1, 44.8. The characterization of α -KgCN and α -KgCN- d_4 by 13 C NMR did not show the presence of α -Kg. Furthermore, Green and Williamson [31] reported that no free acid (α -Kg) was evident in their final product.

2.3. Sample preparation

Swine plasma (100 μ L) was spiked with internal standard (IS), α -KgCN- d_4 (20 μ L of 100 μ M), and 1% formic acid in acetonitrile (400 μ L) to initiate protein precipitation. The resulting solution (pH of approximately 2), was then vortexed for 5 min and centrifuged for 15 min at 16,000 \times g (13,100 rpm, room temperature). After centrifugation, an aliquot of the supernatant was transferred to a 4 mL screw-top vial and dried under N_2 (g) for 20 min at room temperature (Reacti-vap III, Pierce, Rockford, IL, USA). The volume of supernatant transferred was evaluated at 100, 300, and 400 μ L, with 300 μ L producing the optimum LC conditions in terms of peak symmetry and band broadening. After drying, the sample was reconstituted with formic acid (10 μ L of 10 M) and water (300 μ L) and was syringe-filtered (Teflon, 0.22 μ m) to remove particulates. The volume of water for reconstitution was optimized at 300 μ L, based on peak symmetry and band broadening. After filtration, an aliquot (100 μ L) of the filtrate was transferred to a glass insert (150 μ L) which was placed in a screw-top autosampler vial (2 mL) and analyzed by ultra-high performance liquid chromatography tandem mass spectrometry (UHPLC-MS-MS).

2.4. Analysis of α -KgCN

Analysis of α -KgCN was conducted by UHPLC-MS-MS on a Shimadzu UHPLC (LC-20AD, Shimadzu Corp., Kyoto, JPN) and an AB Sciex Q-trap 5500 MS (Applied Biosystems, Foster City, CA, USA). Samples were separated by reversed-phase (RP) chromatography using a Phenomenex Synergi 2.5 μ Fusion-RP 100 A column (2.00 \times 50 mm) (Phenomenex, Torrance, CA, USA). Mobile phases consisted of 1% formic acid in H_2O (mobile phase A, pH 2.1) and 1% formic acid in MeOH (mobile phase B). An aliquot (10 μ L) of the sample was separated by gradient flow at 40 °C with a flow rate of 0.15 mL/min. The concentration of B was increased from 0% to 100% over 2 min, held at 100% for 1 min, and then ramped back down to 0% over 1 min and held constant for 2 min to re-equilibrate the column between samples. Detection of α -KgCN was achieved using electrospray ionization (ESI)-MS-MS operating in negative polarity. N_2 (50 psi) was used as the curtain gas. The ion source was operated at -4500 V and a temperature of 750 °C with a flow rate of 90.0 psi for both the nebulizer (GS1) and heater (GS2) gasses. The collision cell was operated with an entrance potential of -10.0 V and a collision potential of -11.0 V at a medium collision gas (N_2) flow rate. α -KgCN and α -KgCN- d_4 were analyzed in the MS by multiple reaction monitoring (MRM) with the parameters outlined in Table 1.

Table 1
Selected MRM transitions, optimized declustering potentials (DPs) and collision energies (CEs) for the detection of α -KgcCN and α -KgcCN- d_4 by MS–MS analysis.

Compounds	Q1 Mass (m/z)	Q3 Mass (m/z)	Time (min)	DP (V)	CE (V)
α -KgcCN (quantitation)	172.0	145.1	40.0	–26.47	–11.53
α -KgcCN (identification)	172.0	57.0	40.0	–32.85	–24.82
α -KgcCN- d_4 (quantitation)	176.1	149.0	40.0	–26.92	–13.28
α -KgcCN- d_4 (identification)	176.1	61.2	40.0	–31.76	–29.00

2.5. Calibration and quantification

α -KgcCN spiked swine plasma calibration standards (0.2, 0.3, 0.5, 1, 3, 5, 10, 30, 50, 100, and 300 μ M) were prepared and analyzed to evaluate the linear range. Quality control (QC) standards at low, medium, and high concentrations (0.75, 4, and 20 μ M) were used to determine the inter- and intra-assay accuracy and precision. The intra-assay accuracy and precision were determined over 1 day with quintuplicate analysis of each QC standard, and inter-assay accuracy and precision were evaluated over 3 days (within a 9 calendar day period) with quintuplicate analysis of the QC standards each day.

2.6. Stability and recovery

The stability of α -KgcCN in swine plasma was assessed at each storage condition using low (0.75 μ M) and high (20 μ M) QC standards (each in triplicate). Short-term stability experiments were evaluated for the stability of α -KgcCN in the autosampler (prepared samples), on the bench-top, and over multiple freeze–thaw cycles. For autosampler stability, QC standards were prepared, placed in an autosampler at 15 °C, and analyzed at 0, 2, 4, 8, 12 and 24 h. For bench-top stability, the QC standards were allowed to stand at room temperature for 0, 2, 4, 8, 12 and 24 h prior to analysis. Freeze–thaw stability was conducted over three cycles after the QC standards were initially analyzed (cycle 0). Each cycle consisted of storage at –80 °C for 24 h, thawing the standards unassisted at room temperature, preparing and analyzing the applicable QC standards, and refreezing the remaining (non-analyzed) standards. This protocol was continued until three cycles had elapsed. Long-term stability experiments were also conducted under various storage conditions (–80, –20 and 4 °C) for various times (0, 1, 2, 5, 12, 20, and 30 days). Low and high QC standards were prepared and stored at the desired temperature until analyzed.

Recovery experiments were conducted in order to determine the ability of the sample preparation protocol to extract α -KgcCN from swine plasma. Swine plasma was spiked with α -KgcCN at low, medium, and high QC concentrations and compared to aqueous α -KgcCN samples at the same nominal concentrations. The recovery was calculated as a percentage by dividing the concentration of the low, medium, and high QC standards in plasma ($n = 5$ for each) against the same concentration of aqueous α -KgcCN ($n = 5$ for each).

2.7. Data analysis

Calibration curves were developed by plotting the ratio of the MRM (172.0–145.1 m/z) peak area for the analyte (α -KgcCN) and the MRM (176.1–149.0 m/z) peak area for the internal standard (α -KgcCN- d_4) as a function of the α -KgcCN concentration (μ M) in plasma. Both weighted ($1/x$ and $1/x^2$) and unweighted calibration curves were prepared by least squares and a weighted ($1/x^2$) linear fit was found to best fit the calibration data as determined by the inspection of residual plots. The limit-of-detection (LOD) was determined at a signal-to-noise ratio of 3 over 3 separate days of analysis ($n = 5$ for each day) with baseline noise calculated as peak-to-peak noise directly adjacent to the α -KgcCN peak.

Precision was calculated as a percent relative standard deviation (%RSD) by dividing the standard deviation by the mean for each calibrator and QC standard. Accuracy (%) was determined by dividing the calculated concentration by the nominal concentration for each calibrator and QC standard. A %RSD of less than 15% and a percent accuracy of $100 \pm 20\%$ were used as criteria for inclusion of calibration standards and determination of the ULOQ and LLOQ. Stability was calculated as a percentage by dividing the concentration of the QC standard (low or high) from each time point (days or hours) by the concentration of the QC standard at time zero (the control). The α -KgcCN was considered stable under a particular storage condition if this ratio was $\geq 85\%$.

3. Results and discussion

3.1. Analysis of α -KgcCN from swine plasma

The mass spectra of α -KgcCN and α -KgcCN- d_4 produced by ESI(–)–MS are shown in Fig. 2. Fig. 2A shows the mass spectrum of α -KgcCN with the ions important for the analysis of α -KgcCN identified. The m/z ratio of 172.0 corresponds to the molecular ion of α -KgcCN with the loss of a proton ($[M-H]^-$). The m/z ratio of 144.7 corresponds to the molecular ion of the precursor, α -Kgc, minus a proton. The m/z ratio of 101.0 corresponds to the loss of a carboxyl group from α -Kgc. The m/z ratio of 44.8 is a common fragment for a carboxyl group. ESI(–)–MS was also conducted on α -KgcCN- d_4 and its mass spectrum is shown in Fig. 2B. α -KgcCN- d_4 showed similar fragmentation compared with α -KgcCN with the exception of a mass difference of +4 m/z for each major fragment, besides m/z 44.8, because of the replacement of 4 hydrogen atoms with deuterium atoms in the labeled compound.

Fig. 3 shows representative chromatograms of α -KgcCN spiked swine plasma and cyanide-exposed swine plasma (pre- and post-exposure). The α -KgcCN elutes at approximately 1.6 min with some degree of tailing, which is most likely caused by the interaction of exposed silica support with α -KgcCN. The tailing did not interfere with quantification of α -KgcCN. Furthermore, the method shows excellent selectivity for α -KgcCN as shown by the absence of co-eluting peaks in the pre-exposure swine plasma chromatogram. In fact, no other peaks are seen in the pre-exposure swine plasma chromatogram.

3.2. Linear dynamic range

Standard curves were generated in the range of 0.2–300 μ M α -KgcCN in swine plasma. Calibration standards at 0.2, 100, and 300 μ M were found to be outside the LLOQ or ULOQ, resulting in a linear dynamic range from 0.3 to 50 μ M as described by a weighted ($1/x^2$) curve validated over 3 separate days of analysis (within 9 calendar days). Therefore, the dynamic range of α -KgcCN in swine plasma is over 2 orders of magnitude. The LOD was found to be 200 nM α -KgcCN in swine plasma validated over a 7-day period with 3 separate days of analysis ($n = 7$ for each day).

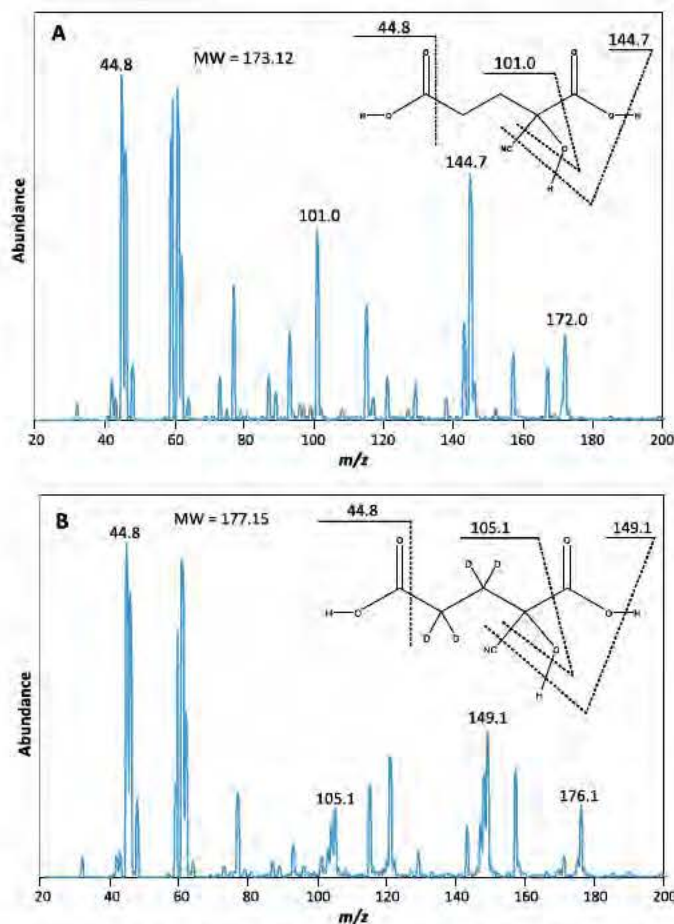


Fig. 2. ESI(-) mass spectra of α -KgCN (A) and α -KgCN- d_4 (B) with identification of the abundant ions (A) The α -KgCN ion at 172.0 m/z corresponds to $[M-H]^-$ and the ion at 144.7 m/z corresponds to $[\alpha\text{-Kg-H}]^-$, the precursor to α -KgCN. (B) The α -KgCN d_4 ion at 176.1 m/z corresponds to $[M-H]^-$ and the ion at 149.1 m/z corresponds to $[\alpha\text{-Kg-}d_4\text{-H}]^-$. Insets: Structures of α -KgCN (A) and α -KgCN- d_4 (B) with abundant fragments indicated.

3.3. Accuracy and precision

The intra- and inter-assay accuracy and precision were evaluated for low, medium, and high QC standards over 3 days of analysis (Table 2). The method produced good accuracy and precision for the concentrations tested, with intra-assay precision $\leq 11\%$ and inter-assay precision $\leq 13\%$ for all QC standards, and accuracy within $\pm 10\%$ of the nominal QC concentration. The accuracy and precision of analytical methods are typically considered acceptable if the %RSD (precision) is less than 15% and the percent accuracy of back-calculated concentrations is between 80% and 120% as compared to the nominal concentration.

3.4. Stability and recovery

The short-term stability of α -KgCN in swine plasma was evaluated on the bench-top and in the autosampler over 24 h. Prepared

samples of α -KgCN exhibited excellent stability in the autosampler, with no more than 15% deviation from the control. Furthermore, freeze-thaw experiments showed that α -KgCN was stable in swine plasma at -80°C over the 3 cycles tested. Conversely, the bench-top stability of α -KgCN was poor with α -KgCN concentrations falling significantly below 85% of the control within 2 h, showing that α -KgCN is quickly eliminated from swine plasma at room temperature.

The long-term stability of α -KgCN was evaluated for 30 days at -80 , -20 and 4°C . The α -KgCN was stable for 30 days at -80°C , for 1 day at -20°C , and was quickly eliminated at 4°C , for both low and high QC concentrations. The results of the long-term study suggest that α -KgCN spiked swine plasma samples should be stored at -80°C when possible. If samples need to be stored at -20°C , they should be analyzed as soon as possible. Storage at $> -20^\circ\text{C}$ is not recommended for plasma samples.

Table 2
The accuracy and precision of α -K_gCN in swine plasma by UHPLC-MS-MS.

Nominal concentration (μ M)	Intra-assay accuracy (%) ^a	Inter-assay accuracy (%) ^b	Intra-assay precision (XRSD) ^a	Inter-assay precision (XRSD) ^b
0.75	100	97	11	8.9
4	110	104	11	13
20	107	104	5.0	8.4

^a Mean for 1 day of validation ($n=5$).

^b Mean for 3 days of validation ($n=15$).

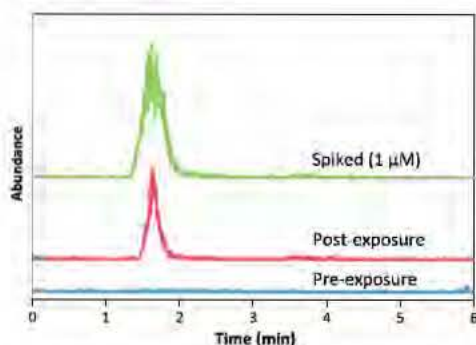


Fig. 3. Chromatograms of α -K_gCN spiked swine plasma (upper trace) and the plasma of cyanide-exposed swine, pre-exposure (lower trace) and post-exposure (middle trace). The chromatograms represent the signal response of the MRM transition 172.0→145.1 m/z .

The recovery of α -K_gCN from swine plasma at low, medium, and high QC concentrations was 14%, 22%, and 27%, respectively. Acidification of the swine plasma before spiking in α -K_gCN, did not significantly increase the recovery (25%, 23%, and 30% for low, medium and high QC standards, respectively). Heating the swine plasma to precipitate proteins and cooling back to room temperature before spiking in α -K_gCN actually decreased the recovery (7%, 4%, and 4% for low, medium, and high QC standards, respectively). Because enzyme activity should at least be reduced when heating and acidifying the plasma, the consistently low recovery is most likely due to facile equilibrium between α -K_g and α -K_gCN. Consequently, cyanide may undergo various side reactions that remove it from the swine plasma such as protein binding [3,14], ATCA formation [7,32], or evaporation of HCN [4,33]. Further experiments will be considered to address these concerns. A potential avenue for future research in this area would be to compare α -K_gCN spiked aqueous and plasma samples by mass spectral analysis to elucidate reactions involving α -K_gCN.

3.5. The analysis of cyanide-exposed swine plasma

The described method was applied to the analysis of α -K_gCN in plasma samples obtained from cyanide-exposed swine. Fig. 3 shows representative chromatograms of plasma collected from swine before and after cyanide exposure. The peak for α -K_gCN observed around 1.6 min and the absence of co-eluting peaks in the pre-exposed swine sample indicate that the analysis is selective for α -K_gCN. Overall, the results indicate that the analytical method presented can be used to quickly and easily analyze α -K_gCN in the plasma of cyanide-exposed swine.

3.6. α -K_gCN as a marker of cyanide exposure

The suggested use of α -K_gCN as a cyanide biomarker was confirmed with the observation of α -K_gCN in the plasma of

cyanide-exposed swine after exposure (Fig. 3). The major advantage of using α -K_gCN as a biomarker is that it was not detected endogenously in the plasma. The disadvantages of using α -K_gCN as a cyanide marker are poor recovery and limited stability in plasma. Although the stability of α -K_gCN was poor under most conditions, it was shown to be stable for at least 30 days at -80°C , which is significantly better than cyanide and thiocyanate in plasma (found to be stable for 2 and 5 days, respectively [34]) but worse than ATCA (found to be stable for at least 3 months under a variety of storage conditions [7]). Further studies on the toxicokinetic behavior of α -K_gCN were undertaken in order to further evaluate its use as a marker of cyanide poisoning [35].

4. Conclusions

An analytical method for the determination of α -K_gCN, a potential alternative marker of cyanide exposure, was created and validated. This method shows the ability to detect α -K_gCN in swine plasma at low concentrations, as indicated by an LOD of 200 nM. Furthermore, α -K_gCN can be quantified accurately and precisely in swine plasma, at sub- μ M concentrations. The method allows α -K_gCN to serve as a biological marker for cyanide exposure and should aid in studies of therapeutic treatment of cyanide exposure with α -K_g. Future work will include the application of the method to analyze α -K_gCN from the plasma of cyanide-exposed swine and investigations pertaining to the low recovery of α -K_gCN from swine plasma. To our knowledge, the method developed here is the first reported analytical method for detecting the cyanide detoxification product, α -K_gCN, in any matrix.

Acknowledgements

The research was supported by the CounterACT Program, National Institutes of Health Office of the Director, and the National Institute of Allergy and Infectious Diseases, Inter-agency Agreement Numbers Y1-OD-0690-01/A-120-B.P2010-01, Y1-OD-1561-01/A120-B.P2011-01, AOD12060-001-00000/A120-B.P2012-01 and the USAMRICD under the auspices of the US Army Research Office of Scientific Services Program Contract No. W911NF-11-D-0001 administered by Battelle (Delivery order 0079, Contract No. TCN 11077). We gratefully acknowledge the funding from the Oak Ridge Institute for Science and Education (ORISE) and the support from a U.S. Dept. of Education, Graduate Assistance in Areas of National Need (GAANN), award to the Department of Chemistry & Biochemistry (P200A100103). We thank the National Science Foundation Major Research Instrumentation Program (Grant Number CHE-0922816), the state of South Dakota, and South Dakota State University for funding the AB SCIEX QTRAP 5500 LC/MS/MS. The authors would like to acknowledge Dr. George Perry, Animal and Range Science (South Dakota State University) for providing swine plasma. Furthermore, the authors are thankful to Dr. Vikhyat Bebartha, Susan M. Boudreau, RN, BSN, Maria G. Castaneda, MS, Toni E. Vargas, PA-C, MHS, and Patricia Dixon, MHS from the Clinical Research Division, Wilford Hall Medical Center (Lackland Air Force Base, San Antonio, TX) for providing potassium cyanide-exposed swine plasma. The opinions or assertions

contained herein are the private views of the authors and are not to be construed as official or as reflecting the views of the Department of the Army, the National Institutes of Health, the National Science Foundation or the Department of Defense.

References

- [1] F.P. Simeonova, L. Fishbein, *Concise Int. Chem. Assess. Doc.* 61 (2004) 1.
- [2] L. Szinicz, *Toxicology* 214 (2005) 167.
- [3] M.J. Pasco, C.R. Hauer, R.F. Stack, C. O'Hehir, J.R. Barr, G.A. Eadon, *Chem. Res. Toxicol.* 20 (2007) 677.
- [4] S.I. Baskin, J.B. Kelly, B.I. Maliner, G.A. Rockwood, C.K. Zoltani, in: S.I. Baskin, T. Brewer, F. Sidell, E. Takafuji, D. Franz (Eds.), *Textbook of Military Medicine, Medical Aspects of Chemical and Biological Warfare*, Borden Institute, Fort Detrick, 1997, p. 271.
- [5] P. Lindquist, H. Rosling, B. Sorbo, L. Tibblin, *Clin. Chem.* 33 (1987) 1228.
- [6] S.J.S. Flora, J.A. Romano, S.I. Baskin, K. Sekhar (Eds.), *Pharmacological Perspectives of Toxic Chemicals and Their Antidotes*, Springer, 2004, p. 484.
- [7] B.A. Logue, N.P. Kirschten, I. Petrikovics, M.A. Moser, G.A. Rockwood, S.I. Baskin, *J. Chromatogr.* 819 (2005) 237.
- [8] B. Ballantyne, *Clin. Toxicol.* 11 (1977) 195.
- [9] S. Murray, B.G. Lake, S. Gray, A.J. Edwards, C. Springall, E.A. Bowey, G. Williamson, A.R. Boobis, N.J. Gooderha, *Carcinogenesis* 22 (2001) 1413.
- [10] B.A. Logue, W.K. Maserek, G.A. Rockwood, M.W. Keebaugh, S.I. Baskin, *Toxicol. Mech. Methods* 19 (2009) 202.
- [11] C.V. Vinnakota, N.S. Peetha, M.G. Perrizo, D.G. Ferris, R.P. Oda, G.A. Rockwood, B.A. Logue, *Biomarkers* 17 (2012) 625.
- [12] J.C.C. Yu, S. Martin, J. Nasr, K. Stafford, D. Thompson, I. Petrikovics, *World J. Methodol.* 2 (2012) 33.
- [13] I. Petrikovics, D.E. Thompson, G.A. Rockwood, B.A. Logue, S. Martin, P. Jayanna, J.C. Yu, *Biomarkers* 16 (2011) 686.
- [14] S.I. Youso, G.A. Rockwood, J.P. Lee, B.A. Logue, *Anal. Chim. Acta* 677 (2010) 24.
- [15] S.I. Youso, G.A. Rockwood, B.A. Logue, *J. Anal. Toxicol.* 36 (2012) 265.
- [16] A. Astier, F.J. Baud, *J. Chromatogr.* 667 (1995) 129.
- [17] P.F. Chatzimisichelakidis, V.F. Samanidou, R. Verpoorte, I.N. Papadoyannis, *J. Sep. Sci.* 27 (2004) 1181.
- [18] W. Butte, H.H. Riemann, A.J. Walle, *Clin. Chem.* 28 (1982) 1778.
- [19] R.M. Black, D. Noort, in: T.T. Marrs, R.L. Maynard, F. Sidell (Eds.), *Chemical Warfare Agents: Toxicology and Treatment*, Wiley and Sons, West Sussex, England, 2007, p. 127.
- [20] P. Houeto, J.R. Hoffman, M. Imbert, P. Levillain, F.J. Baud, *Lancet* 346 (1995) 605.
- [21] A.H. Hall, R. Dart, C. Bogdan, *Ann. Emerg. Med.* 49 (2007) 806.
- [22] S.W. Borron, M. Stonerook, F. Reid, *Clin. Toxicol.* 44 (2006) 3.
- [23] O. Karim, A. Zayed, S. Baraghetli, M. Qadi, R. Ghanem, *IOAB J.* 2 (2011) 23.
- [24] I. Ahmad, W. Hussain, *Pak. J. Pharm. Sci.* 6 (1993) 23.
- [25] J.C. Norris, W.A. Udey, A.S. Hume, *Toxicology* 62 (1990) 275.
- [26] B.M. Wagner, F. Donnerumma, R. Winterteiger, W. Windischhofer, H. Leis, *J. Anal. Bioanal. Chem.* 396 (2010) 2629.
- [27] R. Bhattacharya, P.V.L. Rao, R. Vijayaraghavan, *Toxicol. Lett.* 128 (2002) 185.
- [28] R. Bhattacharya, R. Vijayaraghavan, *Hum. Exp. Toxicol.* 21 (2002) 297.
- [29] R. Bhattacharya, R. Vijayaraghavan, *Biomed. Environ. Sci.* 4 (1991) 452.
- [30] S.J. Moore, J.C. Norris, I.K. Ho, A.S. Hume, *Toxicol. Appl. Pharmacol.* 82 (1986) 40.
- [31] D.E. Green, S. Williamson, *Biochem. J.* 31 (1937) 617.
- [32] H.T. Nagasawa, S.E. Cummings, S.I. Baskin, *Org. Prep. Proced. Int.* 36 (2004) 178.
- [33] F. Moriya, Y.J. Hashimoto, *J. Forensic Sci.* 46 (2001) 1421.
- [34] R.K. Bhandari, R.P. Oda, S.I. Youso, I. Petrikovics, V.S. Bebarata, G.A. Rockwood, B.A. Logue, *Anal. Bioanal. Chem.* 404 (2012) 2287.
- [35] B.L. Mitchell, R.K. Bhandari, V.S. Bebarata, G.A. Rockwood, G.R. Boss, B.A. Logue, *Toxicol. Lett.* (2013), <http://dx.doi.org/10.1016/j.toxlet.2013.07.008>, in press.

APPENDIX VI

Toxicology Letters 222 (2013) 83–89



Contents lists available at ScienceDirect

Toxicology Letters

journal homepage: www.elsevier.com/locate/toxlet



Toxicokinetic profiles of α -ketoglutarate cyanohydrin, a cyanide detoxification product, following exposure to potassium cyanide



Brendan L. Mitchell^a, Raj K. Bhandari^a, Vikhyat S. Bebart^b, Gary A. Rockwood^c,
Gerry R. Boss^d, Brian A. Logue^{a,*}

^a Department of Chemistry and Biochemistry, South Dakota State University, Brookings, SD 57007, USA

^b Medical Toxicology, San Antonio Military Medical Center, San Antonio, TX 78234, USA

^c Analytical Toxicology Division, US Army Medical Research Institute of Chemical Defense, Aberdeen Proving Ground, MD 21010, USA

^d Department of Medicine, University of California, San Diego, La Jolla, CA 92093-0652, USA

HIGHLIGHTS

- The toxicokinetic behavior of α -KgCN in swine was investigated.
- Measuring plasma α -KgCN provides definitive confirmation of cyanide exposure.
- Treatment of cyanide poisoning with cobinamide renders α -KgCN an ineffective diagnostic marker.

ARTICLE INFO

Article history:

Received 6 May 2013

Received in revised form 5 July 2013

Accepted 7 July 2013

Available online xxx

Keywords:

Cyanide exposure

α -Ketoglutarate cyanohydrin

Toxicokinetics

α -Ketoglutarate

ABSTRACT

Poisoning by cyanide can be verified by analysis of the cyanide detoxification product, α -ketoglutarate cyanohydrin (α -KgCN), which is produced from the reaction of cyanide and endogenous α -ketoglutarate. Although α -KgCN can potentially be used to verify cyanide exposure, limited toxicokinetic data in cyanide-poisoned animals are available. We, therefore, studied the toxicokinetics of α -KgCN and compared its behavior to other cyanide metabolites, thiocyanate and 2-amino-2-thiazoline-4-carboxylic acid (ATCA), in the plasma of 31 Yorkshire pigs that received KCN (4 mg/mL) intravenously (IV) (0.17 mg/kg/min). α -KgCN concentrations rose rapidly during KCN administration until the onset of apnea, and then decreased over time in all groups with a half-life of 15 min. The maximum concentrations of α -KgCN and cyanide were 2.35 and 30.18 μ M, respectively, suggesting that only a small fraction of the administered cyanide is converted to α -KgCN. Although this is the case, the α -KgCN concentration increased >100-fold over endogenous concentrations compared to only a three-fold increase for cyanide and ATCA. The plasma profile of α -KgCN was similar to that of cyanide, ATCA, and thiocyanate. The results of this study suggest that the use of α -KgCN as a biomarker for cyanide exposure is best suited immediately following exposure for instances of acute, high-dose cyanide poisoning.

© 2013 Elsevier Ireland Ltd. All rights reserved.

1. Introduction

Cyanide can be found in food (Vetter, 2000), smoke from fires (Becker, 1985; Brenner et al., 2010a; Purser et al., 1984), and cigarettes (Xu et al., 2011, 2012), and industrial facilities (Ma and Dasgupta, 2010; Smith et al., 2010; Zdrojewicz et al., 1996). It is easily procured and could be used as a weapon of mass destruction (Viswanath and Ghosh, 2010). Human exposure to cyanide

produces toxic effects by binding to the iron and copper in the active site of cytochrome c oxidase, thereby inhibiting the enzyme (Baskin et al., 2004). Depending on the dose, this can result in histotoxic anoxia (Baskin et al., 2004), cellular hypoxia (Conn, 1978), respiratory failure (Conn, 1978; Fasco et al., 2007; Way, 1984), and eventual death. Because cyanide is a rapidly acting poison, and cyanide exposure is relevant to both the military and public sectors, toxicokinetic information on cyanide and its detoxification products is important for understanding the behavior of cyanide following exposure. Cyanide can be metabolized and detoxified through a number of routes, including those outlined in Fig. 1. The two major routes of cyanide detoxification are conversion to thiocyanate in the presence of a sulfur donor (Ansell and Lewis, 1970; Baskin et al., 2004) and production of 2-amino-2-thiazoline-4-carboxylic acid (ATCA) from reaction with cystine (Ansell and

Abbreviations: α -KgCN, α -ketoglutarate cyanohydrin; α -Kg, α -ketoglutarate.

* Corresponding author at: Department of Chemistry and Biochemistry, South Dakota State University, Box 2202, Brookings, SD 57007, USA. Tel.: +1 605 688 6698; fax: +1 605 688 6364.

E-mail address: brian.logue@sdstate.edu (B.A. Logue).

0378-4274/\$ – see front matter © 2013 Elsevier Ireland Ltd. All rights reserved.
<http://dx.doi.org/10.1016/j.toxlet.2013.07.008>

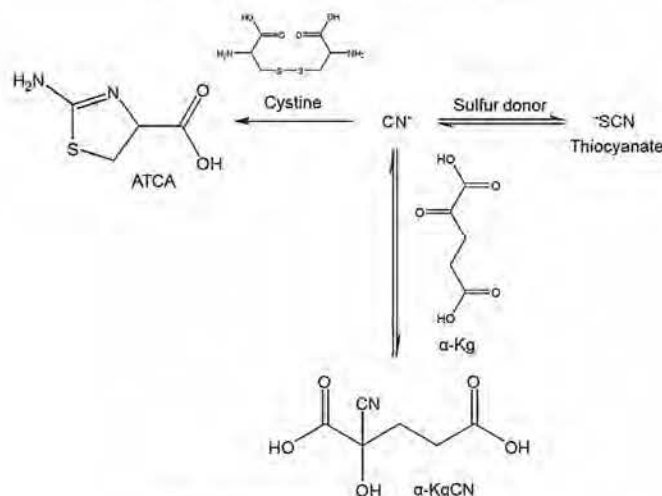


Fig. 1. Cyanide metabolism and detoxification pathways.

Lewis, 1970; Nagasawa et al., 2004). As an alternative detoxification pathway, cyanide can react with endogenous α -ketoglutarate (α -Kg) to form α -ketoglutarate cyanohydrin (α -KgCN) (Baskin et al., 2004; Baskin and Brewer, 1997) in animals. This detoxification pathway is likely important when the thiocyanate and ATCA pathways are overwhelmed, and will be investigated in this study.

Evaluation of the toxicokinetic behavior of cyanide and its breakdown products provides insight into the best marker for verification of cyanide exposure. Such studies have been conducted for cyanide (Dirikolu et al., 2003; Leuschner et al., 1991; Sousa et al., 2003) and its major detoxification products, thiocyanate (Leuschner et al., 1991; Sousa et al., 2003) and ATCA (Petrikovics et al., 2012), in various animal models. The results of these studies are presented in Table 1. Leuschner et al. (1991) investigated the toxicokinetics of cyanide in rats following acute potassium cyanide exposure by gavage at 1.0 mg KCN/kg body weight. The time of peak concentration (T_{max}), 2 min, suggests that cyanide is rapidly distributed with this mode of exposure. Leuschner et al. (1991) also performed a chronic cyanide exposure study over a 13-week period. In that study, the blood cyanide concentrations ranged from 16.0 to 25.5 μ M and the thiocyanate plasma concentrations ranged from 341 to 877 μ M for rats given KCN at 160 mg/kg body weight per day in drinking water. The results of the 13-week study suggested that

chronic cyanide exposure at the dose used does not lead to saturation of cyanide detoxification pathways (Leuschner et al., 1991). Sousa et al. (2003) evaluated the toxicokinetics of blood cyanide and plasma thiocyanate in rats and pigs following oral potassium cyanide exposure at 3.0 mg KCN/kg body weight; over a 24 h period, blood cyanide concentrations ranged from 0.5 to 89.0 μ M and 1.0 to 57.5 μ M, and thiocyanate plasma concentrations ranged from 19.0 to 58.1 μ M and 18.0 to 42.8 μ M, in rats and pigs respectively. The results of this study suggest that about 65–75% of absorbed cyanide is converted to thiocyanate, which is in close agreement with the 80% predicted by Ansell and Lewis (1970). Petrikovics et al. (2012) studied the toxicokinetics of ATCA in rats following intravenous (IV) injection of ATCA at 100 mg/kg body weight. Although this study did not address the *in vivo* generation of ATCA from cyanide exposure, it is one of the first studies to address the distribution and elimination of ATCA. The plasma ATCA ranged from 0.96 to 18.5 μ M, and showed a consistent 5-fold increase over endogenous concentrations between 2.5 and 48 h post-exposure (Petrikovics et al., 2012). These findings suggest that the use of ATCA as a biomarker is promising, but further evaluation of the toxicokinetics of ATCA following cyanide exposure should be undertaken.

Recently, Mitchell et al. (2013) established an analytical method to quantify the cyanide detoxification product, α -KgCN, but a toxicokinetic profile of α -KgCN following cyanide exposure has not been performed. Knowledge of α -KgCN's toxicokinetic profile will provide a better understanding of cyanide's absorption and elimination by this alternative pathway and might show that α -KgCN has advantages over other markers of cyanide exposure for verification of cyanide exposure. Therefore, we completed a toxicokinetic analysis of α -KgCN in potassium cyanide-exposed swine and compared it with data for cyanide and its other detoxification products. We also studied the behavior of cyanide and its detoxification products during administration of cobinamide, a next-generation treatment for cyanide exposure (Brenner et al., 2010a,b; Broderick et al., 2006; Chan et al., 2010, 2011; Zou et al., 2012). Furthermore, α -Kg has been suggested as a cyanide antidote (Bhattacharya et al., 2002; Bhattacharya and Vijayaraghavan, 1991, 2002; Hume et al., 1995; Mathangi et al., 2011; Norris et al., 1990; Tulsawani et al., 2005), and the results of this study may be important for α -Kg therapeutic studies.

Table 1

Toxicokinetic parameters for cyanide, thiocyanate, and ATCA in rats and swine. C_{max} , T_{max} , and $t_{1/2}$ are designated as the peak blood or plasma concentration, peak time, and elimination half-life, respectively.

Species	Analyte ^a	C_{max} (μ M)	T_{max} (min)	$t_{1/2}$ (min)
Rats	Cyanide	6.2 ^b , 89.0 ^c	2 ^b , 15 ^c	14 ^b , 38 ^c
	Thiocyanate	58.1 ^d	360 ^c	348 ^c
	ATCA	18.5 ^d	120 ^d	150 ^d
Swine	Cyanide	57.5 ^c	30 ^c	32 ^c
	Thiocyanate	42.8 ^c	360 ^c	297 ^c

^a Cyanide was analyzed from whole blood, and thiocyanate and ATCA were analyzed from plasma.

^b Leuschner et al. (1991).

^c Sousa et al. (2003).

^d Petrikovics et al. (2012).

2. Experimental

2.1. Reagents and materials

All reagents and materials were at least HPLC grade. α -K₂CN and α -K₂CN-d₂ were synthesized as previously reported (Mitchell et al., 2013). Labeled thiocyanate (Na¹⁵C¹⁵N) and cyanide (Na¹³C¹⁵N) were acquired from Isotech (Miamisburg, OH). Labeled ATCA-d₂ was synthesized in the lab of Dr. Nagasawa at the Department of Veterans Affairs Medical Center (Minneapolis, MN). Aquohydroxocobinamide was synthesized as described previously, and converted to a dinitro derivative by adding two molar equivalents of sodium nitrite (Chan et al., 2010, 2011). Sodium cyanide, sodium tetraborate decahydrate, sodium hydroxide, and Millex®-GV syringe filters (0.22 µm) were purchased from Fisher Scientific (Fair Lawn, NJ). Sodium thiocyanate was obtained from Acros Organics (Morris Plains, NJ). Formic acid (LC/MS grade) and pentafluorobenzyl bromide (PFB-Br) were obtained from Thermo Scientific (Rockford, IL). Tetrabutylammonium sulfate (TBAS) was purchased from Sigma-Aldrich (St. Louis, MO). ATCA was obtained from Chem-Impex International (Wood Dale, IL). Oasis mixed-mode cationic exchange (MCX) columns were acquired from Waters Corporation (Milford, MA). *N*-methyl-*N*-trimethylsilyl-trifluoroacetamide (MSTFA) was acquired from Pierce Chemical Company (Rockford, IL).

2.2. Animal studies

The animal studies were conducted at Wilford Hall Medical Center (Lackland Air Force Base, TX) in accordance with The Guide for the Care and Use of Laboratory Animals, and were approved by the Wilford Hall Clinical Research Division Institutional Animal Care and Use Committee; Wilford Hall is accredited by the American Association for Laboratory Animal Science. A total of 31 Yorkshire pigs (~50 kg) were sedated, intubated, and anesthetized with isoflurane. KCN was injected intravenously at 0.17 mg/kg/min until apnea occurred. At one minute post-apnea, the animals received either saline by IV injection (control group, *N* = 11) or 12.5 mg/kg cobinamide by IV (*N* = 10) or intraosseous (IO) (*N* = 10) injection. Arterial blood was sampled prior to cyanide exposure, 5 min after the start of cyanide infusion, at apnea, and at 2, 4, 6, 8, 10, 20, 30, 40, 50, and 60 min post-apnea. EDTA was added to an aliquot of blood, and the plasma was separated from the red blood cells by centrifugation and shipped on ice to South Dakota State University. Upon receipt, the EDTA-treated plasma was frozen and stored at -80 °C until used.

2.3. Preparation and analysis of swine plasma for α -K₂CN

Plasma was prepared and analyzed for α -K₂CN according to a previously established method (Mitchell et al., 2013). Briefly, 1% formic acid in acetonitrile was added to the plasma, and the precipitate was removed by centrifugation. The resulting supernatant was concentrated by drying under N₂(g) and then reconstituted in aqueous formic acid. The reconstituted sample was analyzed using ultrahigh-performance liquid chromatography tandem mass spectrometry, and α -K₂CN was quantified by monitoring the 172.0 to 145.1 *m/z* transition.

2.4. Preparation and analysis of swine plasma for cyanide and thiocyanate

Cyanide and thiocyanate were measured simultaneously according to Bhandari et al. (2012). Briefly, tetrabutylammonium sulfate and pentafluorobenzyl bromide (PFB-Br) were added to plasma, followed by vortexing for 2 min, and heating at 70 °C for 1 h. Samples were then centrifuged at 9300 × *g* for 4 min, and the organic layer was analyzed by chemical ionization gas-chromatography mass-spectrometry (GC-MS) with ions 208 and 240 *m/z* selected for quantification of PFB-CN and PFB-SCN, respectively.

2.5. Preparation and analysis of swine plasma for ATCA

Plasma was analyzed for ATCA according to Logue et al. (2005). Briefly, proteins were precipitated from the plasma by addition of 1% HCl in acetone (v/v). The supernatant was diluted with 0.1 M HCl and applied to a mixed-mode cation exchange solid phase extraction column. After washing the column, ATCA was eluted using NH₄OH:CH₃OH:H₂O (25:50:25) in 0.1 M HCl, and the samples were dried at 40 °C. MSTFA in hexane (30% v/v) was added to the dried samples, and they were heated at 50 °C for 1 h to chemically modify ATCA to ATCA-(TMS)₃ for GC-MS analysis with ion 362 *m/z* used for quantification.

2.6. Toxicokinetic and data analysis

Toxicokinetic parameters were determined according to methods described by the World Health Organization (1986) and Shargel et al. (2005). Analysis of α -K₂CN was completed with a one-compartment model, with *C*_{max}, *T*_{max}, *t*_{1/2} and elimination constants (*K*_e) obtained from the concentration-time curves. Area under the curve ([AUC]) after apnea was also determined from the concentration-time curve using the trapezoidal rule (Shargel et al., 2005). *C*_{max}/*C*_{baseline} was determined by dividing the maximum plasma concentration by the baseline concentration. The α -K₂CN data for the cobinamide and control animals were analyzed with a one-way analysis of variance and Bartlett's test for equal variances, which showed a

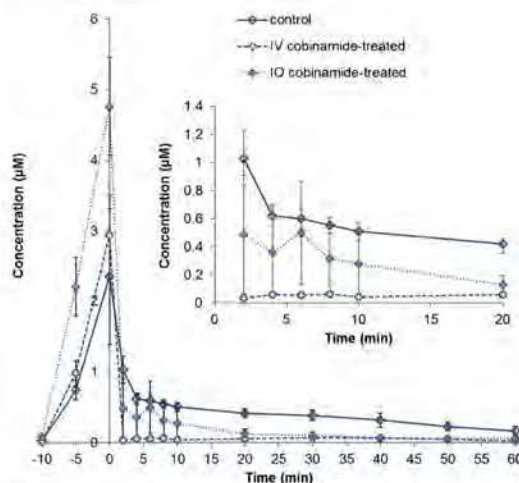


Fig. 2. Toxicokinetic profile of α -K₂CN in control, IV cobinamide-treated, and IO cobinamide-treated swine. Apnea, pre-exposure and 5 min infusion sample points are designated as “time 0, -10, and -5”, respectively. The plasma sampled at time zero was drawn prior to treatment, the -10 time point was obtained before infusion and the -5 time point was collected 5 min after exposure. Error bars denote standard error of the mean (SEM). Inset: “zoomed” representation of the plasma concentrations from 2 to 20 min post-apnea.

significance difference among the three groups. Therefore, two-tailed unpaired *t*-tests with Welch's correction were applied to each time point to evaluate statistical differences between the groups.

3. Results

3.1. Behavior of α -K₂CN after cyanide exposure

The plasma α -K₂CN concentration similarly increased in all three experimental groups during cyanide infusion, but decreased with different kinetics after cyanide was stopped (at the onset of apnea) and cobinamide was injected (Fig. 2). In the control saline-treated group (solid line), the α -K₂CN concentration showed a typical exponential decrease for the duration of the experiment. In the group treated with IV cobinamide (dashed line), α -K₂CN concentrations showed a more rapid decrease compared to the control group. In the group treated with IO cobinamide (dotted line), the α -K₂CN concentrations fell at a similar rate to the IV-treated group, but the concentrations did not fall quite as low and were still well above baseline up to 10 min post-apnea. Significant differences between the control and IV cobinamide-treated groups were observed at all points except -5 and 0 min. Significant differences between control and IO cobinamide-treated groups were observed at -10, -5, 20, 30, and 50 min. In contrast, significant differences between the IV and IO cobinamide-treated groups were only found pre-apnea.

3.2. Comparison of the toxicokinetic profile of α -K₂CN, cyanide, thiocyanate, and ATCA

The toxicokinetic profile of α -K₂CN, ATCA, and cyanide in control animals were generally similar, with the exception that plasma cyanide concentrations were considerably higher compared to ATCA and α -K₂CN (Fig. 3). Also to be noted is that plasma ATCA did not decrease as rapidly as α -K₂CN, likely because ATCA

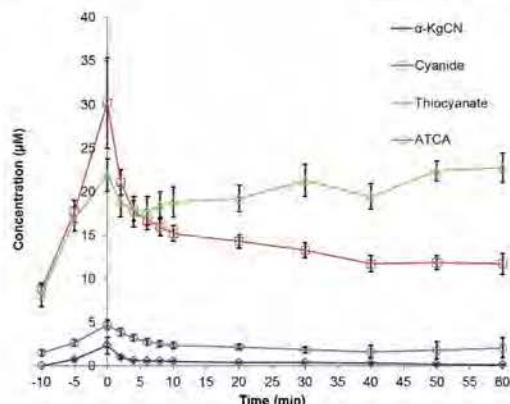


Fig. 3. Toxicokinetic profile of α -KgCN, cyanide, thiocyanate, and ATCA in control swine. Apnea, pre-exposure and 5 min infusion sample points are designated as "time 0, -10, and -5", respectively. The plasma sampled at time zero was drawn prior to treatment, the -10 time point was obtained before infusion and the -5 time point was collected 5 min after exposure. Error bars denote SEM.

formation is not an equilibrium reaction, as is production of α -KgCN. Thiocyanate behaved quite differently compared to the other cyanide exposure markers, decreasing directly after apnea (2 and 4 min) and then rising gradually for the duration of the experiment (Fig. 3).

In the animals treated with IV cobinamide, cyanide, thiocyanate, ATCA and α -KgCN showed the typical increase in concentration prior to apnea as cyanide was being absorbed and distributed (Fig. 4). However, cyanide concentrations increased sharply at 2 min post-apnea and then decreased. ATCA concentrations increased until 4 min post-apnea, before starting to decrease. Thiocyanate and α -KgCN concentrations both decreased immediately following apnea, but thiocyanate then gradually increased starting at 2 min post-apnea.

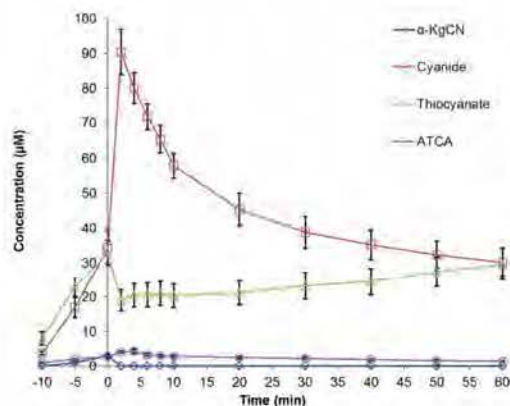


Fig. 4. Toxicokinetic profile of α -KgCN, cyanide, thiocyanate, and ATCA in IV cobinamide-treated swine. Apnea, pre-exposure and 5 min infusion sample points are designated as "time 0, -10, and -5", respectively. The plasma sampled at time zero was drawn prior to treatment, the -10 time point was obtained before infusion and the -5 time point was collected 5 min after exposure. Error bars denote SEM.

Table 2
Toxicokinetic parameters for α -KgCN, cyanide, and ATCA in control animals following IV-infusion of KCN (0.17 mg/kg/min) until apnea.

Analyte	C_{max} (μ M)	$t_{1/2}$ (min)	K_e	[AUC] (μ M min)	$C_{max}/C_{baseline}$
α -KgCN	2.35	15	0.0462	25.6	102.2
Cyanide ^a	30.18	27	0.0258	474.4	3.1
ATCA ^a	4.73	14	0.0499	75.4	3.4

^a The toxicokinetic data for cyanide and ATCA in swine plasma will be reported by Bhandari et al.

3.3. Toxicokinetics of α -KgCN, cyanide, and ATCA

Toxicokinetic parameters for α -KgCN, cyanide and ATCA in control animals are presented in Table 2; values for thiocyanate could not be determined due to the increasing concentrations observed after apnea. A one-compartment model best represents the toxicokinetic behavior of α -KgCN post-apnea, similar to Bhandari et al. (Publication pending) for cyanide and ATCA. α -KgCN, cyanide, and ATCA all exhibited T_{max} at apnea (0 min). Among all the markers, cyanide provided the highest $t_{1/2}$ and C_{max} values (although both could not be determined for thiocyanate). α -KgCN and ATCA produced similar toxicokinetic values.

4. Discussion

The increase in plasma α -KgCN concentrations before apnea, when cyanide is being infused, shows that a portion of the cyanide administered is quickly converted to α -KgCN. After apnea, when the cyanide infusion is stopped, the metabolism and distribution of cyanide dominates and α -KgCN concentrations rapidly decrease. Because α -KgCN formation is an equilibrium reaction (Fig. 1), the rapid decrease in cyanide rapidly consumes α -KgCN as the equilibrium favors the reactants. The sudden decrease in α -KgCN levels in the IV and IO cobinamide-treated animals post-apnea was expected considering that cobinamide was administered just after apnea. Cobinamide has a high affinity for two cyanide ions (Brenner et al., 2010b), and, therefore, free cyanide in the plasma is rapidly sequestered after treatment, causing a decrease in free cyanide, which leads to the consumption of α -KgCN as the equilibrium shifts toward the production of α -Kg and cyanide (Fig. 1).

Comparing the cobinamide-treated groups to the control animals, the main difference occurs immediately following apnea, when plasma cyanide sharply increases and α -KgCN sharply decreases. The increase in cyanide and decrease of α -KgCN in the treated animals is likely the result of rapid cyanide extraction from the red blood cells into the plasma through cobinamide sequestration of cyanide (Nath et al., 2013). This phenomenon would result in less free cyanide in the plasma even though the total (free and sequestered) cyanide concentration increases. The sequestration of cyanide causes a sudden decrease in α -KgCN concentrations. ATCA also showed an increase in concentration until about 4 min post-apnea, which could be explained by conversion of small amounts of free cyanide released by dicyano cobinamide or aquocyanocobinamide (Blackledge et al., 2010).

Thiocyanate also showed interesting behavior in the control and cobinamide-treated animals. The increase in thiocyanate concentrations, as cyanide is infused into the animal, is expected because of the large fraction of cyanide converted to thiocyanate as the major detoxification pathway of cyanide (Ansell and Lewis, 1970; Baskin et al., 2004; Sousa et al., 2003). After the infusion is stopped, a sudden decrease in the thiocyanate concentration occurs, because less free cyanide is available and the combination of thiocyanate distribution and elimination is more rapid than the conversion of cyanide to thiocyanate. Over time, the rate of conversion of cyanide to thiocyanate increases as rhodanese's activity increases

(rhodanese is the enzyme mainly responsible for enzymatic conversion of cyanide to thiocyanate) (Wrobel and Frendo, 1992; Wrobel et al., 2004). After 2–4 min, thiocyanate elimination is not fast enough to match the rate of conversion of cyanide to thiocyanate, causing a buildup of thiocyanate in the plasma (Wrobel and Frendo, 1992; Wrobel et al., 2004). Chan et al. (2010) also observed an increase in plasma thiocyanate concentrations as cyanide was released from red blood cells and converted to thiocyanate.

We found a statistical difference between the α -K_gCN concentrations of the control and cobinamide-treated animals, suggesting that α -K_gCN is eliminated from the plasma at a faster rate when cobinamide is administered. Animals receiving IV cobinamide showed the fastest elimination of α -K_gCN from the plasma, but it was certainly comparable to that in animals receiving IO cobinamide, suggesting the two routes of administration allowed similar distribution profiles for cobinamide. Previous studies conducted in Gottingen minipigs have shown that IO- and IV-administration of the cyanide antidote, hydroxocobalamin, to non-cyanide-poisoned animals produce similar distribution profiles (Murray et al., 2012). Significant differences were also seen pre-apnea in all groups, which can be explained due to interanimal variability.

Comparison of the toxicokinetic parameters of α -K_gCN to those of cyanide and ATCA (Table 2), shows that α -K_gCN behaves similarly to ATCA, although ATCA had the largest K_e value, suggesting it is eliminated faster from the plasma than cyanide or α -K_gCN. Comparison of the [AUC] values, establishes that α -K_gCN had the lowest overall plasma concentrations throughout the study, supported by its fast rate of elimination, low C_{max} concentrations, and low baseline concentrations. We will present a more detailed description of the toxicokinetic behavior of cyanide, thiocyanate and ATCA in a future publication.

Plasma concentrations of α -K_gCN were relatively low in all animals compared to cyanide and thiocyanate because a relatively low amount of cyanide was detoxified by the α -K_gCN pathway. It has been suggested that about 80% of cyanide is converted to thiocyanate in the presence of a sulfur donor (Ansell and Lewis, 1970; Baskin et al., 2004; Sousa et al., 2003) and another 15–20% of cyanide is metabolized by L-cystine to produce ATCA (Ansell and Lewis, 1970). This would suggest that only a small percentage of cyanide is converted to other detoxification products in non-treated (control) animals, including cyanocobalamin (Astier and Baud, 1995; Butte et al., 1982; Chatzimichalakis et al., 2004) and cyanide-protein adducts (Fasco et al., 2007; Youso et al., 2010, 2012), which is consistent with the low plasma concentrations of α -K_gCN. Based on the measured α -K_gCN concentrations and detoxification of cyanide by the thiocyanate and ATCA pathways, we estimate that about 0.1–1.7% of the cyanide dose was converted to α -K_gCN. This estimation was done by dividing the maximum concentrations of α -K_gCN by the total maximum concentrations of cyanide, thiocyanate, ATCA and α -K_gCN of cobinamide-treated and control animals after factoring in the distribution of cyanide between red blood cells and plasma (70–96% of blood cyanide resides in the red blood cells (Baar, 1966; Lundquist et al., 1985). The percentage of cyanide in plasma increases as the cyanide dose increases, because the red blood cells become saturated with cyanide (Lundquist et al., 1985). Further studies (i.e., radioisotope experiments) would have to be undertaken to accurately calculate how much cyanide participates in the α -K_gCN pathway.

This study suggests that use of α -K_gCN as a biomarker for cyanide exposure would be most applicable in instances of acute, high-dose cyanide poisoning soon after exposure. The major advantage of using α -K_gCN as a marker for cyanide exposure is the low, if not undetectable, levels of endogenous α -K_gCN in the plasma, making cyanide exposure easy to detect from elevated

α -K_gCN concentrations. Comparing the maximum cyanide, thiocyanate, ATCA and α -K_gCN plasma concentrations to their endogenous (baseline) concentrations, shows that α -K_gCN has a much higher $C_{max}/C_{baseline}$, suggesting that measuring plasma α -K_gCN can provide a definitive confirmation of cyanide exposure. Although there are several potential advantages of α -K_gCN as a cyanide exposure marker, its rapid elimination, especially in the presence of cobinamide, may limit its use.

To our knowledge, this work provides the first reported toxicokinetic profile of α -K_gCN in any animal. The ability to measure α -K_gCN in plasma would be beneficial in studies using α -K_g as a cyanide antidote (Bhattacharya et al., 2002; Bhattacharya and Vijayaraghavan, 1991, 2002; Hume et al., 1995; Mathangi et al., 2011; Tulsawani et al., 2005). The equilibrium constant for the formation of α -K_gCN ($K_{f,\alpha-KgCN}$) was estimated by assuming the reaction was at equilibrium at apnea. The α -K_gCN concentration (2.35 μ M) was divided by the remaining cyanide concentration (i.e., 30.18 μ M – 2.35 μ M = 27.83 μ M) and the remaining endogenous α -K_g concentration (i.e., 23.95 μ M – 2.35 μ M = 21.60 μ M (Dabek et al., 2005)). Based on the calculated equilibrium constant ($K_{f,\alpha-KgCN} = 3.9 \times 10^{-3}$), the conversion of α -K_g into α -K_gCN is not favorable. Therefore, the use of α -K_g as a therapeutic may not be very effective, but further studies would have to be undertaken to determine α -K_gCN's efficacy in minimizing the lethality of cyanide following exposure.

Future work should address the absorption, distribution, and elimination of α -K_gCN in other animals to determine the most appropriate animal model for evaluating the behavior of α -K_gCN in humans following cyanide exposure. Rigorously determining the $K_{f,\alpha-KgCN}$, and the amount of cyanide that participates in the α -K_gCN pathway, would produce a clear picture of the role of α -K_g in cyanide detoxification, both naturally and as a therapeutic.

Conflict of interest statement

The authors declare no conflict of interest.

Acknowledgements

The research was supported by the CounterACT Program, National Institutes of Health Office of the Director, Grant Nu. U01NS058030, the National Institute of Allergy and Infectious Diseases, Inter agency Agreement Number AOD12060-001-00000/A120-B.P2012-01 and the USAMRICD under the auspices of the US Army Research Office of Scientific Services Program Contract No. W911NF-11-D-0001 administered by Battelle (Delivery order 0079, Contract No. TCN 11077). We gratefully acknowledge the support from a U.S. Dept. of Education, Graduate Assistance in Areas of National Need (GAANN), award to the Department of Chemistry & Biochemistry (P200A100103). We thank the National Science Foundation Major Research Instrumentation Program (Grant Number CHE-0922816) for funding the AB SCIEX QTRAP 5500 LC/MS/MS. The LC/MS/MS instrumentation was housed in the South Dakota State University Campus Mass Spectrometry Facility which was supported by the National Science Foundation/EPSCoR Grant No. 0091948 and the State of South Dakota. The authors would like to acknowledge Dr. George Perry, Animal and Range Science (South Dakota State University) for providing swine plasma. Furthermore, the authors are thankful to Susan M. Boudreau, RN, BSN, Maria G. Castaneda, MS, Toni E. Vargas, PA-C, MHS, and Patricia Dixon, MHS from the Clinical Research Division, Wilford Hall Medical Center (Lackland Air Force Base, San Antonio, TX) for providing potassium cyanide-exposed swine plasma. The opinions or assertions contained herein are the private views of the

authors and are not to be construed as official or as reflecting the views of the Department of the Army, Department of the Air Force, the National Institutes of Health, or the Department of Defense.

References

- Ausell, M., Lewis, F.A.S., 1970. Review of cyanide concentrations found in human organs. Survey of literature concerning cyanide metabolism, normal, nonfatal, and fatal body cyanide levels. *Journal of Forensic Medicine* 17, 148–155.
- Astier, A., Baud, F.J., 1995. Simultaneous determination of hydroxocobalamin and its cyanide complex cyanocobalamin in human plasma by high-performance liquid chromatography. Application to pharmacokinetic studies after high-dose hydroxocobalamin as an antidote for severe cyanide poisoning. *Journal of Chromatography, B: Biomedical Applications* 667, 129–135.
- Baar, S., 1966. The micro determination of cyanide: its application to the analysis of whole blood. *Analyst* 91, 268–272.
- Baskin, S.I., Brewer, T.G., 1997. Cyanide poisoning. In: Sidell, F.R., Takafuji, E.T., Franz, D.R. (Eds.), *Medical Aspects of Chemical and Biological Warfare*. Borden Institute, Washington, D.C., pp. 271–286.
- Baskin, S.I., Petrikovics, I., Kurche, J.S., Nicholson, J.D., Logue, B.A., Maliner, B.L., Rockwood, G.A., 2004. Insights on cyanide toxicity and methods of treatment. In: Flora, S.J.S., Romano, J.A., Baskin, S.I., Selkar, K. (Eds.), *Pharmacological Perspectives of Toxic Chemicals and their Antidotes*. Narosa Publishing House, New Delhi, India, pp. 105–146.
- Becker, C.E., 1985. The role of cyanide in fires. *Veterinary and Human Toxicology* 27, 487–490.
- Bhandari, R.K., Oda, R.P., Youso, S.L., Petrikovics, I., Beberta, V.S., Rockwood, G.A., Logue, B.A., 2012. Simultaneous determination of cyanide and thiocyanate in plasma by chemical ionization gas chromatography mass spectrometry (CI-CC-MS). *Analytical and Bioanalytical Chemistry* 404, 2287–2294.
- Bhattacharya, R., Rao, P.V.L., Vijayaraghavan, R., 2002. In vitro and in vivo attenuation of experimental cyanide poisoning by α -ketoglutarate. *Toxicology Letters* 128, 185–195.
- Bhattacharya, R., Vijayaraghavan, R., 1991. Cyanide intoxication in mice through different routes and its prophylaxis by alpha-ketoglutarate. *Biomedical Environmental Science* 4, 452–460.
- Bhattacharya, R., Vijayaraghavan, R., 2002. Promising role of α -ketoglutarate in protecting against the lethal effects of cyanide. *Human and Experimental Toxicology* 21, 297–303.
- Blackledge, W.C., Blackledge, C.W., Criesel, A., Mahon, S.B., Brenner, M., Pilz, R.B., Boss, G.R., 2010. New facile method to measure cyanide in blood. *Analytical Chemistry* 82, 4216–4221.
- Brenner, M., Kim, J.G., Mahon, S.B., Lee, J., Kreuter, K.A., Blackledge, W., Mukai, D., Patterson, S., Mohammad, O., Sharma, V.S., Boss, G.R., 2010a. Intramuscular cobinamide sulfite in a rabbit model of sublethal cyanide toxicity. *Annals of Emergency Medicine* 55, 352–363.
- Brenner, M., Mahon, S.B., Lee, J., Kim, J., Mukai, D., Goodman, S., Kreuter, K.A., Ahdout, R., Mohammad, O., Sharma, V.S., Blackledge, W., Boss, G.R., 2010b. Comparison of cobinamide to hydroxocobalamin in reversing cyanide physiologic effects in rabbits using diffuse optical spectroscopy monitoring. *Journal of Biomedical Optics* 15, 017001/017001–017001/017008.
- Broderick, K.E., Potluri, P., Zhuang, S., Scheffler, L.E., Sharma, V.S., Pilz, R.B., Boss, G.R., 2006. Cyanide detoxification by the cobalamin precursor cobinamide. *Experimental Biology and Medicine* 231, 641–649.
- Butte, W., Riemann, H.H., Walle, A.J., 1982. Liquid-chromatographic measurement of cyanocobalamin in plasma, a potential tool for estimating glomerular filtration rate. *Clinical Chemistry* 28, 1778–1781.
- Chan, A., Balasubramanian, M., Blackledge, W., Mohanmad, O.M., Alvarez, L., Boss, G.R., Bigby, T.D., 2010. Cobinamide is superior to other treatments in a mouse model of cyanide poisoning. *Clinical Toxicology* 48, 709–717.
- Chan, A., Craunshaw, D.L., Morrell, A., Patterson, S.E., Nagasawa, H.T., Briggs, J.E., Kozocas, J.A., Mahon, S.B., Brenner, M., Pilz, R.B., Bigby, T.D., Boss, G.R., 2011. The combination of cobinamide and sulfanegen is highly effective in mouse models of cyanide poisoning. *Clinical Toxicology* 49, 366–373.
- Chatzimichalidis, P.F., Samanidou, V.F., Verpoorte, R., Papadoyannis, I.N., 2004. Development of a validated HPLC method for the determination of B-complex vitamins in pharmaceuticals and biological fluids after solid phase extraction. *Journal of Separation Science* 27, 1181–1188.
- Conn, E.E., 1978. Cyanogenesis, the production of cyanide, by plants. In: Keeler, R.F., Van Kampen, K.R., James, L.F. (Eds.), *Effects of Poisonous Plants on Livestock*. Academic Press, San Diego, pp. 301–310.
- Dabek, M., Kruszewska, D., Filip, R., Hotowy, A., Pierzynowski, L., Wojtasz-Pajak, A., Szymanczyk, S., Valverde, P.J.L., Werpachowska, E., Pierzynowski, S.G., 2005. α -Ketoglutarate (AKG) absorption from pig intestine and plasma pharmacokinetics. *Journal of Animal Physiology and Animal Nutrition* 89, 419–426.
- Dirikolu, L., Hughes, C., Harkins, D., Boyles, J., Bosken, J., Lehner, F., Troppmann, A., McDowell, K., Tobin, T., Sebastian, M.M., Harrison, L., Crutchfield, J., Baskin, S.I., Fitzgerald, T.D., 2003. The toxicokinetics of cyanide and mandelonitrile in the horse and their relevance to the mare reproductive loss syndrome. *Toxicology Mechanisms and Methods* 13, 199–211.
- Fasco, M.J., Hauer, C.R., Stack, R.F., O'Hehir, C., Barr, J.R., Eadon, G.A., 2007. Cyanide adducts with human plasma proteins: albumin as a potential exposure surrogate. *Chemical Research in Toxicology* 20, 677–684.
- Hume, A.S., Mozingo, J.R., McIntyre, B., Ho, I.K., 1995. Antidotal efficacy of alpha-ketoglutaric acid and sodium thiosulfate in cyanide poisoning. *Journal of Toxicology – Clinical Toxicology* 33, 721–724.
- Leuschner, J., Winkler, A., Leuschner, F., 1991. Toxicokinetic aspects of chronic cyanide exposure in the rat. *Toxicology Letters* 57, 195–201.
- Logue, B.A., Kirschten, N.P., Petrikovics, I., Moser, M.A., Rockwood, G.A., Baskin, S.I., 2005. Determination of the cyanide metabolite 2-aminothiazoline-4-carboxylic acid in urine and plasma by gas chromatography-mass spectrometry. *Journal of Chromatography, B: Analytical Technologies in the Biomedical and Life Sciences* 819, 237–244.
- Lundquist, P., Rosling, H., Sverbo, B., 2011. Determination of cyanide in whole blood, erythrocytes, and plasma. *Clinical Chemistry* 57, 591–595.
- Ma, J., Dasgupta, P.K., 2010. Recent developments in cyanide detection: a review. *Analytica Chimica Acta* 673, 117–125.
- Mathangi, D.C., Shyamala, R., Vijayashree, R., Rao, K.R., Ruckmani, A., Vijayaraghavan, R., Bhattacharya, R., 2011. Effect of alpha-ketoglutarate on neurobehavioral, neurochemical and oxidative changes caused by sub-chronic cyanide poisoning in rats. *Neurochemical Research* 36, 540–548.
- Mitchell, B.L., Rockwood, G.A., Logue, B.A., in press 2013. Quantification of α -ketoglutarate cyanohydrin in swine plasma by ultra-high performance liquid chromatography tandem mass spectrometry. *Journal of Chromatography B*, <http://dx.doi.org/10.1016/j.jchromb.2013.06.029>.
- Murray, D.B., Edleston, M., Thomas, S., Jefferson, R.D., Thompson, A., Dunn, M., Vidler, D.S., Cutton, R.E., Blain, P.G., 2012. Rapid and complete bioavailability of antidotes for organophosphorus nerve agent and cyanide poisoning in minipigs after intrasosseous administration. *Annals of Emergency Medicine* 60, 424–430.
- Nagasawa, H.T., Cummings, S.E., Baskin, S.I., 2004. The structure of ITCA, a urinary metabolite of cyanide. *Organic Preparations and Procedures International* 36, 178–182.
- Nath, A.K., Roberts, L.D., Liu, Y., Mahon, S.B., Kim, S., Ryu, J.H., Werdich, A., Januzzi, J.L., Boss, G.R., Rockwood, G.A., MacRae, C.A., Brenner, M., Gerszten, R.E., Peterson, R.T., 2013. Chemical and metabolomic screens identify novel biomarkers and antidotes for cyanide exposure. *The FASEB Journal*, <http://dx.doi.org/10.1096/fj.12.225037>.
- Norris, J.C., Udey, W.A., Hume, A.S., 1990. Mechanism of antagonizing cyanide-induced lethality by alpha-ketoglutaric acid. *Toxicology* 62, 275–283.
- Petrikovics, I., Yu, J.C.C., Thompson, D.E., Jayanna, P., Logue, B.A., Nasr, J., Bhandari, R.K., Baskin, S.I., Rockwood, G., 2012. Plasma persistence of 2-aminothiazoline-4-carboxylic acid in rat system determined by liquid chromatography tandem mass spectrometry. *Journal of Chromatography, B: Analytical Technologies in the Biomedical and Life Sciences* 891–892, 81–84.
- Purser, D.A., Grimshaw, P., Berrill, K.R., 1984. Intoxication by cyanide in fires: a study in monkeys using polyacrylonitrile. *Archives of Environmental Health* 39, 394–400.
- Shargel, L., Wu-Pong, S., Yu, A.B.C., 2005. *Applied Biopharmaceutics and Pharmacokinetics*, fifth ed. McGraw-Hill, New York, pp. 1–892.
- Smith, J.N., Keil, A., Likens, J., Noll, R.J., Cooks, R.G., 2010. Facility monitoring of toxic industrial compounds in air using an automated, fieldable, miniature mass spectrometer. *Analyst* 135, 994–1003.
- Sousa, A.B., Manzano, H., Soto-Blanco, B., Gorniak, S.L., 2003. Toxicokinetics of cyanide in rats, pigs and goats after oral dosing with potassium cyanide. *Archives of Toxicology* 77, 330–334.
- Tulsawani, R.K., Debnath, M., Pant, S.C., Kumar, O., Prakash, A.O., Vijayaraghavan, R., Bhattacharya, R., 2005. Effect of sub-acute oral cyanide administration in rats: Protective efficacy of alpha-ketoglutarate and sodium thiosulfate. *Chemico-Biological Interactions* 156, 1–12.
- Vetter, J., 2000. Plant cyanogenic glycosides. *Toxicon* 38, 11–36.
- Viswanath, D.S., Ghosh, T.K., 2010. Chemical terrorism: classification, synthesis and properties. In: Ghosh, T.K., Preias, M.A., Viswanath, D.S., Loyalka, S.K. (Eds.), *Science and Technology of Terrorism and Counterterrorism*. CRC Press, Boca Raton, pp. 283–300.
- Way, J.L., 1984. Cyanide intoxication and its mechanism of antagonism. *Annual Review of Pharmacology and Toxicology* 24, 451–481.
- World Health Organization, 1986. *Environmental Health Criteria 57: Principles of Toxicokinetic Studies*. World Health Organization, Geneva, Switzerland, pp. 1–166.
- Wrabel, M., Prendo, J., 1992. The effect of cAMP and some sulfur compounds upon the activity of mercaptopyruvate sulfurtransferase and rhodanase in mouse liver. *Folia Biologica* 40, 11–14.
- Wrabel, M., Jurkowska, H., Sliwa, L., Srebro, Z., 2004. Sulfurtransferases and cyanide detoxification in mouse liver, kidney, and brain. *Toxicology Mechanisms and Methods* 14, 331–337.
- Xu, Y., Zhang, X., Liu, W., Ma, Y., Rui, X., Yang, S., Jin, Y., Chen, Y., Miao, M., 2011. Effect of smoking regime on HCN yields in mainstream cigarette smoke. *Zhongguo Yanco Xuebao* 17, 4–7.
- Xu, Y., Zhang, X., Liu, W., Zhang, T., Duan, Y., Chen, J., Ma, Y., Rui, X., Chen, Y., Miao, M., 2012. Effect of the equilibrium time on hydrogen cyanide delivery in mainstream smoke. *Yingyong Huagong* 41, 1140–1142, 1146.
- Youso, S.L., Rockwood, G.A., Lee, J.P., Logue, B.A., 2010. Determination of cyanide exposure by gas chromatography-mass spectrometry analysis of cyanide-exposed plasma proteins. *Analytica Chimica Acta* 677, 24–28.

- Youso, S.L., Rockwood, G.A., Logue, B.A., 2012. The analysis of protein-bound thiocyanate in plasma of smokers and non-smokers as a marker of cyanide exposure. *Journal of Analytical Toxicology* 36, 265–269.
- Zdrojewicz, Z., Koziol, J., Januszewski, A., Steicwko, A., 1996. Evaluation of concentrations of magnesium, zinc, copper, and calcium in workers exposed to organic solvents, hydrogen cyanide, and harmful physical factors. *Medycyna Pracy* 47, 217–225.
- Zou, Z., Cheng, J., Ye, F., Dan, G., Cai, Y., Wang, J., Dong, Z., 2012. Research programs on antidotes and detection of cyanide and progress in the USA. *Junshi Yixue* 36, 465–470.

APPENDIX VII

Author's personal copy

Journal of Chromatography B, 949–950 (2014) 94–98



Contents lists available at ScienceDirect

Journal of Chromatography B

journal homepage: www.elsevier.com/locate/chromb



Determination of 3-mercaptopyruvate in rabbit plasma by high performance liquid chromatography tandem mass spectrometry



Michael W. Stutelberg^a, Chakravarthy V. Vinnakota^a, Brendan L. Mitchell^a, Alexandre R. Monteil^b, Steven E. Patterson^b, Brian A. Logue^{a,*}

^a Department of Chemistry and Biochemistry, South Dakota State University, Avera Health and Science Center 131, Box 2202, Brookings, SD, 57007, USA
^b Center for Drug Design, University of Minnesota, 516 Delaware Street SE, Minneapolis 55455, MN, USA

ARTICLE INFO

Article history:
Received 21 June 2013
Received in revised form 2 January 2014
Accepted 5 January 2014
Available online 18 January 2014

Keywords:
Cyanide antidote
3-Mercaptopyruvate
Sulfanegen
Liquid chromatography–tandem mass spectrometry

ABSTRACT

Accidental or intentional cyanide poisoning is a serious health risk. The current suite of FDA approved antidotes, including hydroxocobalamin, sodium nitrite, and sodium thiosulfate is effective, but each antidote has specific major limitations, such as large effective dosage or delayed onset of action. Therefore, next generation cyanide antidotes are being investigated to mitigate these limitations. One such antidote, 3-mercaptopyruvate (3-MP), detoxifies cyanide by acting as a sulfur donor to convert cyanide into thiocyanate, a relatively nontoxic cyanide metabolite. An analytical method capable of detecting 3-MP in biological fluids is essential for the development of 3-MP as a potential antidote. Therefore, a high performance liquid chromatography tandem mass spectrometry (HPLC–MS–MS) method was established to analyze 3-MP from rabbit plasma. Sample preparation consisted of spiking the plasma with an internal standard (¹³C₅-3-MP), precipitation of plasma proteins, and reaction with monobromobimane to inhibit the characteristic dimerization of 3-MP. The method produced a limit of detection of 0.1 μM, a linear dynamic range of 0.5–100 μM, along with excellent linearity ($R^2 \geq 0.999$), accuracy ($\pm 9\%$ of the nominal concentration) and precision ($<7\%$ relative standard deviation). The optimized HPLC–MS–MS method was capable of detecting 3-MP in rabbits that were administered sulfanegen, a prodrug of 3-MP, following cyanide exposure. Considering the excellent performance of this method, it will be utilized for further investigations of this promising cyanide antidote.

© 2014 Elsevier B.V. All rights reserved.

1. Introduction

Humans are exposed to cyanide (LD_{50} , human = 1.1 mg/kg) [1,2] in a variety of ways, such as ingestion of some edible plants (spinach or cassava), industrial operations, smoke inhalation from fires and/or cigarettes, and terrorist activities [3,4]. Once cyanide is absorbed, it inhibits the enzyme cytochrome c oxidase in the electron transport system, thereby disrupting aerobic metabolism. There are currently three U.S. Food and Drug Administration (FDA) approved cyanide treatments: hydroxocobalamin, sodium nitrite, and sodium thiosulfate [2,5–7].

Hydroxocobalamin (vitamin B_{12a}) is a large molecular-weight cyanide antidote that detoxifies cyanide by sequestration. It forms a very strong bond with cyanide because of the high affinity of cyanide for the central cobalt atom ($K_A \approx 10^{12} M^{-1}$) [8]. Cyanide binds to cobalt to produce cyanocobalamin (vitamin B₁₂) [9–11], which resides in the plasma and is excreted in urine. The

potential adverse effects of hydroxocobalamin are generally mild and include elevated blood pressure, decreased heart rate, rashes, and red coloring of the skin, tears, urine and sweat [12,13]. The recommended dose of hydroxocobalamin is 5 g (administered over 15 min). Because of the high dose needed for optimum therapeutic effect, hydroxocobalamin must be administered intravenously [2,14], limiting the applicability of hydroxocobalamin in mass casualty situations.

Similar to hydroxocobalamin, the mechanism of action of sodium nitrite is to sequester cyanide from cytochrome c oxidase. However, the sequestration of cyanide is indirect. Sodium nitrite causes the conversion of hemoglobin to methemoglobin, which has a high affinity towards cyanide [14,15]. Recently, another mechanism of action of sodium nitrite was proposed as the prominent method of detoxification in which nitrite is converted to nitric oxide, which subsequently displaces cyanide bound to the active site of cytochrome c oxidase [16,17]. Although sodium nitrite works well to detoxify cyanide, it is toxic at large concentrations [5,18] and has a small therapeutic window. Sodium nitrite is especially toxic when smoke inhalation has occurred, due to the conversion of hemoglobin to methemoglobin, which reduces the oxygen carrying

* Corresponding author. Tel.: +1 605 688 6698; fax: +1 605 688 6364.
E-mail address: brian.logue@sdsu.edu (B.A. Logue).

capacity of the blood [18]. Due to its limited therapeutic efficacy, sodium nitrite is typically administered in tandem with sodium thiosulfate.

Sodium thiosulfate detoxifies cyanide by donating a sulfur to convert cyanide to the much less toxic thiocyanate [18–20]. Therefore, sodium thiosulfate belongs to a class of cyanide therapeutics known as sulfur donors, which utilize sulfurtransferase enzymes as catalysts. Sodium thiosulfate utilizes rhodanese, which is mainly found in the liver and kidneys [14,19], leaving the heart and central nervous system less protected and the main locations of cyanide toxicity [14]. It also has a slow onset of action, attributed to slow entry into cells and the mitochondria [5]. This necessitates its use in combination with faster acting therapeutics, typically sodium nitrite.

Considering that current cyanide antidotes each have major limitations, alternative cyanide antidotes are being investigated [5,8,21]. One such alternate antidote is 3-mercaptopyruvate (3-MP). Similar to sodium thiosulfate, 3-MP acts as a sulfur donor to produce thiocyanate but is instead catalyzed by 3-mercaptopyruvate sulfurtransferase (3-MST) [19,21,22]. Sulfanegen, a prodrug of 3-MP (i.e., sulfanegen converts to 3-MP upon administration), has been found to be highly effective in reversing cyanide toxicity [14,20,21,23,24]. Although a method for the detection of 3-MP by HPLC from mouse tissue has been proposed [25], a multistep, lengthy (>60 min), and high temperature (95 °C) modification of 3-MP is necessary. Therefore, the objective of this study was to develop a simple and sensitive analytical method for the analysis of 3-MP from rabbit plasma to facilitate further development of 3-MP as a cyanide antidote.

2. Experimental

2.1. Reagents and standards

All solvents were LC–MS grade unless otherwise noted. Ammonium formate and 3-mercaptopyruvate (3-MP; $\text{HSCH}_2\text{COCOOH}$) were purchased from Sigma–Aldrich (St. Louis, MO, USA). Acetone (HPLC grade, 99.5%) was purchased from Alfa Aesar (Ward Hill, MA, USA). Isotopically-labeled 3-MP ($\text{HS}^{13}\text{CH}_2^{13}\text{CO}^{13}\text{COOH}$) was synthesized and provided by the Center for Drug Design, University of Minnesota (Minneapolis, MN, USA) [21]. Millex tetrafluoropolyethylene syringe filters (0.22 μm , 4 mm, Billerica, MA, USA) were obtained through Fisher Scientific (Pittsburgh, PA, USA). Monobromobimane (MBB) was obtained from Fluka Analytical (Buchs, Switzerland) and a standard solution (500 μM) was prepared in LC–MS grade water and stored at 4 °C. 3-MP calibration standards and quality controls (QCs) were prepared from a 5 mM stock solution by serial dilution with rabbit plasma. The internal standard solution was prepared from a stock solution of 1 mM isotopically-labeled 3-MP in LC–MS grade water and stored at 4 °C.

2.2. Biological fluids

Rabbit plasma was obtained from two sources, a commercial vendor and a study used to evaluate effectiveness of sulfanegen in cyanide-exposed rabbits. For method development and validation, rabbit plasma (EDTA anti-coagulated) was purchased from Pel-Freez Biological (Rogers, AR, USA) and stored at -80°C until used. Rabbit plasma from sulfanegen efficacy studies was gathered at the Beckman Laser Institute at the University of California–Irvine. Rabbits were intramuscularly anesthetized, intubated and placed on isoflurane. Cyanide was administered at 0.47 mg/min intravenously until apnea (13 min), sulfanegen deanol (0.4 mmol) was then administered intravenously at apnea. Blood was drawn from the rabbits at baseline (i.e., before cyanide exposure), 5 min after

the start of cyanide infusion, at apnea, then 2.5, 5, 7.5, 10, 15 and 30 min after apnea. Blood was drawn into heparin collection tubes and plasma was immediately separated from blood. Plasma samples were then shipped on dry ice to South Dakota State University for analysis. Upon arrival, the plasma samples were stored at -80°C until analyzed.

2.3. Sample preparation

Plasma (100 μL , 3-MP spiked or nonspiked) was added to a 2 mL centrifuge tube along with an internal standard (100 μL of 15 μM 3-MP- $^{13}\text{C}_3$). Protein from the plasma was precipitated by addition of acetone (300 μL) and the samples were cold-centrifuged (Thermo Scientific Legend Micro 21R centrifuge, Waltham, MA, USA) at 8 °C for 30 min at 13,100 rpm (16,500 $\times g$). An aliquot (100 μL) of the supernatant was then transferred into a 4 mL glass vial and dried under N_2 . (Note: Glass vials were used in our laboratory mainly because of practical limitations of the N_2 drier.) The samples were reconstituted with 5 mM ammonium formate in 9:1 water:methanol (100 μL). Underivatized 3-MP initially produced unacceptable chromatographic behavior under all conditions evaluated because of the characteristic dimerization of 3-MP [26–28]. Therefore, MBB (100 μL , 500 μM) was added to prohibit 3-MP dimerization by converting the thiol group, which is necessary for dimerization, to a sulfide. The samples were heated on a block heater (VWR International, Radnor, PA, USA) at 70 °C for 15 min to produce a 3-MP-bimane (3-MPB) complex (Fig. 1). The reacted samples were then filtered with a 0.22 μm tetrafluoropolyethylene membrane syringe filter into autosampler vials fitted with 150 μL deactivated glass inserts for HPLC–MS–MS analysis. It should be noted that when the number of samples were above the maximum limit of the sample apparatus (e.g., the centrifuge), the samples that were not being actively prepared were stored in a standard refrigerator (4 °C) to impede degradation of the analyte.

2.4. HPLC–MS–MS analysis of 3-MPB

A Shimadzu UHPLC (LC 20A Prominence, Kyoto, Japan) coupled to a 5500 Q-Trap mass spectrometer (AB Sciex, Framingham, MA, USA) along with an electrospray ion source was used for HPLC–MS–MS analysis. Separation was performed on a Phenomenex Synergi Fusion RP column (50 \times 2.0 mm, 4 μm 80 Å) with an injection volume of 10 μL from samples stored in a cooled autosampler (15 °C). Mobile phase solutions consisted of 5 mM aqueous ammonium formate with 10% methanol (Mobile Phase A) and 5 mM ammonium formate in 90% methanol (Mobile Phase B). A gradient of 0–100% B was applied over 3 min, held constant for 0.5 min, then reduced to 0% B over 1.5 min. The total run-time was 5.1 min with a flow rate of 0.25 mL/min, and a 3-MPB retention time of about 2.75 min. The electrospray interface was kept at 500 °C with zero air nebulization at 90 psi in positive ionization mode with drying and curtain gasses held at 60 psi each. The ion-spray voltage, declustering potential, collision cell exit potential, and channel electron multiplier voltage were 4500, 121, 10, and 2600 V, respectively. Multiple-reaction-monitoring (MRM) transitions of 311 \rightarrow 223.1 and 311 \rightarrow 192.2 m/z for 3-MPB and 314 \rightarrow 223.1 and 314 \rightarrow 192.2 m/z for the internal standard-bimane complex were used with collision energies of 30.5 and 25 V, respectively. The dwell time was 100 ms for both transitions. Analyst software (Applied Biosystems version 1.5.2) was used for data acquisition and analysis.

2.5. Calibration, quantification and limit of detection

For validation of the analytical method, we generally followed the FDA bioanalytical method validation guidelines [29]. The lower limit of quantification (LLOQ) and upper limit of quantification

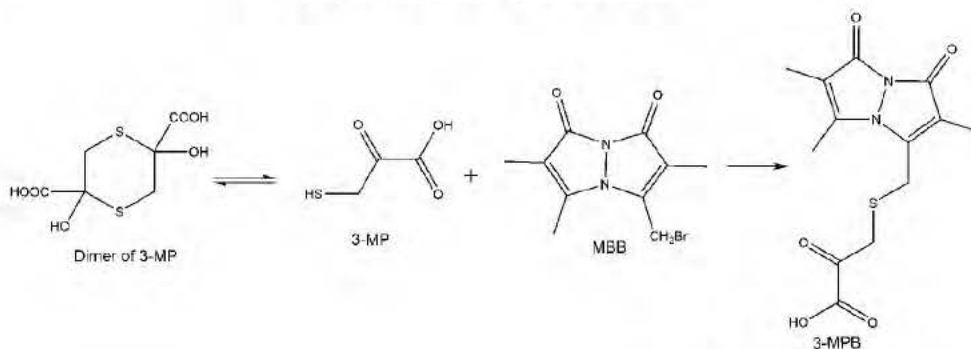


Fig. 1. 3-MP in equilibrium with its dimer and its reaction with MBB to form a stable 3-MPB complex.

(ULOQ) were defined using the following inclusion criteria: 1) calibrator precision of <15% RSD, and 2) accuracy of $\pm 15\%$ of the nominal calibrator concentration back-calculated from the calibration curve. The initial calibration curve was prepared with 0.2–500 μM calibration standards (0.2, 0.5, 1, 2, 5, 10, 20, 50, 100, 200, and 500 μM) in plasma to determine the linear range, with the range later decreased to 0.5–100 μM for the optimized method. A calibration curve was also prepared in aqueous solution and compared to the plasma calibration curve to assess potential matrix effects. For all other experiments, calibration standards and QCs were prepared in rabbit plasma. QCs (N=5) were prepared at three concentrations not included in the calibration curve: 1.5 μM (low QC), 7.5 μM (medium QC) and 35 μM (high QC). The internal standard was prepared daily and added to each sample, calibration standard and QC during sample preparation. QCs were prepared fresh each day in quintuplicate during intra-assay (daily) and inter-assay (over three separate days, within six calendar days) analyses and were used to calculate intra-assay and inter-assay accuracy and precision.

The limit of detection (LOD) was determined by analyzing multiple concentrations of 3-MP below the LLOQ and determining the lowest 3-MP concentration that reproducibly produced a signal-to-noise ratio of 3, with noise measured as the peak-to-peak noise directly adjacent to the 3-MP peak. It should be noted that 3-MP is inherently present in plasma of mammals [19,22] and was typically seen in rabbit plasma at concentrations below the limit of detection in this study.

2.6. Stability and recovery

To evaluate the stability of 3-MP, low and high QCs were stored at various temperatures (room temperature (RT), 4 $^{\circ}\text{C}$, -20°C , and -80°C) and analyzed over multiple storage times. When storage stability samples were analyzed, internal standard was added as the QCs were prepared for analysis. Stability of 3-MP was calculated as a percentage of the initial concentration ("time zero"), with 3-MP considered stable if the concentration of a stored sample was within 10% of time zero. Long-term stability was conducted at three storage conditions (4, -20 , and -80°C). The samples were analyzed in triplicate after 1, 2, 8, 15, 30, and 45 days. Autosampler stability of 3-MPB was determined after typical preparation of low and high QCs and storage in the autosampler for approximately 2, 4, 8, 12, and 24 h. For freeze-thaw stability of 3-MP, each set of low and high QCs was prepared in triplicate. Initially, one set of QCs (low and high) was analyzed. The other standards were stored at -80°C for 24 h. All standards were then thawed unassisted at RT and one

set of QCs was analyzed. The remaining QCs were replaced in the -80°C freezer. This process was repeated twice more for three total freeze-thaw cycles.

For recovery, five aqueous low, medium and high QCs were prepared, analyzed, and compared with equivalent concentrations of plasma QCs. Recovery of 3-MP was calculated as a percentage by dividing the analyte plasma concentration with the calculated aqueous QC concentration.

3. Results and discussion

3.1. HPLC-MS/MS analysis of 3-MP from rabbit plasma

Under biological conditions, 3-MP is in rapid equilibrium with its dimer [30]. This equilibrium is difficult to control and results in poor chromatographic behavior. Because MBB reacts with the thiol group of 3-MP [26,27], which is essential for dimerization, a single 3-MPB complex is created (Fig. 1), which produced excellent chromatographic behavior. Fig. 2 shows representative chromatograms of spiked and nonspiked 3-MPB in

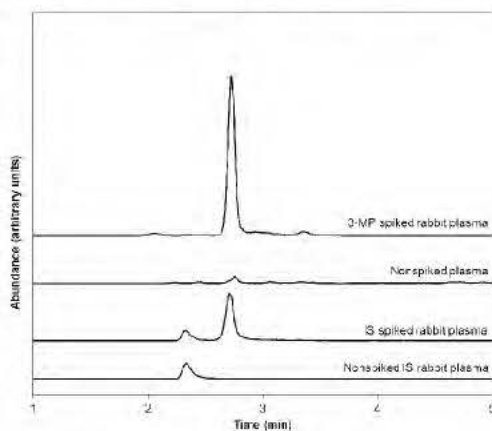


Fig. 2. Representative chromatograms of 3-MP spiked (20 μM) and nonspiked rabbit plasma, monitoring the 311 \rightarrow 223.1 m/z transition. The internal standard 314 \rightarrow 223.1 m/z spiked and nonspiked in rabbit plasma is also shown. 3-MPB elutes at approximately 2.75 min. A small endogenous concentration of 3-MP can be observed in the nonspiked rabbit plasma.

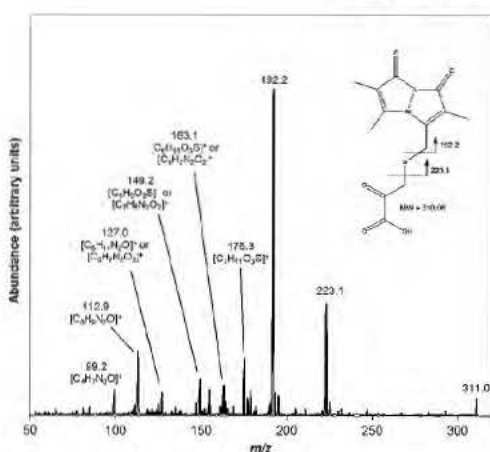


Fig. 3. The mass spectrum of the 3-MPB complex with tentative identification of the abundant ions. The 3-MPB ion at 311 m/z corresponds to [M-H].

plasma, with 3-MPB eluting at approximately 2.75 min. The method shows good selectivity for 3-MPB with no co-eluting peaks ($R_s = 3.07$ from the nearest peak at 3.3 min), although the nonspiked rabbit sample shows a small endogenous 3-MP concentration [19,21,22,24]. Considering the rabbit plasma analyzed for this study in aggregate, it is estimated that the endogenous concentration of 3-MP in rabbits is between 0.05 and 0.1 μM . The endogenous concentration of 3-MP has not been previously estimated due to rapid metabolism in vivo [21–23,31] and the lack of a sensitive analytical technique.

The mass spectrum of 3-MPB, with tentative abundant ion assignments, is displayed in Fig. 3. The 311 \rightarrow 223.1 and 311 \rightarrow 192.2 transitions were selected as the quantification and identification transitions, respectively. The corresponding transitions for the internal standard, 314 \rightarrow 223.1 and 314 \rightarrow 192.2, were also monitored to correct for multiple sources of potential analysis error.

The simple sample preparation and short chromatographic analysis time for the method presented here permit rapid analysis of numerous plasma samples. The analysis of an individual sample using this method typically lasted approximately 1 h and 10 min, including 1 h for sample preparation and 7 min for chromatographic analysis (including equilibration time). Using conservative estimates, approximately 90 parallel samples could be prepared and analyzed in a 24 h period.

3.2. Linear range, limit of detection, and sensitivity

Calibration curves of 3-MP were constructed in the range of 0.2–500 μM in rabbit plasma. The signal ratio of each sample, defined as the peak area for each calibrator divided by its corresponding internal standard peak area was used as the

corrected signal. Upon analysis of the calibration standards using non-weighted and weighted ($1/x$ and $1/x^2$) calibration curves, 0.2, 200, and 500 μM standards were excluded because they did not meet the accuracy and/or precision inclusion criteria. The linear range for the method was 0.5–100 μM for 3-MP when using a $1/x^2$ weighted linear regression of the calibrators with a correlation coefficient (R^2) > 0.999. The LOD was 0.1 μM and the LLOQ and ULOQ of the method were 0.5 and 100 μM , respectively. Moderate matrix effects were observed for 3-MP analysis with the slope of the calibration curve in plasma reduced as compared to aqueous. Attempts were made to reduce the matrix effects using solid-phase extraction (i.e., weak, strong, and mixed-mode anion exchange stationary phases were tested for 3-MP, and C18-type stationary phases were tested for 3-MPB) with no reduction observed. Therefore, it is necessary to prepare all calibration standards in rabbit plasma to determine accurate concentrations of 3-MP.

3.3. Accuracy and precision

Accuracy and precision were determined by quintuplicate analysis of the low, medium, and high QCs (1.5, 7.5, and 35 μM , respectively) on three different days (within 6 calendar days; Table 1). The intra-assay accuracy ($\pm 9\%$) and precision ($< 7\%$ RSD) and the inter-assay accuracy ($\pm 5\%$) and precision ($< 6\%$ RSD) for the method were excellent relative to the typical precision and accuracy of analytical methods for the quantification of small molecules from plasma samples.

3.4. Stability and recovery

Long-term storage stability of 3-MP in spiked plasma was evaluated at 4, -20 and -80 $^\circ\text{C}$, with short-term stability evaluated at RT. Autosampler (2, 4, 8, 12 and 24 h) and freeze-thaw stability (3 cycles) were also evaluated. While 3-MP was stable at -80 $^\circ\text{C}$ for at least 45 days, it was quickly removed from plasma at RT, 4, and -20 $^\circ\text{C}$ (i.e., <1 day) and during freeze-thaw cycles (i.e., 3-MP was stable for only one freeze-thaw cycle). Lower storage temperatures generally increased the stability of 3-MP, likely due to a decrease in enzymatic activity. In the autosampler, 3-MPB was stable for at least 24 h (i.e., the measured concentrations were within 10% of the initial concentrations). The results from the stability study suggest that if storage is necessary, plasma samples should be frozen immediately and stored at -80 $^\circ\text{C}$. Samples should then be prepared immediately after thawing, but can be stored on an autosampler for at least 24 h after preparation.

The recovery of 3-MP for low, medium and high QCs was 81, 75, and 75% respectively. These recoveries were below 90% but were very consistent. Incomplete recovery can be explained by facile enzyme catalyzed conversion of 3-MP in the plasma [19,22,30] and may be an area for further improvement of the method.

3.5. Analysis of sulfanegen-exposed rabbits

The validated HPLC-MS-MS method was applied to the analysis of plasma from rabbits exposed to cyanide and subsequently treated with sulfanegen [14,20,21,24]. The HPLC-MS-MS analysis

Table 1
The accuracy and precision of 3-mercaptopyruvate analysis in spiked rabbit plasma by HPLC-MS-MS.

Concentration (μM)	Intra-assay accuracy ^a	Intra-assay precision ^a	Inter-assay accuracy ^b	Inter-assay precision ^b
1.5	102	8.87	103	5.13
7.5	98	2.39	100	2.74
35	108	2.97	105	2.95

^a QC method validation (N=5) for Day 1.

^b QC mean from three different days of method validation (N=15).

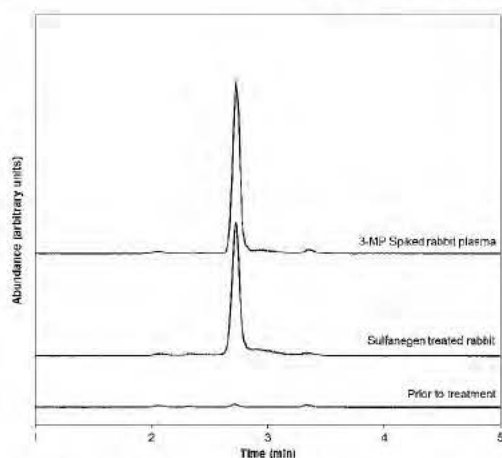


Fig. 4. HPLC-MS-MS chromatograms of 3-MP spiked rabbit plasma, plasma from a sulfanegen treated rabbit and plasma from the same rabbit prior to sulfanegen treatment. The 3-MP signal in the sulfanegen treated rabbits corresponds to 18 μ M.

of the plasma of sulfanegen treated and untreated rabbits is shown in Fig. 4, alongside a chromatogram of 3-MP spiked rabbit plasma. Sulfanegen treated rabbits showed greatly elevated 3-MP concentrations compared to untreated rabbits. Overall, Fig. 4 confirms that the method presented here has the ability to detect elevated 3-MP concentrations from sulfanegen treated rabbits and may be applied to future studies of this next generation cyanide therapeutic. A full pharmacokinetic analysis of sulfanegen in rabbits by the described method will be reported in the near future.

4. Conclusion

An HPLC-MS-MS method for the detection of 3-MP was developed which features simple sample preparation, excellent accuracy and precision, an excellent detection limit, and has a linear range of over 2 orders of magnitude. While Ogasawara et al. [25] reported an HPLC-fluorescence method for the analysis of 3-MP in mouse tissue, the method presented here featured simple and low-temperature sample preparation (i.e., 3-MP is highly unstable at high temperatures), rapid analysis, a reduced lower limit of quantification, a wider linear dynamic range, and the ability to analyze 3-MP from plasma of sulfanegen treated rabbits, which will facilitate the study of 3-MP prodrugs (e.g., sulfanegen) as treatments for cyanide poisoning.

Acknowledgements

We gratefully acknowledge the support from a U.S. Dept. of Education, Graduate Assistance in Areas of National Need (GAANN) award to the Department of Chemistry & Biochemistry (P200A100103). We thank the National Science Foundation Major Research Instrumentation Program (Grant Number CHE-0922816) for funding the AB SCIEX QTRAP 5500 LC-MS-MS. We also would like to acknowledge the support by the CounterACT Program, National Institutes of Health Office of the Director (NIH OD), and the

National Institute of Neurological Disorders and Stroke (NINDS), (Grant Number U01NS058087-06). In addition, the LC-MS-MS instrumentation in the South Dakota State University Campus Mass Spectrometry Facility used in this study was obtained with support from the National Science Foundation/EPSCoR (Grant No. 0091948) and the State of South Dakota. Furthermore, the authors are thankful to Dr. Sari B. Mahon from the Beckman Laser Institute and Dr. Matthew Brenner from the Division of Pulmonary and Critical Care (University of California-Irvine, Irvine, CA) for providing sulfanegen treated rabbit plasma. The opinions or assertions contained herein are the private views of the authors and are not to be construed as official or as reflecting the views of the National Science Foundation, the National Institutes of Health or the CounterACT Program.

References

- [1] C.D. Barnes, L.G. Etherington, *Drug Dosages in Laboratory Animals—A Handbook*, University of California Press, Berkeley, USA, 1973.
- [2] T.F. Cummings, *Occ. Med.* 54 (2004) 82–85.
- [3] R.K. Bhandari, R.P. Oda, S.L. Youso, I. Petrikovics, V.S. Beberta, G.A. Rookwood, B.A. Logue, *Anal. Bioanal. Chem.* 404 (2012) 2287–2294.
- [4] B.A. Logue, D.M. Hinkens, S.I. Baskin, G.A. Rookwood, *Crit. Rev. Anal. Chem.* 40 (2010) 122–147.
- [5] A.H. Hall, J. Sifers, F. Baud, *Crit. Rev. Toxicol.* 39 (2009) 541–552.
- [6] R. Gracia, G. Shepard, *Pharmacotherapy* 24 (2004) 1358–1365.
- [7] A.H. Hall, B.H. Rhumack, *J. Emerg. Med.* 5 (1987) 115–121.
- [8] K.E. Broderick, P. Potluri, S. Zhuang, I.E. Scheffler, V.S. Sharma, R.B. Riz, G.R. Boss, *Exp. Biol. Med.* (2006) 841–849.
- [9] T.C. Marrs, J.P. Thompson, *Clin. Toxicol.* 50 (2012) 875–885.
- [10] S.W. Borron, F.J. Baud, P. Barriot, M. Imbert, C. Bismuth, *Ann. Emerg. Med.* 49 (2007) 794–801.
- [11] H.A. Schwertner, S. Valtier, V.S. Beberta, *J. Chromatogr. B* 905 (2012) 10–16.
- [12] C.E. Becker, N.L. Benowitz, J.C. Forsyth, A.H. Hall, P.D. Mueller, J. Osterloh, *J. Toxicol.: Clin. Toxicol.* 31 (1993) 277–294.
- [13] C. Brunel, C. Widmer, M. Augsburger, F. Dussy, T. Fracasso, *Forensic Sci. Int.* 223 (2012) e10–e12.
- [14] M. Brenner, J.G. Kim, J. Lee, S.B. Mahon, D. Lemor, R. Ahdout, G.R. Boss, W. Blackledge, L. Jann, H.T. Nagasawa, S.E. Patterson, *Toxicol. Appl. Pharm.* 248 (2010) 269–276.
- [15] C.A. DesLauriers, A.M. Burda, M. Wahl, *Am. J. Ther.* 13 (2008) 161–165.
- [16] L.K. Cambal, M.R. Swanson, Q. Yuan, A.C. Weitz, H.-H. Li, B.R. Pitt, L.L. Pearoe, J. Peterson, *Chem. Res. Toxicol.* 24 (2011) 1104–1112.
- [17] L.L. Pearoe, E.L. Bominaar, B.C. Hill, J. Peterson, *J. Biol. Chem.* 278 (2003) 52139–52144.
- [18] M.C. Reade, S.R. Davies, P.T. Morley, J. Dennett, I.C. Jacobs, *Emerg. Med. Australas.* 24 (2012) 225–238.
- [19] G.E. Isom, J.L. Borowitz, S. Mukhopadhyay, in: C. McQueen (Ed.), *Comprehensive Toxicology*, 2010, pp. 485–500.
- [20] S.E. Patterson, A.R. Monteil, J.F. Cohen, O.L. Crankshaw, R. Vince, H.T. Nagasawa, *J. Med. Chem.* (2013).
- [21] H.T. Nagasawa, D.J.W. Goon, D.L. Crankshaw, R. Vince, S.E. Patterson, *J. Med. Chem.* 50 (2007) 6462–6464.
- [22] A. Spallarossa, F. Forlani, A. Carpen, A. Armirotti, S. Paganì, M. Bolognesi, D. Bordo, *J. Mol. Biol.* 335 (2004) 583–593.
- [23] N. Nagahara, T. Ito, M. Minami, *Histol. Histopathol.* 14 (1999) 1277–1288.
- [24] K.G. Belani, H. Singh, D.S. Beebe, P. George, S.E. Patterson, H.T. Nagasawa, *R. Vince, Anesth. Analg.* 114 (2012) 956–961.
- [25] Y. Ogasawara, T. Hirokawa, K. Matsushima, S. Koike, N. Shibuya, S. Tanabe, K. Ishii, *J. Chromatogr. B* 931 (2013) 56–60.
- [26] N.S. Kosower, E.M. Kosower, in: W.B. Jakoby, O.W. Griffith (Eds.), *Methods in Enzymology*, Academic Press, INC, Orlando, FL, USA, 1987, pp. 76–84.
- [27] R.C. Fahey, G.L. Newton, in: W.B. Jakoby, O.W. Griffith (Eds.), *Methods in Enzymology*, Academic Press, INC, Orlando, FL, USA, 1987, p. 85.
- [28] *Sample Preparation in Chromatography*, Elsevier, Boston, MA, USA, 2002, pp. 473–524.
- [29] Food and Drug Administration, *Guidance for industry bioanalytical method validation*, Food and Drug Administration, Rockville, MD, 2001.
- [30] A.J.L. Cooper, M.T. Haber, A. Meister, *J. Biol. Chem.* 257 (1982) 816–826.
- [31] T. Ubuoka, J. Ohta, W.B. Yao, T. Abe, T. Teraoka, Y. Kurozumi, *Amino Acids* 2 (1992) 143–155.